MINERAL NUTRITION IN WHITE SPRUCE SEEDS AND SOMATIC EMBRYOS

MINERAL NUTRITION IN WHITE SPRUCE (*PICEA GLAUCA*) SEEDS AND SOMATIC EMBRYOS

By

DARYL ANDREW REID, B.Sc.

A Thesis

Submitted to the School of Graduate Studies

in Partial Fulfilment of the Requirements

for the Degree

Master of Science

McMaster University

MASTER OF SCIENCE (1998) McMASTER UNIVERSITY
(Biology) Hamilton, Ontario

TITLE: Mineral Nutrition in White Spruce (*Picea glauca*) Seeds and Somatic Embryos.

AUTHOR: Daryl Andrew Reid, B.Sc.
(McMaster University)

SUPERVISOR: Dr. J.N.A. Lott

NUMBER OF PAGES: xvi, 220

ABSTRACT

The mineral nutrient storage reserves in various parts of white spruce (*Picea glauca*) seeds and somatic embryos were investigated. Somatic embryos are produced in tissue culture from single cells or small groups of cells. These cells are induced to produce a callus, which is then stimulated to produce mature somatic embryos that are desiccated down to moisture content levels comparable to those of a mature dry seed.

Morphological comparisons revealed that somatic and zygotic embryos are very similar. Somatic embryos of white spruce; however, were larger, had a flared arrangement of cotyledons, had more prominent suspensor regions, had intercellular spaces in the ground meristem tissue and had ground meristem cells that had divided in several planes of division.

Using a wet ashing protocol, anion exchange resins and the molybdenum blue colourimetric reaction, the total levels of P and the amount of P bound to phytic acid were measured. Phytic acid (or phytate) is the major nutrient storage compound in seeds. Although differences were found on a dry weight basis, a single somatic and a single zygotic embryo had similar levels of P. Somatic embryos produced in different batches varied in their levels of phytic acid, but a somatic embryo could have similar levels of phytic acid as a zygotic embryo. The large female gametophyte contained 86% of the total P and 95% of the total phytic acid in a single seed.

Electron microscopy and energy dispersive x-ray analysis found phytate-rich globoids in the procambium and ground meristem tissues of both types of embryos. Globoids

contained high P, moderate K and Mg, and little if any Ca, Fe and Zn. Globoids were generally larger and more frequent in zygotic embryos. Globoids from the cotyledon procambium of zygotic embryos also contained moderate levels of Fe. Iron-rich particles (possible Fe-phytate deposits) were found in the protoderm, procambium and ground meristem of both types of embryos. These deposits contained high P and Fe, moderate K and Mg, and little if any Ca and Zn. Globoid and Fe-rich particle compositions were similar in both embryo types, but significantly higher Fe:P ratios were found in zygotic embryos.

Atomic absorption spectroscopy was used to measure total K, Mg, Ca, Fe and Zn levels. Although differences were found on a dry weight basis, a single white spruce somatic or zygotic embryo contained similar levels of all these elements. The female gametophyte contained high levels of these elements and the seed coat contained considerable Ca.

Potassium leakage during imbibition in germination medium revealed that a single somatic and zygotic embryo of white spruce leaked similar levels of K. Pretreatment of somatic embryos in a high relative humidity environment resulted in decreased potassium leakage by 80 and 120 min. of imbibition. The seed coat was found to reduce the amounts of K leaked. Surface cells in dry somatic and zygotic embryos were found to be wrinkled, but cells in zygotic embryos were more shrunken in appearance. During imbibition, cells became more turgid; but after 120 min. of imbibition, surface cells still showed signs of wrinkling.

To date, this is the first major report of mineral nutrition in white spruce seeds and is the first comprehensive comparison of mineral nutrients in white spruce seeds and somatic embryos. These results may be useful in producing complete artificial white spruce seeds.

ACKNOWLEDGEMENTS

I wish to thank Dr. John Lott for allowing me the opportunity to work in his lab. His support and encouragement throughout my studies and in my personal life are greatly appreciated. I would also like to thank Dr. Gary Leppard and Dr. Elizabeth Weretilnyk for being on my supervisory committee and for giving me helpful advice on my work.

I would like to thank Dr. Larry Fowke from the University of Saskatchewan and Dr. Stephen Attree from the Pacific Bio. Tech. Incorporation for their advice and generous supply of tissue samples for this thesis. Thank you to Dr. Irene Ockenden and Klaus Schultes for their technical assistance in various parts of this work. I especially would like to thank Marcia West for her support, advice, technical assistance and friendship throughout my work.

Finally, I would like to thank all my family and friends for their continual support and understanding throughout my university career. I would especially like to thank my mother and father for always being there to support me in whatever I chose to do.

TABLE OF CONTENTS

LIST OF TABLES

LIST OF FIGURES

CHAPTER 1:

INTRODUCTION

The focus of this thesis is the study of mineral nutrient storage in dry white spruce (*Picea glauca*) seeds and desiccated white spruce somatic embryos (embryos produced in tissue culture). Various techniques were used to study total phosphorus, phytic acid phosphorus (PA-P), potassium, magnesium, calcium, iron and zinc levels in somatic embryos and various seed tissues. In addition, the mineral nutrient composition of two storage deposits, both believed to be phytate, were studied using energy dispersive x-ray analysis. Finally, potassium leakage and surface damage during imbibition was investigated and the effects of high relative humidity (RH) pretreatment on the levels of potassium leakage during imbibition were measured.

Pinaceae

White spruce is one of 40 recorded species in the *Picea* genus (Young and Young, 1992). *Picea* is one of 10 genera in the Pinaceae (pine) family (Stewart, 1983). Members of the Pinaceae have needle-like leaves and, with the exception of one species, all are found in the Northern Hemisphere (Stewart, 1983). *Pinus*, which is considered the oldest genus in the pine family, evolved by the Lower Cretaceous period approximately 135 million years ago (Stewart, 1983). All subsequent genera in Pinaceae appeared in the Early Tertiary period

approximately 65 million years ago, but phylogenetic relationships in the pine family are still uncertain and require more research to produce an accurate phylogeny (Farjon, 1990).

The spruces (*Picea*) evolved in North Eastern Asia and are currently found widely distributed in the Northern Hemisphere (Young and Young, 1992). These medium-to-tall evergreen conifers have become a key source of lumber and pulpwood due to their quality wood; which is strong, fine-grained, even-textured, long-fibered and light-weight (Young and Young, 1992). Spruces are also important to lumbering and reforestation industries because they are especially well adapted to tolerate extreme cold and wind (Young and Young, 1992). Consequently, spruces are often found growing on high mountain slopes and in areas as far north as the tree line (Young and Young, 1992). Spruces are capable of growing on soils with low concentrations of N, P, K, Ca and Mg as well as on acidic soils (pH 4-5) or basic soils derived from limestone (Farjon, 1990). The wide range of habitats in which *Picea* can survive makes it an attractive genus for widespread reforestation practices.

White spruce, which reaches heights of 40-50 m, can be found at elevations between 5 and 1900 m above sea level (Farjon, 1990). At approximately 30 years of age, white spruce trees develop seed-bearing cones and continue to produce these cones once every 2 to 6 years (Young and Young, 1992). The yellow male strobili (1-2 cm long) are laterally and axillary located while female cones (3-7 cm long) are terminally located, especially in the upper part of the crown (Farjon, 1990). White spruce seeds are small (2-3 mm long) with dark brown to black seed coats. Pollination in white spruce occurs in May with cone ripening by August and seed dispersal in September (Young and Young, 1992). White spruce was first cultivated in 1700 and continues to be an economically important species (Young and Young, 1992).

Zygotic Embryogenesis

Embryogenesis in conifers involves the formation of a zygotic embryo surrounded by nutritive female gametophyte (or megagametophyte) tissue. The female gametophyte is surrounded by a hard protective seed coat. Zygotic embryogenesis in conifers has been described and reviewed previously (Chowdhury, 1962; Singh, 1978; Norstog, 1982; Tautorus *et al.*, 1991; Attree and Fowke, 1993; Misra, 1994). The diploid zygotic embryo is formed by the fusion of a functional sperm cell with the egg cell (Singh, 1978). This single fertilization separates gymnosperm seed development from angiosperm seed development, which involves double fertilization (Attree and Fowke, 1993; Misra, 1994). With single fertilization, the multicellular female gametophyte originates from the functional megaspore and since it begins to develop prior to fertilization, this tissue is haploid (Misra, 1994). This large tissue, which supplies nutrients to the developing embryo and young seedling, represents a substantial initial investment of energy that is wasted if successful fertilization does not occur (Steeves, 1983). Zygotic embryo development occurs entirely surrounded by the female gametophyte.

Conifer zygotic embryo development can be divided into two phases: (1) a brief proembryo phase, which occurs inside the region that was called the egg cell prior to fertilization, and (2) the embryo phase, which occurs following proembryo elongation into the cellular female gametophyte tissue (Singh, 1978; Owens and Molder, 1984a; 1984b). Often the embryo phase is divided into early, mid and late stages based on morphological changes (Misra, 1994). The following is a detailed description of zygotic embryogenesis in *Picea* based on previous descriptions of conifer zygotic embryogenesis and as depicted in Figure 1

(Buchholz, 1918; Singh, 1978; Owens and Molder, 1979; Singh and Owens, 1980; Owens and Blake, 1985; Krasowski and Owens, 1993).

The proembryo phase begins with the fertilization of the egg nucleus. The fertilized egg nucleus divides giving two free nuclei (Fig. 1A), which both divide synchronously giving four free nuclei in the egg cell (Fig. 1B). These four nuclei divide again and the cell walls form to give two tiers of four cells each, called the 8-celled proembryo (Fig. 1C). Each cell divides giving a 16-celled proembryo consisting of four tiers with four cells in each tier (Fig. 1D). Starting from the tip of the proembryo the tiers are; the apical tier, suspensor tier, rosette tier and finally the open tier. The cells of the suspensor tier elongate and push the apical tier up through the archegonial jacket (layer of cells surrounding the original egg cell) into the nutritive female gametophyte, marking the end of the proembryo phase (Fig. 1E).

During the early stages of the embryo phase, the apical tier cells divide to form the terminal embryonal cells and the subterminal suspensor cells, called secondary suspensor cells. This division again pushes the embryonal cells further into the female gametophyte (Fig. 1F). The embryonal cells then divide to give an embryonal mass (Fig. 1G). The basal cells in this mass continue to divide and elongate to add to the thick secondary suspensor. The distal cells in the mass divide to form a club-shaped embryo (Fig. 1H), which continues to enlarge (mid-embryo stage). The enlarging embryo fills the corrosion cavity in the female gametophyte and the late-embryo stage is marked by the development of well-defined root and shoot apices, elongation of the hypocotyl and cotyledons, and the development of provascular tissues (procambium). From the root meristem, a massive root cap forms. During late stages of development, storage products accumulate within the seed tissues. Then, once all the cells

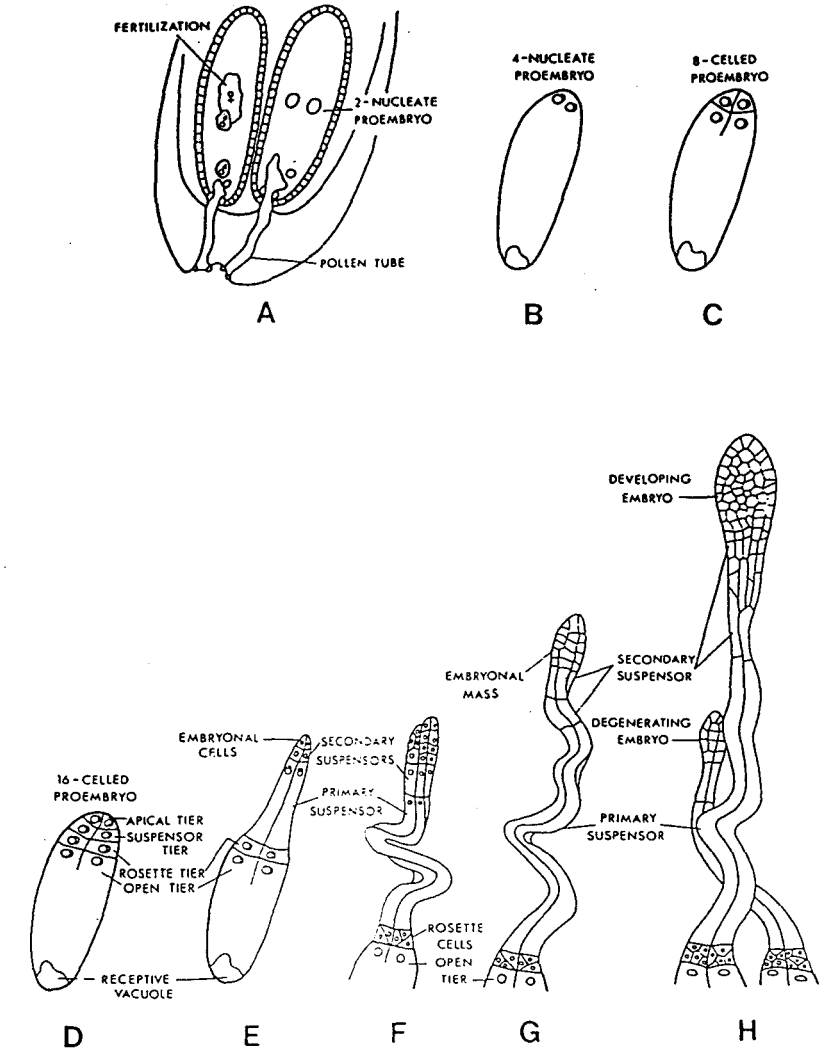

Figure 1: Fertilization and zygotic embryogenesis in *Picea*. Following fertilization, the zygote nucleus divides into two free nuclei within the old egg cell, which is surrounded by female gametophyte tissue (A). Each nucleus then divides giving four free nuclei (B). Since this figure illustrates longitudinal sections, only half of each tier in the following diagrams are illustrated. Each nucleus divides again and cell walls develop giving two tiers of four cells each (C). Cell division occurs again (D) and the suspensor tier elongates pushing the apical tier into the female gametophyte (E). The apical tier cells divide pushing the embryonal cells further into the female gametophyte (F) and the embryonal mass is formed (G). Basal cells divide to add to the suspensor region while the distal cells develop into the club-shaped embryo (H). Generally one embryo will fully mature, while the other embryos degenerate (From Owens and Blake, 1985).

within the seed have finished accumulating reserves, the mature seed becomes dormant until the germination processes are initiated.

Most conifers undergo either cleavage polyembryony or simple polyembryony (Tautorus *et al.*, 1991). Cleavage polyembryony is the process in which multiple embryos develop from cells originating from a single zygote (Attree and Fowke, 1993). In cleavage polyembryony, the apical tier of four cells from a single proembryo divides into four columns of cells, any of which can develop into a separate embryo (Chowdhury, 1962). Since all the embryos originate from the same proembryo, they are all genetically identical (Chowdhury, 1962). Typically only one of these embryos fully mature while the others abort, but the mechanism and factors influencing which embryo becomes dominant are not well understood (Buchholz, 1918; Dogra, 1967; Owens and Blake, 1985). Cleavage polyembryony commonly occurs in the genera *Abies*, *Cedrus*, *Keteleeria*, *Pinus* and *Tsuga* (Buchholz, 1926; 1931; Chowdhury, 1962; Owens and Molder, 1984b). Cleavage polyembryony is what occurs in tissue culture production of somatic embryos.

Simple polyembryony is common in the genera *Larix*, *Picea*, *Pseudolarix* and *Pseudotsuga* (Buchholz, 1939; Chowdhury, 1962). This type of polyembryony occurs when multiple eggs in a single ovule are fertilized and grow into embryos (Singh, 1978). Each proembryo in this case is produced from fertilization by a gamete from a different pollen grain than the other proembryos in the ovule and is thus genetically different (Tautorus *et al.*, 1991). Again, normally only one proembryo matures while the others abort. Of the two types of polyembryony, simple polyembryony is considered to be more primitive since no cleavage is involved (Chowdhury, 1962).

Somatic Embryogenesis

Somatic embryogenesis is the production of embryos from single cells or small groups of vegetative cells using tissue culture techniques (Ammirato, 1983). The first description of haploid somatic embryos was for the cycad, *Zamia floridana* (LaRue, 1948; 1954). These haploid somatic embryos were produced by culturing haploid female gametophytes. In 1967, the first production of diploid somatic embryos was reported from culturing *Zamia integrifolia* zygotic embryos (Norstog and Rhamstine, 1967). The first production of angiosperm somatic embryos was reported independently by Reinert (1958; 1959) and Steward *et al.* (1958) for carrot (*Daucus carota*). Following this, advancements in angiosperm somatic embryo production proceeded at a faster rate than those for gymnosperm cultures.

The production of conifer somatic embryos was first reported in 1985 by three independent groups of researchers. Hakman *et al.* (1985) and Chalupa (1985) reported successful somatic embryogenesis by culturing Norway spruce (*Picea abies*) zygotic embryos. In the same year, Nagmani and Bonga (1985) described the production of haploid European larch (*Larix decidua*) somatic embryos from cultured female gametophytes. A large volume of research has since been devoted to optimizing culture conditions to produce somatic embryos for a vast number of species. Somatic embryos now produced for several species are morphologically very similar to natural zygotic embryos and initiation of somatic embryos for previously uncultured species is being reported on a regular basis.

Somatic embryogenesis involves the reactivation of many of the events in zygotic embryogenesis with the eventual production of embryos having shoot and root apices

(Tautorus *et al.*, 1991; Attree and Fowke, 1993). As reviewed by Tautorus *et al.* (1991), most of the initial attempts at conifer somatic embryogenesis between 1968 and 1980 resulted in the production of polarized embryo-like structures, termed embryoids, which in no case developed into complete somatic embryos. Conifer somatic embryogenesis can be divided into three major stages: induction, development of immature embryos, and maturation (Misra, 1994).

Induction of embryogenic cultures refers to the production of a mass of cells, which will later be stimulated to produce immature somatic embryos (Misra, 1994). This requires an initial supply of cells from a tissue source, referred to as the explant. The terminology used to describe stages in tissue culture is sometimes confusing when discussing this mass of cells induced in this initial stage. Although less commonly seen, undifferentiated parenchyma cells, referred to as callus tissue, may develop from the explant and can be used to produce somatic embryos (Misra, 1994). More frequently, in conifer tissue cultures the mass of cells induced from the explant is an organized mass of compact embryonal cells with associated suspensors, much like early stages of zygotic embryogenesis (Misra, 1994). These organized cell masses are referred to in literature as embryonal masses, stage 1 somatic embryos, embryonal suspensor masses, proembryo calli or embryogenic calli (Tautorus *et al.*, 1991; Misra, 1994).

Typically somatic embryos are induced using seed tissues as the explant source. Haploid conifer embryogenic cultures have only been successfully produced from explants of female gametophyte tissue (Attree and Fowke, 1993). Haploid cultures have been established for several species including European silver fir (*Abies alba*) (Schuller *et al.*, 1989) and Eastern white pine (*Pinus strobus*) (Finer *et al.*, 1989). Diploid embryogenic cultures of

conifers are most readily induced using zygotic embryo explants (Attree and Fowke, 1993). Immature zygotic embryos have been widely used to induce somatic embryo development in species such as Norway spruce (Hakman *et al.*, 1985), Douglas-fir (*Pseudotsuga menziesii*) (Durzan and Gupta, 1987), and Western larch (*Larix occidentalis*) (Thompson and von Aderkas, 1992). Mature zygotic embryos have also been used for species like redwood (*Sequoia sempervirens*) (Bourgkard and Favre, 1988), white spruce (Tremblay, 1990), and sitka spruce (*Picea sitchensis*) (Krogstrup, 1990).

Seed tissue explants of conifers are typically induced to produce a mass of cells using low osmotic conditions (1-3% sucrose) and plant growth regulators (PGRs), usually 5 μM cytokinin and 10 μM auxin (Attree and Fowke, 1993; Misra, 1994). The only exception to this induction media is with the genus *Abies*, which requires cytokinin as the only PGR (Schuller *et al.*, 1989; Nørgaard and Krogstrup, 1991). In general, spruces and larches yield embryogenic tissues better than pines. To improve pine induction, explants consisting of both zygotic embryo and female gametophyte tissues are often used (Attree and Fowke, 1993). Genotype has also been demonstrated to influence the ability of seed tissues to induce tissue cultures. The geographic source of white spruce seeds significantly affects its ability to induce embryogenic tissue (Tremblay, 1990). In addition to this, the induction of somatic embryogenesis is under strong additive genetic control in white spruce (Park *et al.*, 1993). Optimal induction in white spruce occurs when seed tissues are used from seeds stored for two months at 4°C (Hakman and Fowke, 1987). Initiation has been reported using tissues from seeds stored for as long as 11 years at 3 to 5°C for white spruce (Tremblay, 1990). Black spruce (*Picea mariana)* seeds stored at -18°C for 13 years and red spruce (*Picea*

rubens) seeds stored at -20°C for 20 years have also been used to initiate cultures (Tautorus *et al.*, 1990; Harry and Thorpe, 1991).

Several studies have investigated the use of older tissue sources for somatic embryo induction so as to allow selection of explant sources based on preferred characteristics. Using vegetative tissues as the explant source would provide a tissue culture that is genetically identical to that of the plant from which the explant was collected. Having seeds as the explant source results in a culture that is not genetically identical to the explant, because a seed is fertilized by pollen from another tree. Using cotyledons from 7 to 8 day old white spruce seedlings, Toivonen and Kartha (1988) were able to induce culture lines. Similarly, Krogstrup (1986) induced cultures using 7 day old cotyledons from seedlings of Norway spruce using pretreatment with cytokinin. Attree *et al.* (1990) were able to use shoots and cotyledons from 12 to 30 day old black spruce and white spruce seedlings without cytokinin pretreatment. The age of the explant tissue was further lengthened by Mo and von Arnold (1991), who developed embryogenic cultures from 36 day old Norway spruce seedlings.

The ability to produce callus from established plants was reported by Ruaud *et al.* (1992), who used needles from 14 month old somatic embryo-derived plants of Norway spruce to induce callus. In a more recent study of Norway spruce, Westcott (1994) produced embryogenic callus from buds and needles of trees between 2 and 26 years old. As the age of the source increased, the productivity of the cultures from needle explants decreased (Westcott, 1994). At 26 years of age, bud explants were found to be significantly more productive explants than needles (Westcott, 1994). Chavez *et al.* (1992) also demonstrated callus induction using the pinnae from leaves of mature trees of the cycad, *Ceratozamia*

mexicana. Expanding the ability to use mature tissues from conifer species will significantly improve the ability to select for specific tree characteristics.

A very promising system now being used in combination with somatic embryogenesis is the isolation of totipotent protoplasts (plant cells lacking cell walls), which can be used to induce somatic embryo development. Conifer protoplasts can be isolated from vegetative tissues like cotyledons, needles and roots and will divide in culture to form colonies of cells (Tautorus *et al.*, 1991). Typically, however, in order to get plant regeneration, embryogenic cell suspensions must be used as the source of protoplasts (Tautorus *et al.*, 1991). Gupta and Durzan (1987) first demonstrated conifer somatic embryo production from protoplasts for loblolly pine (*Pinus taeda*) isolated from embryogenic cell suspensions. Isolated protoplasts from embryogenic suspension cultures of white spruce started to divide in 24 h and the first somatic embryos were recovered after 23 days, which later were successfully converted to plants (Attree *et al.*, 1987; 1989a). They later reported improved somatic embryo regeneration from protoplasts isolated from immature zygotic embryos of white spruce (Attree *et al.*, 1989b). More recently, Kunitake *et al.* (1995) successfully regenerated plants from protoplasts isolated from the mesophyll of the upper 4-5 mature leaves of 40 day old prairie gentian (*Eustoma grandiflorum*) plants, offering a new system to use older vegetative tissues for somatic embryo production.

The transfer of desirable genes into protoplasts, which are then used to develop somatic embryos, may improve forestry production as well as provide a useful system to isolate, map and better understand genes and their functions (Tautorus *et al.*, 1991). Protoplasts provide a convenient system for direct gene transfer practices. Electroporation

of DNA into conifer protoplasts has resulted in the expression of the luciferase gene in Douglas-fir and loblolly pine (Gupta *et al.*, 1988). Expression of the chloramphenicol acetyl transferase gene was also reported following electroporation as well as polyethylene glycol (PEG) mediated uptake using protoplasts of white and black spruce (Bekkaoui *et al.*, 1988; Tautorus *et al.*, 1989; Wilson *et al.*, 1989).

Maintaining cultures to allow immature somatic embryos to further develop involves exposure to media that resembles the induction media in that it contains auxin, cytokinin and a low concentration of sucrose (Attree and Fowke, 1993). This step involves the processes of cleavage polyembryony, in which immature somatic embryos form from the mass of embryonal cells (Misra, 1994). Several culture systems can be used to produce large numbers of immature somatic embryos. Flasks which are shaken or agitated are commonly used to maintain cultures, provided sub-culturing is performed before carbohydrates become limiting (Lulsdorf *et al.*, 1992). Liquid cultures in these flasks are prone to rapid changes in embryogenic potential and vitality so a reserve supply of somatic embryos is commonly used to re-establish the liquid culture (Attree and Fowke, 1993). Typically, stationary reserve supplies of somatic embryos are maintained on semi-solidified medium in Petri dishes and must be sub-cultured every 2-4 weeks in order to prevent browning and potential cell death (Attree and Fowke, 1993). Costs involved in keeping these reserve supplies may be reduced by storing them at low temperatures between 0 and 10°C for up to one year as sealed stationary cultures (Joy *et al.*, 1991; Attree and Fowke, 1993). For mass production these cost saving procedures may prove to be valuable to industrial success.

Relatively new systems being used to maintain cultures are mechanically stirred and

airlift bioreactors, both of which are vessels with uniform flows of liquid medium (Tautorus *et al.*, 1991). Bioreactors are expensive to use but are convenient because conditions (temperature, pH and degree of agitation) can be more accurately measured and controlled thus allowing production of a more homogeneous culture (McDonald and Jackman, 1989). Somatic embryos of black spruce and interior spruce (*Picea glauca-engelmanii*), which were produced using bioreactors, showed no signs of sheer stress due to mechanical agitation (Tautorus *et al.*, 1992). Using three bioreactors continuously (approximately seven times a year) can produce approximately 125,000 white spruce somatic embryos and using 25 units continuously can produce approximately one million embryos in a single year (Attree *et al.*, 1994). Using a bioreactor consisting of a flat absorbent pad over liquid culture medium, vigorous desiccation-tolerant white spruce somatic embryos were successfully produced (Attree *et al.*, 1994).

Cryopreservation of cultures in liquid nitrogen also holds potential for maintaining cultures while quality assessments of the somatic embryos and plants derived from these embryos can be made. Typically, embryogenic cell cultures of immature embryos are submerged in liquid nitrogen following treatment with a cryoprotectant combination of sorbitol and dimethylsulfoxide. Kartha *et al.* (1988) precultured white spruce cell cultures in sorbitol and then, following exposure to dimethylsulfoxide, cooled the cultures to -30°C at a rate of $0.3°Cmin^{-1}$ before submerging the cryovials in liquid nitrogen. These cultures produced viable embryos after one year storage. Similar results were found with interior spruce (Cyr *et al.*, 1994) and black spruce (Klimaszewska *et al.*, 1992). Kristensen *et al.* (1994) cryopreserved sitka spruce suspension cultures in liquid nitrogen, but found that only

the cells on the periphery of the embryonic region of the immature embryos survived storage. In an attempt to avoid using cryoprotectants, Attree *et al.* (1995) stored mature white spruce somatic embryos at -20°C for one year and 76-84% of the embryos converted to plantlets. These techniques allow several genetic lines to be preserved until needed to mass produce embryos.

Somatic embryo maturation involves the application of abscisic acid (ABA) and raised osmotic concentrations (Attree and Fowke, 1993). Frequently other PGRs may be included in this maturation media to improve development (Attree and Fowke, 1993). Often prior to exposing immature embryos to ABA, the embryos are pretreated for one week with 1-3% sucrose and activated charcoal to reduce auxin and cytokinin levels (Becwar *et al.*, 1987; 1989; Roberts *et al.*, 1990a; 1990b). In order to produce fully mature embryos it is necessary to use ABA to prevent or slow down cleavage polyembryogenesis, resulting in developmentally synchronized somatic embryos that are receptive to ABA (Attree and Fowke, 1993; Gupta *et al.*, 1993; Misra, 1994). A reduction in the auxin concentration may be responsible for this, but some studies indicate that cytokinin may still be required during early stages of maturation (Attree and Fowke, 1993).

Abscisic acid has many roles in embryo maturation. In zygotic embryo development, ABA accumulates during the mid and late stages of seed development preventing precocious germination (Kermode, 1990). Genes responsive to ABA are induced to transcribe mRNAs responsible for the accumulation of storage reserves (proteins, lipids, and starch) as well as late embryogenesis abundant (LEA) proteins, which are believed to have a role in desiccation tolerance (Skriver and Mundy, 1990). In comparison to the role of ABA in zygotic embryo

development, ABA shows the same effects on storage product accumulation in somatic embryos (Hakman *et al.*, 1990; Roberts *et al.*, 1990a; Misra *et al.*, 1993). Initially, ABA concentrations around 8-12 μM were used for conifer somatic embryo production (Becwar *et al.*, 1987; 1989; Hakman and von Arnold, 1988). It has been found, however, that somatic embryos tend to lose sensitivity to ABA during maturation so more recent protocols use ABA levels as high as 40 μM in order to maintain cultures longer without precocious germination (Attree and Fowke, 1993). Several other factors affect the levels of ABA required and consequently each genotype for a species and each culture procedure must be individually tested to find the optimal ABA levels.

The type of osmoticum used in combination with ABA has been shown to greatly affect somatic embryo development. Often sucrose was used as the osmoticum but higher molecular weight osmotica like PEG 4000 and dextrans have been used to improve embryo development (Attree and Fowke, 1993). Two desired outcomes of maturation are to stimulate storage product accumulation and to lower tissue water content so as to produce somatic embryos more like desiccated zygotic embryos. Low molecular weight osmotica, like sucrose, cross the cell walls causing water loss from the living part of the cell, leading to plasmolysis (Attree *et al.*, 1991; Attree and Fowke, 1993). Over long exposure times the sucrose will be absorbed by the living part of the plant cell, which stimulates water re-entry (deplasmolysis or osmotic recovery) resulting in no reduction in the water content (Attree *et al.*, 1991; Attree and Fowke, 1993). Polyethylene glycol 4000 and dextrans are large enough that they do not enter the cell wall of cells in somatic embryos, since the permeability limit of the cell wall is 30 Å (Attree *et al.*, 1995). Thus turgor pressure in the symplast is reduced by

these osmotica and no plasmolysis or osmotic recovery is observed (Attree *et al.*, 1991; Attree and Fowke, 1993). The elimination of solute accumulation within the cell also reduces the toxic effects associated with solute build-up that occurs when permeating osmotica are used (Attree *et al.*, 1991; Attree and Fowke, 1993).

Maturation of white spruce somatic embryos with PEG 4000 and ABA has resulted in improved embryo quality (Attree *et al.*, 1991; 1992; 1994; 1995; Misra *et al.*, 1993; Leal *et al.*, 1995). While maturation with permeating osmotica, such as sucrose, resulted in the absence of some crystalloid and matrix proteins in protein bodies, somatic embryos produced with PEG 4000 resulted in the production of these proteins and tripled the total protein content per mg tissue (Joy *et al.*, 1991; Misra *et al.*, 1993). Polyethylene glycol 4000 also increased dry weights while decreasing moisture contents (MCs) and improved the maturation frequency 3-fold (Attree *et al.*, 1991). Using PEG 4000 also increased 9-fold the levels per embryo of the major storage lipid, triacylglycerol, to levels five times higher than in a single zygotic embryo (Attree *et al.*, 1992). A combination of ABA and PEG 4000 was found to be more optimal in reducing precocious germination then use of ABA or PEG 4000 alone (Attree *et al.*, 1991).

The final step in producing highly viable somatic embryos is to dry the embryos down to moisture levels similar to zygotic embryos in dry seeds. Seed drying is required to switch seeds from the processes involved in maturation to those involved in germination, but full drying is not necessarily required (Bewley and Black, 1985; Kermode, 1990; Attree and Fowke, 1993). Late embryogenesis abundant proteins are now considered to produce desiccation tolerance in embryos and LEA transcripts have been found in the late stages of

white spruce somatic embryo maturation (Skriver and Mundy, 1990; Leal and Misra, 1993). Both partial and full embryo drying have been found to improve germination and plant recovery from conifer somatic embryos. Partial drying of mature interior spruce somatic embryos at high (> 95%) RH resulted in improved germination frequency, improved seedling root and shoot elongation, and decreased germination times (Roberts *et al.*, 1990b). Partial drying, which resulted in successful germination, has also been reported for white spruce somatic embryos (Kong and Yeung, 1992). Full drying of white spruce somatic embryos to water levels below those of zygotic embryos has been achieved using a two step drying procedure (Attree *et al.*, 1991; 1992; 1994; 1995). Maturation with ABA and PEG 4000 followed by drying in RH environments (starting at 81% and finishing at 43%) resulted in major decreases in moisture levels (Attree *et al.*, 1995). Several studies have also found that improvements in treatments that promote storage reserve accumulation also promote desiccation tolerance (Attree and Fowke, 1993).

Germination and plant growth from somatic embryos has been reported for many species. Conifer somatic embryos have typically germinated using half strength PGR-free media containing 2-3% sucrose (von Arnold and Hakman, 1988; Becwar *et al.*, 1989; Attree *et al.*, 1995). Embryos on the filter paper are imbibed approximately one week under low light and then regenerating plantlets are manually separated and further maintained under low light in the same media combination as above (Attree *et al.*, 1995). Once the plantlets have well developed roots they are transferred to soil for further growth. Attree *et al.* (1994) reported that 80% of the white spruce somatic embryos produced in Petri dishes and 92% of the embryos produced in bioreactors successfully converted to plants. It is, however, not

clear whether the germination media fully replaces the role of the female gametophyte in a seed (Cyr *et al.*, 1991).

With the development of better drying regimes, the germination and plantlet recovery frequencies have been greatly improved. Plantlets derived from somatic embryos have now been established on soil for many species. Seedlings derived from somatic embryos have now been planted in field tests and reforestation pilot projects are underway to reforest large areas with these seedlings. The final step needed to produce artificial seeds is to package the somatic embryos in a manner mimicking the female gametophyte and seed coat. These seed parts act as protection for zygotic embryos by slowing down imbibition, resulting in less swelling damage to the embryo. Somatic embryos lack this protection and are thus prone to greater imbibitional damage. Coatings could provide physical protection while supplying nutrients, antibiotics, fungicides and PGRs (Attree and Fowke, 1993). Several attempts to encapsulate hydrated angiosperm somatic embryos with hydrogels like sodium alginate were first reported by Redenbaugh *et al.* (1991). Hydrated Norway spruce somatic embryos encapsulated in 2-3% sodium alginate germinated at a frequency of 90% (Fourré *et al.*, 1991). Attempts to encapsulate white spruce somatic embryos in non-hydrated water soluble compounds allowed somatic embryos to be desiccated and regenerated in a controllable manner (Attree and Fowke, 1993). In order to properly develop an artificial seed, more information about the mineral nutrition in natural seeds must be obtained to allow the production of synthetic seeds with equivalent mineral nutrient supplies.

Objectives

The goals of this project were to investigate various aspects of mineral nutrient storage in white spruce seeds and somatic embryos as well as to study imbibitional damage and potassium leakage during imbibition. This thesis consists of the following studies:

1) A scanning electron microscopy and light microscopy study to introduce the reader to the tissue arrangements in somatic embryos. This light microscopy survey was compared to previous observations of white spruce zygotic embryos and female gametophytes (Reid, 1996). Included in this chapter will be an image analysis study of somatic embryos, which was used to develop a selection criterion for somatic embryos. Also included are the measurements of MC in somatic embryos and various parts of white spruce seeds (Chapter 2).

2) Measurement of total phosphorus in somatic embryos produced using typical maturation media and altered maturation media, as well as, in various parts of seeds. Measurements of the amount of phosphorus bound to phytic acid in these same somatic embryos and seed parts were done (Chapter 3).

3) The use of transmission electron microscopy and energy dispersive x-ray microanalysis to study the mineral nutrient composition of globoids (phytate deposits in protein bodies) and Fe-rich particles (believed to be Fe-associated phytate deposits in plastids) from various regions and tissues of somatic embryos. These findings were compared to globoid and Fe-rich particle compositions in white spruce seeds (Reid, 1996) (Chapter 4).

4) Measurement of total potassium, magnesium, calcium, iron and zinc in somatic embryos and various seed tissues using atomic absorption spectroscopy (Chapter 5).

5) Study of potassium leakage and surface damage to somatic and zygotic embryos during imbibition. Potassium leakage was measured using atomic absorption spectroscopy and surface damage observed using an environmental scanning electron microscope (ESEM). The effects of pretreating somatic embryos in a high RH environment on potassium leakage were investigated (Chapter 6).

6) Conclusion and summary of the key findings in this thesis (Chapter 7).

Abbreviations

AAS - atomic absorption spectroscopy

ABA - abscisic acid

DW - dry weight

EDX analysis - energy dispersive x-ray analysis

ESEM - environmental scanning electron microscope

HCl - hydrochloric acid

HNO_3 - nitric acid

H_2O_2 - hydrogen peroxide

H_2SO_4 - sulfuric acid

LEA proteins - late embryogenesis abundant proteins

LV medium - Litvay's medium

MC - moisture content

PA-P - phytic acid-phosphorus

P/B - peak-to-background

PEG - polyethylene glycol

PGR - plant growth regulator

RH - relative humidity

SEM - scanning electron microscope

STEM - scanning transmission electron microscope

TCA - trichloroacetic acid

CHAPTER 2:

SCANNING ELECTRON MICROSCOPY, LIGHT MICROSCOPY, IMAGE ANALYSIS AND MOISTURE CONTENT OF WHITE SPRUCE SEEDS AND SOMATIC EMBRYOS

Introduction

A conventional scanning electron microscope (SEM) is designed for viewing surface details of a sample. In an SEM, the electron beam is focused onto a small spot, which is then scanned over the specimen surface to produce an image of the surface (Hayat, 1978). As electrons from the electron beam interact with the specimen; some electrons are inelastically scattered, which produces secondary electrons (Newbury *et al.*, 1986). Secondary electrons are produced when loosely-bound electrons on the surface of the sample, in a region called the conduction-band, are ejected by the incoming electrons from the electron beam (Goldstein *et al.*, 1981). The energy transfer in the conduction-band is relatively low, typically in the range of 1 to 50 eV (Newbury *et al.*, 1986). Due to this low energy of the secondary electrons, secondary electrons cannot escape from deep inside the tissue and are therefore only released from approximately the outermost 5 to 10 nm of the sample (Hayat, 1978; Newbury *et al.*, 1986). In this way only the surface details are seen in the image, producing an image that appears 3-dimensional.

Biological samples possess some characteristics that must be accounted for when using an SEM. Many biological specimens are hydrated and when placed into the high vacuum chamber of an SEM the cells collapse due to water evaporation, which can distort

and damage the sample. To avoid this damage, specimens can be rapidly frozen to reduce ice crystal formation or the specimen can be dehydrated. Another characteristic of biological specimens is that they are electrical insulators and thus conduct electricity poorly (Hayat, 1978). Due to this property, negative charges accumulate on the surface of the sample, which causes an intensely bright image due to electrical charging (Hayat, 1978). In order to eliminate or reduce charging to tolerable levels; samples are coated with a thin film of metal, which acts as a ground to conduct away the negative charge (Hayat, 1978; Goldstein *et al.*, 1981). Additional advantages of metal coating are an increased production of secondary electrons and decreased specimen damage from the electron beam (Hayat, 1978).

A common method of applying this metal coating is with a sputter-coater. Bombardment of a metal plate with energetic particles (like ionized argon atoms) results in metal ions being ejected from the plate at random angles, coating the entire surface of the specimen (Goldstein *et al.*, 1981). Several metals have been used for coating. Gold is commonly used because it gives a high level of secondary electron discharge, can be obtained in a pure form, and is fine grained so that the sample surface is not distorted (Hayat, 1978).

In addition to studies on surface details, light microscopy is often used to obtain information on general cell arrangements and cellular structures. The sample is either viewed in its natural state or is fixed and/or embedded prior to sectioning. A vast number of organelle and compound specific stains have been utilized. A common stain used is toluidine blue. Toluidine blue is a metachromatic stain, which refers to the fact that some tissue structures will stain a colour that is different from the colour of the dye (O'Brien and McCully, 1981). With toluidine blue stain; red and purple colours are thought to be formed

due to the stacking of dye ions, which are bound together by water molecules (O'Brien and McCully, 1981). As more dye is bound as stacked aggregates, the colour of the structure shifts towards the red end of the visible light spectrum (O'Brien and McCully, 1981). Due to different binding sites and spaces for dye stacking within different cell structures, toluidine blue is very useful for distinguishing various cellular structures (O'Brien and McCully, 1981).

In this study, scanning electron microscopy and light microscopy were used to introduce the reader to the tissue arrangements and general morphologies of white spruce somatic and zygotic embryos. Toluidine blue was used to stain light microscopy sections because it stains the storage proteins of protein bodies, which are protein plus mineral nutrient storage organelles. Globoids, spherical mineral nutrient deposits within protein bodies, stain differently than the protein body matrix and therefore can be distinguished. The composition of globoids will be dealt with in more detail in Chapters 3 and 4. In addition, image analysis of somatic embryos was used to develop the selection criteria for choosing somatic embryos of similar size to allow the elimination of very large or small embryos. Lastly, the moisture contents of white spruce somatic embryos and various parts of white spruce seeds were measured.

Materials and Methods

Seed Source

White spruce (*Picea glauca*) seeds and somatic embryos were obtained from Dr. L.C. Fowke of the Department of Biology at the University of Saskatchewan. Seeds were collected from the Big River and Christopher Lake regions north of Saskatoon, Saskatchewan. Seed coats were removed and zygotic embryos were excised using fine forceps.

Various batches of somatic embryos were prepared as outlined by Attree *et al.* (1994; 1995) and shipped on the filter paper supports in plastic Petri dishes. The basal medium used was that described by Litvay *et al.* (1981) at half-strength (0.5 LV) and supplemented with 250 mg/l glutamine and 500 mg/l casein hydrolysate. Suspension cultures of immature somatic embryos were maintained in 0.5 LV medium containing 1% sucrose and PGRs (9 μM 2,4-dichlorophenoxyacetic acid and 4.5 μM benzyladenine). These suspension cultures were established from agar cultures of immature somatic embryos, which had been established using zygotic embryos as the explant tissue source. The suspension cultures were then precultured for one week in 0.5 LV medium, 3% sucrose and PGRs at 0.20 strength.

The precultured immature somatic embryos were washed, resuspended (20% w/v) in medium lacking PGRs and spread evenly over filter paper supports (Whatman no. 2) on top of development medium in Petri dishes. The embryos were developed using 0.5 LV medium with 3% sucrose, 7.5% (w/v) PEG 4000 (Fluka Chemical Corp.), 0.8% Difco Bitek agar (Canlab, Mississauga, Ontario), and 20 μM autoclaved ± racemic ABA (Sigma Chemical

Co.). The plated embryos were kept in the darkness for approximately 8 weeks to mature. After fully developing, the embryos were dried for 4 weeks in open Petri dishes in a 63% RH environment as done by Attree *et al.* (1991).

In addition to these somatic embryos, several batches of embryos were produced with maturation media containing various levels of *myo*-inositol and sucrose to investigate the effect of the treatments on levels of total P and PA-P in somatic embryos. Normally the maturation media contains 0.005% *myo*-inositol and 3% sucrose. The four treatments were produced by altering both *myo*-inositol and sucrose concentrations to take into account osmotic conditions. These four treatments were produced in four separate runs with each run consisting of one plate for each treatment condition. The treatments were done using the following media compositions: 0% *myo*-inositol plus 3% sucrose, 0.15% *myo*-inositol plus 2.5% sucrose, 0.3% *myo*-inositol plus 2.0% sucrose, and 0.6% *myo*-inositol plus 1.5% sucrose.

Scanning Electron Microscopy

White spruce somatic embryos and zygotic embryos were attached to aluminum stubs using double-sided tape. Samples were then gold coated using a Polaron sputter coating unit E 5100 (Polaron Equipment Ltd., Watford, England) and viewed using an ISI model DS130 SEM (International Scientific Instruments, Inc., Santa Clara, CA).

Light Microscopy

Somatic embryos were fixed in 5% glutaraldehyde in 0.2 M pH 7.0 phosphate buffer for 3 h. Following fixation, embryos were washed with 0.2 M pH 7.0 phosphate buffer for 1 h and then dehydrated through a graded ethanol series (20, 40, 60, 80, 90, 95, and 100% ethanol) for 20 to 30 min. per concentration. Infiltration was carried out overnight at room temperature using catalysed Solution A from a JB-4 embedding kit (Polysciences, Warrington, PA). Samples were then placed into molds and filled with an embedding solution consisting of a 40:1 ratio of catalysed Solution A:Solution B from the JB-4 embedding kit. Aluminum chucks were placed in the molds and sealed with hot wax. The chucks were filled with the embedding solution and the resin was polymerized for 3 h at room temperature.

Using a JB-4 Porter-Blum microtome (Sorvall, Norwall, CT), dry sections 3 μm thick were cut using glass knives and the sections were placed on warm water to flatten out. Sections were collected onto glass slides, dried on a slide warmer for several min. and placed in a 65°C oven overnight. Sections were stained for 4 min. with 1% toluidine blue solution, washed for 1 min. with distilled water and air dried. Cover slips were fixed to the slides using Montant DPX and air dried. Using a camera on a Carl Zeiss RA light microscope (Carl Zeiss, West Germany) pictures were taken.

Image Analysis

To develop a standard selection process for using somatic embryos of reasonably uniform size, 100 somatic embryos were randomly selected from a typical plate and used for image analysis. Using graph paper with a square of known dimensions, an image was

collected using a video camera (MTI-65, Dage-MTI Inc., Michigan City, Ind.) mounted on a copy stand. This image was transferred to a PGT IMIX-II computer system (Princeton Gamma-Tech., Princeton, NJ) and numbered points were placed on all four corners of the square image. A calibration file was then created by using a calibration program to indicate the correct measurements of the square.

Once calibrated, the 100 somatic embryos were laid out on a black background so that no two embryos were touching. Using the same video camera in the same position, an image of the 100 embryos was collected. This image was transferred to the PGT IMIX-II computer system as a grey-tone digital image and the brightness and contrast were adjusted accordingly. Using a painter program the image was converted to a binary colour image using grey-level conversion. With this binary colour image the mean, minimum, maximum, median and standard deviation for the length of the embryos was measured using a feature analysis program. Embryos within 1.5 standard deviations of the average length were used for all the experiments reported in this thesis. This selection procedure provided a sufficient quantity of embryos to study while still eliminating extremely large and small embryos.

Moisture Content

Aluminum weighing pans were heated in an oven (Blue M Electric Company, Blue Island, Illinois, USA) and cooled in a desiccator before weighing. Sample sizes used were: 180 zygotic embryos, 180 female gametophytes, 80 somatic embryos and 50 whole seeds. Each of the above samples were done in triplicate. The corresponding female gametophytes from the seeds used to make one sample of zygotic embryos were used to make one female

gametophyte sample. Whole seeds were cut in half to allow moisture release from the tissues enclosed by the hard seed coats. Samples were weighed in dry aluminum pans and placed in the oven at 85 ± 2 °C. Weights were taken at 1, 2, 3 and 24 h intervals, until a constant weight was obtained on at least two consecutive measurements. Using the formula of Allen *et al.* (1974), the MCs were determined by dividing the loss in weight on drying (g) by the initial sample weight (g) and multiplying by 100. Values for seeds without seed coats were calculated by combining the value for each sample of zygotic embryos with the value for the corresponding female gametophytes. Statistical differences between means were determined using the MINITAB analysis of variance test. When a difference was found, Tukey's test (Zar, 1984) was used to determine which means differed at $P > 0.05$.

Results

Light Microscopy and Scanning Electron Microscopy

White spruce somatic embryos were shipped on filter paper. Often, on a single filter paper, several hundred somatic embryos were densely packed (Fig. 2). Typically, somatic embryos had six cotyledons but embryos were found with five or seven cotyledons. Comparison of somatic embryos to various parts of a seed revealed that somatic embryos are often much larger than zygotic embryos and female gametophytes (Fig. 3). Surrounding the female gametophyte of a white spruce seed is a dark brown seed coat (Fig. 3).

Somatic embryos can easily be distinguished from zygotic embryos in that somatic embryos have a flared arrangement of the cotyledons and a prominent suspensor region, which is equivalent to the smaller root cap in a zygotic embryo (Fig. 4). In somatic embryos, the cotyledons are rounded in cross-section and do not cover the shoot apex (Fig. 5); whereas, in zygotic embryos the cotyledons are more triangular in cross-section and are densely packed together to protect the shoot apex (Fig. 6). In Fig. 6, the cotyledons have been pulled back a little due to mechanical disruption during specimen preparation. Since somatic embryos are produced in tissue culture, embryos at slightly different stages of maturation can be present on a single plate. Figure 7 illustrates a somatic embryo that was in the process of cotyledon fission when the growth of the cultured embryos was stopped and desiccation begun. With somatic embryos produced using more refined purification protocols, these less mature embryos are largely eliminated from the plates.

In white spruce somatic embryos there are three main tissue regions: protoderm,

ground meristem and procambium (Fig. 8). The protoderm is a single cell layer of rectangular cells that surrounds the entire embryo. Inside the protoderm is the ground meristem, which consists of multiple layers of oval-to-square cells in the plane of section. Finally, the core of the embryo consists of multiple layers of rectangular cells in the plane of section, which are elongated in the plane of the hypocotyl-root axis. This procambium extends from within a few cells of the tips of the cotyledons down to the root apex region. The same tissue regions were also present in white spruce zygotic embryos (Fig. 9) (Reid, 1996). Frequently, ground meristem cells in zygotic embryos were very uniform in size, were in discrete rows and had few intercellular spaces (Fig. 9). In somatic embryos, however, ground meristem cells were frequently divided in numerous directions and many intercellular spaces were observed (Fig. 8).

The protoderm of a somatic embryo often contained a number of protein bodies with no evident globoids (Fig. 10). The protoderm of a zygotic embryo also contained protein bodies that appeared to lack globoids (Fig. 11) (Reid, 1996). Often the ground meristem just inside the protoderm contained protein bodies with prominent globoids in zygotic embryos (Fig. 11); whereas in somatic embryos, protein bodies in the first rows of ground meristem contained few if any identifiable globoids (Fig. 10).

The ground meristem was the tissue that differed the most between the two embryo types. In zygotic embryos, the ground meristem contained cells with many protein bodies having prominent globoids (Fig. 9). In somatic embryos, ground meristem cells tended to have fewer protein bodies displaying prominent globoids (Fig. 12). In addition, ground meristem cells from somatic embryos had larger translucent regions within the cell, which may

represent large lipid deposits or fixation artifacts (Fig. 12).

The procambium of somatic embryos (Fig. 13) closely resembled that found in zygotic embryos by Reid (1996). These cells had no intercellular spaces and contained significant numbers of protein bodies, but the number of globoid-containing protein bodies was much less than in the ground meristem.

Image Analysis and Moisture Content

The average length per somatic embryo was 2.91 mm and the median length was 2.84 mm. The minimum length was 1.81 mm and the maximum length was 5.21 mm. The standard deviation for length was 0.70 mm. Therefore the range of sizes of somatic embryos used for all subsequent experiments was 1.86 mm to 3.96 mm in length (1.5 standard deviations above and below the mean length).

Mean MC values are given in Table 1. Somatic embryos had significantly higher MC values than any part of the white spruce seeds. The tissues within a seed had very similar MC levels with the innermost tissue of a seed (the zygotic embryo) having the highest MC. The large seed coats had the lowest MC as shown by the difference between the values for seeds without seed coats and whole seeds.

Figure 2: Culture Plate of Mature Desiccated White Spruce Somatic Embryos. Note the dark yellow embryos of variable sizes within one plate. Scale bar = 2 mm.

Figure 3: White Spruce Somatic Embryo and Various Parts of White Spruce Seeds. From left to right: whole seed, female gametophyte (seed without seed coat), zygotic embryo and somatic embryo. Scale bar = 1 mm.


2


3

Figures 4 to 7: Conventional Scanning Electron Micrographs of White Spruce Somatic and Zygotic Embryos.

Figure 4: Micrograph of a somatic embryo (left) and a zygotic embryo (right). Note that the somatic embryo has flared cotyledons (C), a long hypocotyl (H) and a distinct suspensor region (S). Zygotic embryos have closely appressed cotyledons (C). Scale bar = 500 μm.

Figure 5: Flared array of cotyledons of a somatic embryo with an exposed shoot apex. The cotyledons are rounded and surround the shoot apex, which has a crack likely due to handling during specimen preparation. Scale bar = 200 μm.

Figure 6: This micrograph shows the triangular-shaped cotyledons of a zygotic embryo due to the dense packing of the cotyledons. The shoot apex is not visible in a zygotic embryo. Scale bar = 150 μm.

Figure 7: Micrograph of a white spruce somatic embryo demonstrating cotyledon fission. Note that the tips of each of the two newly forming cotyledons (asterisks) are now visible. Also the cotyledons are not yet spread apart far enough to fully reveal the shoot apex surface. Scale bar = 200 μm.

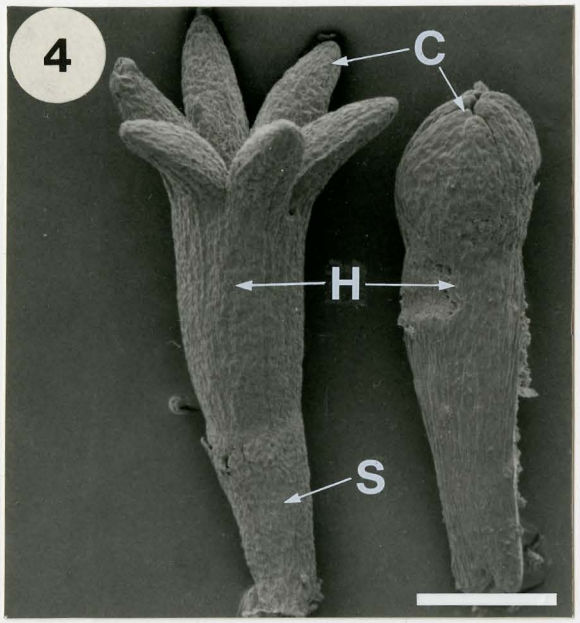
4
C
H
S

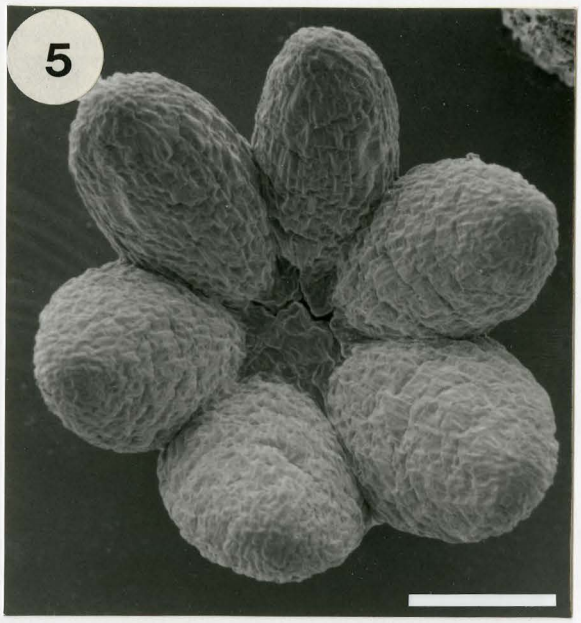
5

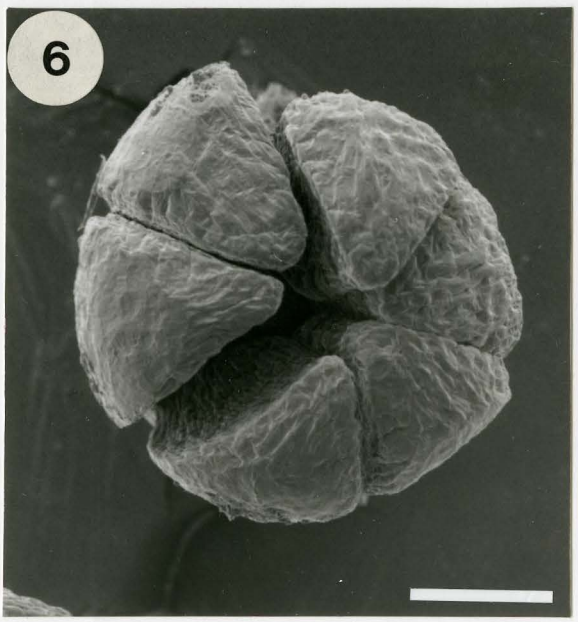
6

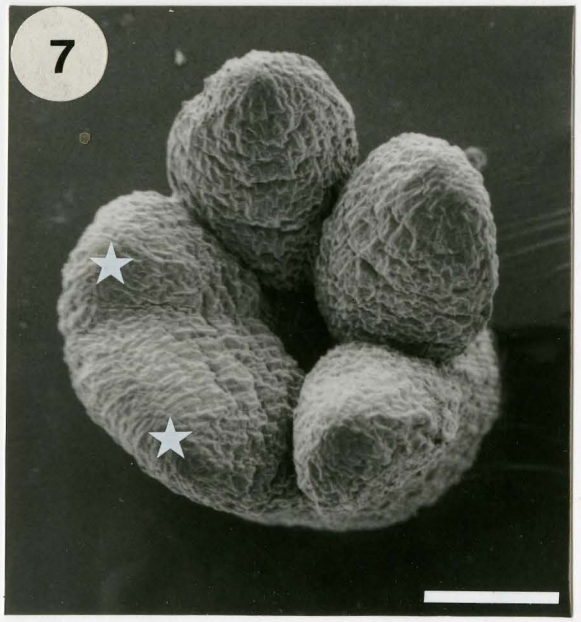
7

Figures 8 to 13: Light Micrographs of Sections from White Spruce Somatic Embryos Compared to Light Micrographs of White Spruce Zygotic Embryos, Taken From Reid (1996).

Figure 8: Hypocotyl of a somatic embryo. Note the three tissue regions: protoderm (Pt), ground meristem (Gm) and procambium (Pc). Also note the protein bodies (P), intercellular spaces (I) and dark nuclei (N). Scale bar = 150 μm.

Figure 9: Cotyledon of a zygotic embryo. Note the three tissue regions: protoderm (Pt), ground meristem (Gm) and procambium (Pc). Protein bodies (P) are visible with translucent globoids (G). Scale bar = 50 μm.

Figure 10: Protoderm in the hypocotyl of a somatic embryo. This micrograph shows protoderm cells (Pt) and ground meristem cells (Gm). Protein bodies (P) in the protoderm lack globoids and the first few rows of ground meristem cells have no visible globoid-containing protein bodies in this micrograph. Scale bar = 20 μm.

Figure 11: Zygotic embryo protoderm from the hypocotyl region. In this micrograph the protein bodies (P) in the protoderm (Pt) have no globoids, but the protein bodies in the ground meristem (Gm) have distinct globoids (G). Scale bar = 20 μm.

Figure 12: Ground meristem cells from the hypocotyl of a somatic embryo. This micrograph shows ground meristem cells that are almost completely divided. These cells contain protein bodies with distinct globoids (G). Also note the large intercellular spaces (I) in the ground meristem region. Scale bar = 20 μm.

Figure 13: Procambial cells from the hypocotyl of a white spruce somatic embryo. These rectangular cells have numerous protein bodies (P), but no globoid-containing protein bodies are visible in this micrograph. Scale bar = 20 μm.

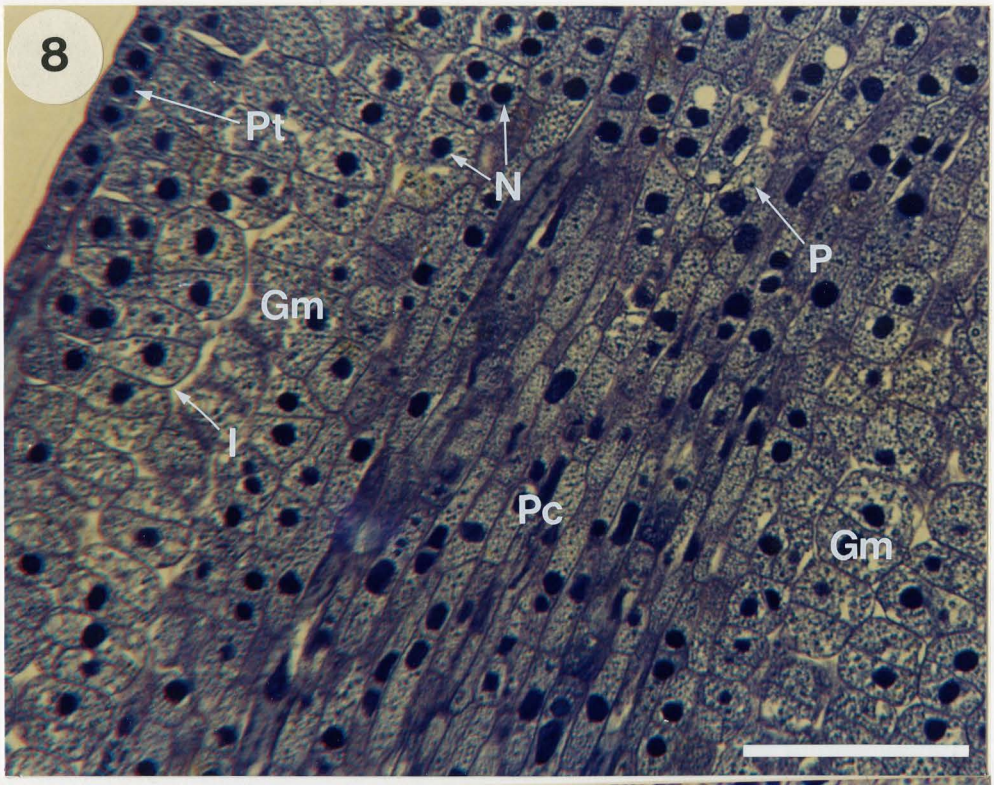
8
Pt
N
P
Gm
I
Pc
Gm

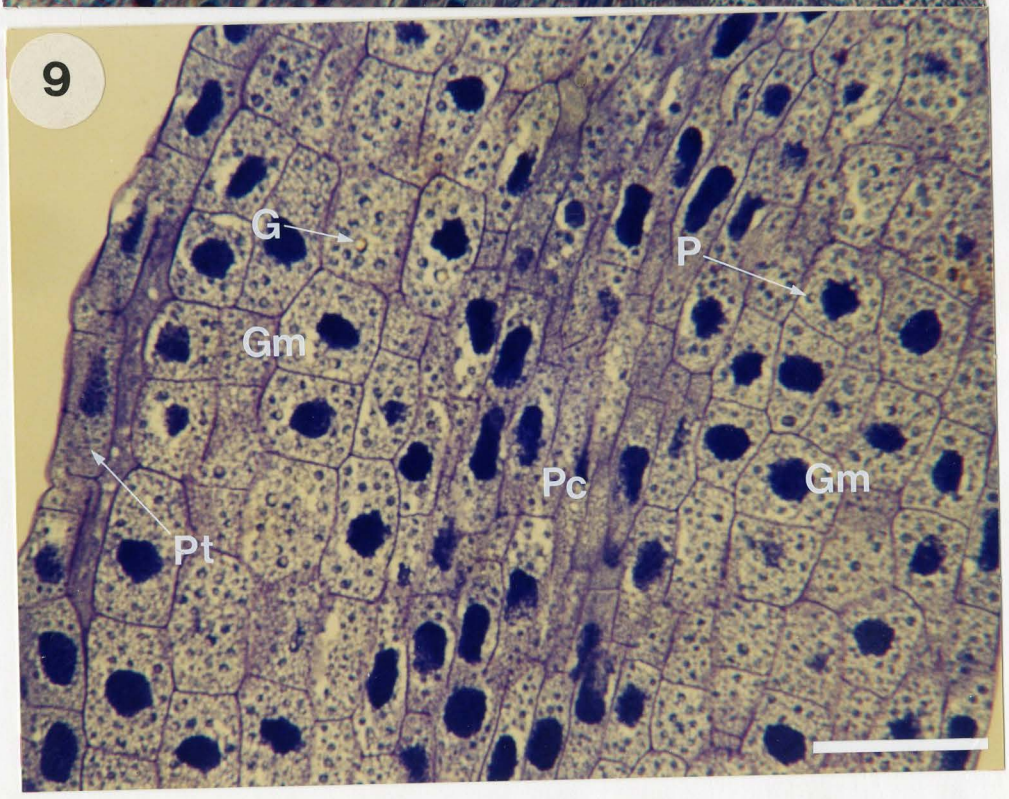
9
G
P
Gm
Pc
Gm
Pt

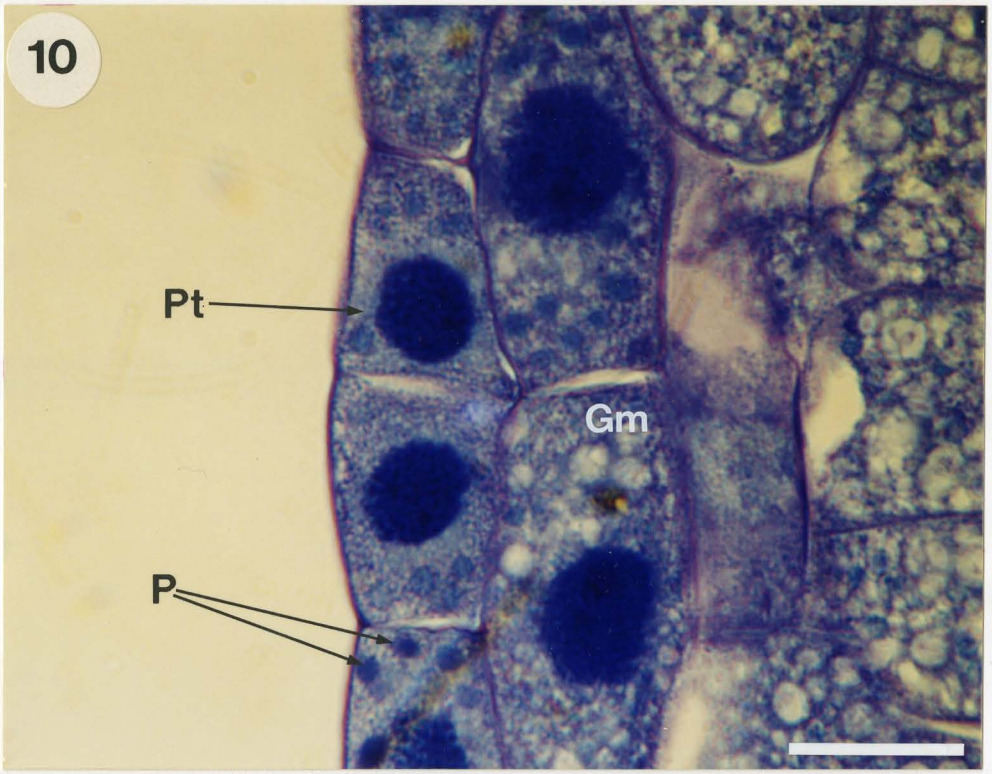
10
Pt
Gm
P

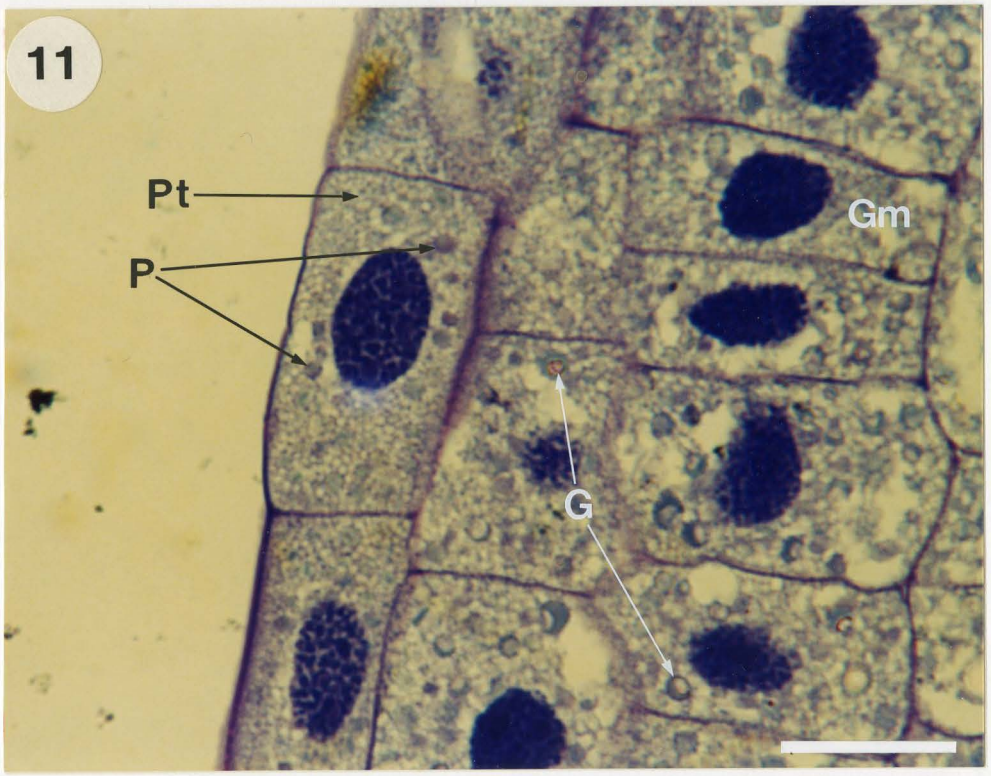
11
Pt
P
Gm
G

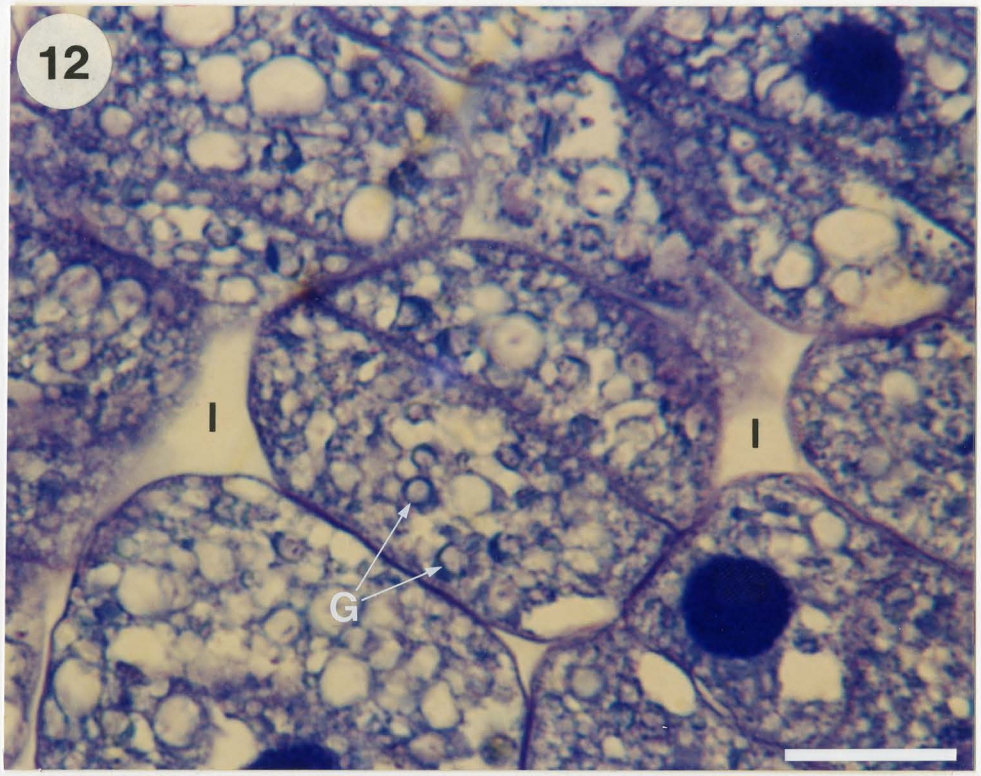
12
I
I
G

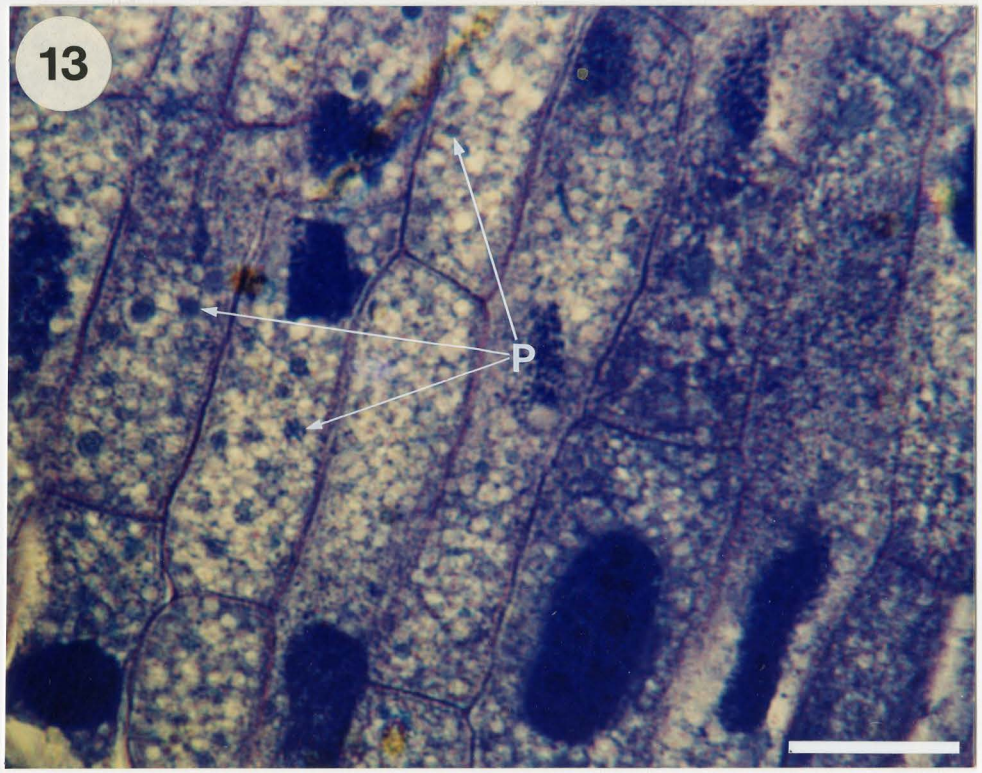
13
P

Table 1: Mean moisture content (±SD) for white spruce somatic embryos, zygotic embryos, female gametophytes, seeds without seed coats and whole seeds at 85 ± 2 °C.

Sample	Number per Sample	Mean Moisture Content (%)
Somatic Embryos	80	7.66 ± 0.17 **a**
Zygotic Embryos	180	4.76 ± 0.12 **b**
Female Gametophytes	180	4.42 ± 0.25 **bc**
Seeds Without Seed Coats	180	4.46 ± 0.22 **bc**
Whole Seeds	50	4.19 ± 0.06 **c**

Note: Each mean was calculated using three values. Each MC followed by the same letter is not significantly different at $P > 0.05$. Values for seeds without seed coats were calculated using values for zygotic embryos and female gametophytes.

Discussion

Seeds of white spruce consist of a hard outer seed coat (or testa) covering the female gametophyte, which in turn surrounds the zygotic embryo (Bewley and Black, 1985). The seed coat acts as a protective barrier and it imposes dormancy on the zygotic embryo by providing mechanical restraint on embryo growth (Downie and Bewley, 1996). Within the seed, the zygotic embryo is partly separated from the female gametophyte by a small cavity called the corrosion cavity. During germination, nutrients liberated from the female gametophyte are released into this cavity and absorbed by the embryo (Maheshwari and Singh, 1967). Often, due to inadequate pollen exposure, white spruce seeds are found lacking zygotic embryos and the percentage of seeds that germinate varies from year to year (Owens and Molder, 1979; Caron *et al.*, 1993). For these reasons, production of large numbers of somatic embryos offers a potentially more efficient way of producing seedlings for reforestation practices than by using seed collection methods. The somatic embryos used for this thesis had a 100% germination frequency (Stephen Attree, personal communication).

Light microscopy and scanning electron microscopy have been previously used to compare zygotic and somatic embryos of various species. Comparisons of angiosperm zygotic and somatic embryos, like alfalfa (*Medicago sativa*), using an SEM have revealed significant morphological differences during development (Xu and Bewley, 1992). Light microscopy and scanning electron microscopy comparisons of white spruce zygotic and somatic embryos have found that the general morphology and anatomy of these two types of embryos are very similar (Attree *et al.*, 1992; Fowke *et al.*, 1994). Although morphological and anatomical similarities of white spruce somatic and zygotic embryos have been previously

published, repeating these structural investigation techniques can be very useful when discussing general structures and tissues present in these embryos. Also, it is important to repeat these studies to observe any morphological changes that may occur as the culturing system for somatic embryos is improved.

Scanning electron microscopy in this current study found many similarities between white spruce somatic and zygotic embryos, but some distinct differences were also found. Zygotic embryos had cotyledons that were tightly packed together; whereas, somatic embryos had a flared array of cotyledons. This difference in cotyledon arrangement has commonly been used as a morphological feature in distinguishing between conifer somatic and zygotic embryos. Recent advances in culturing white spruce somatic embryos in bioreactors have resulted in the production of smaller somatic embryos that have closed cotyledon arrangements resembling zygotic embryos (Stephen Attree, personal communication). Occasionally, somatic embryos at various stages of development can be present on the same culture plate. Embryos with cotyledons in the process of developing sometimes were found on the plates used here. The emergence of two cotyledons as one large structure, which then splits, has been previously reported for white spruce somatic embryos (Fowke *et al.*, 1994).

In addition to the cotyledon arrangement, white spruce somatic embryos were different from zygotic embryos in that somatic embryos had a prominent suspensor region. Conifer zygotic embryos have an analogous region called the root cap, which is not as prominent as the suspensor of a somatic embryo. In somatic embryos, this suspensor region was often approximately 1/3 of the length of the hypocotyl-root axis of the embryo. This long suspensor region on a somatic embryo represents the point where the embryo develops from

the callus and is likely so large due to the fact that these embryos develop from a relatively large mass of callus.

Using light microscopy, somatic embryos were found to have three tissue types: protoderm, ground meristem and procambium. These same tissue regions have been described in detail for zygotic embryos of white spruce (Owens and Molder, 1979; Krasowski and Owens, 1993; Reid, 1996). Cells within these tissue regions from the two types of embryos generally were similar in shape and had similar protein bodies.

One difference between the two types of embryos was the presence of large intercellular spaces in the ground meristem of somatic embryos. These intercellular spaces are very prominent during development and likely result from the absence of mechanical resistance during somatic embryo development (Kong and Yeung, 1992). Desiccation of white spruce somatic embryos has been shown to significantly reduce these intercellular spaces (Kong and Yeung, 1992). As seen here, mature desiccated somatic embryos still have considerable intercellular spaces.

A second difference found using light microscopy was with the pattern in which cell division had taken place in the ground meristem. Somatic embryos had cell arrangements due to cells dividing in various planes of division and occasionally cells adjacent to one another had divided in very different planes. Again this is likely due to the absence of mechanical restraint in somatic embryo development, which allows the embryos to expand in length to produce larger embryos. Zygotic embryo ground meristem tissue had been formed by more uniform patterns of division with distinct rows of cells arranged parallel to the hypocotyl-root axis (Reid, 1996). In general, white spruce somatic embryos are anatomically very similar to

zygotic embryos in spite of these few differences.

Desiccation of seed tissues is believed to result in the switch from the pattern of gene expression in the developmental processes to the pattern of gene expression associated with the processes of germination (Bewley and Black, 1985; Kermode and Bewley, 1985). In this study, white spruce seeds had MC's less than 5% and somatic embryos had MC's of 7.66%. Similar MC's for somatic embryos of white spruce were reported by Attree *et al.* (1994). Drying of white spruce somatic embryos to 5% MC has also been reported (Attree *et al.*, 1995). These low MC's allow easier storage of somatic embryos, while maintaining embryo viability, and results in mature somatic embryos similar in MC to zygotic embryos. The MC values calculated here were used throughout this thesis to express measurements of mineral nutrients on a dry weight (DW) basis.

CHAPTER 3:

MEASUREMENT OF TOTAL PHOSPHORUS AND PHYTIC ACID PHOSPHORUS

Introduction

Phosphorus is an essential plant macronutrient and is present in phospholipid membranes, DNA, RNA, ATP, ADP and several sugar phosphates in metabolic processes (Glass, 1989; Salisbury and Ross, 1992). Traditionally, the use of colour reactions and spectrophotometry have been the basis of P determinations. Most of the procedures used involve the formation of heteropolyacids like molybdophosphate or vanadomolybdophosphate in acidic solutions. It has been found that while being less stable, the molybdophosphate reduction method is more sensitive and better for detection of low P concentrations than the vanadomolybdophosphate method (Tušl, 1972).

The molybdophosphate reduction protocol begins with adding an acidic solution containing an excess of ammonium molybdate. The molybdate ions react with the orthophosphate ions in the sample producing molybdophosphoric acid ($H_3[P(Mo_3O_{10})_4]$), which has a yellow colour (Boltz and Mellon, 1948). Reduction of this complex with hydroquinone and sodium sulfite produces a stable blue colour with an intensity proportional to the inorganic P content (Briggs, 1924). It has been found that adding sodium sulfite after adding hydroquinone improves the colour intensity and proportionality of the colour to the P concentration (Briggs, 1924). Using this colour reaction gives a detection limit of 0.05

µg/ml with an optimal measuring range of 0.5 to 10 µg/ml (Štupar *et al.*, 1987).

In the molybdenum blue method, only orthophosphates react with molybdate to give the molybdophosphoric acid complex (Motomizu *et al.*, 1983). Consequently, in order to measure total P, all the P-containing compounds within the tissue must be converted to orthophosphate. This is done by breaking down the organic matter either by wet ashing in strong acids or bases or by dry ashing at high temperatures (Ashton, 1936). Often both procedures produce comparable results (Ashton, 1936; Isaac and Johnson, 1975). Some studies, however, have found wet ashing to be superior over dry ashing (Stuffins, 1967; Griffiths and Thomas, 1981; Ockenden *et al.*, 1997). Other studies have found that dry ashing produces better results (Tušl, 1972; Munter *et al.*, 1979; Clegg *et al.*, 1981).

There are advantages and disadvantages to using either wet or dry ashing procedures. Typically, wet ashing involves the use of nitric and sulfuric acids with low heat to digest the tissue and occasionally hydrogen peroxide is used to remove any colour (Gorsuch, 1970). Dry ashing involves initial charring of the sample at low heat to remove volatile materials that may ignite at high temperatures resulting in tissue loss (Gorsuch, 1970). The sample is then fully oxidized at higher temperatures (often 450 to 550°C) in a muffle furnace. Wet ashing is faster and less prone to volatilization and retention of elements in the apparatus due to the use of low temperatures and liquids (Gorsuch, 1970). Dry ashing on the other hand allows the use of larger sample sizes, requires less attention and often involves fewer reagents, which decreases background problems due to elements in the reagents (Gorsuch, 1970). When beginning to measure phosphorus in a new tissue type it is recommended to try both procedures and then the most appropriate procedure can be chosen based on the consistency

of results along with sample quantity.

Often the majority of a seed's total P is present as part of *myo*-inositol hexa*kis*phosphoric acid or phytic acid (Johnson and Tate, 1969; Lott, 1984). Phytic acid consists of a 6-carbon ring with a phosphate group on each carbon and provides mineral nutrients during germination and early stages of seedling development (Brown *et al.*, 1961; Johnson and Tate, 1969; Lott and Ockenden, 1986). Phytic acid is typically found in seeds as a mixed cation salt called phytate (or phytin), which is generally the major P store in seeds (Cosgrove, 1966; Johnson and Tate, 1969; Raboy, 1990). Typically, 50 to 80% of a seed's total P may be bound as phytic acid (Greenwood, 1989; Lott *et al.*, 1995a).

In order to measure the amounts of P bound as phytic acid, the phytic acid component of the tissue must be extracted and purified. Kikunaga *et al.* (1985) found that extraction in 2.4% hydrochloric acid (HCl) was better than trichloroacetic acid (TCA), while Cilliers and van Niekerk (1986) found no difference between HCl and TCA. This study uses HCl as the extracting acid. Following extraction, the phytic acid component must be separated from other compounds extracted by the acid. A common technique to accomplish this involves columns containing anion exchange resin. The resin used here is a crosslinked copolymer of styrene and divinylbenzene with quaternary ammonium functional groups (Gjerde and Fritz, 1987; Korkisch, 1989). Bound to the ammonium functional group are counterions (chloride ions in this study), which will be replaced by the phytic acid during the separation procedures. Following this, the separated phytic acid is removed from the column using an appropriate acid and digested using the wet ashing procedures used for total P. Levels of P bound in phytic acid are then measured using the molybdenum blue colourimetric procedure.

In this study the total P and the amount of PA-P was measured for various parts of white spruce seeds and for white spruce somatic embryos produced using maturation media varying in sucrose and *myo*-inositol concentrations.

Materials and Methods

Wet Ashing

The digestion procedures of Ellis and Morris (1983) and Ockenden *et al.* (1997) were used with all the types of samples. Each sample of zygotic embryos consisted of embryos from 85 seeds. The female gametophytes from those same 85 seeds were used as one female gametophyte sample. Whole seed samples consisted of 60 seeds each. Samples of somatic embryos consisted of 45 somatic embryos each and separate samples were tested for two batches of somatic embryos produced independently with normal maturation media. In addition, samples of somatic embryos from batches matured on altered maturation media were tested to study the effect on total P and PA-P levels. The four maturation media treatments used were: 3.0% sucrose plus 0% *myo*-inositol; 2.5% sucrose plus 0.15% *myo*-inositol; 2.0% sucrose plus 0.3% *myo*-inositol; and 1.5% sucrose plus 0.6% *myo*-inositol. These combinations were chosen to provide a large range of *myo*-inositol concentrations while compensating for osmotic conditions within the media. For all sample types, four separate aliquots were prepared and tested for total P. All the above samples were done in quadruplicate and means calculated.

Each sample was weighed and then placed into a 100 ml digestion tube (7900 Tube, 25 mm x 200 mm, VWR Scientific of Canada Ltd., Toronto) with one glass bead. To each tube, 3.0 ml of concentrated nitric acid (HNO_3) was added followed by 0.5 ml of concentrated sulfuric acid (H_2SO_4). All tubes were placed in a Kjeldahl digestion unit (Gallenkamp, England) and heated. Frequent tapping of the tubes was done for about 15 min. until the

solutions within all the tubes were bubbling sufficiently to avoid sudden bursts of acid from the tubes. The tubes were heated until white fumes filled the tubes (1.5 to 2 h). Fuming was considered complete when it was no longer possible to see through the digestion tube. The tubes were then removed from the digestion unit and allowed to cool to room temperature. Seven drops of 30% hydrogen peroxide (H_2O_2) (w/v) were added to each tube containing zygotic or somatic embryos to complete the digestion and remove any colour from the solution (Organ *et al.*, 1988). The tubes were placed back in the digestion unit and heated until fumes reappeared. In order to complete the digestion of the female gametophyte and whole seed samples, four additions of 7 drops of 30% H_2O_2 (w/v) each were used with heating to fuming between each addition in order to remove all the colour. Finally, all tubes were cooled to room temperature and a few ml of deionized water were added to each tube.

Each digested solution of zygotic or somatic embryos was carefully transferred to a separate 10 ml volumetric flask using a small glass funnel and a glass rod. The glass bead from the tube was collected in the funnel. Two washes of the digestion tube were performed using a few ml of deionized water per wash and transferred to the flask. The glass rod and funnel were further washed into the flask and the combined solution was taken up to volume with deionized water. Each solution was transferred to a glass scintillation vial and stored in the refrigerator until needed for the molybdenum blue colourimetric reaction.

Digested samples of female gametophytes and whole seeds were transferred in a similar fashion to separate 25 ml volumetric flasks. Several washes of each tube were added to the respective flasks and the flasks were taken up to volume with deionized water. To dilute these samples, 2 ml from each sample was pipetted into 10 ml volumetric flasks and

taken up to volume. This final solution was transferred to glass scintillation vials and stored in the refrigerator until needed for the molybdenum blue colourimetric reaction.

Molybdenum Blue Colourimetric Reaction for Phosphorus

The molybdenum blue procedure outlined in AOAC (1990) and Plaami and Kumpulainen (1991) was used. For this colour reaction three solutions were required. An ammonium molybdate solution was used which consisted of 300 ml of 0.067 M ammonium molybdate (BDH Inc., Toronto, ON) and 200 ml of 37.5% H_2SO_4 (v/v). The second solution required was a 0.045 M solution of hydroquinone (BDH Inc., Toronto, ON) with 2 to 3 drops of concentrated H_2SO_4 used to retard oxidation. Thirdly, a 1.59 M solution of sodium sulfite (J.T. Baker Inc., Phillipsburg, NJ) was needed. Finally, a phosphate standard solution was prepared by diluting a standard solution of phosphate (Aldrich Chemical Company, Inc., Milwaukee, WI), which contained 0.5 mg phosphate per ml, to give a final solution containing 0.0245 mg P per ml. All solutions were stored in the refrigerator until needed.

One ml of each of the zygotic embryo solutions and two ml of each of the somatic embryo, female gametophyte and whole seed solution were pipetted into separate 10 ml volumetric flasks. Several 1 ml standard samples were also pipetted into 10 ml volumetric flasks. Additionally, one 10 ml volumetric flask was set aside for the reagent blank. To the reagent blank, 1 ml of molybdenum solution was added followed by 1 ml of hydroquinone solution and finally 1 ml of sodium sulfite solution. The flask was made up to volume with deionized water and shaken vigorously. This process was sequentially repeated for each flask containing a sample solution, trying to keep approximately 1 min. for the addition of the

solutions to each flask.

One hour after the reagent blank was prepared, readings were taken on a Zeiss PMQ II spectrophotometer (Carl Zeiss, West Germany) at 650 nm. Using plastic disposable cuvettes (Styrene Cuvettes, 1 cm x 1 cm) the reagent blank plus three test samples were placed into the spectrophotometer and their absorbancies were read. The blank was changed half way through all the readings due to the build up of air bubbles. When changing the solution in a cuvette, the cuvette was first washed twice with some of the new test sample.

Using all the readings for the phosphate standard, an average standard absorbancy reading was calculated. A standard factor was calculated by dividing the theoretical amount of P per ml in the standard (24.5 μg P/ml) by the mean absorbancy reading for the standards. The absorbancy reading for each sample was multiplied by this factor to give the corrected μg P per ml in the sample. These values were then multiplied by the appropriate dilution factor to give the μg P in each digested sample. Dividing these values by the corresponding DW (g) gave the μg P per g DW. Additionally, the μg of P per embryo, female gametophyte or whole seed was calculated for each sample. Using the values obtained for zygotic embryos and their corresponding female gametophytes, the total amount of P for seeds without seed coats was calculated.

Statistical differences between means were determined using the MINITAB analysis of variance test. When a difference was found, Tukey's test (Zar, 1984) was used to determine which means differed at $P > 0.05$.

Extraction of Phosphorus-Containing Compounds for Phytate Analysis

For each sample type tested for total P, four samples were used for phytate analysis. Each zygotic embryo sample had 110 to 130 embryos and the female gametophytes from these same 110 to 130 seeds were combined to make one female gametophyte sample. Whole seed samples consisted of 75 seeds each. Samples of somatic embryos consisted of 130 to 200 somatic embryos each and samples were run for two batches of embryos produced using the normal maturation media as well as for each of the four treated conditions. Using an agate mortar and pestle, samples were individually ground up and weighed. Using the extraction procedure outlined by AOAC (1990), phosphorus-containing compounds were extracted from this tissue using 2.4% HCl (w/v). Samples of zygotic and somatic embryos were placed into separate 50 ml Erlenmeyer flasks with 15 ml of 2.4% HCl and placed on a shaker (Eberbach Corporation, Ann Arbor, Michigan) for 2.5 h. Every 15 to 20 min., the flasks were taken out and swirled to get pieces of tissue off the sides of the flasks and to loosen up the tissue on the bottom of the flasks. Female gametophyte and whole seed samples were placed into separate 125 ml Erlenmeyer flasks with 25 ml of 2.4% HCl and were shaken for 2.5 h.

After shaking, the solutions were transferred to 50 ml plastic centrifuge tubes (Nalgene, round bottomed) and centrifuged for 15 min. at 10,000 rpm (12,000 x g) in a Sorvall Superspeed RC2-B Centrifuge (Ivan Sorvall Inc., Newtown, Connecticut) cooled to 5 °C. The supernatants were decanted into new Erlenmeyer flasks using glass funnels and Whatman No. 41 slow ashless filter paper. These extracts were then transferred to glass scintillation vials and stored in the refrigerator.

Column Separation

Column separation of phytate from the extracts was done as described by AOAC (1990) and Plaami and Kumpulainen (1991). Plastic columns (Econo Bio-Rad 0.7 x 15 cm) with 5 cm of tygon tubing attached to the bottoms were placed in clamps on retort stands. Metal clamps were placed on the tygon tubing to control the flow rate of the column. Approximately 0.5 g samples of Bio-Rad analytical grade anion exchange resin (AG 1-X8 200-400 mesh chloride form) were weighed and made into slurries with deionized water. Each slurry was then transferred to a column and the column was filled with deionized water. The resin was allowed to settle for at least 30 min. and the clamp was tightened so as to prevent any water loss. The final resin bed was approximately 1 cm in height.

The flow rate of each column was adjusted to 10 drops per min. and this rate was checked periodically throughout the separation. Once the rate was set and the column nearly dry, 15 ml of deionized water was applied to the column. Additions of solutions to the columns were done slowly enough to avoid disrupting the resin beds. Once the water was just above the resin bed, 15 ml of 0.7 M NaCl was applied to the column to maximize binding sites for phytic acid and phosphate. After the 0.7 M NaCl was almost completely through the column, 15 ml of deionized water was added to the column using a clean pipet.

Three ml of each concentrated extract was then pipetted into a separate graduated cylinder and taken up to 30 ml with deionized water. When the water had almost completely drained from the column, the extract solution was applied. Each extract was run on two columns to give duplicate samples. After all the extract was added to the column, the cylinder was washed with a few ml of deionized water and transferred to the column just before the

resin went dry. One additional wash was also done and transferred to the column. Again the resin was washed with 15 ml of deionized water followed by 15 ml of 0.1 M NaCl to remove inorganic phosphate from the resin.

After the NaCl was completely through the column, the waste beakers were removed and clean 100 ml beakers were placed under the columns. Sixty ml of 2 N HCl was applied to each column to remove the phytic acid from the resin. The entire column separation took between 5 and 8 h depending on the individual column. In total, 8 columns were run for each of the zygotic embryos, female gametophytes, whole seeds, two batches of normally produced somatic embryos and the four somatic embryo batches produced with altered maturation media.

Each beaker, containing extracted phytate from a column, was then placed on a SYBRON thermolyne 2600 hot plate (Thermolyne Corporation, Dubuque, Iowa) set at low-medium heat. The HCl was evaporated away until approximately 3 ml of solution remained in each beaker. After cooling, the solutions were transferred to digestion tubes using a glass rod with two additional washes each and digested as described for wet ashing. No H_2O_2 was needed to complete the digestion. Each digested sample of zygotic or somatic embryos was transferred to 10 ml volumetric flasks, taken up to volume with deionized water and 6 ml from each was used for the molybdenum blue colour reaction as described previously. Each digested sample of female gametophytes and whole seeds was transferred to 25 ml volumetric flasks and taken up to volume with deionized water. Five ml of each female gametophyte solution was then transferred to separate 10 ml volumetric flasks, taken up to volume and 6 ml of each solution was used for the molybdenum blue colourimetric

reaction as described previously. For each whole seed sample, 8.4 ml was pipetted into a 10 ml volumetric flask, which was taken up to volume and 6 ml was used for the colour reaction.

For each column the μg PA-P per g DW, μg PA-P per tissue and the % PA-P of the total P was calculated. The % PA-P of the total P was calculated based on levels of P and PA-P measured per tissue. By combining values for zygotic embryos and female gametophytes, values were calculated for seeds without seed coats. The μg PA-P per g DW for seeds without seed coats was calculated by adding the levels found in both zygotic embryos and female gametophytes and dividing by the combined DW's. The μg PA-P per tissue was simply calculated by addition of the levels in a single zygotic embryo and a single female gametophyte. The % PA-P of the total P in seeds without seed coats was calculated based on the levels of P and PA-P measured per tissue.

Statistical differences between means were determined using the MINITAB analysis of variance test. When a difference was found, Tukey's test (Zar, 1984) was used to determine which means differed at $P > 0.05$.

Results

Total Phosphorus

Total P levels in somatic embryos and various parts of seeds are summarized in Table 2 and illustrated in Figures 14 and 15. When expressed per g DW, the two separate batches of somatic embryos produced on normal maturation media varied slightly with both batches having less P than zygotic embryos. Zygotic embryos, female gametophytes and seeds without seed coats (combined zygotic embryos and female gametophytes) had similar P levels per g DW. Whole seeds had less P per g DW than the individual parts of the seed, but still had more P than either of the two batches of somatic embryos.

Expressing total P per tissue shows that while there is still a slight difference between the two batches of somatic embryos, there is no significant difference between a single somatic embryo from either batch and a single zygotic embryo. A single female gametophyte contains approximately 7.4 times more P than a single zygotic embryo. As shown by the differences between a whole seed and a seed without a seed coat, only 2.5% of the total P in a single seed was in the seed coat.

Total P for batches of somatic embryos matured using media of varying sucrose and *myo*-inositol levels are summarized in Table 3. Results showed that both total P per g DW and total P per tissue did not vary significantly from treatment-to-treatment. All four treatments produced embryos with P levels per g DW slightly higher than those produced using the typical maturation media (Compare Table 2 to Table 3).

Table 2: Mean (± SD) total phosphorus levels in white spruce somatic embryos and various parts of white spruce seeds expressed per g DW and per tissue.

Sample	Number per Sample	µg P per g DW	µg P per tissue
Somatic Embryos Batch 1	45	6382.50 ± 101.53 **a**	2.07 ± 0.14 **a**
Somatic Embryos Batch 2	45	6887.39 ± 76.43 **b**	2.22 ± 0.08 **a**
Zygotic Embryos	85	10697.48 ± 207.67 **c**	1.84 ± 0.05 **a**
Female Gametophytes	85	11630.28 ± 158.97 **d**	13.57 ± 0.44 **b**
Seeds Without Seed Coats	85	11509.90 ± 130.52 **d**	15.41 ± 0.47 **c**
Whole Seeds	60	7820.61 ± 124.07 **e**	15.81 ± 0.51 **c**

Note: Each mean was calculated using 4 values. Values for seeds without seed coats were calculated using the values for zygotic embryos and the values for female gametophytes. Values in a single column that are followed by the same letter are not significantly different at $P > 0.05$.

Figure 14: Bar graph of total P expressed per g DW for white spruce somatic embryos and various parts of white spruce seeds.

Figure 15: Bar graph of total P expressed per tissue for white spruce somatic embryos and various parts of white spruce seeds.

14

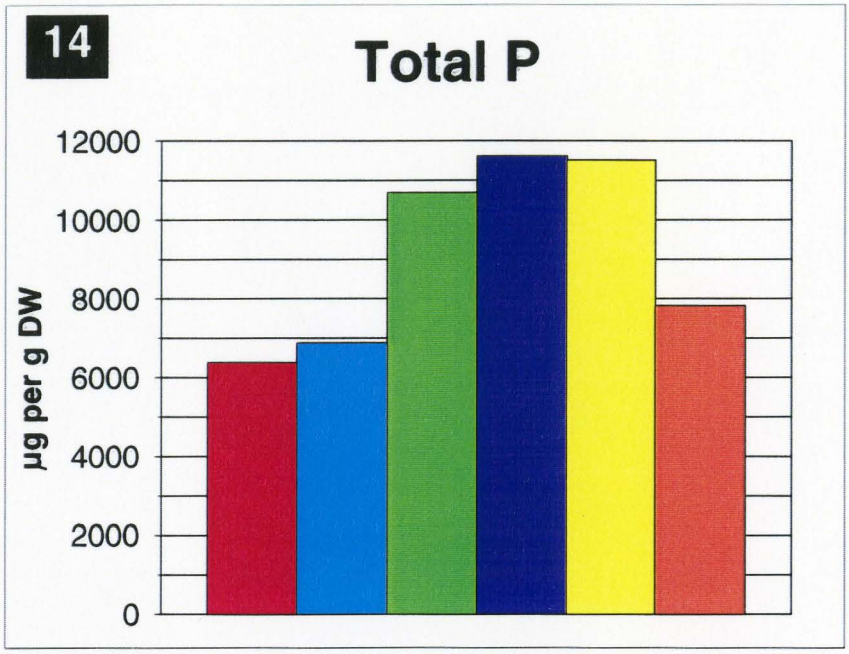
Total P
12000
10000
8000
6000
4000
2000
0
µg per g DW

15

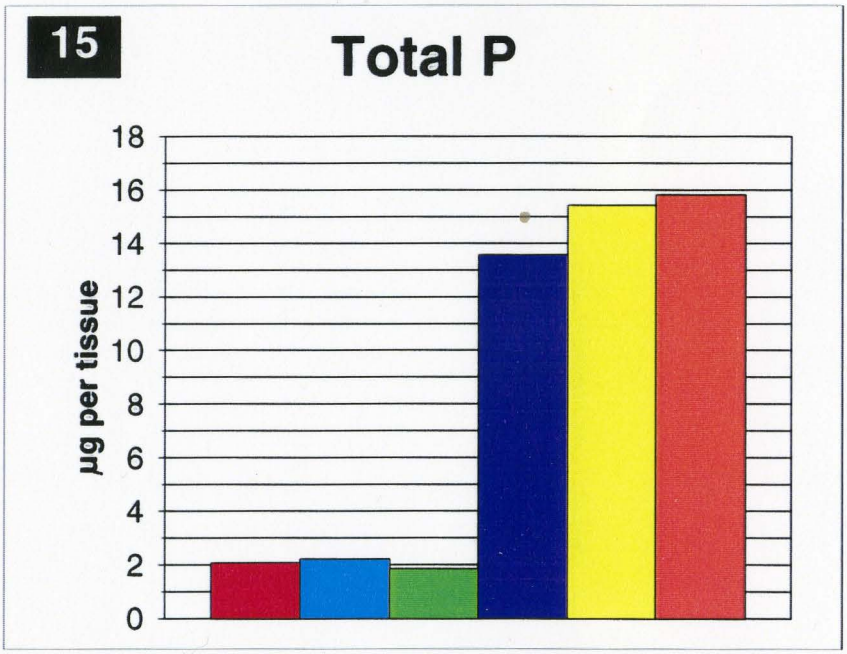
Total P
18
16
14
12
10
8
6
4
2
0
µg per tissue

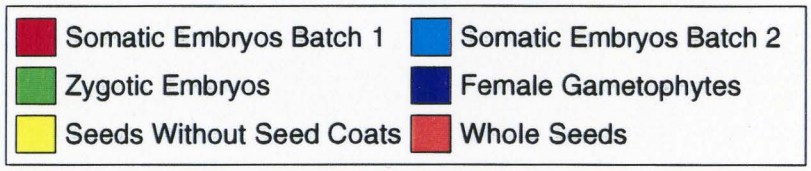
Somatic Embryos Batch 1
Somatic Embryos Batch 2
Zygotic Embryos
Female Gametophytes
Seeds Without Seed Coats
Whole Seeds

Table 3: Mean (± SD) total phosphorus levels for white spruce somatic embryos matured on various combinations of sucrose and *myo*-inositol. Comparison of treatment-to-treatment differences.

Sample	Number per Sample	µg P per g DW	µg P per tissue
3.0% sucrose plus 0.0% *myo*-inositol	45	7269.18 ± 278.49 **a**	1.87 ± 0.05 **a**
2.5% sucrose plus 0.15% *myo*-inositol	45	7189.41 ± 360.49 **a**	2.06 ± 0.22 **a**
2.0% sucrose plus 0.3% *myo*-inositol	45	7481.45 ± 558.84 **a**	1.97 ± 0.21 **a**
1.5% sucrose plus 0.6% *myo*-inositol	45	7754.06 ± 296.45 **a**	1.93 ± 0.25 **a**

Note: Each mean was calculated using 4 values. Values in a single column that are followed by the same letter are not significantly different at $P > 0.05$.

The batches of treated embryos were produced in four Runs with each Run consisting of one plate of each of the four treatment conditions. To determine if there was variation per Run, a mean value for each Run was calculated using the four plates in the Run. Runs 1 and 2 were produced simultaneously and separately from Runs 3 and 4, which were also produced simultaneously. Table 4 shows the μg P per g DW and the μg P per tissue for each of the Runs. No significant differences were found between the Runs for either calculation.

Phytic Acid Phosphorus

Levels of PA-P for somatic embryos and various parts of seeds are given in Table 5 and illustrated in Figures 16 to 18. Expressing PA-P levels per g DW shows that the two batches of somatic embryos vary significantly. Batch 2 had approximately 2.2 times more PA-P per g DW than Batch 1. Batch 2 also had higher total P levels (Table 1). Zygotic embryos had 4.4 and 2.1 times more PA-P than somatic embryos Batch 1 and Batch 2, respectively. Female gametophytes contained high PA-P levels per g DW, having approximately 2.9 times more PA-P than zygotic embryos. Combining zygotic embryos and female gametophytes reduced the level of PA-P per g DW from those obtained for female gametophytes alone. Adding the seed coats (whole seeds) again significantly reduced the PA-P levels per g DW from values calculated for seeds without seed coats.

Comparing PA-P levels per tissue shows that Batches 1 and 2 differ approximately 2.3 fold with Batch 2 being higher. A single zygotic embryo has PA-P levels similar to a single somatic embryo from Batch 2. When statistically compared with female gametophytes, seeds without seed coats, and whole seeds; zygotic and somatic embryos do not vary

Table 4: Mean (± SD) total phosphorus levels for white spruce somatic embryos matured on various combinations of sucrose and *myo*-inositol. Comparison of Run-to-Run differences.

Sample	Number per Sample	µg P per g DW	µg P per tissue
Run 1	45	7437.55 ± 480.70 **a**	1.79 ± 0.15 **a**
Run 2	45	7495.92 ± 299.96 **a**	1.96 ± 0.17 **a**
Run 3	45	7387.63 ± 298.66 **a**	2.12 ± 0.16 **a**
Run 4	45	7373.49 ± 663.19 **a**	1.96 ± 0.18 **a**

Note: Each mean was calculated using 4 values. Values in a single column that are followed by the same letter are not significantly different at $P > 0.05$.

Table 5: Mean (± SD) phytic acid phosphorus levels in white spruce somatic embryos and various parts of white spruce seeds expressed per g DW, per tissue and as a percentage of the total phosphorus.

Sample	Number per Sample	µg PA-P per g DW	µg PA-P per tissue	% PA-P of Total P
Somatic Embryos Batch 1	130	783.08 ± 70.99 **a**	0.22 ± 0.03 **a**	12.27 ± 1.11 **a**
Somatic Embryos Batch 2	150	1692.74 ± 86.66 **b**	0.51 ± 0.03 **a**	24.58 ± 1.26 **b**
Zygotic Embryos	110-130	3473.55 ± 298.35 **c**	0.54 ± 0.08 **a**	32.47 ± 2.79 **c**
Female Gametophytes	110-130	10139.33 ± 106.50 **d**	12.02 ± 1.02 **b**	87.18 ± 0.92 **d**
Seeds Without Seed Coats	110-130	9362.36 ± 101.14 **e**	12.56 ± 1.08 **b**	81.34 ± 0.88 **e**
Whole Seeds	75	6875.15 ± 104.05 **f**	12.67 ± 0.58 **b**	80.17 ± 3.64 **e**

Note: Each mean was calculated using 8 values. Values for seeds without seed coats were calculated using the values for zygotic embryos and the values for female gametophytes. Values in a single column that are followed by the same letter are not significantly different at $P > 0.05$.

Figure 16: Bar graph of PA-P for white spruce somatic embryos and various parts of white spruce seeds expressed per g DW.

Figure 17: Bar graph of PA-P for white spruce somatic embryos and various parts of white spruce seeds expressed per tissue.

Figure 18: Bar graph of PA-P for white spruce somatic embryos and various parts of white spruce seeds expressed as a percentage of total P.

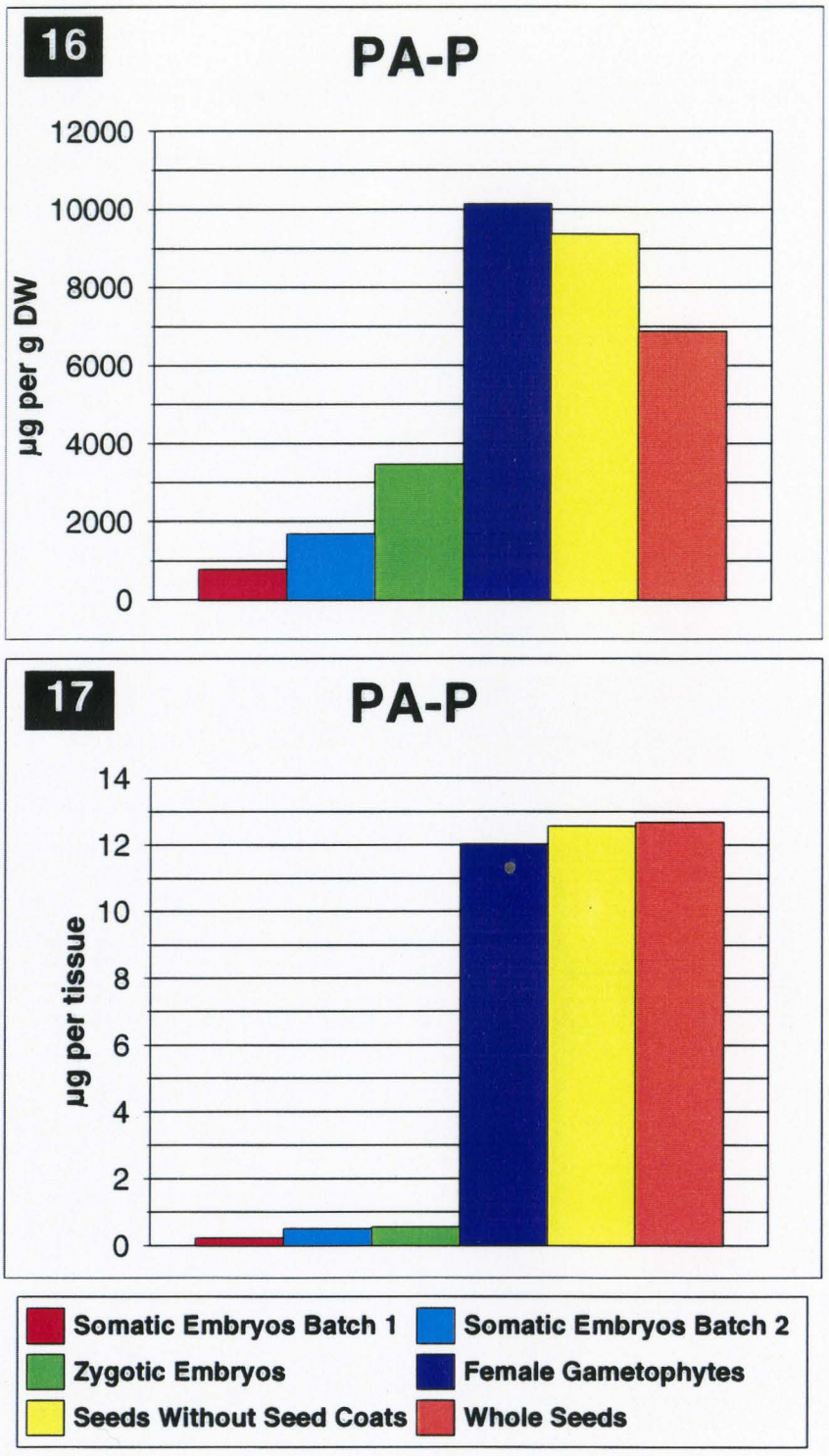
16
PA-P
12000
10000
8000
6000
4000
2000
0
µg per g DW
17
PA-P
14
12
10
8
6
4
2
0
µg per tissue
Somatic Embryos Batch 1
Somatic Embryos Batch 2
Zygotic Embryos
Female Gametophytes
Seeds Without Seed Coats
Whole Seeds

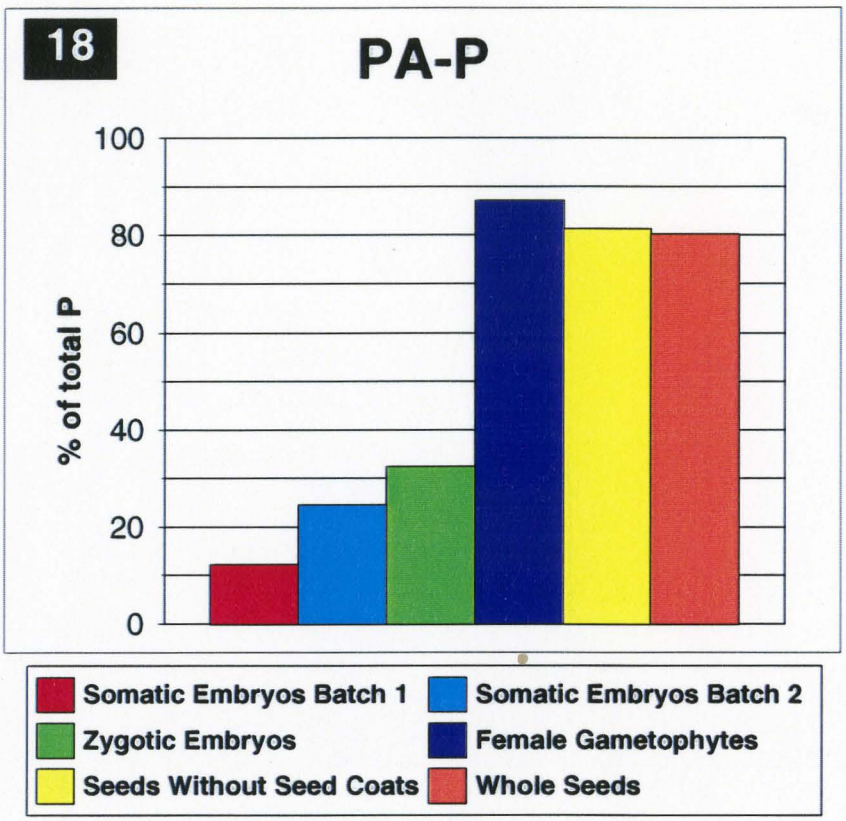
18
PA-P
100
80
60
40
20
0
% of total P
Somatic Embryos Batch 1
Somatic Embryos Batch 2
Zygotic Embryos
Female Gametophytes
Seeds Without Seed Coats
Whole Seeds

significantly. Even though there are no statistical differences, Batch 1 somatic embryos had noticeably lower PA-P per tissue than both Batch 2 somatic embryos and the zygotic embryos. Combining zygotic embryos with female gametophytes increased the levels of PA-P per tissue but the majority of PA-P was within the female gametophyte. Comparison of a seed without a seed coat to a whole seed shows that there is no significant level of PA-P in the seed coats.

Expression of PA-P values as a percentage of total P showed that the majority of P in female gametophytes, seeds lacking seed coats and whole seeds is in the form of PA-P. Zygotic embryos had 2.7 times less of the total P bound to phytic acid as compared to female gametophytes. Both batches of somatic embryos had similar percentages of P bound to phytic acid and both batches had significantly lower percentages of PA-P than zygotic embryos.

Table 6 summarizes the PA-P results for each of the four treatment conditions for somatic embryos. Comparing the different treatments shows no significant differences in PA-P due to the levels of sucrose and *myo*-inositol in the maturation media. When expressed per g DW, per tissue and as a % of the total P, each treatment condition produced embryos with PA-P levels in the range found with Batches 1 and 2 (Table 5).

Comparing treatment conditions shows that Runs 1 and 2 do not vary significantly and both are significantly different from Runs 3 and 4 (Table 7). Runs 3 and 4 also do not vary significantly (Table 7). Runs 1 and 2 produced embryos with PA-P levels similar to Batch 1 somatic embryos (Table 5). Runs 3 and 4 produced embryos with significantly higher PA-P levels than Runs 1 and 2 but lower than Batch 2 somatic embryos (Table 5). Most of the variation was found to be from run-to-run rather than from treatment-to-treatment.

Table 6: Mean (± SD) phytic acid phosphorus levels for white spruce somatic embryos matured on various combinations of sucrose and *myo*-inositol. Comparison of treatment-to-treatment differences.

Sample	Number per Sample	µg PA-P per g DW	µg PA-P per tissue	% PA-P of Total P
3.0% sucrose plus 0.0% *myo*-inositol	200	1171.29 ± 391.99 **a**	0.29 ± 0.11 **a**	15.81 ± 5.38 **a**
2.5% sucrose plus 0.15% *myo*-inositol	200	1214.71 ± 454.67 **a**	0.34 ± 0.14 **a**	16.39 ± 6.23 **a**
2.0% sucrose plus 0.3% *myo*-inositol	200	1048.42 ± 334.31 **a**	0.28 ± 0.10 **a**	14.14 ± 4.58 **a**
1.5% sucrose plus 0.6% *myo*-inositol	200	1230.26 ± 349.05 **a**	0.31 ± 0.12 **a**	16.59 ± 4.78 **a**

Note: Each mean was calculated using 8 values. Values in a single column that are followed by the same letter are not significantly different at $P > 0.05$.

Table 7: Mean (± SD) phytic acid phosphorus levels for white spruce somatic embryos matured on various combinations of sucrose and *myo*-inositol. Comparison of Run-to-Run differences.

Sample	Number per Sample	µg PA-P per g DW	µg PA-P per tissue	% PA-P of Total P
Run 1	200	762.84 ± 124.46 **a**	0.20 ± 0.02 **a**	10.26 ± 1.67 **a**
Run 2	200	916.78 ± 119.74 **a**	0.21 ± 0.03 **a**	12.23 ± 1.60 **a**
Run 3	200	1445.53 ± 204.35 **b**	0.39 ± 0.06 **b**	19.57 ± 2.77 **b**
Run 4	200	1539.54 ± 200.40 **b**	0.42 ± 0.05 **b**	20.88 ± 2.72 **b**

Note: Each mean was calculated using 8 values. Values in a single column that are followed by the same letter are not significantly different at $P > 0.05$.

Discussion

In seeds, P-containing compounds can be classified into four main groups: nucleic acids, inorganic P compounds, phosphatides and phytates (Lolas and Markakis 1975). Phytic acid is of interest to humans because it has been implicated in anaemias, rickets, osteoporosis and bone deformities (Taylor, 1965; Zarei *et al.*, 1972; Berlyne *et al.*, 1973). In addition, phytic acid chelates numerous elements decreasing their availability to digestive tracts of monogastric animals and has been implicated in peptic digestion inhibition (Barré, 1956; Lolas and Markakis, 1975; Bassiri and Nahapetian, 1977; Jaffe, 1981). Phytate acts as a source of phosphate, inositol and cations (monovalent and divalent); which are mobilized to support growth of the developing seedling until the root system is adequately formed (Lott, 1984; Greenwood, 1989).

When white spruce somatic embryos were compared to various parts of white spruce seeds, it was found that on a DW basis somatic embryos had significantly less total P than any seed parts. Since somatic embryos are significantly larger than zygotic embryos and therefore have higher DW's, these differences indicate that zygotic embryo tissue has its P reserves packed more densely than somatic embryos. There was some small variation between the two batches of somatic embryos. Female gametophytes had slightly higher P per g DW than zygotic embryos. Whole seeds had significantly lower total P levels than seeds without seed coats indicating that the seed coats have very low P levels. In a comprehensive study on eleven *Pinus* species by West and Lott (1993a), the total P levels ranged from 7,000 to 14,800 µg per g DW for zygotic embryos and from 5,200 to 15,600 µg per g DW for female gametophytes. The levels found in white spruce seeds place both zygotic embryos and female

gametophytes in the middle of the ranges reported for *Pinus*. Overall, white spruce seeds most closely resemble the results for one batch of Swiss Mountain pine (*Pinus mugo*) reported by West and Lott (1993a).

Expression of total P per tissue resulted in a very different comparison. There was no significant difference in P levels for the two batches of somatic embryos. A single somatic embryo from either batch had similar P levels to a single zygotic embryo. Clearly, when size differences are eliminated and a single embryo is analysed as a complete unit, these two types of embryos are very similar in P levels. Female gametophyte tissue contained the bulk of the P in the seed. Comparison of whole seeds with seeds without seed coats shows very low amounts of P within the seed coat itself. West and Lott (1993a) reported ranges of P per tissue in *Pinus* to be from 4 to 111 μg for zygotic embryos and from 40 to 1273 μg for female gametophytes. White spruce has significantly less total P per seed than any of these *Pinus* species, since white spruce seeds are smaller than any *Pinus* seeds studied by West and Lott (1993a).

Phytic acid biosynthesis in seeds is still not fully understood but three possible biosynthetic pathways have been proposed as reviewed by Greenwood (1989) and Lott *et al.* (1995a). One pathway involves using ATP to sequentially add phosphate groups to *myo*-inositol-1-phosphate to give the hexaphosphate. A second proposed pathway is similar to the first, but blocks of phosphate are added rather than a single phosphate group at a time. The last pathway suggests that hexaphosphate is produced via some yet unknown intermediate. Recent studies on second messenger production have indicated the possibility of phytic acid being synthesized via polyphosphoinositide intermediates (reviewed by Loewus

et al., 1990).

Measurements of phytic acid in somatic embryos revealed considerable variation between different batches of somatic embryos. Total amounts of PA-P per g DW was two times higher in Batch 2 somatic embryos than in Batch 1 somatic embryos. Both batches contained significantly less PA-P per g DW than zygotic embryos. Female gametophytes were found to have very high levels of PA-P. Expressing PA-P values per tissue shows that while a somatic embryo from each batch varied by 2.3 times, a somatic embryo can be produced with PA-P levels approaching those found in a zygotic embryo. The lower levels of PA-P found in a Batch 1 somatic embryo, which had similar total P levels to a Batch 2 somatic embryo and a zygotic embryo, indicates that these embryos contained the required amounts of P but had not packaged it into phytic acid. The female gametophyte tissue of a seed contained the bulk of the PA-P within the seed. Comparing values for seeds with and without seed coats shows very little PA-P within the seed coat.

Traditionally, PA-P levels have been reported in the literature as a percentage of the total P present. In this study, the female gametophyte tissue had almost 55% more of its P in the form of phytic acid than a zygotic embryo. This large difference between female gametophyte tissue and zygotic embryos illustrates the importance of taking the time to dissect out the zygotic embryo from the female gametophyte. As the results for seeds without seed coats shows, combining the zygotic embryo with the female gametophyte gives a high % PA-P due to the overwhelming influence of the large female gametophyte. Somatic embryos had values that still varied, but the fact that Batch 2 somatic embryos still closely resemble zygotic embryos indicates that this culture system for white spruce is sufficient

enough to produce somatic embryos very similar to zygotic embryos.

Previous studies of PA-P as a % of the total P in other species have found large variations. Levels as low as 38% have been reported for wheat (*Triticum aestivum*) grains, but levels varied in this study between 38% and 94% for various wheat varieties (Bassiri and Nahapetian, 1977). Large variations in % PA-P have also been found for oats (*Avena sativa*) and for bean (*Phaseolus vulgaris*) seeds (Ashton and Williams, 1958; Lolas and Markakis, 1975). Comparison of white spruce seeds to levels in the various species summarized by Lott (1984), shows that, on a whole seed basis, white spruce is in the high end of values typically found. Since no previous study has been done on PA-P in conifer seeds, it is not possible without further study to ascertain if these levels are typical of other conifers or of gymnosperms in general. It is clear however, that white spruce zygotic embryos have very little of the total P in phytic acid when compared to other species.

In an attempt to alter the levels of PA-P in somatic embryos, various batches were developed on maturation media with varying proportions of *myo*-inositol and sucrose. These combinations were chosen to provide a large range of *myo*-inositol while compensating for osmotic changes. The theoretical basis for these media alterations was that since phytic acid consists of phosphorylated *myo*-inositol, altering this component of the media may affect levels accumulating in the embryos. Total P results revealed that maturation on different media combinations had no significant affect on levels accumulating in the embryos. In fact, the majority of variation occurred between runs rather than between treatments. In all treatments, including media completely lacking *myo*-inositol, the total P levels were very consistent indicating that other regulatory factors must be optimizing the amount of P within

the embryos.

Although total P did not change under these treatments, PA-P levels were still measured to test whether more of this P was packaged into phytic acid due to more *myo*-inositol being available. Results of PA-P levels revealed that there was no significant differences between treatments with all treatments giving levels between those found for the two batches of somatic embryos matured on normal media. Again the majority of variation was found between runs. The fact that treatment without *myo*-inositol gave similar PA-P levels to other treatments would indicate that this sugar is acting more as an osmoticum than as a carbon source for phytic acid biosynthesis.

In black spruce and red spruce it was found that sucrose alone or sucrose plus *myo*-inositol resulted in the same quality of somatic embryo production, indicating their roles as being at least partly osmotic (Tremblay and Tremblay, 1991). The results here are encouraging from a tissue culture perspective in that somatic embryos appear to go through the steps of producing phytic acid from raw materials as would occur in a zygotic embryo. Biochemical studies on phytic acid biosynthesis would be a logical next step. If somatic embryos do in fact follow similar biosynthetic pathways to produce phytic acid as zygotic embryos do, the ease of getting somatic embryos at various stages of development makes this tissue culture system very attractive to biochemists.

The higher levels of PA-P seen in Batch 2 somatic embryos versus Batch 1 may be a result of using different purification steps. Batch 1 somatic embryos were produced using the conventional methods of condensing embryos onto one filter paper. Subsequent to the production of Batch 1 somatic embryos, advances were made in improving the ability to

purify a sample of somatic embryos that are more uniform in size to eliminate extreme deviants from the batch. This new purification step has not yet been published and therefore cannot be discussed in this current format. Improving the purification steps would ultimately eliminate those embryos that are more prone to have deviating levels of PA-P, thus improving the mean PA-P levels for that batch.

Further research into both improving purification steps and in producing somatic embryos with higher P and PA-P levels would be very beneficial for commercial applications. Studying nutrient-loaded black spruce seedlings, Malik and Timmer (1995) found that seedlings with identical height and biomass compared to non-treated seedlings had 43%, 76% and 33% more N, P and K, respectively, likely due to luxury consumption. Nutrient-loaded seedlings have been found to have a higher root production and improved seedling resistance to nutrient and moisture stress (van den Driessche, 1985; Timmer and Miller, 1991). Treatment of sitka spruce with P caused an 8-fold increase in P content and a 3-fold increase in tree growth compared to seedlings not given this P (Proe and Millard, 1995). Production of somatic embryos with increased P levels along with treatment of seedlings in the nursery prior to outplanting may provide an efficient way to mass produce trees of improved growth and quality.

CHAPTER 4:

TRANSMISSION ELECTRON MICROSCOPY AND ENERGY DISPERSIVE X-RAY ANALYSIS OF GLOBOIDS AND FE-RICH PARTICLES

Introduction

Energy dispersive x-ray (EDX) analysis is a convenient tool for studying the elemental compositions of specific spots or larger areas within the sample and allows the simultaneous detection of elements with a high detection sensitivity (Lott and Spitzer, 1980). When using a beryllium window on the detector the analysis is restricted to detecting elements with atomic number 11 (Na) and higher (Chandler, 1977). EDX analysis can only be used to detect elements and thus cannot be used to directly identify compounds.

Using a scanning transmission electron microscope (STEM), the electron beam can be focused on a specific spot in the tissue. As the electrons from the electron beam interact with the specimen various changes can occur (Chandler, 1977; 1979). One of the several changes that can occur is the release of an x-ray with an energy characteristic of the atom from which the x-ray was released (Chandler, 1977; 1979). As the electron beam interacts with the atom it knocks out an inner shell electron resulting in an ionised atom (Chandler, 1977; 1979). The energy required by the incident electron beam to eject an inner shell electron is commonly referred to as the absorption edge or the critical excitation potential (Chandler, 1977). Since inner shells in an atom have lower energies, electrons from outer orbitals fall to fill the gap in the atom (Chandler, 1977; 1979). The electron filling this gap

may lose energy in the form of an x-ray photon, which has the exact energy as the potential energy difference between the two shells (Chandler, 1977; 1979). In turn, an electron in an even higher orbital can fall to fill this new gap thus creating a cascade of falling electrons giving a spectrum of x-ray emissions from that atom (Chandler, 1979). Heavier atoms have more complex spectra due to the presence of more electron orbitals that allow more possible inter-shell transitions (Chandler, 1977).

The number of x-ray counts for a given peak is proportional to the number of atoms for that element in the area of sample being tested. The total number of counts in a peak includes background from the production of continuum or Bremsstrahlung x-rays (Bozzola and Russell, 1992). Continuum x-rays (also called white radiation) are produced by the deceleration of inelastically-scattered electrons as the beam electrons pass through the coulomb field of the nucleus (Bozzola and Russell, 1992). The intensity of the continuum is proportional to the atomic number of the atom as well as the electron beam energy (Goldstein *et al.*, 1981; Watt, 1985; Friel, 1995). The intensity of the x-ray energy also depends on the proximity of the passing electrons to the nucleus with higher energy x-rays produced when the electrons pass closer to the nucleus (Bozzola and Russell, 1992). Due to the overlap of characteristic and continuum x-rays it can be difficult to detect trace elements, especially at lower x-ray energies where the continuum x-rays are more prominent (Goldstein *et al.*, 1981).

To obtain the net counts for a given element, the background or continuum x-ray counts for that peak must be subtracted in order to get a representative value of the number of characteristic x-rays (Barbi, 1979). This is especially important for simultaneously studying several elements since each element has a different background and thus peak heights may be

similar while net counts are very different. A useful format to express peak values is in the form of peak-to-background (P/B) ratios, which have been defined as the number of counts above the background for a peak divided by the number of background counts (Ockenden and Lott, 1991). As this ratio becomes very small, the ability to distinguish a peak from the continuum x-rays becomes more difficult (Chandler, 1977). Using numerical values rather than visual comparisons of spectra allows compensations for variations in sample thickness and density in addition to reducing the effects of uneven sample topography on x-ray collection (Lott *et al.*, 1978b; Ockenden and Lott, 1991).

Using a STEM with an x-ray detector allows the researcher to accurately and easily select areas for EDX analysis within the tissue. One common way to prepare tissue for EDX analysis is to dehydrate, embed and section while trying to maintain the elemental integrity of the tissues to be sampled. Using a low-water-content preparation procedure, which involves starting with 80% ethanol to allow some initial swelling of dry tissue, results in better infiltration of seed tissues while maintaining water concentrations low enough so as to prevent the extraction of water-soluble phytates (Yatsu, 1983; Lott *et al.*, 1984). Using dry glass knives also prevents loss of elements, which may occur if sections are cut into water-filled boats (Skilnyk and Lott, 1992).

When analysing discrete spots the data is often portrayed as a spectrum of peaks, but x-ray data can also be displayed as a digital map when larger areas are scanned. These maps are useful to display the spatial distribution of elements within a sample and can be used to display concentration gradients (Friel, 1995). X-ray maps use x-rays produced through the same interaction of the electron beam and the sample as described earlier. Mapping is

different in that larger areas are scanned rather than discrete points (Friel, 1995). In this way maps can identify areas containing high concentrations of elements, which can then be analysed more fully using spot analysis (spectral EDX analysis). Traditionally, analog maps were used which simply display the distribution as a series of dots on a photograph (Friel, 1995). More modern maps (digital maps) take a digital image and each pixel within the image contains the number of x-rays collected (Friel, 1995). In this way digital mapping can produce maps where the elemental composition of every pixel can be used to produce maps of different elements giving each element a different colour (Friel, 1995). Digital mapping is, however, restricted in many systems due to peak overlaps for different elements. Various elements have overlapping x-ray energies and these usually cannot be separated in a map, which therefore prevents accurate estimations of their presence.

Globoids (or globoid crystals) are naturally electron-dense deposits within seed protein bodies and are composed of phytate. Due to their natural electron density and relatively large size, these inclusions are convenient particles for spectral EDX analysis. EDX analysis of globoids from different tissues and species have shown the presence of P, Mg and K with occasional storage of Ca, Mn, Na, Zn, Ba and Fe (Lott, 1984; Lott *et al.*, 1995a). Globoid composition has been studied in various tissues from several species including perisperm tissue, embryonic tissue, female gametophyte tissue, and endosperm (West and Lott, 1993b; Lott *et al.*, 1995b; West *et al.*, 1995). Variations in the elemental compositions of globoids have been found from species-to-species, organ-to-organ, tissue-to-tissue, cell-to-cell and within one cell (Lott, 1981; 1984).

Studying seeds from eleven *Pinus* species, West and Lott (1993b) found small

($\leq$ 0.33 μm in diameter) naturally electron-dense inclusions in membrane-bound structures resembling proplastids and termed them Fe-rich particles based on spectral EDX analysis. These inclusions were found throughout the female gametophyte and in the protoderm, ground meristem, procambium, shoot apex and root apex of the zygotic embryos (West and Lott, 1993b). These particles contained high P and Fe, moderate levels of K and Mg, and traces of Ca, Mn, and Zn (West and Lott, 1993b). Based on the similarities of EDX analysis spectra of Fe-rich particles, globoids and precipitated ferric phytate, West and Lott (1993b) proposed that these particles could represent storage deposits of Fe-rich phytate. The high levels of P also suggests that these deposits are not phytoferritin inclusions, which is a common storage compound found in chloroplasts (Pittermann *et al.*, 1996).

In this chapter digital x-ray mapping was used to illustrate elemental distributions within cells from different tissue regions in white spruce somatic embryos and seeds. In addition to this, the elemental compositions of globoids and Fe-rich particles in various regions of white spruce somatic embryos were investigated using spectral EDX analysis. These spectral EDX analysis results were compared to those from white spruce female gametophytes and zygotic embryos obtained by Reid (1996).

Materials and Methods

Tissue Preparation

The low-water-content preparation procedure of Lott *et al.* (1984) was used to prevent the loss of water-soluble phytate. Desiccated white spruce somatic embryos produced using normal maturation media (Batch 1 somatic embryos) described in Chapter 1 were removed from the filter paper using forceps and placed into 80% ethanol overnight. The embryos were then placed into 100% ethanol for at least 8 h and again in 100% ethanol overnight. To complete the dehydration the embryos were treated with propylene oxide for at least 7 h.

Using a standard hardness Spurr's epoxy resin, the embryos were infiltrated on a tissue rotator using a propylene oxide:Spurr's epoxy resin series (2:1, 1:2, 0:1 and 0:1) for 24 h in each solution. Following infiltration each embryo was sectioned into three regions (cotyledons, hypocotyl and radicle) and each region was placed into a separate rubber mold. All molds were filled with Spurr's resin and allowed to harden in a 70°C oven overnight. Previously studied white spruce zygotic embryos and female gametophytes were prepared using the above protocol (Reid, 1996).

A Reichert OM U2 ultramicrotome (Reichert, Austria) was used to cut thick sections (1-1.5 μm) using dry glass knives. Each section was flattened using eyelashes and cactus spines mounted on wooden sticks and picked up using 100 mesh Formvar-carbon coated copper grids. Drops of 100% ethanol were used to help the sections adhere to the Formvar.

Digital X-ray Mapping

Using the scanning mode of a JEOL-1200 EX-II TEMSCAN microscope (JEOL, Tokyo) and a PGT model IMIX-II microanalysis system (Princeton Gamma-Tech., Princeton, NJ), digital maps were collected at a magnification of 4,000 times. Each map was collected for 34 min. and 8 sec. resulting in a 512 K image containing 204,800 pixels.

Several maps were collected for ground meristem and procambium cells from the hypocotyl of a somatic and a zygotic embryo until a suitably flat area was found to yield a good map. In addition, an x-ray map was collected from female gametophyte tissue. Due to the relatively low amounts of storage material in the protoderm tissue, no maps were collected for this tissue region.

Each x-ray map consisted of P, K, Mg and Fe distributions. Calcium maps could not be used because the major x-ray energies for Ca are overlapped by the minor K x-ray energies. Large amounts of K within the tissue produces strong K signals and therefore strong overlap with Ca. The minor x-ray energies for Cu overlap the major x-ray energies for Zn and due to strong Cu signals from the Cu grids, Zn maps could not be used. There is also overlap of the major Fe x-ray energies with the Mn minor x-ray energies, but due to low levels of Mn within the tissue Fe maps were still useable. X-ray maps were collected by using the following x-ray energy ranges for each element: Mg, 1153.7-1354.3 eV; P, 1905.3-2120.7 eV; K, 3193.7-3432.3 eV; and Fe, 6259.9-6546.1 eV (Beecroft and Lott, 1996).

Spectral EDX Analysis of Globoids and Fe-rich Particles

EDX analysis was carried out at 80 kV and a magnification of 25,000 using the

scanning mode of the JEOL microscope and the PGT microanalysis system. All spectra were collected for 60 sec. with aperture, spot size, tilt and detector distance kept the same for all analyses. Only those spectra collected with greater than 1000 counts/sec. and less than 5% dead time were used.

For each of five somatic embryos, five spectra of globoids from different cells and of different sizes were collected from both the ground meristem and procambium in each of the cotyledon, hypocotyl and radicle regions. Additionally, for each of these same five embryos, five spectra of Fe-rich particles were collected from each of the protoderm, ground meristem and procambium in each of the cotyledon, hypocotyl and radicle regions. Therefore in total, 225 spectra of Fe-rich particles and 150 spectra of globoids were collected.

X-ray counts for all the spectra were collected by integrating the peaks at the selected window widths from Beecroft and Lott (1996): Mg, 1153.7-1354.3 eV; P, 1905.3-2120.7 eV; K, 3193.7-3432.3 eV; Ca, 3568.6-3813.4 eV; Mn, 5758.5-6037.5 eV; Fe, 6259.9-6546.1 eV; Cu, 7891.7-8200.3 eV; and Zn, 8478.9-8795.1 eV. In order to produce the best fit background line for all elements, points were connected at the following eV values: 510, 660, 814, 1453, 1730, 2500, 2800, 3020, 4200, 5400, 8400, 9400 and 11 000 eV (modified from Stewart *et al.*, 1988). Background subtraction was performed for each element in each spectrum by subtracting the number of counts in the background from the total number of counts in the element. Peak-to-background ratios were calculated for each element in each spectrum by using the total number of counts before and after subtraction (Stewart *et al.*, 1988). Ratios of elements to P were also calculated since P represents the main anion to which the elements are bound in phytate.

Due to peak overlaps, correction factors were used to calculate the actual Ca, Fe, and Zn counts in each spectrum. The K_β peak of K overlaps the K_α peak of Ca, therefore a correction factor of 8.80% of the total x-ray counts for the K K_α peak was subtracted from the total counts in the Ca window to give the actual counts for Ca (Pittermann *et al.*, 1996). Similarly, the K_β peak of Mn overlaps the Fe K_α peak, therefore a correction factor of 11.60% of the total x-ray counts for Mn K_α peak was subtracted from the total counts in the Fe window to give a corrected Fe value (Pittermann *et al.*, 1996). Finally, the K_β peak of Cu overlaps the K_α peak of Zn, therefore 2.00% of the net Cu K_α counts was subtracted from the total Zn counts to give a corrected Zn value (Pittermann *et al.*, 1996).

The statistical significance of means was determined by using the MINITAB analysis of variance test. In cases where significance was established, Tukey's test was used to determine which of the means were statistically different at $P > 0.05$ (Zar, 1984). Due to the use of manually predetermined background points and relatively short sampling times, several negative counts were obtained for Ca, Mn, Fe and Zn P/B values as well as for the Ca:P and Fe:P ratios. For each P/B value and ratio, all the negative values from the 375 spectra collected were averaged and any means equal to or less than the absolute value of this mean were considered to be not significantly different from the background line and were assigned a value of zero. Peak-to-background values and ratios of P/B values for individual embryos were analysed to see if there were any significant variations from embryo-to-embryo.

MINITAB's two-sample t-test for the difference between two means at $P > 0.05$ was used to compare spectral EDX analysis values for somatic embryos to values from zygotic embryos, which were obtained under the same conditions used here (Reid, 1996). In the first

comparison, all the globoids in somatic embryos were pooled together and compared to all the globoids pooled together for zygotic embryos. Each element P/B value and each ratio of an element to P in somatic embryo globoids were compared to the corresponding value in zygotic embryo globoids. This was repeated for Fe-rich particles. In the second comparison, P/B values and ratios to P in globoids from the cotyledon procambium of somatic embryos were compared to corresponding values for globoids in the cotyledon procambium of zygotic embryos. This second comparison was repeated for each particle type in each tissue from each embryo region studied.

Results

Naturally electron-dense globoids were found in the ground meristem and procambium in the cotyledons, hypocotyl and radicle regions of somatic embryos. Typically, globoids were found to be 0.5 to 2.0 μm in diameter (Figs. 19 and 20), but were occasionally observed to be 3.0 μm in diameter. Generally only one globoid was observed per protein body, but occasionally as many as three were visible in a section of a protein body. Fe-rich particles were found in the protoderm, ground meristem and procambium from the cotyledons, hypocotyl and radicle regions. Typically Fe-rich particles were 0.14 to 0.25 μm in diameter and were also naturally electron-dense (Figs. 19 and 20). Globoids and Fe-rich particles were found in similar regions of zygotic embryos (Fig. 21) and throughout the female gametophyte (globoids illustrated in Fig. 22) (Reid, 1996). In zygotic embryos globoids ranged from 0.5 to 3 μm in diameter with one to three globoids per section of a protein body. Globoids in zygotic embryos were, however, commonly found to be between 2 and 3 μm in diameter. In female gametophytes, globoids ranged from 0.5 to 6.0 μm in diameter and often more than one were found per section of a protein body. All Fe-rich particles were less than 0.33 μm in diameter in seeds and not found in clusters like globoids.

Ground meristem cells in zygotic embryos (Fig. 23) and somatic embryos (Fig. 24) contained globoids of variable sizes. Globoids in zygotic embryo tissues were commonly larger and more variable in size than those in somatic embryos. Fe-rich particles were also discernable at lower magnifications in sections from both somatic and zygotic embryos. Procambium cells also contained globoids and Fe-rich particles in zygotic embryos (Fig. 25) and somatic embryos (Fig. 26). Generally, globoids were smaller in procambium cells than

in ground meristem cells. Occasionally, larger globoids were found in the procambium cells of zygotic embryos than in somatic embryo procambial tissue. Female gametophyte tissue contained protein bodies, which frequently contained numerous globoids and globoids of very different sizes (Fig. 27). Typical protoderm cells contained little if any electron-dense storage material (Fig. 28). When Fe-rich particles were found, typically no more than 2 or 3 were observed per section of a single protoderm cell.

Figures 29 and 30 illustrate digital x-ray maps for cells in the ground meristem from the hypocotyl of a zygotic embryo and somatic embryo, respectively. In zygotic embryos the globoids were often larger and more frequent than in somatic embryos. In addition to P, K and Mg, globoids in zygotic embryos showed traces of Fe, which were not found in maps for somatic embryos. Fe-rich particles containing P and Fe were found in both types of embryos at similar frequencies and occasionally contained some K in the zygotic embryo ground meristem map (Fig. 29).

Digital x-ray maps of procambium tissue for a zygotic embryo and a somatic embryo are shown in Figs. 31 and 32, respectively. Globoids were more numerous in procambium cells of zygotic embryos compared to somatic embryos (Compare Fig. 31 to 32). In both types of embryos the globoids were generally smaller in the procambium than in the ground meristem (Compare Fig. 29 to 31 and 30 to 32). Globoids in the procambium of both embryos contained P, K and Mg. Fe-rich particles contained Fe, but occasionally identifiable levels of P were also detected (Fig. 31).

Female gametophyte tissue produced digital x-ray maps as shown in Fig. 33. Globoids ranged in size and were frequently larger than any globoid observed in embryo

Figures 19 to 22: Scanning Transmission Electron Micrographs of Globoids and Fe-rich Particles From White Spruce Somatic Embryos, Zygotic Embryos and Female Gametophytes.

Figure 19: Thick section (1-1.5 μm) of the ground meristem of the radicle region from a somatic embryo. Globoids (G) that are variable in size and smaller Fe-rich particles (F) are visible. Scale bar = 2 μm.

Figure 20: Thick section (1-1.5 μm) of somatic embryo hypocotyl ground meristem tissue, fixed using the low-water-content preparation procedure, showing naturally electron-dense globoids (G), located within protein bodies (P), and naturally electron-dense Fe-rich particles (F). Scale bar = 2 μm.

Figure 21: Thick section (1-1.5 μm) from the hypocotyl ground meristem of a zygotic embryo. This micrograph illustrates naturally electron-dense globoids (G) within protein bodies (P) and smaller naturally electron-dense Fe-rich particles (F). Scale bar = 2 μm.

Figure 22: Micrograph of female gametophyte tissue. This micrograph illustrates protein bodies (P) containing globoids (G) ranging in size from 1 to 5.5 μm in diameter. Scale bar = 4 μm.

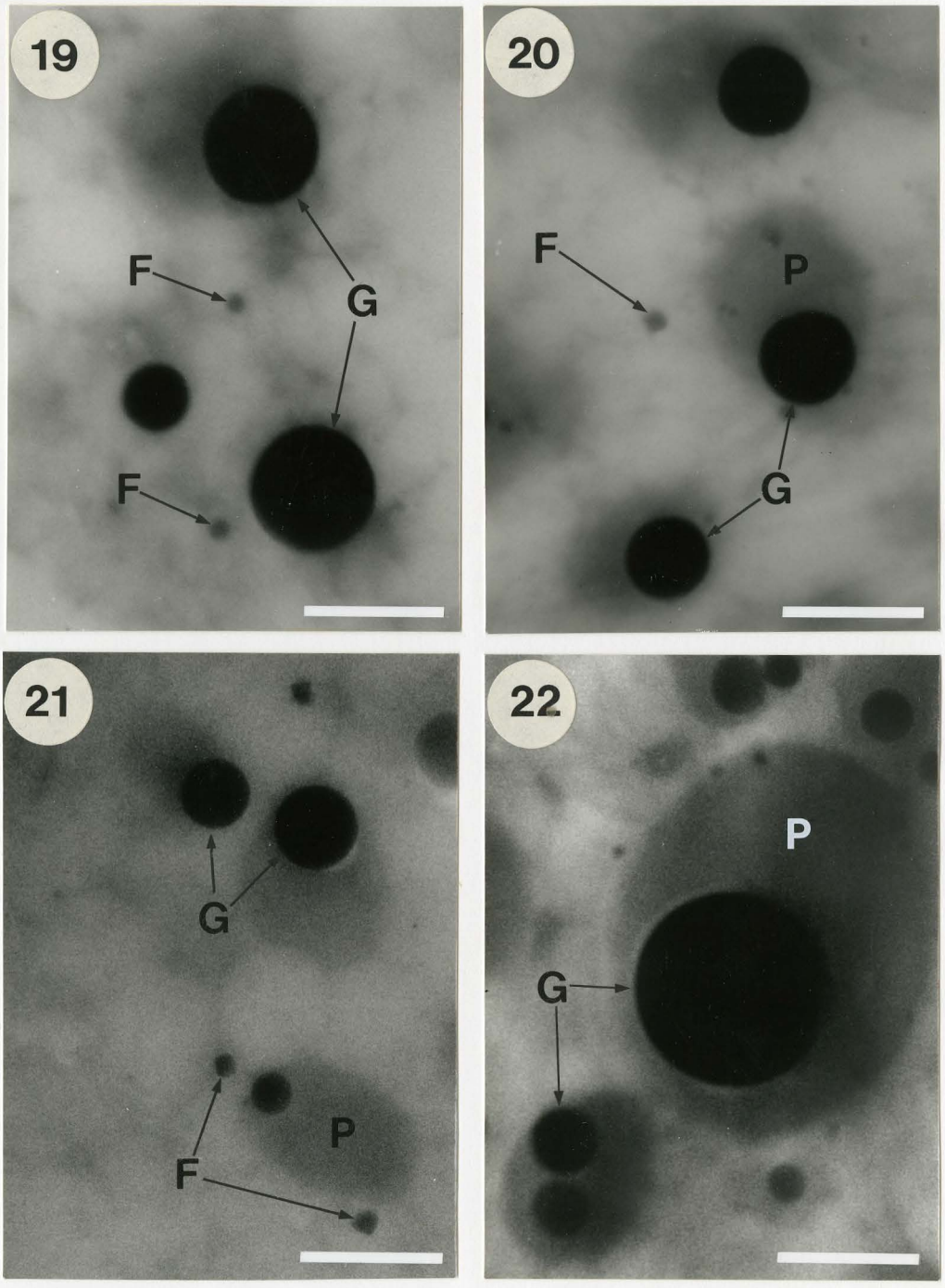
19
F
G
F
20
F
P
G
21
G
P
F
22
P
G

Figures 23 to 28: Scanning Transmission Electron Micrographs of Typical Cells Within White Spruce Somatic Embryos, Zygotic Embryos and Female Gametophytes.

Figure 23: Typical ground meristem cell from the hypocotyl of a zygotic embryo. This micrograph illustrates numerous globoids (G) of variable size and small Fe-rich particles (F) within a single cell. Scale bar = 5 μm.

Figure 24: Ground meristem cell from the hypocotyl of a somatic embryo. Note the multiple globoids (G) and small Fe-rich particles (F). Scale bar = 5 μm.

Figure 25: Elongated hypocotyl procambial cells from a zygotic embryo. Several globoids (G) variable in size are visible as are numerous Fe-rich particles (F). Scale bar = 5 μm.

Figure 26: Typical elongated procambial cells from the hypocotyl region of a somatic embryo. Note occurrence of globoids (G) more uniform in size than in zygotic embryos (Fig. 25). Fe-rich particles (F) are also seen within these cells. Scale bar = 5 μm.

Figure 27: Micrograph of female gametophyte tissue from a seed. This micrograph illustrates the large range in size of globoids (G) and multiple globoids within a single protein body (P). Note the decreased frequency of Fe-rich particles in comparison to embryo tissues. Scale bar = 5 μm.

Figure 28: Protodermal cell from the hypocotyl of a somatic embryo. Note the globoids (G) in the first layer of ground meristem but the absence of naturally-electron dense deposits within the protoderm (Pt). Scale bar = 5 μm.

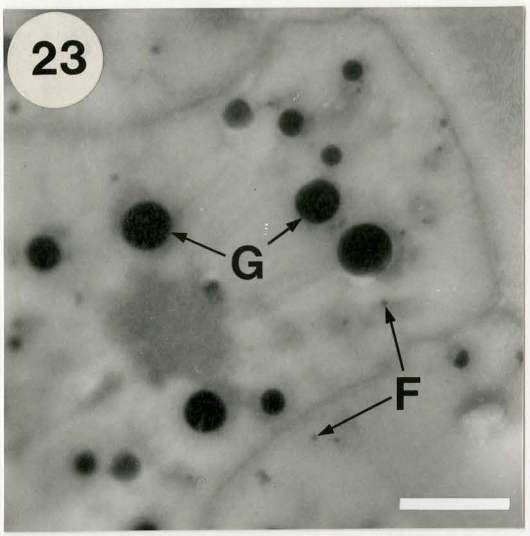
23
G
F

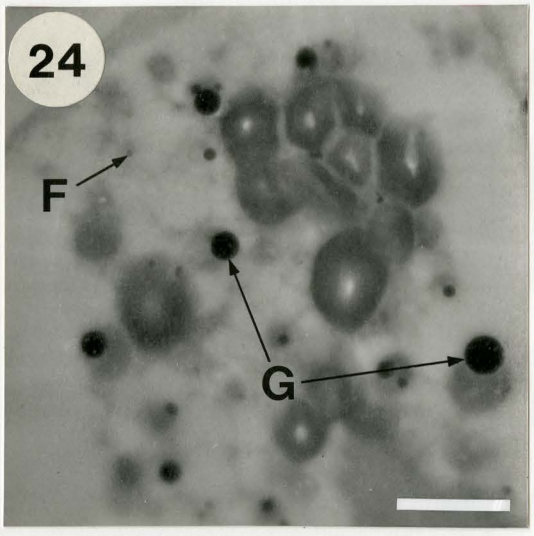
24
F
G

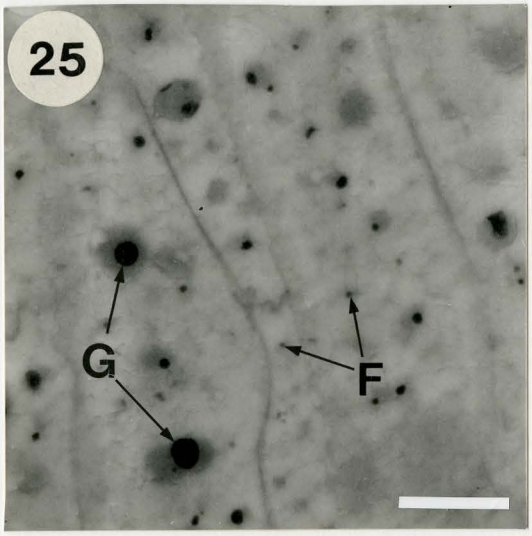
25
G
F

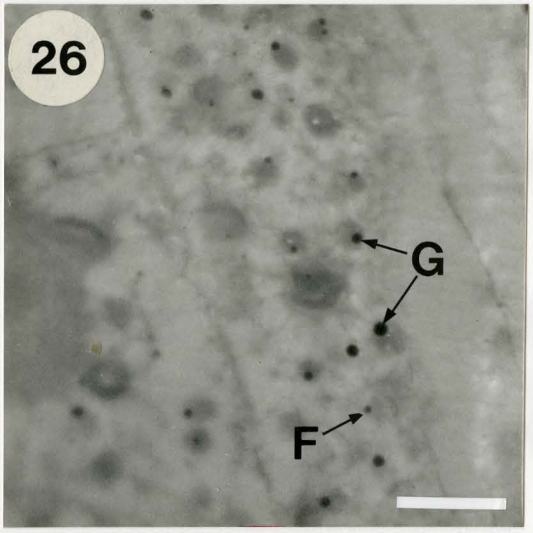
26
G
F

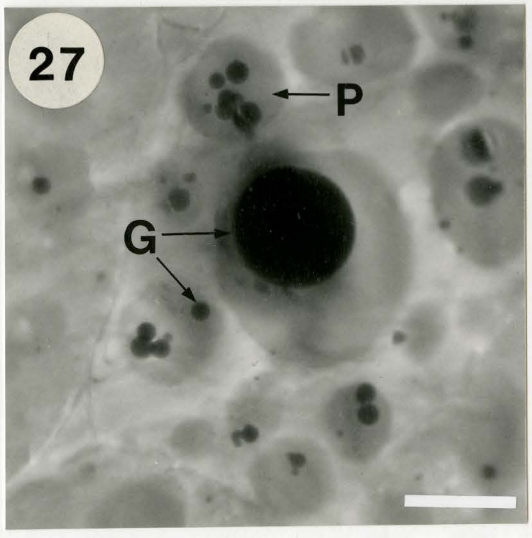
27
P
G

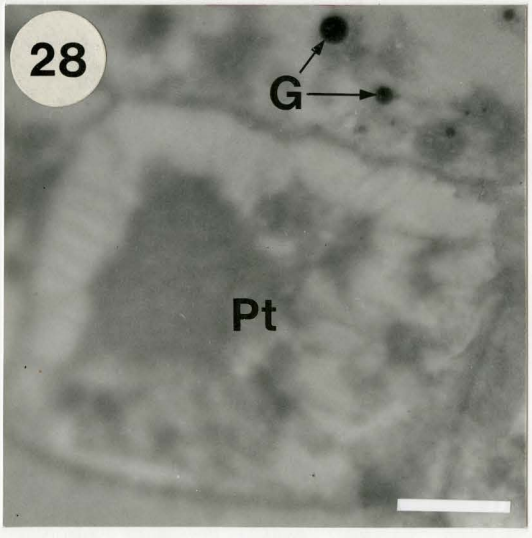
28
G
Pt

Figures 29 to 33: Digital X-ray Maps of Cells from White Spruce Somatic Embryos, Zygotic Embryos and Female Gametophyte Tissue.

Figure 29: Typical ground meristem cell from the hypocotyl of a zygotic embryo. Note the numerous globoids (g) containing P, K, Mg and traces of Fe. Fe-rich particles (arrowheads) show P, Fe and sometimes identifiable K. Magnification = 1200x.

Figure 30: Typical ground meristem cell from the hypocotyl of a somatic embryo. Note the globoids (g) containing P, K and Mg; and the Fe-rich particles (arrowheads) with P and Fe. Magnification = 1200x.

Figure 31: X-ray map of the procambium tissue in a zygotic embryo. This map shows P, K and Mg in globoids (g); and P and Fe in Fe-rich particles (arrowheads). Magnification = 1200x.

Figure 32: Digital x-ray map of somatic embryo hypocotyl procambium tissue. Globoids (g) containing P, K and Mg; and Fe-rich particles (arrowheads) containing Fe are illustrated in this map. Magnification = 1200x.

Figure 33: X-ray map of female gametophyte tissue from a seed. Note the large globoids (g) containing P, K, Mg and Fe; but no visible Fe-rich particles. Magnification = 1200x.

29

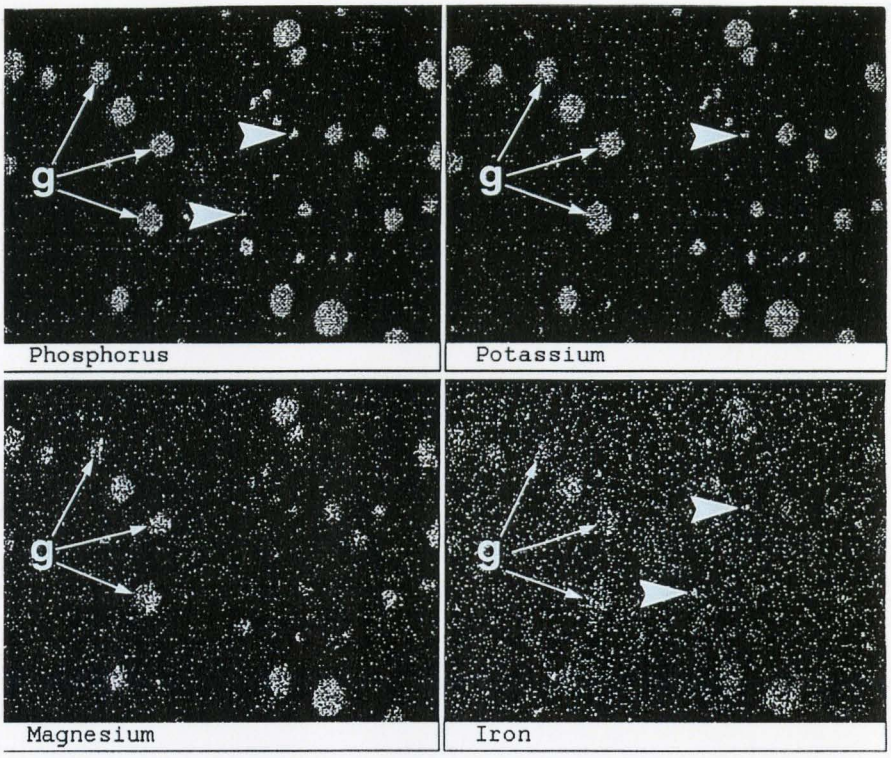
g
g
Phosphorus
Potassium
g
g
Magnesium
Iron

30

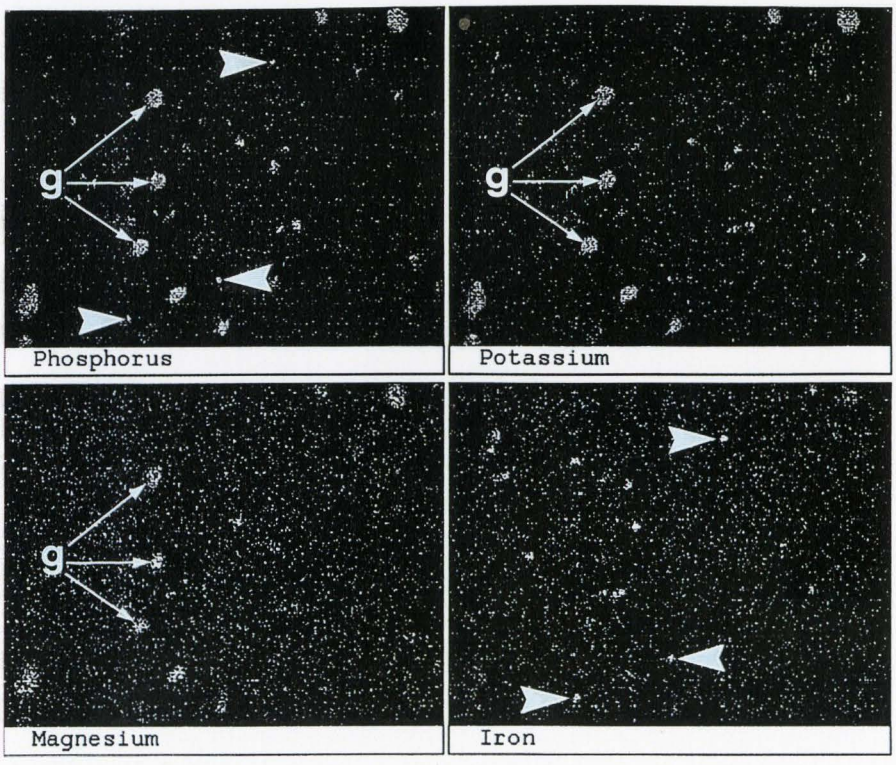
g
g
Phosphorus
Potassium
g
Magnesium
Iron

31

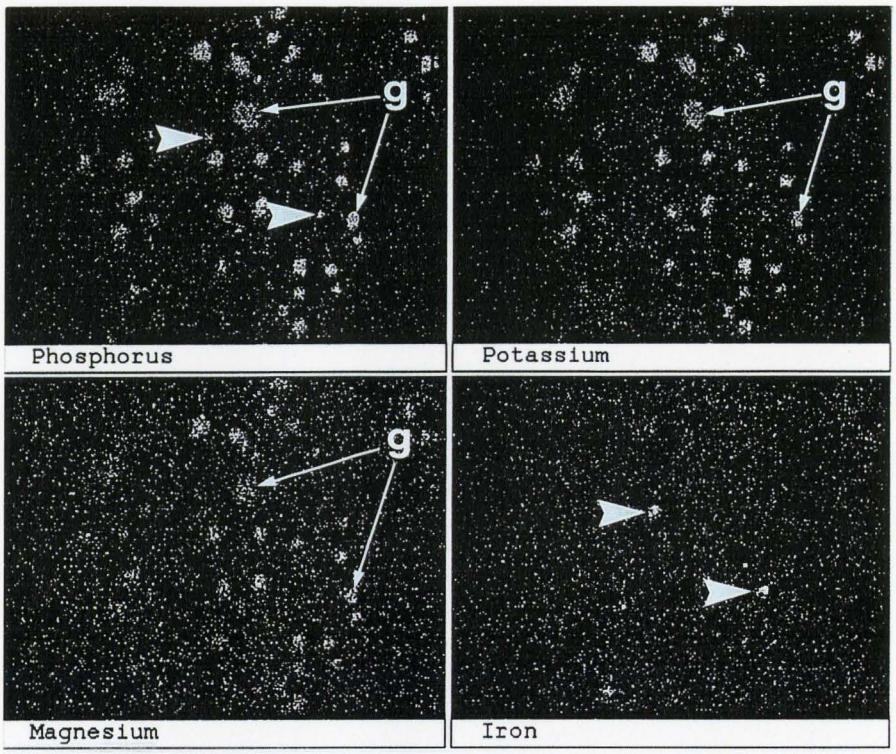
g
g
g
Phosphorus
Potassium
Magnesium
Iron

32

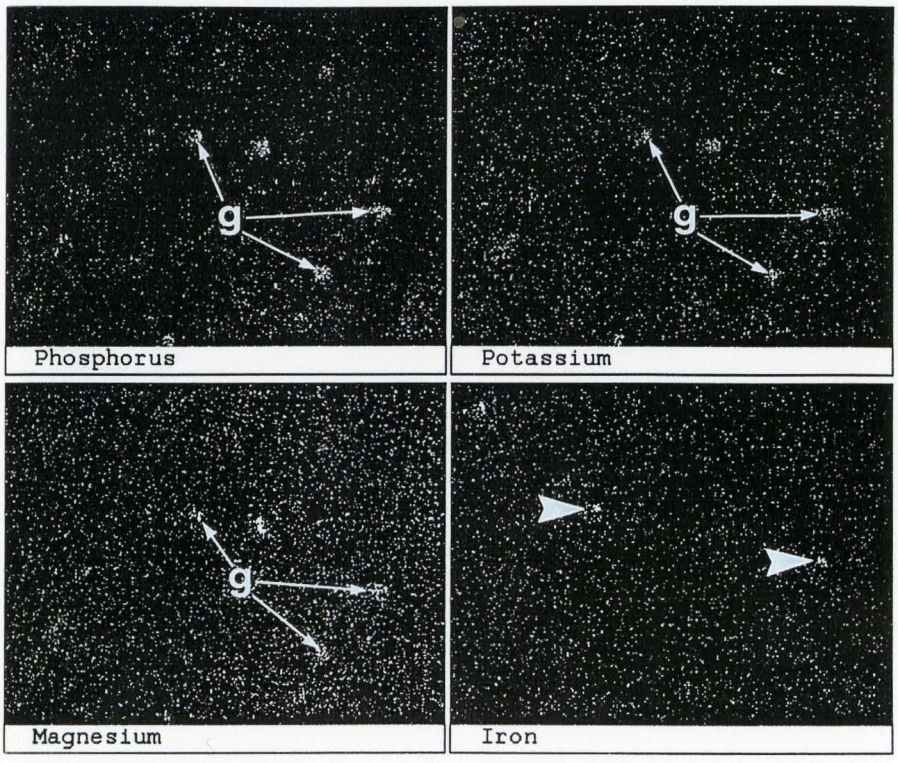
g
g
g
Phosphorus
Potassium
Magnesium
Iron

33

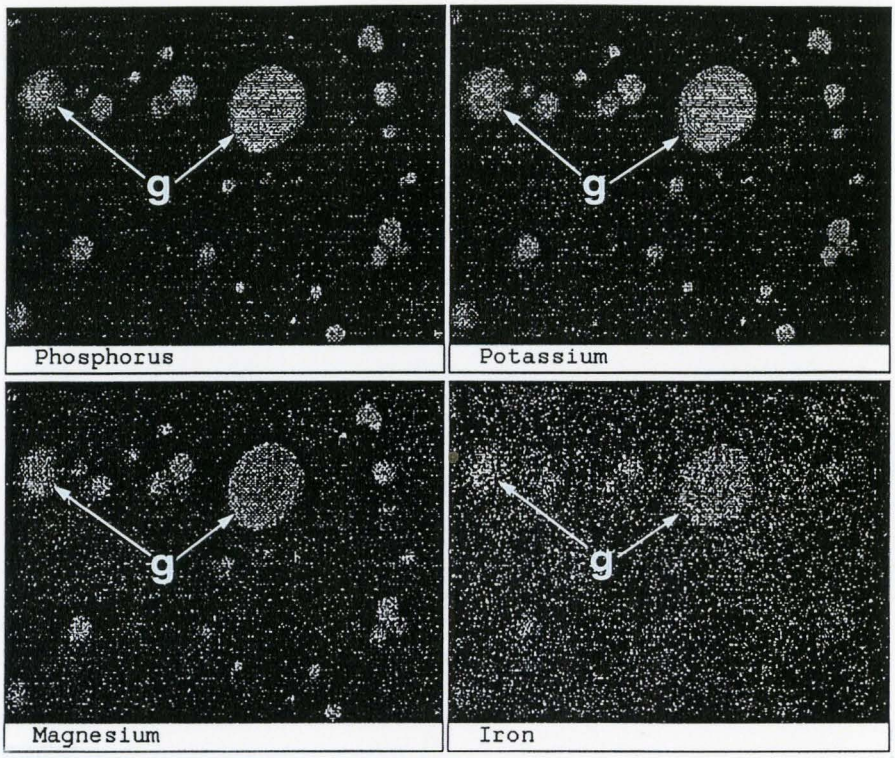

tissues. Globoids contained P, K, Mg and frequently Fe. Note that the map of female gametophyte tissue showed no detectable Fe-rich particles. No maps of protodermal cells were illustrated here due to the lack of significant mineral nutrient storage material.

Comparison of typical EDX analysis spectra (based on P/B values) of globoids from zygotic embryos (Fig. 34) with that from somatic embryos (Fig. 35), shows similar compositions. Typical globoids contained high levels of P with moderate levels of Mg and K (Figs. 34 and 35). This composition was also typical of globoids sampled from female gametophytes (Reid, 1996). One exception to this typical composition was that globoids from the procambium of zygotic embryo cotyledons contained moderate levels of Fe and slightly reduced K and Mg (Fig. 36). Spectra of globoids from the same tissue region in somatic embryos showed no significant levels of Fe and more typical K and Mg levels (Fig. 37).

Fe-rich particles in somatic embryos were found to be similar in composition to those studied in zygotic embryos and female gametophytes (Reid, 1996). All Fe-rich particles contained high P and Fe with moderate to low levels of K and Mg. Fe-rich particles sampled from seeds typically had Fe peaks higher than P peaks (Fig. 38) (Reid, 1996). Typical Fe-rich particles from somatic embryos had P peaks higher than Fe peaks (Fig. 39). Although Fe-rich particles in seeds and somatic embryos differed in the proportions of P to Fe, particles of similar P and Fe proportions were found in both seeds and somatic embryos (Figs. 40 and 41). Comparison of globoid spectra (Figs. 34 to 37) with Fe-rich particle spectra (Figs. 38 to 41), show that K and Mg peaks were often slightly lower in Fe-rich particles.

Figures 34 to 41: EDX Analysis Spectra of Globoids (> 0.03 μm) and Fe-rich Particles (≤ 0.03 μm) From Thick Sections of White Spruce Zygotic and Somatic Embryos.

The energy lines for each element illustrated are as follows: Mg (K_α = 1.2 keV), P (K_α = 2.0 keV), Cl (K_α = 2.6 keV), K (K_α = 3.3 keV, K_β = 3.6 keV), and Fe (K_α = 6.4 keV, K_β = 7.1 keV). Note the peaks at 8.0 keV and 8.9 keV are the Cu K_α and Cu K_β peaks, respectively, from the copper grids used for holding the sections.

Figure 34: Typical EDX analysis spectrum of a globoid from the hypocotyl ground meristem tissue of a zygotic embryo (From Reid, 1996).

Figure 35: EDX analysis spectrum of a typical globoid from the hypocotyl ground meristem tissue of a somatic embryo.

Figure 36: EDX analysis spectrum of a globoid from the cotyledon procambium tissue of a zygotic embryo showing high Fe levels (From Reid, 1996).

Figure 37: EDX analysis spectrum of a globoid from the cotyledon procambium tissue of a somatic embryo showing no detectable Fe levels.

Figure 38: Typical EDX analysis spectrum of an Fe-rich particle from the radicle ground meristem of a zygotic embryo showing the P peak lower than the Fe peak (From Reid, 1996).

Figure 39: Typical EDX analysis spectrum of an Fe-rich particle from the radicle ground meristem of a somatic embryo showing a higher Fe peak than P peak.

Figure 40: EDX analysis spectrum of an Fe-rich particle from the radicle procambium of a zygotic embryo (From Reid, 1996).

Figure 41: EDX analysis spectrum of an Fe-rich particle from the radicle procambium of a somatic embryo showing similar proportions of P and Fe as illustrated in Fig. 40.

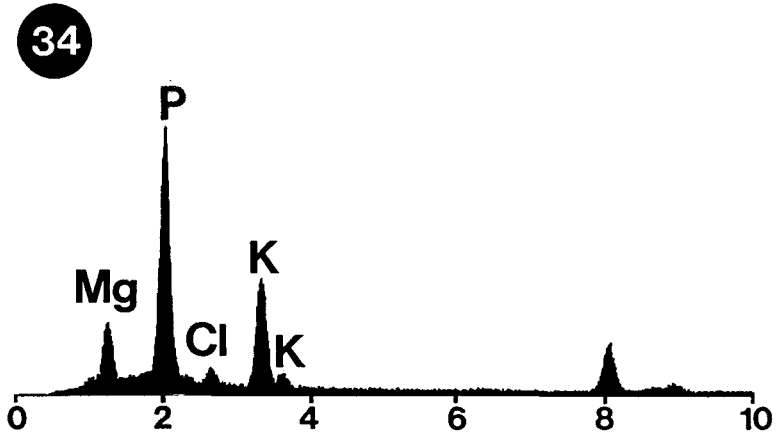
34
P
Mg
Cl
K
K
0
2
4
6
8
10

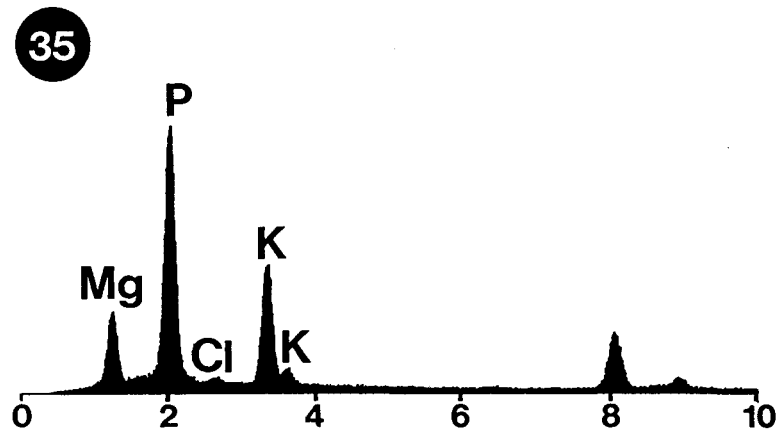
35
P
Mg
Cl
K
K
0
2
4
6
8
10

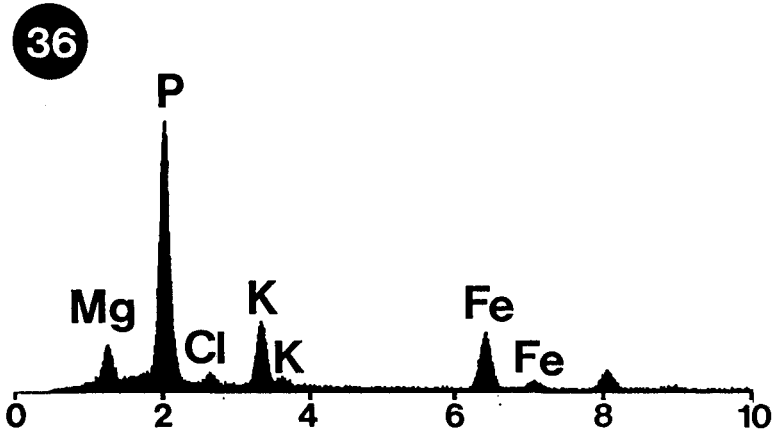
36
P
Mg
Cl
K
K
Fe
Fe
0
2
4
6
8
10

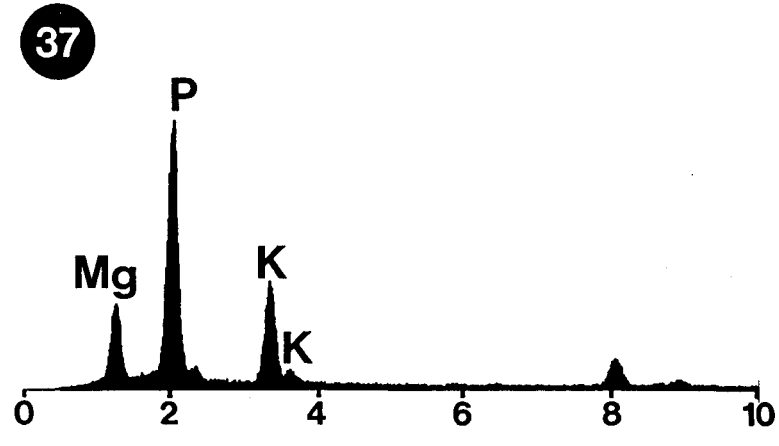
37
P
Mg
K
K
0
2
4
6
8
10

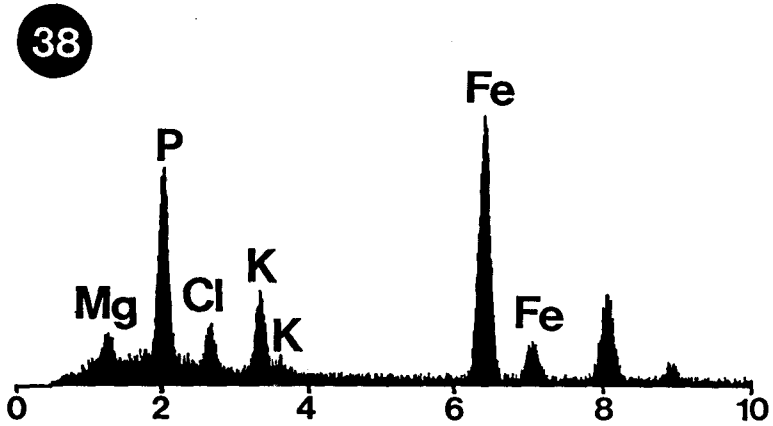
38
Fe
P
Mg
Cl
K
K
Fe
0
2
4
6
8
10

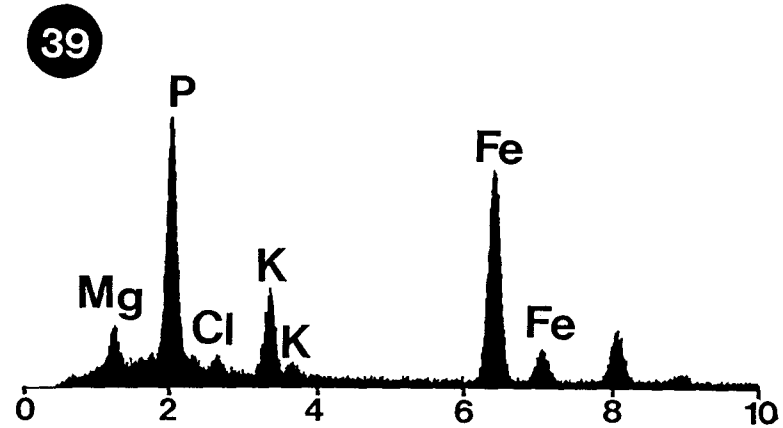
39
P
Fe
Mg
Cl
K
K
Fe
0
2
4
6
8
10

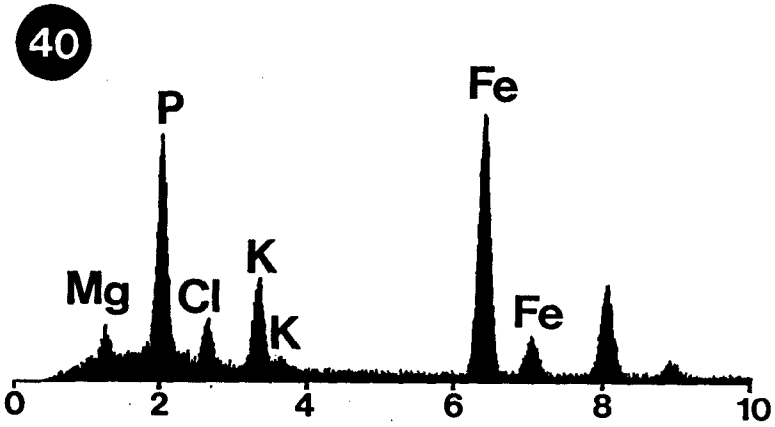
40
Fe
P
Mg
Cl
K
K
Fe
0
2
4
6
8
10

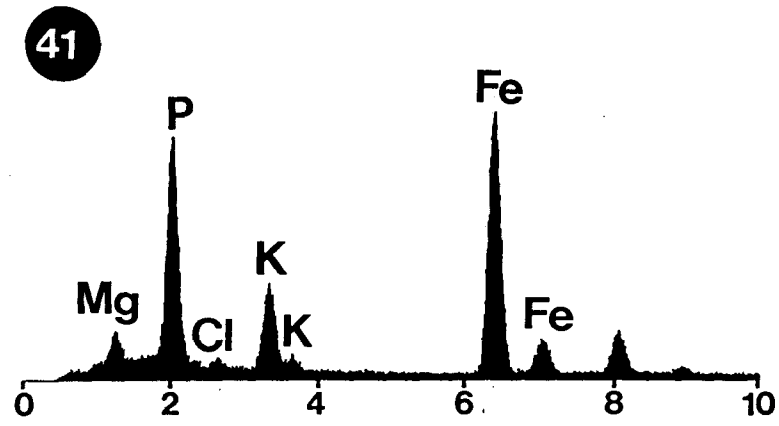
41
Fe
P
Mg
Cl
K
K
Fe
0
2
4
6
8
10

For each of the five somatic embryos sampled, the P/B values and ratios of P/B values are given in Appendix A. No significant differences were found from embryo-to-embryo. The majority of the variation was from particle-to-particle. The mean P/B values for the five somatic embryos combined are illustrated in Table 8. Globoids were found to have mean P/B values for P greater than 10.00 except in the procambium from the hypocotyl and radicle regions. Globoids in the ground meristem of the hypocotyl and radicle regions contained higher K levels than in other regions and all globoids contained very little Fe and Zn. One exception was the presence of higher Zn levels in the cotyledon procambium globoids.

Fe-rich particles had mean P/B values for P ranging from 4.39 to 5.51, which was significantly lower than found in globoids. Fe-rich particles had very high Fe levels with those in the radicle ground meristem having the highest Fe values. Globoids contained higher K and Mg than Fe-rich particles; and in all particles the Ca levels were very low in comparison to P, K and Mg levels. Fe-rich particles contained little if any detectable Zn.

Table 9 summarizes the mean ratios of P/B values for five somatic embryos. Globoids from different regions all had K:P values greater than 0.55 and Mg:P values ranging from 0.41 to 0.46. The Ca:P ratio was very low (less than 0.13) in globoids and both the Fe:P and Zn:P ratios were near or equal to zero. The K:P, Ca:P and Zn:P ratios in Fe-rich particles were very similar to those found for globoids while the Mg:P ratio was lower in Fe-rich particles than in globoids. The Fe:P ratio was higher in Fe-rich particles (between 2.4 and 3.14) than in globoids (between 0.01 and 0.02).

Appendix B shows the P/B values and ratios of P/B values for white spruce zygotic embryos and female gametophytes (Reid, 1996). Globoids and Fe-rich particles in female

gametophytes had similar compositions to those found in somatic and zygotic embryos. Results from the two-sample t-test for P/B values from entire somatic embryos versus entire zygotic embryos are given in Table 10 with raw numbers given in Appendix C. In general, globoids in zygotic embryos had significantly higher P/B values for P, K and Fe than globoids in somatic embryos. Globoids in somatic embryos did show significantly higher Ca P/B values, but Ca levels were very low in globoids from both types of embryos. Fe-rich particles had higher P and K in somatic embryos and higher Zn levels in zygotic embryos, although Zn levels were very low.

Two-sample t-test results for ratios of P/B values for globoids and Fe-rich particles in entire embryos are illustrated in Table 11 with raw numbers given in Appendix C. This comparison showed higher Mg:P and Ca:P ratios in globoids from somatic embryos. The Ca:P ratios for globoids were very low due to low Ca levels. The Fe:P ratio for globoids was especially high in zygotic embryo globoids (10 times higher than in somatic embryos). Ratios of P/B values for Fe-rich particles found that in zygotic embryos the following ratios were higher: Mg:P, Ca:P, Fe:P, and Zn:P. Again the Ca:P and Zn:P ratios were very low for Fe-rich particles in both types of embryos.

Table 12 summarizes the comparison of P/B values from particles in the same tissues in zygotic and somatic embryos using MINITAB's two-sample t-test. When there were significant differences in P for globoids, higher P values were found in zygotic embryos. One exception was that globoids in the cotyledon procambium had significantly higher P in somatic embryos than in zygotic embryos. When significant differences were found in K and Mg these values were higher in globoids from zygotic embryos. Globoids from the cotyledon

procambium, however, had higher Mg levels in somatic embryos. Fe-rich particles had higher P, K and Mg values in somatic embryos. Although Ca was generally very low in both types of particles, when significant differences were found the somatic embryos commonly had the higher levels. Also for both types of particles, when differences were found in Fe and Zn levels they were generally higher in zygotic embryos.

Results from MINITAB's two-sample t-test for ratios of P/B values are illustrated in Table 13. The K:P ratio was found to be not significantly different in the majority of the regions studied. When significant differences were found in particles tested, zygotic embryos had higher K:P values in procambium tissues. Several regions were found to have significantly different Mg:P ratios between the two embryo types. Fe-rich particles in the ground meristem of the cotyledons, hypocotyl and radicle had higher Mg:P ratios in zygotic embryos while globoids in these same regions had higher Mg:P ratios in somatic embryos. The Ca:P ratios showed no clear trends, but when differences were found to be statistically different, somatic embryos frequently had higher levels than zygotic embryos. The Fe:P ratios were found to be significantly higher for zygotic embryos in 11 out of the 15 tested particle locations. Due to the relatively low levels, the Zn:P ratio showed no clear trend.

Table 8: Mean (± SD) peak-to-background ratios of elements in globoids (> 0.33 μm) and Fe-rich particles (≤ 0.33 μm) for various tissues from thick sections of five white spruce somatic embryos.

Organ	Tissue	Particle	P	K	Mg	Ca	Fe	Zn
Cotyledons	Protoderm	Fe-rich Particle	4.39 ± 1.10 **d**	2.62 ± 0.77 **e**	0.88 ± 0.30 **d**	0.53 ± 0.16 **ab**	12.78 ± 3.62 **b**	NS **c**
	Ground Meristem	Fe-rich Particle	5.51 ± 1.56 **d**	3.06 ± 1.16 **e**	1.17 ± 0.38 **d**	0.37 ± 0.25 **bcde**	14.56 ± 4.38 **b**	NS **c**
		Globoid	10.30 ± 2.10 **ab**	6.07 ± 1.39 **bc**	4.18 ± 1.03 **b**	0.37 ± 0.26 **bcde**	0.24 ± 0.18 **a**	0.25 ± 0.26 **bc**
	Procambium	Fe-rich Particle	4.80 ± 1.38 **d**	2.71 ± 1.07 **e**	1.07 ± 0.32 **d**	0.37 ± 0.24 **bcde**	13.94 ± 4.89 **b**	NS **c**
		Globoid	10.21 ± 1.73 **ab**	6.42 ± 1.87 **b**	4.37 ± 0.96 **ab**	0.24 ± 0.15 **def**	0.08 ± 0.08 **a**	0.86 ± 1.00 **a**
Hypocotyl	Protoderm	Fe-rich Particle	4.84 ± 1.10 **d**	3.02 ± 0.82 **e**	1.00 ± 0.18 **d**	0.60 ± 0.16 **a**	13.97 ± 3.85 **b**	NS **c**
	Ground Meristem	Fe-rich Particle	4.74 ± 1.46 **d**	3.55 ± 1.14 **de**	1.02 ± 0.31 **d**	0.31 ± 0.24 **cdef**	13.62 ± 4.51 **b**	NS **c**
		Globoid	11.10 ± 2.10 **a**	8.78 ± 2.52 **a**	4.61 ± 0.69 **ab**	0.17 ± 0.10 **f**	0.23 ± 0.17 **a**	0.14 ± 0.19 **bc**
	Procambium	Fe-rich Particle	4.74 ± 1.33 **d**	3.04 ± 0.78 **e**	1.03 ± 0.38 **d**	0.20 ± 0.12 **ef**	14.08 ± 5.25 **b**	NS **c**
		Globoid	8.67 ± 2.51 **bc**	6.31 ± 1.70 **bc**	3.51 ± 1.13 **c**	0.27 ± 0.15 **def**	0.08 ± 0.12 **a**	0.45 ± 0.53 **b**
Radicle	Protoderm	Fe-rich Particle	4.83 ± 1.25 **d**	3.40 ± 1.03 **e**	0.98 ± 0.22 **d**	0.47 ± 0.16 **abc**	14.65 ± 4.62 **b**	NS **c**
	Ground Meristem	Fe-rich Particle	5.21 ± 1.97 **d**	3.40 ± 1.40 **e**	1.10 ± 0.37 **d**	0.33 ± 0.23 **cdef**	16.35 ± 6.62 **b**	NS **c**
		Globoid	10.58 ± 1.85 **a**	8.29 ± 2.04 **a**	4.82 ± 1.02 **a**	0.41 ± 0.31 **abcd**	0.09 ± 0.20 **a**	0.32 ± 0.48 **bc**
	Procambium	Fe-rich Particle	4.85 ± 2.02 **d**	3.18 ± 1.46 **e**	1.01 ± 0.39 **d**	0.35 ± 0.27 **bcdef**	14.44 ± 6.05 **b**	NS **c**
		Globoid	7.41 ± 2.16 **c**	4.90 ± 1.91 **cd**	3.19 ± 0.74 **c**	0.25 ± 0.10 **def**	0.11 ± 0.18 **a**	NS **c**

Note: 25 spectra were used for each mean. Values in the same column that are followed by the same letter are not significantly different at $P > 0.05$. NS indicates values determined not to be significantly different from the background.

Table 9: Ratios (± SD) of K to P, Mg to P, Ca to P, Fe to P, and Zn to P from peak-to-background ratios for thick sections of five resin embedded white spruce somatic embryos.

Organ	Tissue	Particle	K:P	Mg:P	Ca:P	Fe:P	Zn:P
Cotyledons	Protoderm	Fe-rich Particle	0.60 ± 0.11 **de**	0.20 ± 0.05 **b**	0.13 ± 0.03 **a**	2.94 ± 0.57 **bc**	NS **c**
	Ground Meristem	Fe-rich Particle	0.55 ± 0.14 **e**	0.21 ± 0.04 **b**	0.07 ± 0.04 **bcd**	2.64 ± 0.40 **c**	NS **c**
		Globoid	0.62 ± 0.20 **cde**	0.41 ± 0.06 **a**	0.04 ± 0.03 **def**	0.02 ± 0.02 **a**	0.02 ± 0.03 **bc**
	Procambium	Fe-rich Particle	0.57 ± 0.14 **e**	0.23 ± 0.04 **b**	0.08 ± 0.05 **bc**	2.87 ± 0.45 **bc**	NS **c**
		Globoid	0.64 ± 0.20 **bcde**	0.43 ± 0.06 **a**	0.02 ± 0.02 **ef**	0.01 ± 0.01 **a**	0.08 ± 0.10 **a**
Hypocotyl	Protoderm	Fe-rich Particle	0.63 ± 0.11 **bcde**	0.21 ± 0.03 **b**	0.13 ± 0.03 **a**	2.89 ± 0.49 **bc**	NS **c**
	Ground Meristem	Fe-rich Particle	0.78 ± 0.19 **abc**	0.22 ± 0.05 **b**	0.06 ± 0.05 **cde**	2.87 ± 0.39 **bc**	NS **c**
		Globoid	0.80 ± 0.22 **a**	0.42 ± 0.06 **a**	0.02 ± 0.01 **f**	0.02 ± 0.02 **a**	NS **c**
	Procambium	Fe-rich Particle	0.66 ± 0.13 **abcde**	0.22 ± 0.05 **b**	0.04 ± 0.03 **def**	2.93 ± 0.64 **bc**	NS **c**
		Globoid	0.76 ± 0.19 **abcd**	0.41 ± 0.08 **a**	0.03 ± 0.02 **ef**	0.01 ± 0.02 **a**	0.05 ± 0.07 **ab**
Radicle	Protoderm	Fe-rich Particle	0.70 ± 0.09 **abcde**	0.21 ± 0.04 **b**	0.10 ± 0.04 **ab**	3.05 ± 0.54 **b**	NS **c**
	Ground Meristem	Fe-rich Particle	0.65 ± 0.11 **abcde**	0.22 ± 0.04 **b**	0.07 ± 0.04 **bcd**	3.14 ± 0.43 **b**	NS **c**
		Globoid	0.79 ± 0.16 **ab**	0.46 ± 0.07 **a**	0.04 ± 0.03 **def**	0.01 ± 0.02 **a**	0.03 ± 0.05 **bc**
	Procambium	Fe-rich Particle	0.66 ± 0.13 **abcde**	0.22 ± 0.07 **b**	0.07 ± 0.05 **bcd**	3.01 ± 0.40 **b**	NS **c**
		Globoid	0.66 ± 0.16 **abcde**	0.44 ± 0.06 **a**	0.04 ± 0.02 **def**	0.01 ± 0.02 **a**	NS **c**

Note: 25 spectra were used for each mean. Values in the same column that are followed by the same letter are not significantly different at $P > 0.05$. NS indicates values determined not to be significantly different from the background.

Table 10: Comparison of peak-to-background ratios for somatic and zygotic embryos using MINITAB's two-sample t-test. This comparison compares all the globoids and Fe-rich particles tested from somatic embryos to all the globoids and Fe-rich particles tested from zygotic embryos. Embryo names in bold indicate which embryo type had a significantly higher mean at P > 0.05.

Particle Type	P	K	Mg	Ca	Fe	Zn
Globoids	**Zygotic**	**Zygotic**	NS	**Somatic**	**Zygotic**	NS
Fe-rich Particles	**Somatic**	**Somatic**	NS	NS	NS	**Zygotic**

Note: 225 Fe-rich particle spectra were compared to 225 Fe-rich particle spectra and 150 globoid spectra were compared to 150 globoid spectra. NS indicates no significant difference between the two means.

Table 11: Comparison of ratios of peak-to-background values for somatic and zygotic embryos using MINITAB's two-sample t-test. This comparison compares all the globoids and Fe-rich particles tested from somatic embryos to all the globoids and Fe-rich particles tested from zygotic embryos. Embryo names in bold indicate which embryo type had a significantly higher mean at P > 0.05.

Particle Type	K:P	Mg:P	Ca:P	Fe:P	Zn:P
Globoids	NS	**Somatic**	**Somatic**	**Zygotic**	NS
Fe-rich Particles	NS	**Zygotic**	**Zygotic**	**Zygotic**	**Zygotic**

Note: 225 Fe-rich particle spectra were compared to 225 Fe-rich particle spectra and 150 globoid spectra were compared to 150 globoid spectra. NS indicates no significant difference between the two means.

Table 12: Comparison of peak-to-background ratios for somatic and zygotic embryos using MINITAB's two-sample t-test to compare significant differences between embryos for the same element in the same tissue and same organ.

Organ	Tissue	Particle	P	K	Mg	Ca	Fe	Zn
Cotyledons	Protoderm	Fe-rich Particle	NS	NS	NS	**Zygotic**	**Zygotic**	NS
	Ground Meristem	Fe-rich Particle	NS	NS	NS	**Zygotic**	**Zygotic**	NS
		Globoid	NS	**Zygotic**	NS	**Somatic**	**Zygotic**	**Zygotic**
	Procambium	Fe-rich Particle	NS	NS	**Somatic**	NS	NS	NS
		Globoid	**Somatic**	NS	**Somatic**	NS	**Zygotic**	**Somatic**
Hypocotyl	Protoderm	Fe-rich Particle	**Somatic**	**Somatic**	NS	NS	NS	NS
	Ground Meristem	Fe-rich Particle	**Somatic**	**Somatic**	NS	**Somatic**	NS	NS
		Globoid	NS	NS	NS	NS	NS	**Zygotic**
	Procambium	Fe-rich Particle	**Somatic**	NS	**Somatic**	**Somatic**	NS	NS
		Globoid	**Zygotic**	NS	NS	**Somatic**	**Zygotic**	NS
Radicle	Protoderm	Fe-rich Particle	NS	NS	NS	NS	**Somatic**	**Zygotic**
	Ground Meristem	Fe-rich Particle	**Somatic**	**Somatic**	**Somatic**	NS	**Somatic**	NS
		Globoid	**Zygotic**	NS	NS	**Somatic**	NS	NS
	Procambium	Fe-rich Particle	NS	NS	NS	**Somatic**	NS	NS
		Globoid	**Zygotic**	**Zygotic**	**Zygotic**	**Somatic**	NS	**Zygotic**

Note: 25 spectra were compared to 25 spectra for each entry. Embryo names indicate which embryo type had the higher mean at $P > 0.05$. NS indicates no significant difference between the means.

Table 13: Comparison of K to P, Mg to P, Ca to P, Fe to P, and Zn to P ratios for somatic and zygotic embryos using MINITAB's two-sample t-test to compare significant differences between embryos for the same ratio in the same tissue and same organ.

Organ	Tissue	Particle	K:P	Mg:P	Ca:P	Fe:P	Zn:P
Cotyledons	Protoderm	Fe-rich Particle	**Somatic**	NS	**Zygotic**	**Zygotic**	NS
	Ground Meristem	Fe-rich Particle	NS	**Zygotic**	**Zygotic**	**Zygotic**	NS
		Globoid	NS	**Somatic**	**Somatic**	**Zygotic**	**Zygotic**
	Procambium	Fe-rich Particle	NS	NS	NS	**Zygotic**	NS
		Globoid	**Zygotic**	NS	NS	**Zygotic**	**Somatic**
Hypocotyl	Protoderm	Fe-rich Particle	NS	NS	NS	**Zygotic**	NS
	Ground Meristem	Fe-rich Particle	NS	**Zygotic**	NS	**Zygotic**	NS
		Globoid	NS	**Somatic**	NS	NS	NS
	Procambium	Fe-rich Particle	**Zygotic**	NS	NS	**Zygotic**	NS
		Globoid	NS	NS	**Somatic**	**Zygotic**	NS
Radicle	Protoderm	Fe-rich Particle	NS	**Zygotic**	NS	NS	NS
	Ground Meristem	Fe-rich Particle	NS	**Zygotic**	NS	**Zygotic**	NS
		Globoid	NS	**Somatic**	**Somatic**	NS	NS
	Procambium	Fe-rich Particle	**Zygotic**	NS	**Somatic**	**Zygotic**	NS
		Globoid	NS	**Somatic**	**Somatic**	NS	**Zygotic**

Note: 25 spectra were compared to 25 spectra for each entry. Embryo names indicate which embryo type had the higher mean at $P > 0.05$. NS indicates no significant difference between the means.

Discussion

Seeds store the majority of their mineral nutrients and protein reserves in membrane-bound structures called protein bodies (Spitzer and Lott, 1980). Protein bodies consist of a proteinaceous matrix, which may contain one or more kinds of inclusions (Lott, 1981). Inclusions that may be found in a protein body include protein crystalloids, globoids, soft globoid regions and calcium oxalate crystals (Lott, 1981).

One type of inclusion commonly found in protein bodies is protein crystalloids, which may be angular, irregular or round (Lott, 1980). Protein crystalloids in conifer somatic and zygotic embryos have been thoroughly investigated. In white spruce zygotic embryos, protein crystalloids make up 70 to 80% of the total storage protein and contain proteins with molecular weights of 42, 34.5-35, 22-23 and 8 KDa (Misra and Green, 1990; 1991; Misra *et al.*, 1993). These proteins are disulphide-linked into oligomers of 55 to 57 KDa (Flinn *et al.*, 1991). Maturation of white spruce somatic embryos with ABA and PEG 4000 have resulted in similar protein crystalloid polypeptides as found in zygotic embryos (Misra *et al.*, 1993).

Another type of inclusion often found in protein bodies, which are the focus of this study, are phytate-containing globoids (Lott, 1980). The low-water-content preparation procedures used here were designed to retain the phytate in the tissue. It has been shown that K-phytate and Na-phytate are very water soluble, while phytates containing divalent and trivalent cations tend to be less soluble in water (Brown *et al.*, 1961; Crean and Haisman, 1963). Skilnyk and Lott (1992) found that aqueous fixation can result in major losses of P, Mg and K. Prolonged fixation and washing can cause the complete extraction of globoids (Wada and Maeda, 1979). Using thin sections cut on a water-filled microtome boat, can also

result in major losses of elements into the water-filled boat (Skilnyk and Lott, 1992). Thicker sections cut on dry knives prevent the shattering of globoids as well as eliminating the extraction problems. Since globoids are naturally electron dense, they can be readily identified in these thicker sections and the addition of electron-dense stain can be omitted. Post-fixing with osmium tetroxide, which also adds electron density, can cause large scale extractions of soluble K-containing compounds and should also be omitted (Lott and Buttrose, 1978; Lott and Vollmer, 1979; Lott *et al.*, 1978a).

Observations of thick sections and comparisons of digital x-ray maps in this study revealed that globoids in somatic embryos were found in the same size range (0.5 to 3 μm in diameter) as reported for zygotic embryos (Reid, 1996) Globoids in somatic embryos, however, tended to be in the lower end of this range. In both types of embryos, globoids were larger and more numerous in the ground meristem than in the procambium. In both the ground meristem and procambium, zygotic embryos had more globoids per unit area than somatic embryos. Digital maps of tissues in these embryos showed that globoids had similar compositions (P, K and Mg), but globoids in zygotic embryos commonly showed traces of Fe. Female gametophyte tissue, which contained very large globoids, also demonstrated significant Fe levels in digital x-ray maps.

Peak-to-background values are commonly used to compare EDX analysis spectra, but when analysing P/B values it must be remembered that the values are arbitrary units and should not be directly related to quantitative levels (Lott *et al.*, 1978b). This is because some elements produce a higher yield of x-rays than other elements, thus peaks in an EDX analysis spectrum are not directly proportional to the quantity of element present. When present in

equal concentrations, the P peak will be lower than the peaks for Fe, K and Ca; the Mg peak will be lower than the P peak; and the K and Fe peaks will be almost equal in height (Russ, 1972). These relative peak heights are also dependent upon the accelerating voltage in the electron microscope and on the apparatus used to collect the spectra (Russ, 1972). If all spectra are collected under the same conditions then P/B values are useful in determining differences between spectra for any given element, but inferences about relative concentrations of elements within a single spectrum should be approached with caution. By keeping these limitations in mind P/B values can be very valuable and informative for comparing large numbers of spectra.

Energy dispersive x-ray analysis of individual globoids confirmed the presence of P, K, and Mg in both somatic and zygotic embryos with occasional traces of Fe and little if any Ca or Zn. When data for all the globoids in somatic embryos were pooled together and compared to all the data for globoids in zygotic embryos, it was found that zygotic embryos had significantly higher values for P, K, Fe and Fe:P. Somatic embryos had significantly higher Mg:P ratios. Comparison of globoids from specific tissues in each embryo type showed consistently more Fe in zygotic embryos. This was especially evident in the cotyledon procambium where globoids in zygotic embryos had Fe peaks similar in height to the K.

Energy dispersive x-ray analysis of globoids for white spruce in this study showed similar compositions to globoids from seeds of various *Pinus* species (West and Lott, 1993b). In *Pinus*, there were no significant differences in globoid composition between zygotic embryos of different species and only small differences between globoids from the female gametophyte and zygotic embryo of a single species (West and Lott, 1993b). As found here

for white spruce, the protein bodies in *Pinus* also contained one or more globoids (West and Lott, 1993b). In zygotic and somatic embryos of white spruce, protein bodies often contained one globoid, but as many as three were observed in a single section.

In a study of thin sections from white spruce zygotic embryos and female gametophytes, Krasowski and Owens (1993) reported only one globoid cavity per section of a protein body in zygotic embryos and up to three cavities per section of a protein body in female gametophytes. Observations of thicker sections used in this study contradict the findings of Krasowski and Owens (1993). In fact, female gametophytes typically contained more than three globoids per protein body in a single section (Reid, 1996). This difference can be attributed to the use of thicker sections. Thin sections cause the globoids to be ripped out of the section and often smaller globoids can be completely overlooked. In addition, as globoids are ripped out, some of the proteinaceous matrix may also be removed so that several smaller globoid cavities become one larger cavity. Thick sections are advantageous because the globoids are retained in the section and a more accurate description of protein body composition can be made.

The second type of storage material studied here was Fe-rich particles. These particles were found in zygotic embryos and female gametophytes of *Pinus* and were present in chloroplasts from green cotyledons of seedlings of jack pine (*Pinus banksiana*) (West and Lott, 1993b; Pittermann *et al.*, 1996). Subsequently, Fe-rich particles have also been found in chloroplasts from green cotyledons of white spruce seedlings (unpublished results). Fe-rich particles were found in the protoderm, procambium and ground meristem of white spruce somatic embryos as was reported for zygotic embryos of white spruce (Reid, 1996). These

naturally electron-dense deposits were visible in lower magnification STEM micrographs and could be identified in several digital x-ray maps. EDX analysis of individual Fe-rich particles showed high P and Fe with moderate K and Mg and little if any Ca or Zn. Combining all the Fe-rich particles in white spruce somatic embryos and comparing to all those collected previously from zygotic embryos revealed higher P/B values for P and K in somatic embryos. Zygotic embryos of white spruce had higher Mg:P and Fe:P ratios than somatic embryos. Comparison of specific tissue regions confirmed that Fe-rich particles consistently had higher Mg:P and Fe:P ratios. The composition of Fe-rich particles in white spruce are consistent with those reported by West and Lott (1993b) for *Pinus*.

Recently, seeds from nine genera in the Pinaceae family were studied for the presence and composition of Fe-rich particles (Reid *et al.*, 1998). Reid *et al.* (1998) found that Fe-rich particles are a common characteristic of conifers in the family Pinaceae and that they have similar compositions with the exception of lower Fe:P ratios in *Cedrus* and *Abies*. From EDX analysis studies and comparisons to prepared phytate and phytoferritin deposits, it was proposed that Fe-rich particles represent stores of Fe-rich phytate (West and Lott, 1993b; Pittermann *et al.*, 1996; Reid *et al.*, 1998). The findings of this current study are consistent with that proposal.

CHAPTER 5:
MEASUREMENT OF POTASSIUM, MAGNESIUM, CALCIUM, ZINC AND IRON USING ATOMIC ABSORPTION SPECTROSCOPY

Introduction

Atomic absorption spectroscopy (AAS) has been widely used to measure numerous elements in both biological and non-biological samples. The use of AAS for analytical studies was first reported by Walsh (1955). Since then, many refinements have made AAS a very accurate way to measure small quantities of elements. Tissue samples must be broken down and then taken up into appropriate solutions prior to using AAS. Traditionally, wet and dry ashing (described in Chapter 3) have been used to break down the tissue but several studies have favoured the use of dry ashing (Lambert, 1976; Menden *et al.*, 1977; Isaac, 1980; Ockenden and Lott, 1986). Ashing is commonly followed by acid treatment to make elements in the ash more soluble (Gorsuch, 1970; Ockenden and Lott, 1986). Following this, samples are taken up into appropriate solutions, diluted and then read.

In AAS, liquid samples are measured by aspirating tiny droplets into a flame at 1500-3000°C, using acetylene as a fuel and air as an oxidant (Robinson, 1975). As the liquid sample is decomposed by the flame, free atoms in the ground state absorb photons from the light source to become excited atoms (Robinson, 1975). This reduces the amount of transmitted radiant energy from the flame (Peters *et al.*, 1974). Typically, the sources of radiant energy are hollow cathode lamps filled with gases like He, Ne or Ar (Isaac, 1980). The gas within the lamp becomes ionized by the anode creating a negatively charged ion,

which is then accelerated towards the positively charged cathode (Robinson, 1975). As the charged ion strikes the cathode, metal atoms on the surface of the cathode are dislodged and become excited (Robinson, 1975). These metal atoms return to their ground state by emitting radiation of characteristic wavelengths (Robinson, 1975). The metal used in the cathode is the same metal as that being tested and therefore the emitted radiation in the cathode matches the energy needed to excite atoms in the sample (Isaac, 1980). The radiation transmitted through the flame is filtered by a monochromator, which eliminates background radiation from the gas in the lamp and from the flame, and the filtered radiation is measured using a photodetector (Peters *et al.*, 1974).

Depending on the element of interest, several possible interferences must be taken into consideration when preparing solutions to be measured. These interferences include ionization interference, chemical interference and matrix interference. Depending on which element is being measured, one or multiple interferences may occur.

One interference, which is associated with K samples, is ionization interference. With ionization interference, enough energy is supplied to the sample to allow the K atoms to overcome their ionization potential resulting in ionized K atoms (Isaac, 1980). Since these atoms are no longer in their ground state, they cannot absorb photons and therefore K concentrations are underestimated (Isaac, 1980). To reduce or eliminate ionization interference, an excess of an element like Cs is added to the solution. Cesium atoms ionize easier than K atoms and therefore K stays in its ground state where it is able to be measured (Isaac, 1980).

A second type of interference associated with AAS is chemical interference. In this

type of interference, the element of interest bonds with an anion in the sample to produce a stable compound (Robinson, 1975; Isaac, 1980). This results in the inability of the element of interest to be converted to the ground state and therefore it cannot be measured (Walsh, 1982). Chemical interference is a problem with Ca samples because anions like phosphates, sulphates and silicates bind strongly to Ca (Yofe and Finkelstein, 1958; Rocchiccioli and Townshend, 1968; Allen *et al.*, 1974). To reduce chemical interference, elements like La are added to the solutions because they will bind more readily to the anions and leave Ca in the ground state (Yofe and Finkelstein, 1958). Magnesium samples also experience chemical interference and La must also be added to these samples.

The final potential interference problem in AAS that must be considered is matrix interference. This problem is caused by high levels of dissolved solids or high acid concentrations in the solution, both of which increase the solution's viscosity (Isaac, 1980). This increase in viscosity causes slower aspiration rates, which results in less solution being degraded in the flame at any given time and thus underestimates the overall concentrations (Isaac 1980). Matrix interference can be easily overcome by using appropriate dilutions so that viscosities are kept relatively low (Isaac, 1980).

Atomic absorption spectroscopy is very convenient to use because it has high specificity, relatively few interferences, good detection limits, lower flame temperatures than other techniques and is simple to use (Isaac, 1980). In this chapter, AAS was used to measure K, Mg, Ca, Fe and Zn in white spruce somatic embryos and various parts of white spruce seeds.

Materials and Methods

Potassium, Mg, Ca, Fe and Zn were measured for each of the following: somatic embryos, zygotic embryos, female gametophytes and whole seeds. For each of the above, three samples were tested and mean values calculated. Somatic embryos were pooled together from three plates for each element measured. For measuring K and Mg, samples consisted of 100 somatic embryos, 100 zygotic embryos, 100 female gametophytes or 50 whole seeds. Calcium was tested using 300 somatic embryos, 300 zygotic embryos, 300 female gametophytes or 100 whole seeds per sample. For each Fe sample, 400 to 600 somatic embryos, 400 to 600 zygotic embryos, 400 to 600 female gametophytes or 150 whole seeds were used. Finally, Zn samples consisted of 120 somatic embryos, 120 zygotic embryos, 120 female gametophytes or 30 whole seeds. For each sample of zygotic embryos, the female gametophytes from these same seeds were pooled together as one female gametophyte sample. Using the values measured for zygotic embryos and female gametophytes the levels of each of the above elements were calculated for seeds without seed coats.

The dry ashing procedures used by Ockenden and Lott (1986) and West and Lott (1993a) were used. Samples were weighed in separate porcelain crucibles (Coors Porcelain, Golden, Co.) and slowly charred on a SYBRON thermolyne 2600 hot plate (Thermolyne Corporation, Dubuque, Iowa) set at high heat. For each set of ashed samples, a blank crucible was also treated in the same manner to test for contamination from the preparation procedures. Each crucible was initially placed at the corner of the hot plate until the tissue began to blacken and then the crucibles were moved half way towards the center of the hot

plate until all the tissue had blackened. Final charring was done by placing the crucibles in the center of the hot plate and loosely covering the crucibles with aluminium foil. The samples were charred until no smoke was visible leaving the crucibles. The temperature at the center of the hot plate was approximately 450°C and approximately 45 to 60 min. was required for complete charring. Crucibles were then placed uncovered in a Blue M Electric Company muffle furnace (Blue Island, Illinois) and ashed for 4 h at 550°C.

Following complete ashing, each ashed sample was double acid treated to help release elements from the insoluble components of the ash. The crucibles were placed back on the hot plate at low heat and approximately 1.5 ml of 1:2 (v/v) Aristar HNO_3 in deionized water was added to each crucible. The acid was allowed to completely evaporate away and then approximately 1.5 ml of 1:1 (v/v) HCl in deionized water was added to each crucible. Again the acid was allowed to evaporate away completely.

Each sample of treated ash was then transferred to a volumetric flask with a glass rod and funnel using several applications of approximately 2 ml of the appropriate solution. Remaining solution on the glass rod and funnel was rinsed into the flask and the flask was taken up to volume. Solutions were then transferred to centrifuge tubes and centrifuged for 3 min. at 3000 rpm (1470 x g) in an International Clinical Centrifuge (International Equipment Co., Needham, Mass). Samples were then diluted with the appropriate solutions to concentrations within the readable range of the AAS. Potassium samples were diluted in water until the final dilution, which was done using 1100 ppm $CsCl_2$ solution. Both Mg and Ca ashes were taken up in 5% HCl containing 0.5% La. Iron samples were diluted in 10% HNO_3 and Zn samples were diluted in 1% HNO_3. For each element, a sample of rice flour

(reference number 1568a) from the National Institute of Standards and Technology (Gaithersburg, Maryland) was tested to confirm that the procedures used here were accurately measuring these elements.

Potassium, Mg, Ca and Zn samples were measured on a Varian AA-1275 series atomic absorption spectrophotometer (Varian Techtron Pty. Limited, Springvale, Australia). Iron samples were measured on a Perkin-Elmer 5100 atomic absorption spectrophotometer (Perkin-Elmer Corporation, Norwalk, Connecticut) at the Occupational and Environmental Health Laboratory (McMaster University, Hamilton, Ontario). VWR Scientific standards (VWR Scientific, West Chester, PA) were used at the following concentrations: K (0.2, 0.4, 0.8, 1.2, 1.6, and 2.0 μg/ml), Mg (0.05. 0.1, 0.2, 0.4, 0.6, and 0.8 μg/ml), Ca (0.5, 1, 2, 3, 4, and 5 μg/ml), Fe (0.5, 1, 2, 3, 4, and 5 μg/ml) and Zn (1, 2, 3, 4, and 5 μg/ml). Each standard was made up in the appropriate solution for the element being tested. Standard curves were made for each element by taking triplicate readings for each standard concentration and graphing the mean absorbancy versus the standard concentration. For each sample, readings were also taken in triplicate and the mean absorbancy reading was converted to a concentration value using the standard curve.

Element concentrations were calculated as μg per g DW and as μg per tissue. Statistical differences between means was determined using the MINITAB analysis of variance test. When a difference was found, Tukey's test (Zar, 1984) was used to determine which means differed at $P > 0.05$.

Results

Concentrations of K per g DW and per tissue are given in Table 14 and illustrated in Figs. 42 and 43. On a DW basis, somatic embryos had lower K concentrations than zygotic embryos. Female gametophytes had slightly higher mean values of K per g DW than zygotic embryos, but no statistical differences were found in the various parts of the seeds (not including whole seeds). Expressing K concentrations per tissue showed that a single somatic embryo and a single zygotic embryo contained similar K levels. The large female gametophyte of a seed contained the majority (59%) of a seed's K. As shown by the difference between whole seeds and seeds without seed coats, the seed coat of a single seed contained a significant amount of K (approximately 32% of the seed's total K).

Concentrations of Mg for white spruce somatic embryos and various parts of white spruce seeds are given in Table 14 and illustrated in Figs. 44 and 45. Expressed per g DW, the concentrations of Mg were significantly higher in zygotic embryos. Female gametophyte tissue had significantly higher Mg concentrations than zygotic embryos and whole seeds had concentrations similar to those measured in zygotic embryos per g DW. Calculating Mg per tissue showed that a zygotic embryo had a mean value for Mg that was higher than that for a somatic embryo, but no statistical difference was found. The female gametophyte of a seed contained 85% of the total Mg in the seed and 8.5 times more Mg than the zygotic embryo. Only 5% of a seed's total Mg was found in the seed coat.

Calcium levels per g DW and per tissue are summarized in Table 14 and Figs. 46 and 47. Based on mean values, somatic embryos had more Ca per g DW than zygotic embryos, but no statistical differences were found. Female gametophytes contained 2.2 times more Ca

per g DW than zygotic embryos and whole seeds contained the highest concentrations of Ca per g DW. A single somatic embryo had 2 times more Ca than a single zygotic embryo. Only 2% of the Ca in a seed was found within the zygotic embryo; whereas, 28% of the seed's Ca was found in the female gametophyte. The seed coat contained the bulk of the Ca (approximately 70%) within a seed.

Table 15 and Figs. 48 and 49 illustrate Fe levels per g DW and per tissue. Zygotic embryos had significantly higher Fe per g DW than both somatic embryos and female gametophytes. Somatic embryos and female gametophytes had very similar concentrations of Fe on a DW basis. Expressed per tissue, Fe concentrations were not significantly different in somatic and zygotic embryos. Approximately 68% of the total Fe in a seed was within the female gametophyte and only 16% of the total Fe was within the seed coat of a seed.

Finally, measurements of Zn are summarized in Table 15 and illustrated in Figs. 50 and 51. Zygotic embryos were found to contain more Zn than somatic embryos per g DW and less than female gametophytes. A single somatic embryo and a single zygotic embryo had very similar Zn concentrations. In a single seed, 64% of the total Zn was present in the female gametophyte and 30% of the total Zn was found to be in the seed coat.

Table 14: Element concentrations (± SD) of K, Mg and Ca in white spruce somatic embryos, zygotic embryos, female gametophytes, seeds without seed coats and whole seeds expressed per g DW and per tissue.

Sample	µg K		µg Mg		µg Ca	
	per g DW	per tissue	per g DW	per tissue	per g DW	per tissue
Somatic Embryos	4995.85 ± 341.65 **a**	1.57 ± 0.21 **a**	1771.57 ± 109.64 **a**	0.60 ± 0.04 **a**	118.26 ± 3.14 **a**	0.04 ± 0.00 **a**
Zygotic Embryos	7737.98 ± 308.56 **b**	1.56 ± 0.08 **a**	3707.55 ± 178.03 **b**	0.71 ± 0.08 **a**	94.20 ± 8.76 **a**	0.02 ± 0.00 **a**
Female Gametophytes	8235.90 ± 266.95 **b**	10.21 ± 0.65 **b**	4909.51 ± 149.44 **c**	6.09 ± 0.38 **b**	203.66 ± 5.65 **b**	0.25 ± 0.01 **b**
Seeds Without Seed Coats	8167.02 ± 258.25 **b**	11.77 ± 0.61 **c**	4748.22 ± 105.94 **c**	6.81 ± 0.45 **c**	188.70 ± 4.68 **b**	0.26 ± 0.01 **b**
Whole Seeds	7718.62 ± 256.98 **b**	17.19 ± 0.83 **d**	3344.59 ± 128.38 **b**	7.20 ± 0.22 **c**	421.81 ± 21.79 **c**	0.89 ± 0.06 **c**

Note: Each mean was calculated using 3 values. The values for seeds without seed coats were calculated by combining the values for zygotic embryos and values for female gametophytes. Values in a single column that are followed by the same letter are not significantly different at $P > 0.05$.

Table 15: Element concentrations (± SD) of Fe and Zn in white spruce somatic embryos, zygotic embryos, female gametophytes, seeds without seed coats and whole seeds expressed per g DW and per tissue.

Sample	µg Fe		µg Zn	
	per g DW	per tissue	per g DW	per tissue
Somatic Embryos	143.94 ± 4.62 **ac**	0.04 ± 0.00 **a**	79.95 ± 3.07 **a**	0.03 ± 0.00 **a**
Zygotic Embryos	242.01 ± 12.49 **b**	0.04 ± 0.00 **a**	149.38 ± 8.20 **b**	0.02 ± 0.00 **a**
Female Gametophytes	143.80 ± 3.41 **ac**	0.18 ± 0.01 **b**	195.42 ± 4.79 **c**	0.24 ± 0.00 **b**
Seeds Without Seed Coats	155.95 ± 4.19 **a**	0.22 ± 0.01 **c**	190.40 ± 5.06 **cd**	0.26 ± 0.00 **b**
Whole Seeds	128.10 ± 4.65 **c**	0.26 ± 0.01 **d**	176.22 ± 8.19 **d**	0.37 ± 0.02 **c**

Note: Each mean was calculated using 3 values. The values for seeds without seed coats were calculated by combining the values for zygotic embryos and values for female gametophytes. Values in a single column that are followed by the same letter are not significantly different at $P > 0.05$.

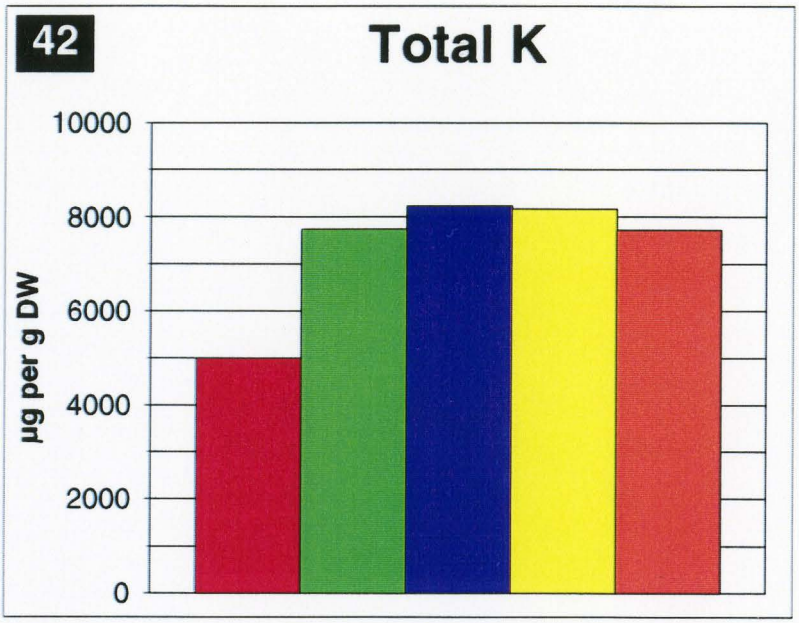
42
Total K
10000
8000
6000
4000
2000
0
µg per g DW

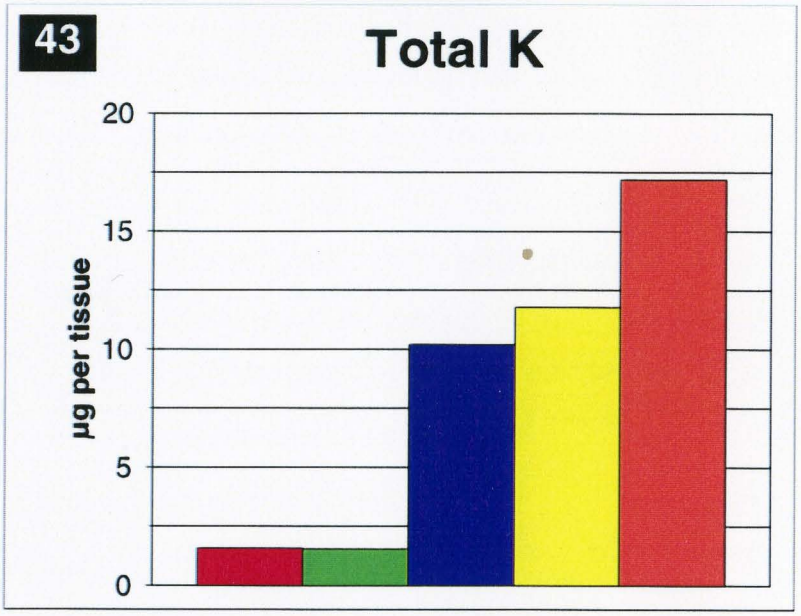
43
Total K
20
15
10
5
0
µg per tissue

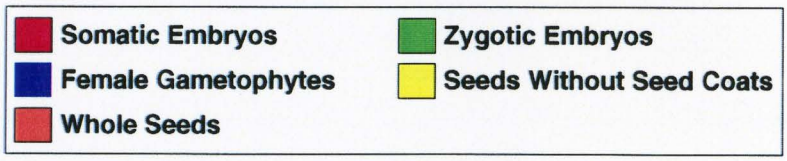
Somatic Embryos
Zygotic Embryos
Female Gametophytes
Seeds Without Seed Coats
Whole Seeds

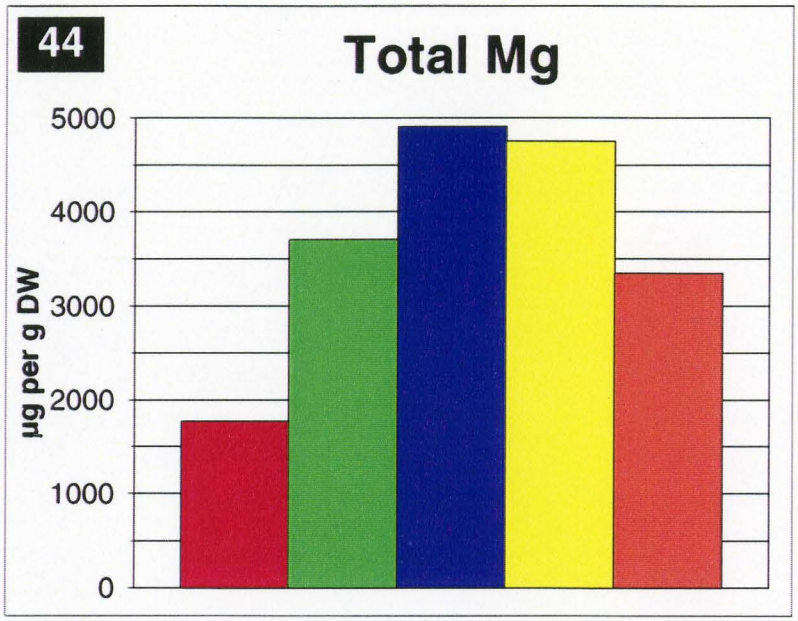
44
Total Mg
5000
4000
3000
2000
1000
0
µg per g DW

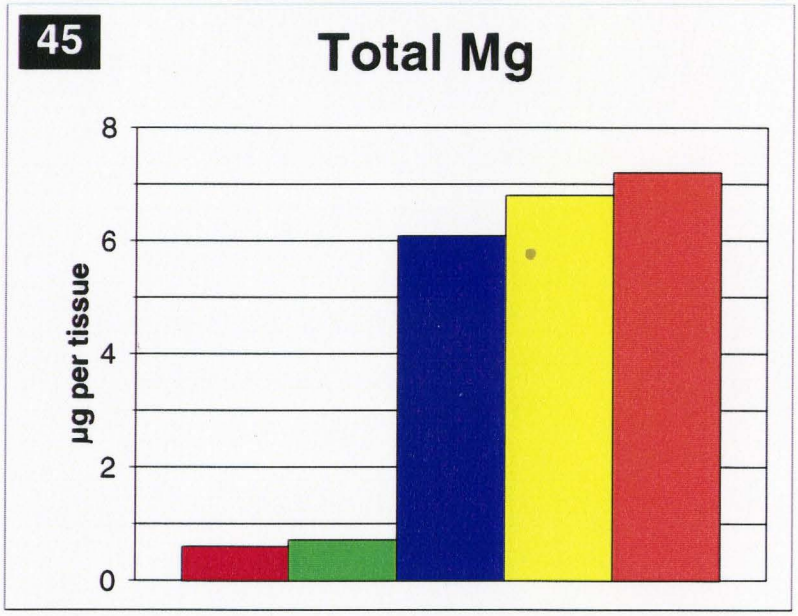
45
Total Mg
8
6
4
2
0
µg per tissue

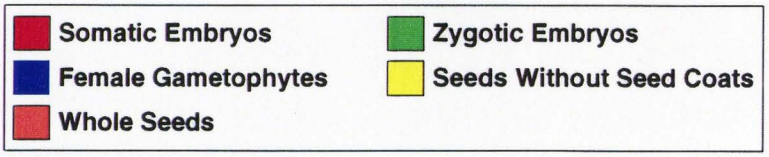
Somatic Embryos
Zygotic Embryos
Female Gametophytes
Seeds Without Seed Coats
Whole Seeds

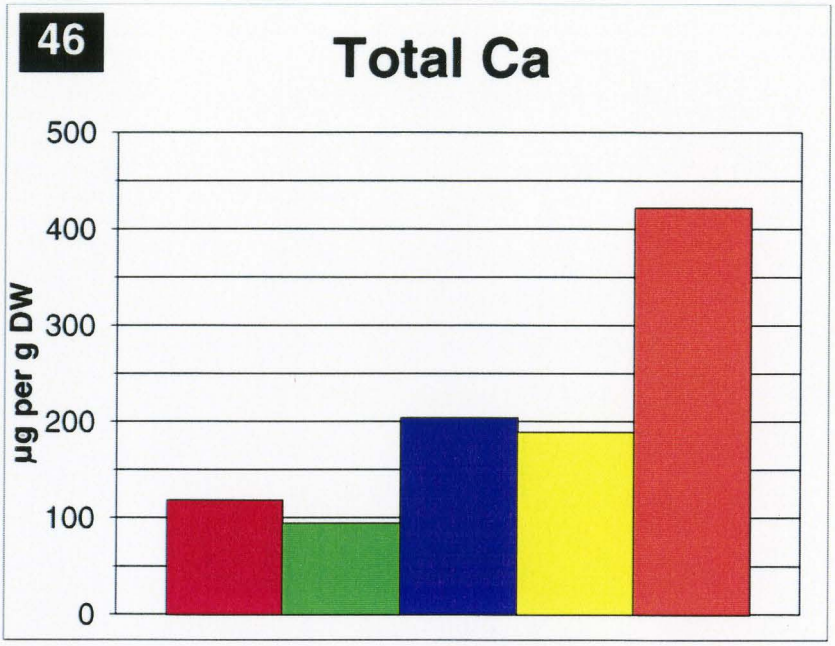
46
Total Ca
500
400
300
200
100
0
µg per g DW

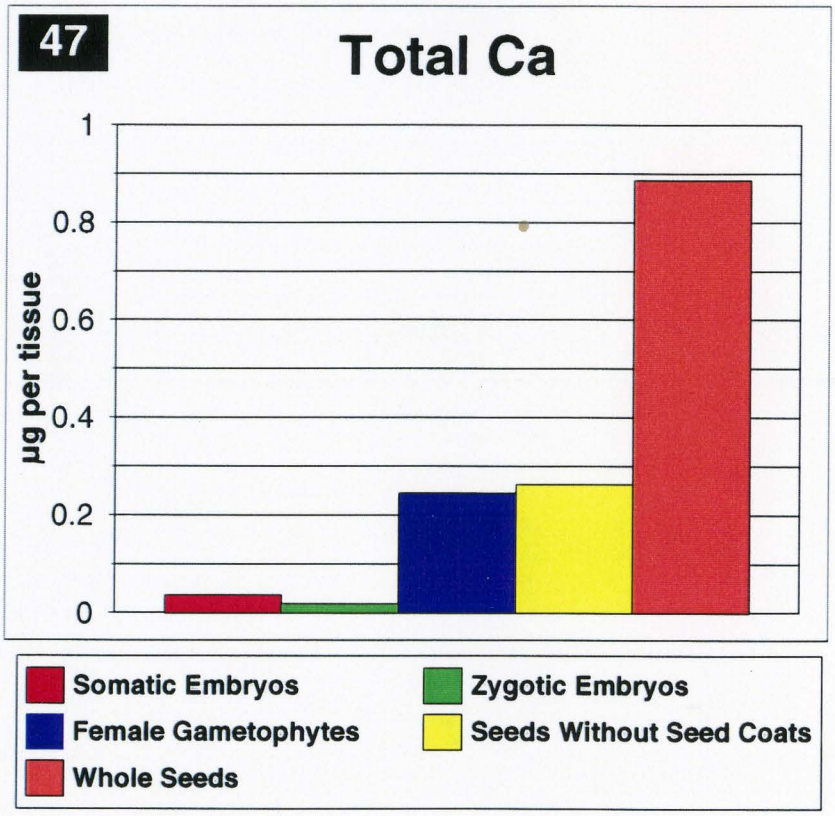
47
Total Ca
1
0.8
0.6
0.4
0.2
0
µg per tissue
Somatic Embryos
Zygotic Embryos
Female Gametophytes
Seeds Without Seed Coats
Whole Seeds

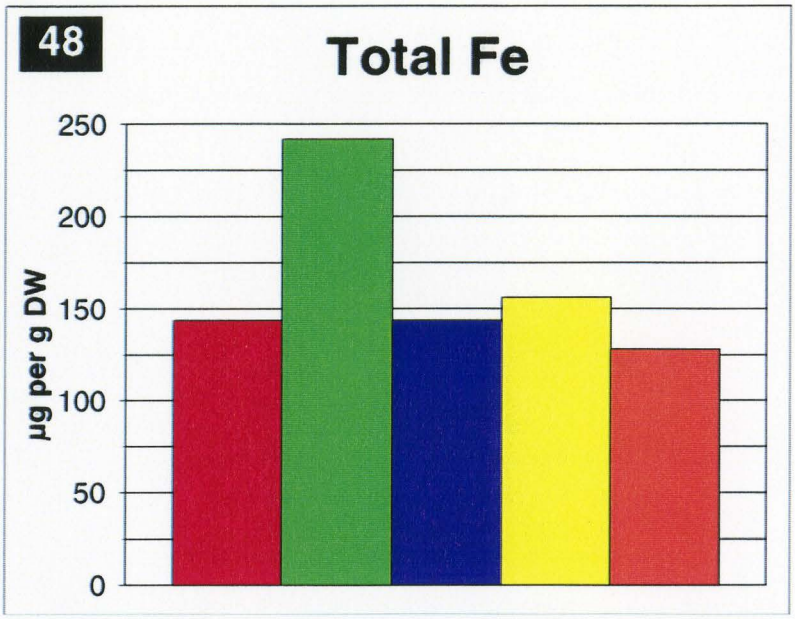
48
Total Fe
250
200
150
100
50
0
µg per g DW

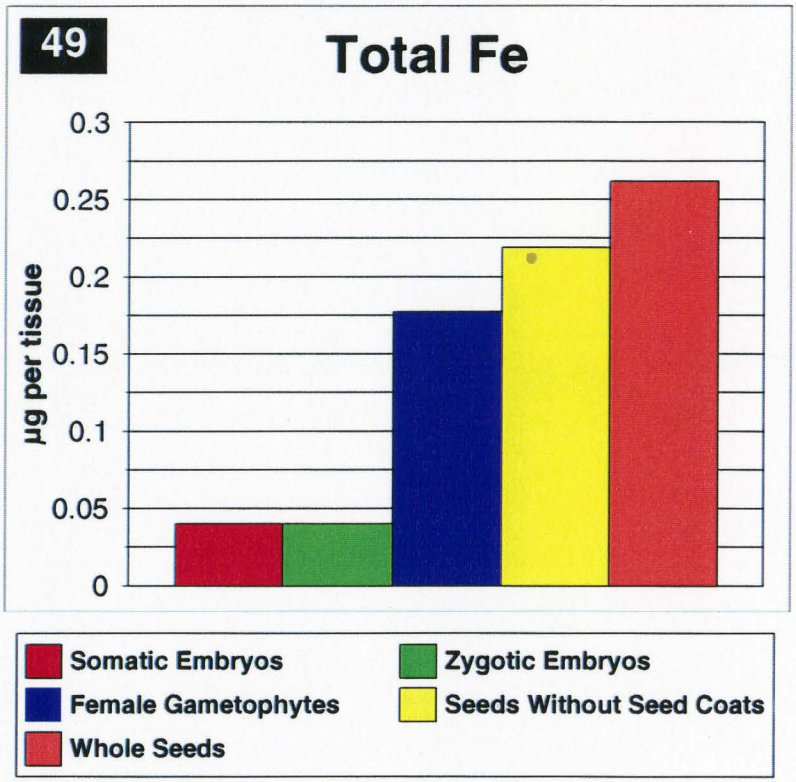
49
Total Fe
0.3
0.25
0.2
0.15
0.1
0.05
0
µg per tissue
Somatic Embryos
Zygotic Embryos
Female Gametophytes
Seeds Without Seed Coats
Whole Seeds

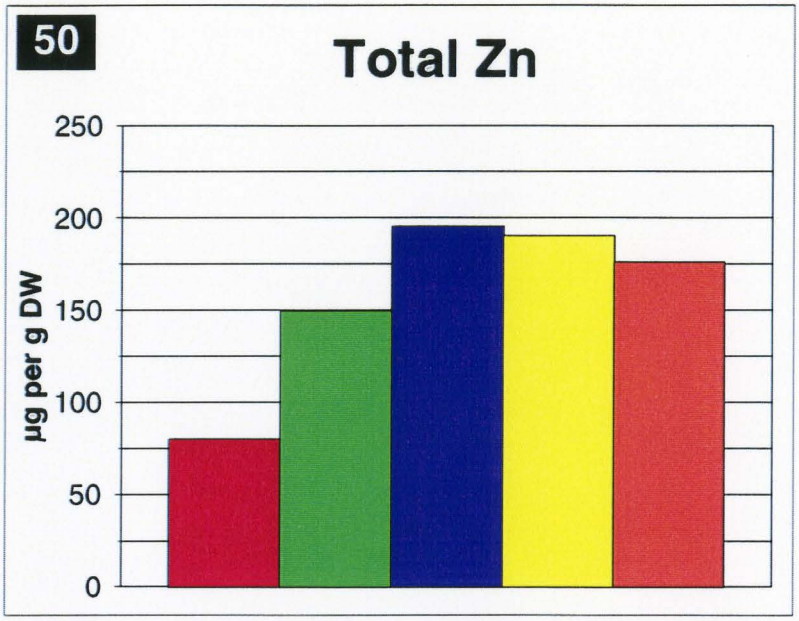
50
Total Zn
250
200
150
100
50
0
µg per g DW

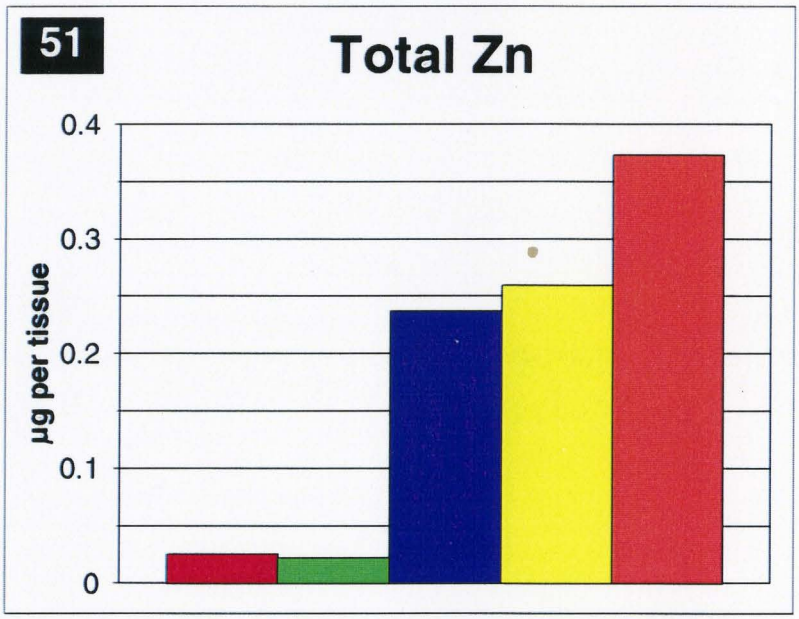
51
Total Zn
0.4
0.3
0.2
0.1
0
µg per tissue

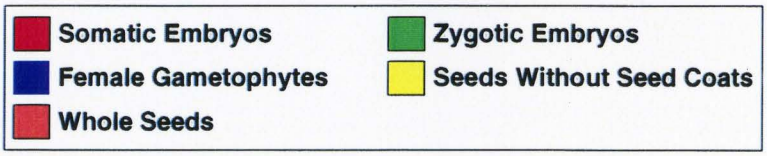
Somatic Embryos
Zygotic Embryos
Female Gametophytes
Seeds Without Seed Coats
Whole Seeds

Discussion

During seed development, mineral nutrients are supplied to the developing seeds by the phloem of the parent plant (Tinker and Läuchli, 1986). Plants will even supply the nutrients required by the seeds at the expense of other structures (Mengel and Kirkby, 1982). For this reason, it could be expected that seeds from various environments will likely be very similar in mineral nutrition levels. Since somatic embryos are germinated on media, it is not always clear whether this media contains the appropriate components to provide the nutrients that are available to a germinating zygotic embryo. Therefore, it is very important to measure mineral nutrients in somatic embryos and compare these to values from seeds to ensure that all the essential elements are present in sufficient quantities.

Besides N, K is the most abundant inorganic nutrient required by plants for metabolic functions and growth. Potassium is a cofactor of over 40 enzymes and has been linked to both enzyme activation and maintaining enzyme structural integrity (Evans and Sorger, 1966; Lüttge and Clarkson, 1989; Taiz and Zeiger, 1991). High levels of K are often present in the cytoplasm of plant cells because it is essential in all the major steps of protein synthesis (Evans and Wildes, 1971; Wyn Jones *et al.*, 1979; Gibson *et al.*, 1984). In addition to these roles, K is involved in cell turgor, cell expansion and the maintenance of electrostatic balance within cells (Lüttge and Clarkson, 1989).

In this study, of the elements measured in white spruce somatic embryos and various parts of white spruce seeds, K was the most abundant element and Mg was the second most abundant. In comparison to K and Mg, the concentrations of Ca, Fe and Zn were relatively low. Measurements of K per g DW were found to be significantly higher in various parts of

white spruce seeds than in somatic embryos of white spruce. White spruce zygotic embryos had K concentrations per g DW similar to those reported for zygotic embryos of jack pine by West and Lott (1993a). Female gametophytes from white spruce seeds were very similar in their concentrations of K per g DW to Scotch pine (*Pinus sylvestris*) and lodgepole pine (*Pinus contorta*) female gametophytes studied by West and Lott (1993a). Concentrations of K per g DW were significantly lower in white spruce somatic embryos than in both white spruce zygotic embryos and in zygotic embryos of various *Pinus* species studied by West and Lott (1993a). Expression of K concentrations per tissue showed that a single somatic embryo and a single zygotic embryo of white spruce had very similar amounts of K. The large female gametophyte in a white spruce seed contained the majority of the seed's K. Potassium concentrations per tissue for white spruce zygotic embryos and female gametophytes were lower than those reported for *Pinus* by West and Lott (1993a). These lower amounts in white spruce are due to the fact that white spruce seeds are smaller than seeds from any of the pine species studied by West and Lott (1993a). Therefore for all the elements measured here, white spruce had lower concentrations per tissue than any amount found in *Pinus*.

The second most abundant element measured in this study was Mg. Magnesium is important in plants because it is a cofactor for several plant enzymes and is a constituent of the porphyrin component of the chlorophyll molecule (Clarkson and Hanson, 1980; Taiz and Zeiger, 1991). Like K, white spruce somatic embryos contained less Mg than zygotic embryos on a DW basis. On a DW basis, white spruce zygotic embryos were similar in concentrations of Mg to zygotic embryos of digger pine (*Pinus sabiniana*) reported by West and Lott (1993a). The large female gametophyte tissue of white spruce seeds most closely

resembled the concentrations of Mg per g DW of female gametophyte tissue from Eastern white pine studied by West and Lott (1993a). White spruce somatic embryos had lower mean concentrations of Mg per tissue than white spruce zygotic embryos, but no statistical differences were found. The large nutritional female gametophyte tissue contained the bulk of the seed's Mg.

Another element measured here was Ca and several roles have been found for Ca in plants. Calcium is required as a cofactor of some enzymes involved in the hydrolysis of ATP and phospholipids (Taiz and Zeiger, 1991). Calcium also acts as a second messenger in transducing external physical and hormonal signals into cellular responses (Poovaiah and Reddy, 1993). Calcium has been shown to play roles in mitosis and cytokinesis in that high Ca levels are associated with the cell plate and spindle fibers during cell division (Hepler and Wayne, 1985). In cell walls, Ca is commonly found in large amounts bound to pectins in the middle lamella of the cell wall (Mengel and Kirkby, 1982).

Measurements of Ca on a DW basis revealed a different trend than that observed for K and Mg. With Ca, white spruce somatic embryos had more Ca than zygotic embryos. Female gametophytes of white spruce had much higher Ca concentrations than zygotic embryos of white spruce on a DW basis. As found with Mg, Ca concentrations per g DW in white spruce zygotic embryos and female gametophytes most closely resembled those found by West and Lott (1993a) for digger pine and Eastern white pine, respectively. Expressing Ca concentrations per tissue showed that a somatic embryo of white spruce had double the Ca concentration as that found in a white spruce zygotic embryo. The bulk of the Ca in a single white spruce seed was found to be in the seed coat. A seed coat is a protective

structure composed of inner and outer cuticle layers surrounding many layers of thick-walled protective cells (Bewley and Black, 1985). Therefore the bulk of the Ca in a seed coat is present in the form of calcium pectate in cell walls (Mengel and Kirkby, 1982).

In this study, Fe was also measured. Iron is an essential element because it is a constituent of many cytochromes and proteins associated with photosynthesis, nitrogen fixation and respiration (Taiz and Zeiger, 1991). White spruce zygotic embryos contained higher Fe concentrations per g DW than somatic embryos or female gametophytes. Iron concentrations per g DW in white spruce zygotic embryos were closest to those reported for lodgepole pine zygotic embryos by West and Lott (1993a). Concentrations of Fe per g DW in white spruce female gametophytes were closest to those reported by West and Lott (1993a) for Eastern white pine female gametophytes. A single white spruce zygotic embryo contained very similar amounts of Fe to a single somatic embryo of white spruce. As with other elements, the larger female gametophyte in a seed contained much more Fe than the zygotic embryo.

The final mineral nutrient studied here was Zn. Zinc can be found bound as complexes with several important substances including: ATP, ADP, organic acids, amino acids, nucleic acids, sugars and metalloenzymes (Shkolnik, 1984; Glass, 1989; Taiz and Zeiger, 1991). Zinc is an essential constituent of many important enzymes like alcohol dehydrogenase, glutamic dehydrogenase and carbonic anhydrase (Taiz and Zeiger, 1991).

Relatively low concentrations of Zn were found in white spruce somatic and zygotic embryos in comparison to elements like K and Mg. On a DW basis, white spruce zygotic embryos had significantly more Zn than white spruce somatic embryos. Female gametophytes

of white spruce had significantly higher Zn concentrations per g DW than zygotic embryos. On a DW basis, white spruce zygotic embryos most closely resembled lodgepole pine zygotic embryos studied by West and Lott (1993a) and white spruce female gametophytes most closely resembled female gametophytes of Scotch pine reported by West and Lott (1993a). A single white spruce somatic embryo had very similar concentrations of Zn to a single zygotic embryo of white spruce. The female gametophyte of a single white spruce seed contained over 10 times more Zn than the zygotic embryo. The seed coat of a white spruce seed also contained significant amounts of Zn.

The female gametophyte of a white spruce seed plays a major nutritional role as shown by the concentrations of K, Mg, Ca, Fe and Zn measured here. A single white spruce somatic embryo is very similar in the levels of these elements to a single zygotic embryo of white spruce. Somatic embryos, however, lack a female gametophyte and must therefore be treated with solutions containing mineral nutrients required for successful germination and seedling growth. Since somatic embryos now being produced for white spruce more closely resemble zygotic embryos (Stephen Attree, personal communication), it would be valuable to know if these embryos have similar mineral nutrient concentrations as those measured in this study. What is clear, is that in order to make the next step towards producing synthetic seeds, the nutritional role of the female gametophyte must be considered and compensated for in artificial seed production.

CHAPTER 6:
A STUDY OF POTASSIUM LEAKAGE AND MORPHOLOGICAL CHANGES IN SURFACE DETAILS DURING IMBIBITION

Introduction

Development of a seedling from a dry seed begins with the uptake of water in a process called imbibition. During the phase of water entry into the seed, many compounds within the seed are leaked into the surrounding environment. Previous studies have shown that sugars, amino acids, organic acids, phenolics, proteins and inorganic ions are leaked during imbibition (Simon and RajaHarun, 1972; Simon, 1974; Duke and Kakefuda, 1981; Schoettle and Leopold, 1984). Inorganic ions like K, Mg, Cl, Ca and Mn have been found to leak during imbibition; but typically K is the major ion leaked (Loomis and Smith, 1980; Givelberg *et al.*, 1984; Bewley and Black, 1985; Lott *et al.*, 1991). It has also been shown that different tissues may leak electrolytes at very different rates (Bruggink *et al.*, 1991). Leakage is of concern because the germination frequency of seeds decreases as the level of leakage increases (Thornton *et al.*, 1990). It has been proposed that excessive leakage may promote pathogen growth, thus increasing the number of seedlings attacked by pathogens (Simon and RajaHarun, 1972; Simon, 1974).

Many explanations have been proposed as to why cells leak so much during the initial stages of imbibition, but there is still considerable controversy in this area of research due to the difficulty in studying the structure of cells in both dry and hydrated states. Often, techniques like ultrathin sectioning and transmission electron microscopy are difficult to use

for dry seed tissues because aqueous fixatives result in imbibition and therefore cellular changes (Thomson and Platt-Aloia, 1982). For this reason, a TEM can best be used to study cell membrane and cell wall structure of hydrated samples. Conventional scanning electron microscopy has been used to study cell walls of dry seeds (Webb and Arnott, 1982). As described in Chapter 2, a conventional SEM is more difficult to use for hydrated tissue samples. Attempts have been made to study cell walls of imbibed tissue and changes in cell wall wrinkling at different hydration levels by using freeze-drying and freeze-etching procedures (Lott, 1974; Lott and Kerr, 1986; Cavdek *et al.*, 1987). Additionally, hydrated white spruce somatic embryos and zygotic embryos have been studied using a low temperature SEM and chemically fixed embryos in a conventional SEM (Fowke *et al.*, 1994). Still, with all these techniques, the tissue must be treated in some fashion prior to observation and artifacts can not be completely ruled out.

A new system now available for studying the surface features of samples is an ESEM. An ESEM has the benefit over a conventional SEM in that the ESEM can observe samples in their hydrated state and with specially designed specimen stages, samples can now be both hydrated and desiccated within the specimen chamber (Danilatos, 1981a; Danilatos and Postle, 1982). Unique features of an ESEM allow the observation of hydrated tissues and these features include: the use of a low vacuum (typically 3-10 Torr) specimen chamber, the use of water vapour within the specimen chamber and multiple pressure limiting apertures.

In a conventional SEM, the specimen chamber is in a high vacuum (typically 10^{-5} Torr) and therefore samples must be dry or frozen to avoid surface distortions, as described in Chapter 2. An ESEM utilizes a low vacuum specimen chamber, which is filled with water

vapour. The use of water vapour (or other appropriate gases) is critical to being able to view a sample within these low vacuum environments. As the electron beam interacts with the specimen, secondary electrons are produced from the sample as described in Chapter 2. In an ESEM, as these secondary electrons accelerate towards the detector, they collide with water molecules within the chamber atmosphere (Meredith *et al.*, 1996). These collisions produce additional secondary electrons and positive ions (Meredith *et al.*, 1996). The positive ions are attracted towards the specimen surface, which helps reduce the charging effects described in Chapter 2 (Meredith *et al.*, 1996). The secondary electrons produced from these collisions then accelerate with the original secondary electrons towards the detector. In this process there is a cascade of collisions, which results in an increased suppression of charging and amplification of the number of electrons being collected by the detector (Meredith *et al.*, 1996). By utilizing water vapour to both reduce charging and to amplify the signal, high resolution images of non-coated samples can be collected.

Having a low vacuum chamber creates problems for an SEM because gas molecules can scatter the electrons in the electron beam, which causes a larger spot size and thus reduced resolution (Danilatos, 1981b). An ESEM has a unique multiple pressure limiting aperture system, which allows the electron gun to be under very high vacuum while the specimen chamber can be at a relatively low vacuum (Danilatos, 1981b). The multiple pressure limiting apertures allow the vacuum to be changed dramatically over several sequential pressure decreases so that the electrons in the electron beam are retained in a sufficient quantity to create an adequate electron beam (Danilatos, 1981b). Utilizing a very short distance (typically 1.5-3 mm) between the detector and the specimen, the electron beam

reaching the specimen is not scattered and good resolution is attainable (Danilatos, 1981b).

In addition to using specimens in their natural state, an ESEM has the advantage in that images are collected and stored on a computer. In an ESEM, the user can archive images on computer disks and then retrieve the images at a convenient time. The computer system associated with an ESEM allows the user to return to an image previously collected and photograph the image to obtain a negative. Using computer images also allows the use of computer imaging software, which can be very convenient for enhancing the contrast of an image. These aspects allow a researcher the freedom to quickly document a sample and then at a convenient time the images can be more thoroughly analyzed and appropriate images selected.

In this chapter, AAS was used to measure K leakage during imbibition of white spruce somatic embryos and various parts of white spruce seeds using a typical white spruce somatic embryo germination medium. Additionally, white spruce somatic embryos were pretreated in a high RH environment to measure the effect of moisture content of the tissues prior to complete imbibition on the total amount of K leaked. A high RH pretreatment has been demonstrated to significantly reduce K leakage in carrot somatic embryos (Tetteroo *et al.*, 1996). Also in this chapter, an ESEM was used to study surface changes during imbibition in white spruce somatic and zygotic embryos.

Methods

Potassium Leakage

Potassium leakage was measured during imbibition of white spruce somatic embryos, zygotic embryos, seeds without seed coats and whole seeds. For each of these, three samples were tested at each of 5, 10, 20, 40, 80 and 120 min. of imbibition. Sample sizes used were: 100 somatic embryos, 60 zygotic embryos, 25 seeds without seed coats and 25 whole seeds. In addition, the effect of a high RH pretreatment on K leakage in white spruce somatic embryos was investigated. For each of three pretreated samples, 120 somatic embryos were imbibed and tested for each of the above imbibition times. Somatic embryos were pretreated by placing each sample into a separate uncovered 25 ml volumetric flask and the flasks were placed into a desiccator containing water. Samples were pretreated in this desiccator for 48 h prior to imbibition. All samples of somatic embryos were taken from a pooled supply of somatic embryos, which were collected from several culture plates.

Samples were imbibed in 25 ml volumetric flasks containing modified germination medium. The germination medium used was that of Attree *et al.* (1995). This medium contained half-strength LV medium (Appendix D) with 2% sucrose and was modified by excluding the 0.6% agar and all K-containing salts. Samples were imbibed in the dark in a CONVIRON growth chamber (Controlled Environments Ltd., Winnipeg, Manitoba) set at 25°C. Flasks were continuously agitated using a TEKTATOR V rotator (Tekpro, Evanston, IL) set at 100 ± 10 rpm. At the appropriate time interval, an aliquot of 3.5 or 5 ml was pipetted into a porcelain crucible. Each sample was only used to measure one imbibition time.

Aliquots of germination medium were also pipetted into crucibles to measure background K concentrations within the medium. Solutions were evaporated on a hot plate (approximately 2 h) and then dry ashed as described in Chapter 5. Samples were processed and measured as described for the study of K in Chapter 5.

Potassium concentrations were expressed as μg K leaked per g DW, μg K leaked per tissue and as a % of the total K present based on DW's (as measured in Chapter 5). Statistical differences between means was determined using the MINITAB analysis of variance test. When a difference was found, Tukey's test (Zar, 1984) was used to determine which means differed at $P > 0.05$.

Environmental Scanning Electron Microscopy

Dry white spruce somatic embryos, zygotic embryos, seeds without seed coats and seed coats were attached to aluminum stubs using double-sided carbon tape. Samples were observed using an ESEM model 2020 (ElectroScan Corporation, Wilmington, MA) and several images were collected. White spruce somatic and zygotic embryos were then attached to stainless steel stubs and imbibed for the various time intervals used for K leakage and using the same medium. Using a Peltier stage (ElectroScan Corporation, Wilmington, MA) cooled with water to 0.5°C, hydrated embryos were observed and images collected. Somatic and zygotic embryos were also imbibed for 2 h in water and viewed in the ESEM.

Images collected by the ESEM were then processed using the PiXision differential hysteresis program (designed by Dr. Klaus-Ruediger Peters, University of Connecticut Health Center, Farmington, CT). This program compares contrast levels in a single pixel to contrast

levels in all the other pixels of the image and is used to eliminate extreme contrasts while enhancing the small contrast differences (Peters, 1995). This produces an image with enhanced details. Images were then cropped to size using Corel Photohouse for Windows95 and were organized into plates using WordPerfect for Windows95. These images were then printed on photographic quality paper using a Sony digital printer model UP-D8800.

Results

Potassium Leakage

Table 16 gives all the amounts of K leaked per g DW. Concentrations of K leaked per g DW for white spruce somatic embryos, pretreated somatic embryos and zygotic embryos are illustrated in Fig. 52. Figure 53 illustrates the amounts of K leaked per g DW for various parts of white spruce seeds. In all types of samples studied, over 45% of the total K leaked per g DW during the entire 120 min. period was leaked within the first 20 min. of imbibition. Following this initial leakage, the rate of K leakage on a DW basis began to decrease significantly. On a DW basis, zygotic embryos leaked the most K while whole seeds leaked the least (almost 4 times less K leaked per g DW than for zygotic embryos). Removal of the seed coats resulted in significant increases in the amount of K leaked per g DW, to levels similar to those found for isolated zygotic embryos. During the initial 40 min. of leakage, somatic embryos and pretreated somatic embryos leaked similar amounts of K, both of which were significantly lower than that found for zygotic embryos. After 40 min. of imbibition, pretreated somatic embryos leaked significantly less K per g DW than untreated somatic embryos.

Concentrations of K leaked per tissue are summarized in Table 17. The values of K leaked per tissue during imbibition of dry white spruce somatic embryos, pretreated somatic embryos and dry zygotic embryos are illustrated in Fig. 54 and values for various parts of white spruce seeds are illustrated in Fig. 55. Approximately 50% of all the K leaked per tissue for all types of samples studied, leaked within the first 20 min. of imbibition.

Throughout the entire 120 min. imbibition period, a single somatic embryo, a single pretreated somatic embryo and a single zygotic embryo leaked similar amounts of K. A single seed without a seed coat leaked the most K, leaking 8 times more K than a single zygotic embryo. A whole seed had a reduced amount of K leakage (approximately 2 times less K leaked than a single seed without a seed coat).

Expressing the amount of K leaked as a % of the total K present (based on values of total K from Table 14) gave the results summarized in Table 18 and illustrated in Figs. 56 and 57. Pretreatment of white spruce somatic embryos resulted in a significant decrease in the % of K leaked at 80 and 120 min. of imbibition. This 17% reduction in the % of K leaked after 120 min. resulted in leakage values for pretreated somatic embryos being significantly similar to values for zygotic embryos. When desiccated white spruce somatic embryos were imbibed, approximately 90% of the K present within the embryos was leaked into the germination medium. The % of total K leaked for seeds without seed coats parallelled those measured for zygotic embryos, but initial leakage within the first 20 min. was significantly lower for seeds without seed coats than for zygotic embryos. Leaving the seed coats intact resulted in significant reductions in the % of total K leaked over the 120 min. imbibing period, to levels approximately 3.5 times lower than measured when seed coats were removed.

Table 16: Potassium leakage (± SD) for dry white spruce somatic embryos, zygotic embryos, seeds without seed coats, whole seeds and somatic embryos pretreated in a high RH environment expressed as µg of K leaked per g DW.

Sample	Time (min.)					
	5	10	20	40	80	120
Somatic Embryos	1270.11 ± 115.50 **a**	1461.49 ± 81.80 **a**	2316.26 ± 270.33 **a**	2883.32 ± 177.04 **a**	4446.84 ± 290.08 **a**	4553.16 ± 181.83 **a**
Pretreated Somatic Embryos	1019.20 ± 185.33 **a**	1572.74 ± 254.67 **a**	2385.73 ± 19.33 **a**	2940.08 ± 366.53 **a**	3287.61 ± 278.95 **b**	3705.00 ± 248.24 **b**
Zygotic Embryos	1681.48 ± 228.07 **c**	2088.24 ± 137.06 **b**	3075.43 ± 121.62 **b**	4056.10 ± 188.41 **b**	5203.34 ± 508.75 **a**	5732.87 ± 311.33 **c**
Seeds Without Seed Coats	898.34 ± 96.02 **ab**	1563.22 ± 70.34 **a**	2470.64 ± 229.61 **a**	3369.96 ± 452.69 **ab**	4698.90 ± 200.98 **a**	5496.54 ± 453.65 **c**
Whole Seeds	541.28 ± 79.61 **b**	700.35 ± 49.56 **c**	1086.19 ± 88.37 **c**	1218.31 ± 154.17 **c**	1280.02 ± 209.30 **c**	1503.61 ± 180.18 **d**

Note: Each mean was calculated using 3 values. Values in a single column that are followed by the same letter are not significantly different at $P > 0.05$.

Table 17: Potassium leakage (± SD) for dry white spruce somatic embryos, zygotic embryos, seeds without seed coats, whole seeds and somatic embryos pretreated in a high RH environment expressed as µg of K leaked per tissue.

Sample	Time (min.)					
	5	10	20	40	80	120
Somatic Embryos	0.29 ± 0.03 **a**	0.32 ± 0.00 **a**	0.59 ± 0.13 **a**	0.70 ± 0.08 **a**	1.04 ± 0.08 **a**	1.05 ± 0.04 **a**
Pretreated Somatic Embryos	0.26 ± 0.05 **a**	0.39 ± 0.06 **a**	0.60 ± 0.01 **a**	0.74 ± 0.10 **a**	0.83 ± 0.08 **a**	0.92 ± 0.07 **a**
Zygotic Embryos	0.25 ± 0.03 **a**	0.32 ± 0.02 **a**	0.50 ± 0.04 **a**	0.65 ± 0.03 **a**	0.84 ± 0.08 **a**	0.94 ± 0.03 **a**
Seeds Without Seed Coats	1.39 ± 0.05 **b**	2.23 ± 0.05 **b**	3.70 ± 0.32 **b**	4.72 ± 0.58 **b**	6.48 ± 0.90 **b**	7.52 ± 0.52 **b**
Whole Seeds	1.19 ± 0.17 **b**	1.54 ± 0.14 **c**	2.39 ± 0.21 **c**	2.70 ± 0.35 **c**	2.81 ± 0.46 **c**	3.31 ± 0.38 **c**

Note: Each mean was calculated using 3 values. Values in a single column that are followed by the same letter are not significantly different at $P > 0.05$.

Table 18: Potassium leakage (± SD) for dry white spruce somatic embryos, zygotic embryos, seeds without seed coats, whole seeds and somatic embryos pretreated in a high RH environment expressed as a % of total K present.

Sample	Time (min.)					
	5	10	20	40	80	120
Somatic Embryos	25.42 ± 2.31 **a**	29.25 ± 1.64 **a**	46.37 ± 5.41 **ab**	57.63 ± 3.42 **a**	89.01 ± 5.80 **a**	91.14 ± 3.64 **a**
Pretreated Somatic Embryos	20.40 ± 3.71 **a**	31.48 ± 5.10 **a**	47.75 ± 0.39 **a**	58.85 ± 7.34 **a**	65.81 ± 5.58 **b**	74.16 ± 4.97 **b**
Zygotic Embryos	21.73 ± 2.95 **a**	26.99 ± 1.77 **a**	39.74 ± 1.57 **b**	52.42 ± 2.44 **ab**	67.24 ± 6.58 **b**	74.09 ± 4.02 **b**
Seeds Without Seed Coats	11.00 ± 1.18 **b**	19.14 ± 0.86 **b**	30.25 ± 2.81 **c**	41.26 ± 5.54 **b**	57.54 ± 2.46 **b**	67.30 ± 5.55 **b**
Whole Seeds	7.01 ± 1.03 **b**	9.07 ± 0.64 **c**	14.07 ± 1.15 **d**	15.78 ± 2.00 **c**	16.58 ± 2.71 **c**	19.48 ± 2.33 **c**

Note: Each mean was calculated using 3 values. Values in a single column that are followed by the same letter are not significantly different at $P > 0.05$.

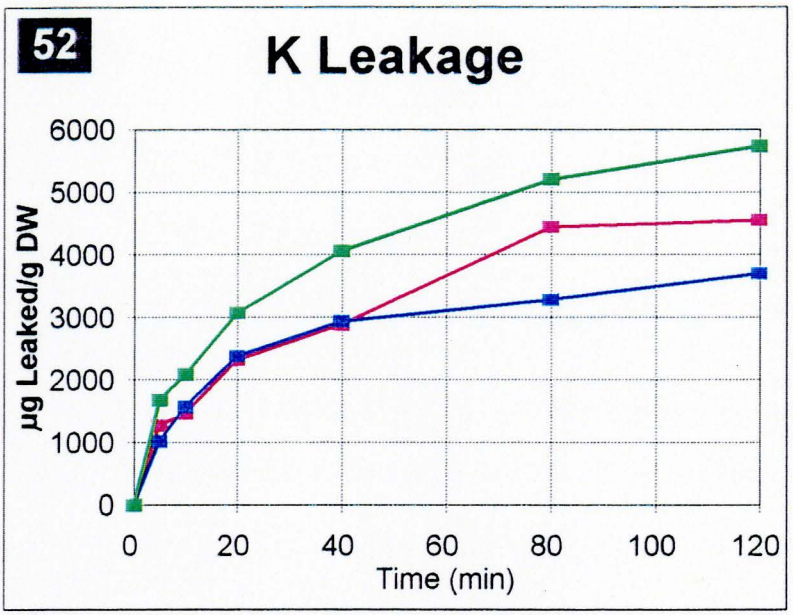
52
K Leakage
µg Leaked/g DW
6000
5000
4000
3000
2000
1000
0
0
20
40
60
80
100
120
Time (min)

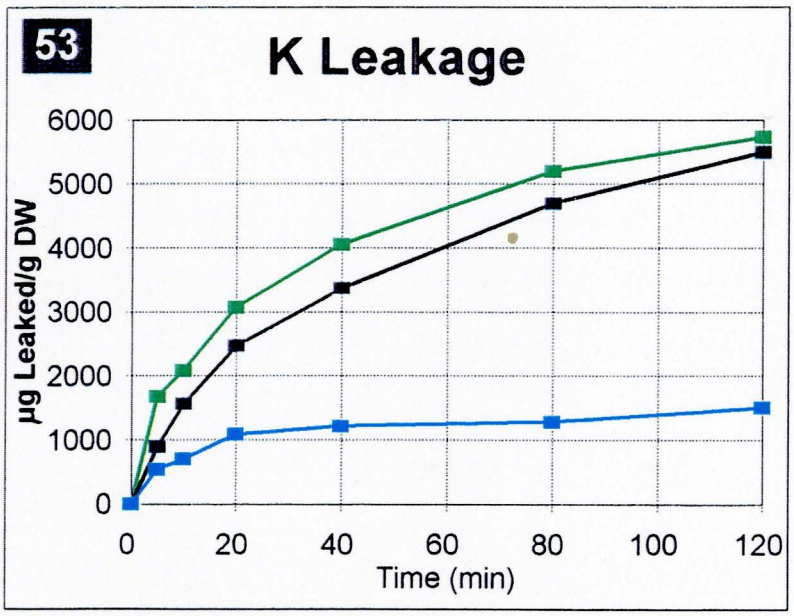
53
K Leakage
µg Leaked/g DW
6000
5000
4000
3000
2000
1000
0
0
20
40
60
80
100
120
Time (min)

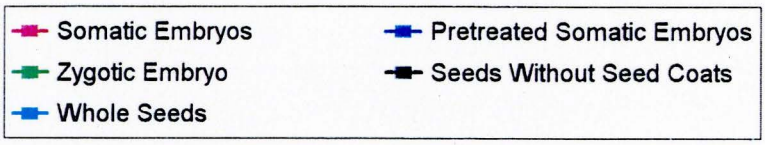
Somatic Embryos
Pretreated Somatic Embryos
Zygotic Embryo
Seeds Without Seed Coats
Whole Seeds

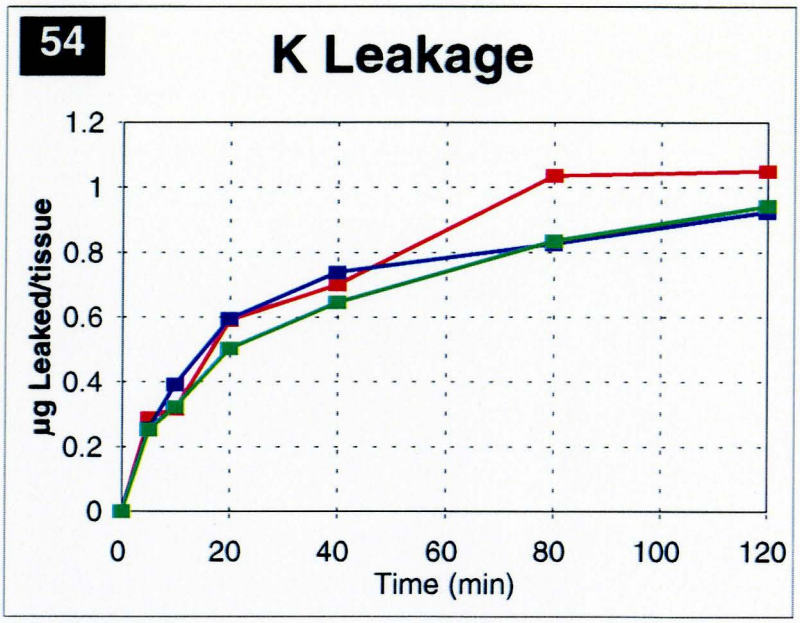
54
K Leakage
µg Leaked/tissue
1.2
1
0.8
0.6
0.4
0.2
0
0
20
40
60
80
100
120
Time (min)

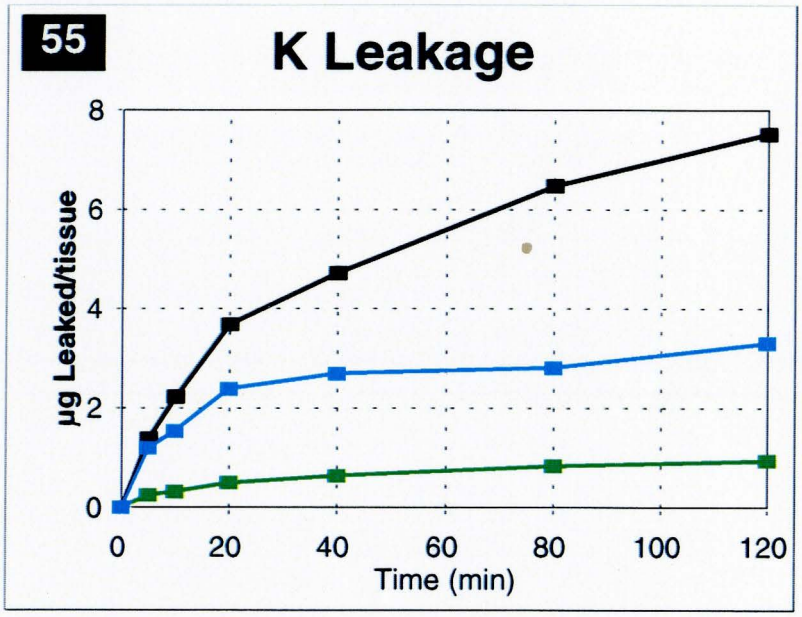
55
K Leakage
µg Leaked/tissue
8
6
4
2
0
0
20
40
60
80
100
120
Time (min)

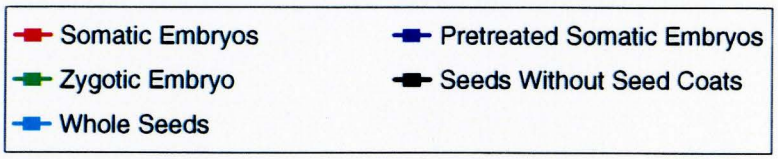
Somatic Embryos
Pretreated Somatic Embryos
Zygotic Embryo
Seeds Without Seed Coats
Whole Seeds

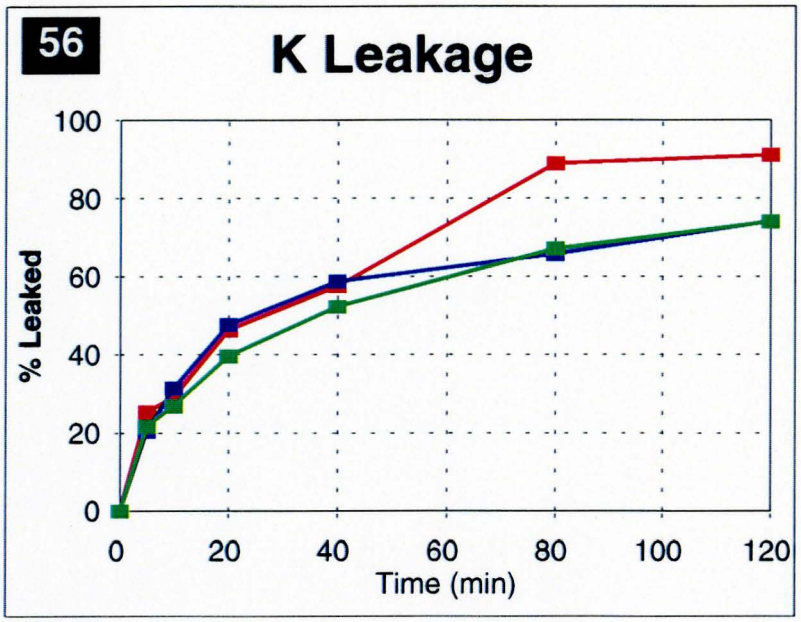
56
K Leakage
% Leaked
100
80
60
40
20
0
0
20
40
60
80
100
120
Time (min)

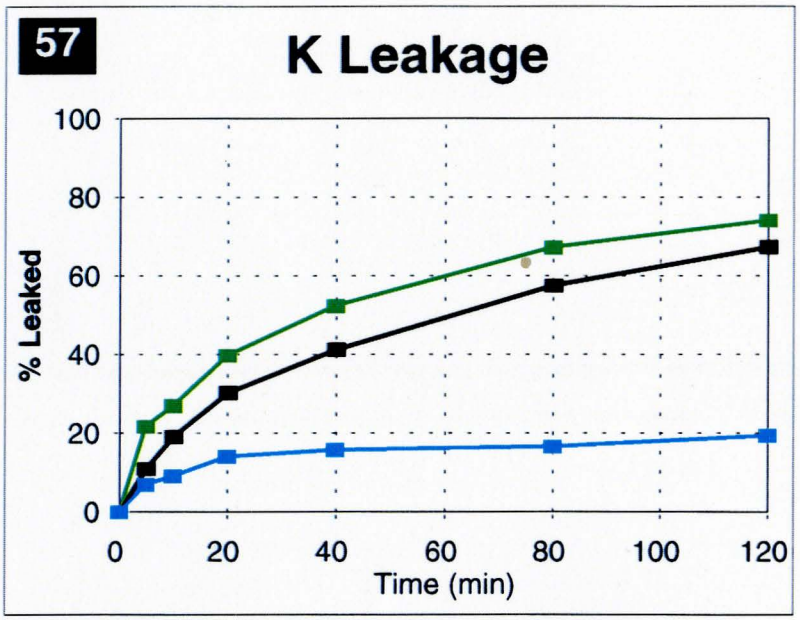
57
K Leakage
% Leaked
100
80
60
40
20
0
0
20
40
60
80
100
120
Time (min)

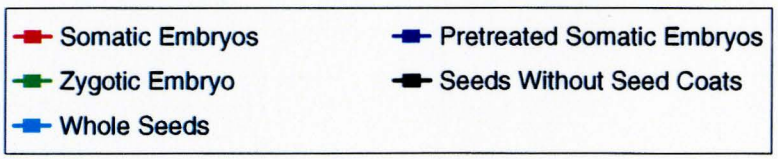
Somatic Embryos
Pretreated Somatic Embryos
Zygotic Embryo
Seeds Without Seed Coats
Whole Seeds

Environmental Scanning Electron Microscopy

Outer and inner surfaces of seed coats from dry white spruce seeds are illustrated in Figs. 58 and 59, respectively. The outer surface of the seed coat is characterized by what appears to be large waxy deposits. The inner surface, however, had some remnants of cellular structure in that rectangular cell shapes were visible. Surrounding the female gametophyte of a dry white spruce seed was a thin fibrous layer (Fig. 60). Removal of this layer from the female gametophyte revealed a surface without distinctive cell wall details (Fig. 61).

For all remaining ESEM micrographs, the left hand column illustrates surface structures in somatic embryos, while the right hand column illustrates equivalent structures in zygotic embryos. For imbibition studies of somatic and zygotic embryos, all samples began as dry embryos. The shoot apex of a desiccated white spruce somatic embryo was flattened and contained surface cells that were very shrivelled (Fig. 62). Figure 63 illustrates the shoot apex of a dry white spruce zygotic embryo following removal of two cotyledons. The shoot apex in a white spruce zygotic embryo also contained highly shrivelled cells, but the apex was smaller and more lobed than the shoot apex of a white spruce somatic embryo (Compare Figs. 62 and 63). The zygotic embryo from a white spruce seed had a shoot apex that was completely enclosed and protected within a cavity formed by the close packing of the cotyledons.

Cotyledons of desiccated white spruce somatic embryos had surface cells arranged in discrete rows and cells had a wrinkled appearance (Fig. 64). In white spruce zygotic embryos, dry cotyledons also contained wrinkled surface cells (Fig. 65), but these cells appeared more shrunken than cells from cotyledons of desiccated somatic embryos.

Imbibition of white spruce somatic embryos in germination medium for 5 min. resulted in cotyledons having surface cells that were still wrinkled in appearance (Fig. 66). Cotyledons of zygotic embryos imbibed for 5 min. in germination medium had similar appearances to those in somatic embryos imbibed for the same period of time, in that surface cells still appeared shrunken and wrinkled (Fig. 67). There were no noticeable changes in appearance of cotyledon surface cells from somatic and zygotic embryos imbibed in germination medium for 40 min. (Figs. 68 and 69) and for 120 min. (Figs. 70 and 71).

The hypocotyl surface of a desiccated white spruce somatic embryo resembled the cotyledon surface, with cells arranged in discrete rows and wrinkled in appearance (Fig. 72). Surface cells in the hypocotyl of a dry zygotic embryo were also arranged in discrete rows and these cells were very shrunken in appearance (Fig. 73). Hydration of a somatic embryo for 5 min. in germination medium resulted in the hypocotyl surface cells having a more turgid appearance, but wrinkling was still evident (Fig. 74). Likewise, after 5 min. hydration of a zygotic embryo in germination medium, cells on the surface of a hypocotyl appeared to be more turgid (Fig. 75) than cells in the dry embryo. In zygotic embryos, swelling was irregular in that some surface cells appeared very turgid while others still exhibited shrunken appearances (Fig. 75). After 40 min. exposure to germination medium, somatic and zygotic embryos still had hypocotyls with some surface cells turgid while others showed wrinkling in the cell walls (Figs. 76 and 77). Somatic embryos exposed to medium for 120 min. had the majority of their hypocotyl surface cells turgid and the cell walls of these cells had a striated pattern running parallel to the hypocotyl-root axis (Fig. 78). Like somatic embryos, after 120 min. of imbibition, the majority of surface cells in hypocotyls of white spruce zygotic embryos

were turgid and a few cells still had wrinkled surfaces (Fig. 79).

The surface of the suspensor region of a desiccated somatic embryo was unorganized in that it contained highly wrinkled and shrunken cells not arranged in any discrete rows (Fig. 80). The surface of the root cap region of a dry zygotic embryo had cells present in more discrete rows than in somatic embryos, contained shrivelled cells and was less distinguishable from the hypocotyl portion of the embryo (Fig. 81). The appearance of these suspensor/root cap regions in both types of embryos did not change throughout the entire imbibition period. Zygotic embryos also often had one side that was very smooth in appearance. This smooth surface never changed in appearance throughout this imbibition regime. Also, somatic and zygotic embryos were imbibed for 2 h in water and the surface of these embryos appeared very turgid and no evidence of wrinkled cells was found indicating complete hydration.

Figures 58 to 63: Environmental Scanning Electron Micrographs of Various Parts of Dry White Spruce Seeds and Somatic Embryos.

Figure 58: The outer surface of the seed coat from a seed. Note the irregular waxy surface of this seed coat. Magnification = 200x.

Figure 59: Inner surface of a seed coat illustrating remnant cellular structures. Magnification = 200x.

Figure 60: Micrograph of the thin fibrous layer surrounding the female gametophyte of a seed. Magnification = 200x.

Figure 61: Surface detail of the female gametophyte from a dry seed. Note the lack of cellular details in the surface of this tissue. Magnification = 85x.

Figure 62: Flattened shoot apex (center of image) in a desiccated white spruce somatic embryo, composed of shrunken cells surrounded by a flared array of cotyledons. Magnification = 200x.

Figure 63: Lobed shoot apex of a dry white spruce zygotic embryo. Note the region below the apex is where two cotyledons were removed to expose the shoot apex within its protective cavity. Also note the shrunken appearance of the cells in the shoot apex region. Magnification = 200x.

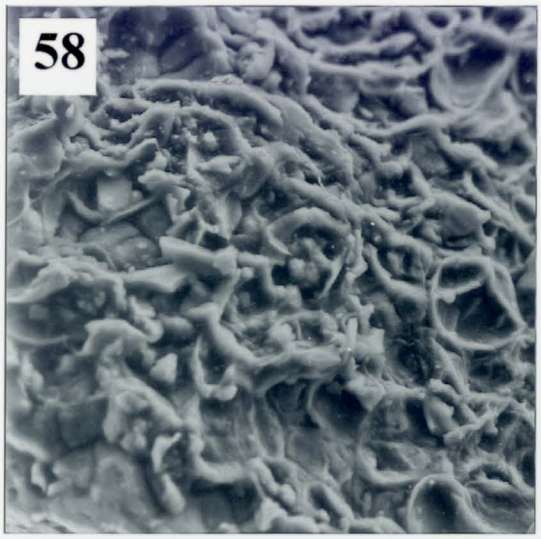
58

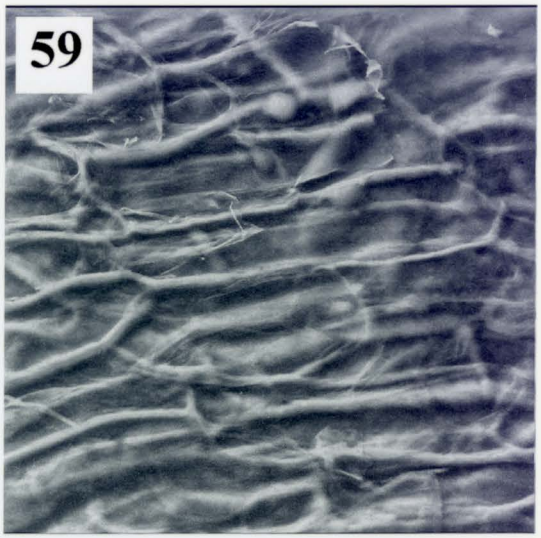
59

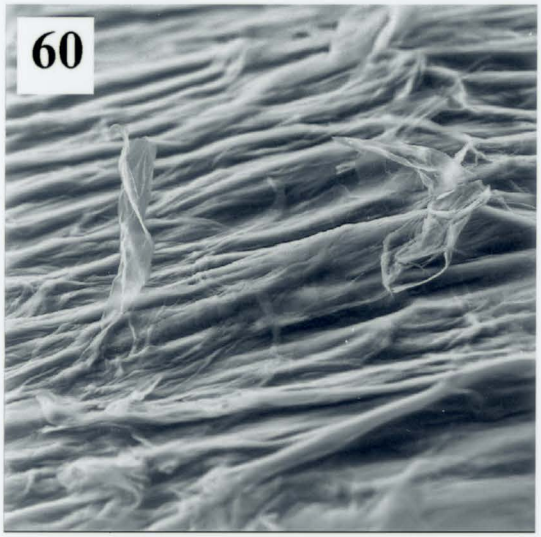
60

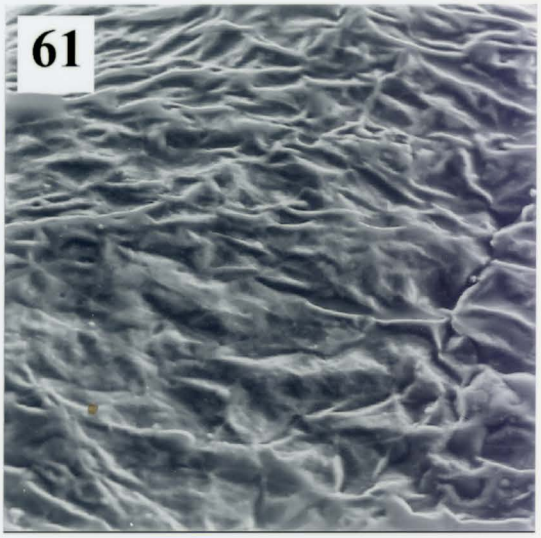
61

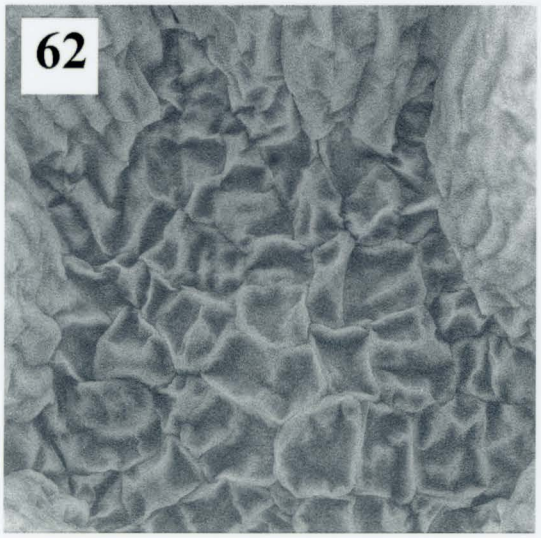
62

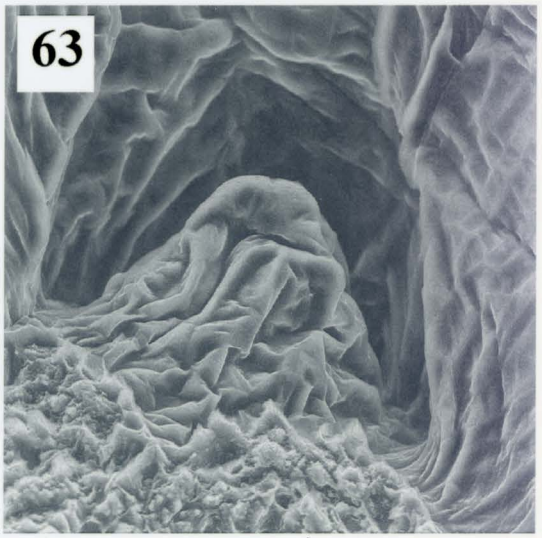
63

Figures 64 to 69: Environmental Scanning Electron Micrographs of Cotyledons From Dry and Imbibed White Spruce Somatic and Zygotic Embryos.

Figure 64: Surface of a desiccated somatic embryo cotyledon. Note the arrangement of shrivelled cells in very discrete rows. Magnification = 200x. Insert illustrates wrinkles in these cells. Magnification of insert = 300x.

Figure 65: Tips of several cotyledons in a dry zygotic embryo. Magnification = 200x. Insert illustrates the shrunken and wrinkled appearance of cells in these cotyledons. Insert Magnification = 300x.

Figure 66: Cotyledon of a somatic embryo imbibed in germination medium for 5 min. Note that these cells still show severe wrinkling. Magnification = 200x.

Figure 67: Zygotic embryo cotyledon following 5 min. imbibition in germination medium. These cells appear more turgid than in the dry state, but swelling is irregular as shown by shrunken areas next to turgid areas. Magnification = 200x.

Figure 68: Somatic embryo cotyledon after 40 min. imbibition in germination medium. Cell morphology is similar to that observed after 5 min. imbibition in that several cells are still wrinkled while others are turgid. Magnification = 200x.

Figure 69: Cotyledon of a zygotic embryo following 40 min. imbibition in germination medium. Note the cells are still shrunken and wrinkled and are similar in appearance to cells from the cotyledon of the somatic embryo imbibed for 40 min. Magnification = 200x.

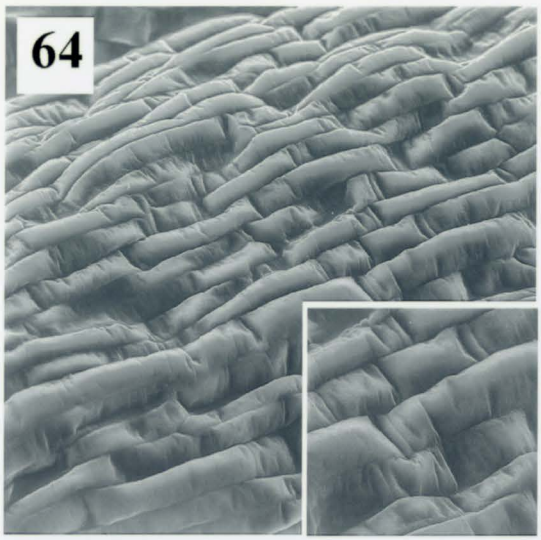
64

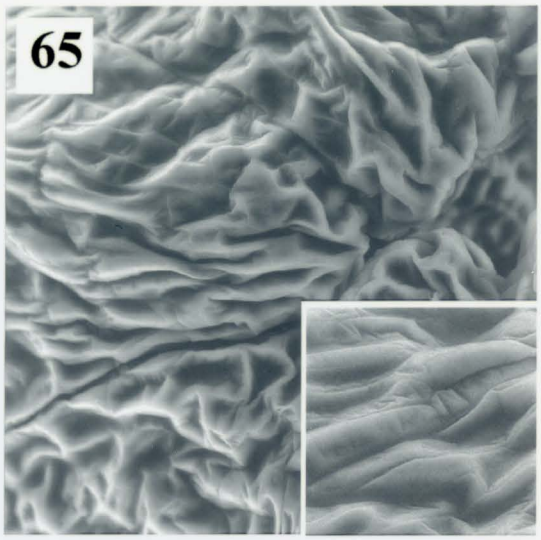
65

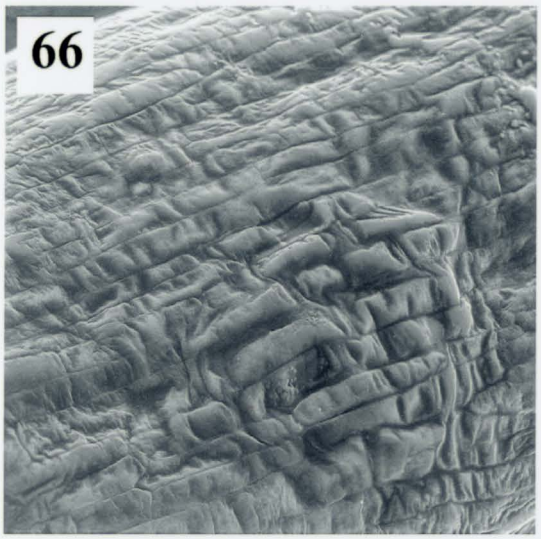
66

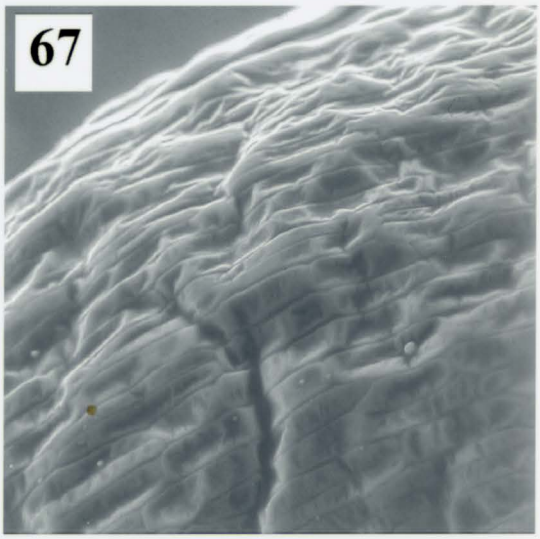
67

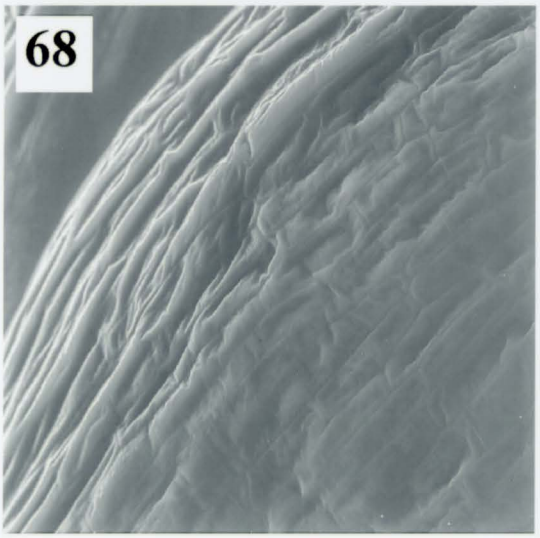
68

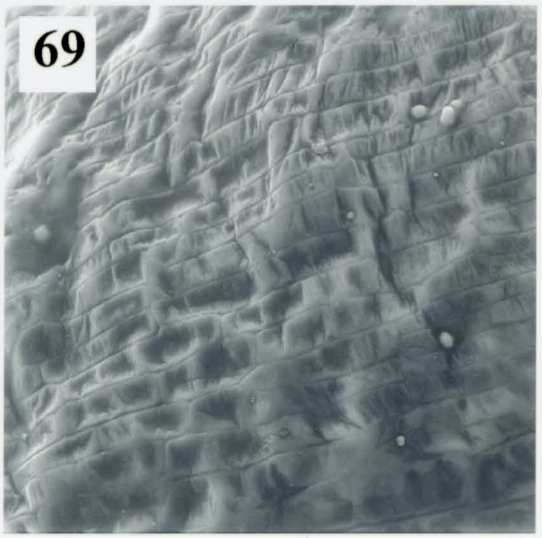
69

Figures 70 to 75: Surface Details of Cells From Cotyledons and Hypocotyls of Dry and Imbibed White Spruce Somatic and Zygotic Embryos as Seen in an ESEM.

Figure 70: Cells from the cotyledon of a somatic embryo imbibed for 120 min. in germination medium. These cells still demonstrate wrinkling and areas that are very shrunken. Magnification = 680x.

Figure 71: Cotyledon of a zygotic embryo imbibed for 120 min. in germination medium. Cells are wrinkled and some cells are still highly shrunken. Magnification = 680x.

Figure 72: Hypocotyl region of a desiccated somatic embryo. Cells are arranged in discrete rows. Magnification = 200x. Insert shows wrinkles in the cell walls of these cells. Magnification of insert = 300x.

Figure 73: Dry hypocotyl of a white spruce zygotic embryo. Note that these cells are arranged in discrete rows. Magnification = 200x. Insert illustrates the shrunken and wrinkled appearance of these cells. Magnification of insert = 300x.

Figure 74: Cells in the hypocotyl of a somatic embryo imbibed for 5 min. in germination medium. Cells appear to be turgid, but some wrinkling is still present. Magnification = 680x.

Figure 75: Hypocotyl of a zygotic embryo following imbibition for 5 min. in germination medium. Note that these cells are more turgid than those shown in Fig. 73, but some cells showed very irregular swelling. Magnification = 680x.

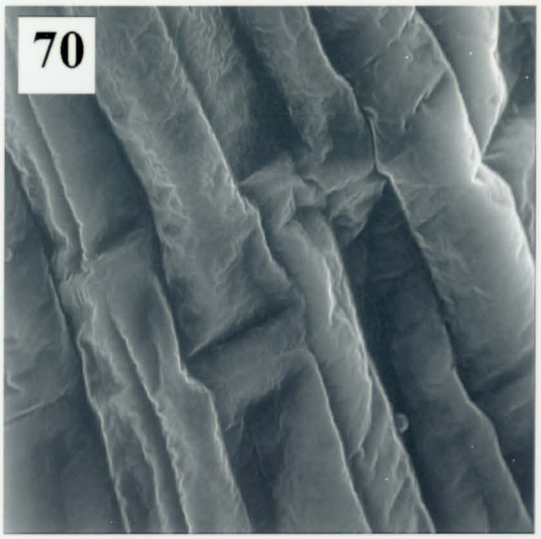
70

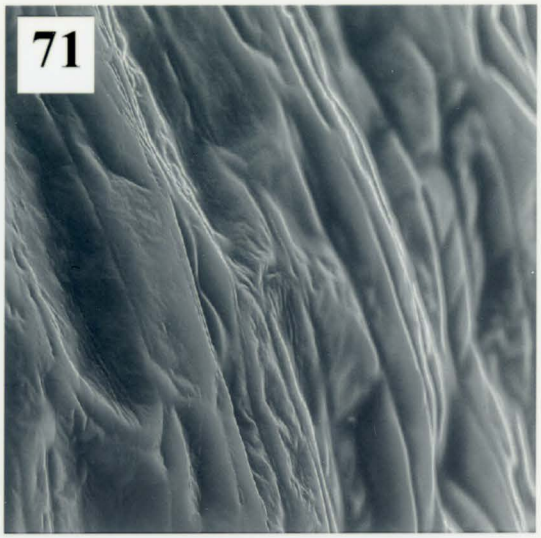
71

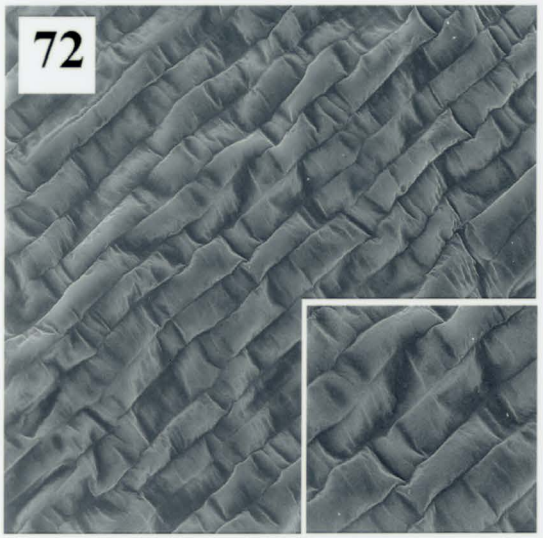
72

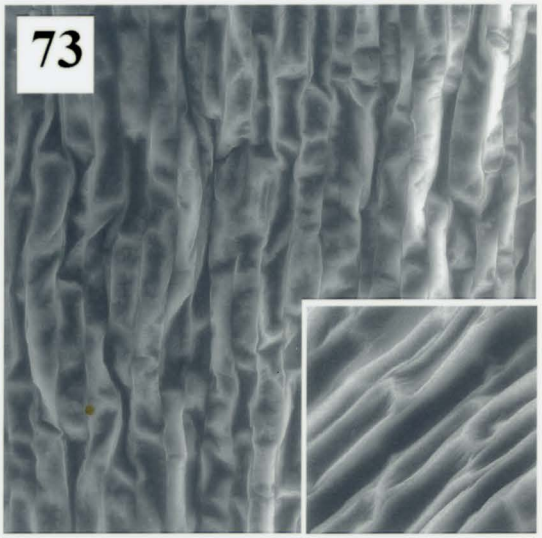
73

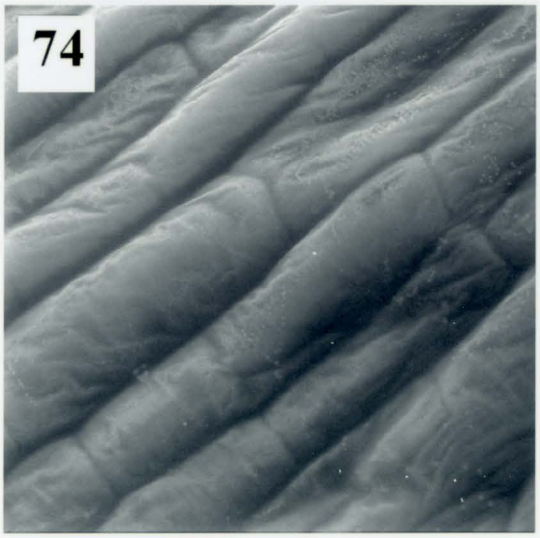
74

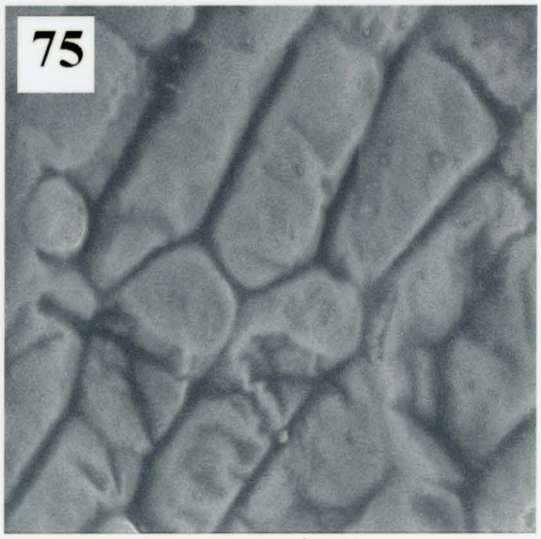
75

Figures 76 to 81: Environmental Scanning Electron Micrographs of the Hypocotyl and Suspensor/Root Cap Regions of Dry and Imbibed White Spruce Somatic and Zygotic Embryos.

Figure 76: Hypocotyl region of a somatic embryo following 40 min. imbibition in germination medium. Cells in this embryo still show some wrinkling. Magnification = 680x.

Figure 77: Zygotic embryo hypocotyl after 40 min. in germination medium. Cells have very similar appearance to those seen in the somatic embryo shown in Fig. 76. Cells still have wrinkled appearances. Magnification = 680x.

Figure 78: Somatic embryo hypocotyl following exposure to germination medium for 120 min. Cells appear more turgid and have numerous fine striations running parallel to the hypocotyl-root axis of the embryo. Magnification = 680x.

Figure 79: Hypocotyl region of a white spruce zygotic embryo after 120 min. imbibition in germination medium. Most cells are turgid with occasional cells still showing evidence of wrinkling. Magnification = 680x.

Figure 80: Suspensor region of a desiccated somatic embryo. Cells were not present in discrete rows. Magnification = 200x. Insert illustrates the highly shrivelled cells found in this region. Magnification of insert = 300x.

Figure 81: Root cap region of a dry zygotic embryo. These cells are arranged in rows. Magnification = 200x. Insert illustrates very shrunken and wrinkled cells in this region. Magnification of insert = 300x.

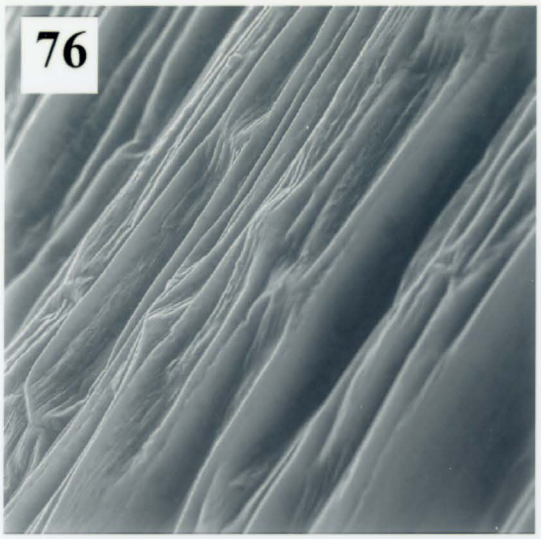
76

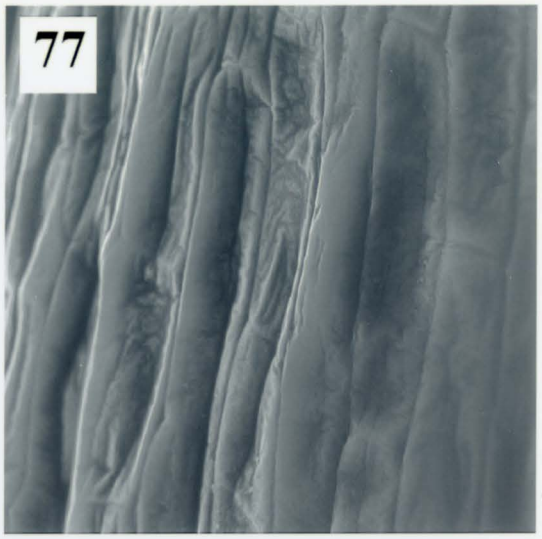
77

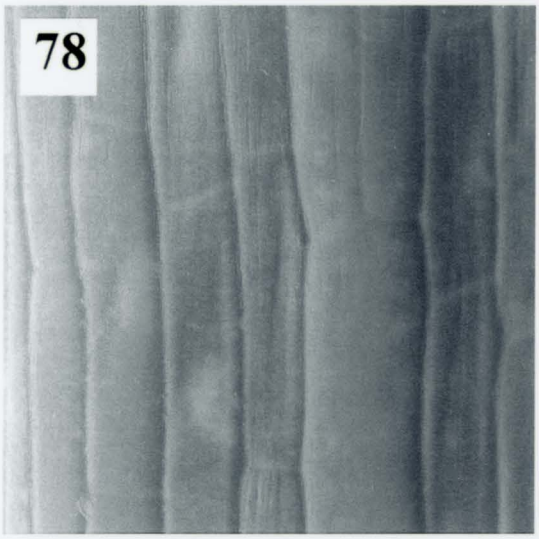
78

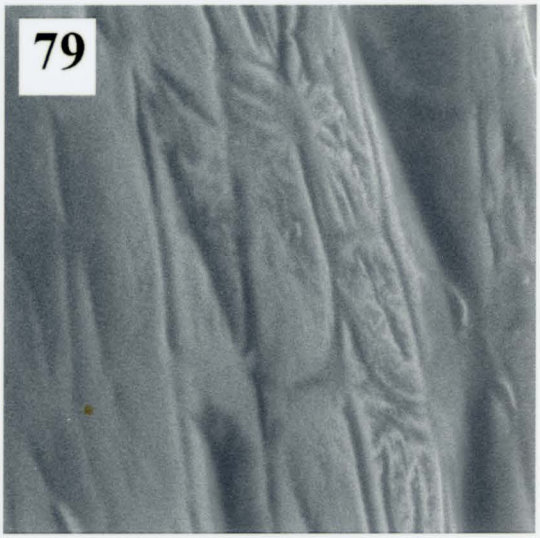
79

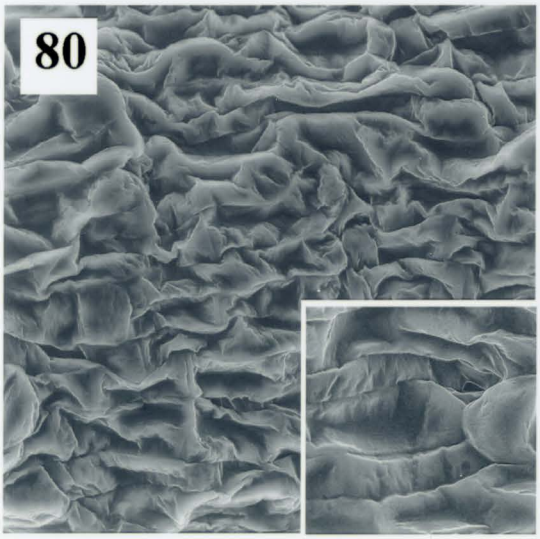
80

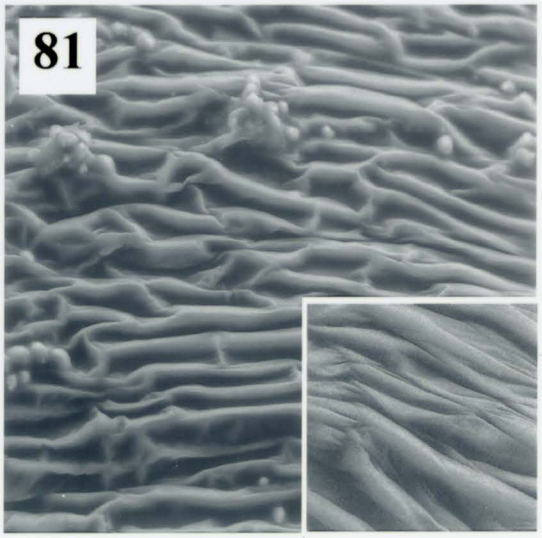
81

Discussion

Imbibition of water into a dry seed results in the resumption of active metabolic activities required to promote the growth of a zygotic embryo into a seedling. In a spruce seed, it has been shown that the cotyledons of the zygotic embryo are the major sites of nutrient uptake from the female gametophyte and translocation of these nutrients to the rest of the embryo (Teasdale and Buxton, 1986; DeCarli *et al.*, 1987). Hydrolysis of protein and lipid stores in zygotic embryos and female gametophytes occurs rapidly within the initial stages of seedling development and are important to support seedling growth until the seedling becomes established (DeCarli *et al.*, 1987; Misra and Green, 1990). Studies of white spruce somatic embryos and zygotic embryos have shown that protein mobilization during germination occurs in a similar fashion for both types of embryos (Misra and Green, 1990; Misra *et al.*, 1993).

Imbibition of white spruce somatic embryos is faster than imbibition of seeds, due to the lack of a seed coat and female gametophyte. It has been estimated that approximately 2 h of imbibition of a white spruce somatic embryo is equivalent to 65 h of imbibition of tissues within a white spruce seed (Attree *et al.*, 1992). Due to this rapid imbibition, white spruce somatic embryos must be carefully imbibed using semi-solidified medium and only after 4 to 6 weeks of seedling growth are these plantlets transferred to soil (Attree and Fowke, 1995). In order to allow plantlet production with less demanding handling protocols, the dynamics of water uptake and solute leakage in somatic embryos must be investigated.

In this study, the levels of K leaked into germination medium was measured for white spruce somatic embryos and various parts of white spruce seeds. This medium was chosen

to, as closely as possible, mimic the conditions under which somatic embryos of white spruce are germinated. Imbibition was performed in the dark, as was done in the initial stages of germination for white spruce somatic embryos as reported by Attree and Fowke (1995). Results show that seeds without seed coats and isolated zygotic embryos of white spruce leak similar amounts of K per g DW and as a % of the total K present. Whole seeds, with intact seed coats, had significantly less leakage of K per g DW and as a % of the total K present. On a per tissue basis, the smaller zygotic embryo leaked less K than a seed without the seed coat and the addition of the seed coat to a seed resulted in significant reductions in the amount of K leaked from a seed. The testa plays a significant role in regulating the water supply to the embryo by slowing down the rate of water absorption (Larson, 1968; Rowland and Gusta, 1977; McDonald *et al.*, 1988). The removal of the seed coat has previously been shown to increase leakage of solutes from other species (Duke and Kakefuda, 1981; Duke *et al.*, 1983). The waxy appearance of the seed coat as revealed in the ESEM is consistent with its role of slowing water entry into the seed.

When desiccated white spruce somatic embryos were imbibed, significantly less K leaked per g DW than occurred with white spruce zygotic embryos. A single somatic embryo and a single zygotic embryo, however, leaked similar levels of K throughout the imbibitional period. When expressed as a % of the total K present, white spruce somatic embryos leaked significantly more K at 80 and 120 min. intervals than did white spruce zygotic embryos. Measurement of K leakage was stopped at 120 min. of imbibition because the rate of K leakage was starting to level off. Pretreatment of desiccated white spruce somatic embryos in a high RH environment for 2 days resulted in significant decreases in K leakage per g DW

and as a % of the total K present for both the 80 and 120 min. time intervals. This pretreatment resulted in the levels leaked per g DW and as a % of the total K present similar to those for zygotic embryos of white spruce. Although pretreatment did not produce significant changes in the amount of K leaked per tissue, a pretreated somatic embryo did have values of K leaked closer to a single zygotic than did an untreated somatic embryo. Pretreatment of carrot somatic embryos in a high RH environment for 4 h was also shown to significantly reduce the % of K leaked during imbibition (Tetteroo *et al.*, 1996). It is believed that this pretreatment allows the membranes to begin reforming distinct bilayer conformations so that imbibition in liquid results in less leakage through the membranes.

It would be expected that embryos with a larger surface area to volume ratio would leak more K because the K present within the embryo would be closer to the surface and therefore more readily lost through diffusion. A white spruce somatic embryo is larger than a zygotic embryo and therefore has a smaller surface area to volume ratio. Theoretically, the larger somatic embryo should lose K slower than a zygotic embryo. From the findings of this study, a single somatic embryo and a single zygotic embryo leaked similar amounts of K, suggesting that the size difference has little effect on the levels of K leaked. It would therefore seem that producing smaller somatic embryos, which would more closely resemble zygotic embryos, would not result in increased leakage during imbibition.

One theory proposed to explain these large losses of solutes during imbibition is that in a dry seed the cell membranes are not present as complete bilayers, but rather as inverted hexagonal plates (Simon, 1974). This theory arises from observations of membranes in brain tissue reported by Luzzati and Husson (1962). Simon (1974) extrapolated this theory to

seeds to suggest that solute leakage occurs due to the hexagonal structure. In this theory, phospholipids are arranged in a pattern that results in the presence of small water-filled channels lined by the heads of the phospholipids (Simon and RajaHarun, 1972; Simon, 1978). In this way, electrolytes diffuse through these pores until the membrane rearranges to form complete bilayers. This hexagonal theory has never been directly proven to occur in dry seeds and it has been argued that data collected concerning temperature effects on membrane leakage directly contradict this theory (Hoekstra and Van der Wal, 1988; Crowe *et al.*, 1989).

A second membrane theory that has been proposed to explain imbibitional solute leakage is a gel-to-liquid crystalline phase transition theory (Crowe *et al.*, 1989). This theory is a modification of the Simon (1974) inverted hexagonal theory in that, according to Crowe *et al.* (1989), membranes in dry seeds have gel phases with phospholipids from each side of the bilayer being aligned with one another. This would allow solutes to more easily pass through the bilayer by moving between aligned phospholipids. Upon hydration, the phospholipids shift to form the liquid phase so that phospholipids on one side of the bilayer are staggered in relation to phospholipids on the other side of the bilayer (Crowe *et al.*, 1989). At this stage, as a solute tries to cross the membrane, the phospholipid on one side restricts its passage (Crowe *et al.*, 1989). This theory was based on work with pollen and has subsequently been repeated on pollen (Hoekstra *et al.*, 1992). This phenomenon has not, however, been demonstrated in seed tissues, but McKersie and Stinson (1980) reported that their work on birdsfoot trefoil (*Lotus corniculatus*) seeds could not be explained by the hexagonal phase theory and they therefore concluded a more subtle change had occurred.

Perhaps the results of McKersie and Stinson (1980) would be better explained according to the gel-to-liquid crystalline theory.

A third explanation for large-scale solute leakage during imbibition, that has been shown in seeds, is that cells physically rupture and extrude their cellular contents. Cellular rupture has been found in embryos of soybean (*Glycine maxima*), navybean (*Phaseolus vulgaris*), pea (*Pisum sativum*) and peanut (*Arachis hypogea*) (Dunn *et al.*, 1980; Duke and Kakefuda, 1981; Schoettle and Leopold, 1984). Spaeth (1989) even reported that streams of intracellular substances ranging in diameter from 0.2 to 1 μm were extruded from imbibed pea cotyledons. This is the only current theory that has been consistently shown in seed tissues from various species.

Surface details of desiccated white spruce somatic embryos, as revealed in the ESEM, showed cells that were wrinkled in appearance. These findings are consistent with observations made previously using sputter coating and a conventional SEM (Fowke and Attree, 1994). Wrinkling of surface cells in dry embryos is believed to be essential for the preservation of plasma membrane-cell wall associations (Webb and Arnott, 1982). The degree of wrinkling is associated with the environment in which desiccation occurred, the presence of varying ratios of storage products within the cells and the composition of the cell walls (Webb and Arnott, 1982). Dry white spruce zygotic embryos were found to contain surface cells that were more shrunken than those in somatic embryos. This may reflect the lower MC in zygotic embryos (Chapter 2) or the presence of higher lipid contents in somatic embryos (Attree *et al.*, 1994; 1995), which may prevent additional shrinkage. Lipids are hydrophobic and therefore upon drying they shrink less, resulting in cells with less

shrinkage.

In a previous SEM survey of somatic and zygotic embryos of white spruce, several techniques were used to study dry and hydrated embryos (Fowke *et al.*, 1994). The use of an ESEM allowed the easy study of both dry and hydrated embryos, eliminating the tissue preparation and possible artifacts associated with the techniques used by Fowke *et al.* (1994). In this current study, surfaces of somatic and zygotic embryos hydrated in water alone appeared turgid and no wrinkling was evident. This was consistent with observations of Fowke *et al.* (1994).

The focus, however, of this current study was changes in surface details during imbibition in gemination medium. Somatic and zygotic embryos of white spruce showed some surface swelling (which was more prominent in the hypocotyl) during imbibition in this medium, but even after 120 min. some signs of wrinkling were still present. No signs of cell rupture were evident in either embryo type. One explanation for the presence of wrinkling after 120 min. is that Attree *et al.* (1991) noted that 2 h of imbibition was required to return white spruce somatic embryos to their predesiccated turgid appearances. Perhaps longer exposure to the germination medium would have resulted in more swelling of these cells. A second possibility is that the high osmotic conditions in the germination medium were sufficient enough to allow only gradual swelling rather than the rapid water influx that occurs with water alone. Germination medium was used here so as to closely mimic treatments of somatic embryos in the lab, but as a seed imbibes water, nutrients liberated from the female gametophyte likely produce a solution surrounding the imbibing zygotic embryo with similarly large amounts of nutrients. Therefore, imbibitional observations in this study are likely more

reflective of the changes that occur during early steps of imbibition of white spruce zygotic embryos than observations of imbibition in water alone. Since somatic embryos are imbibed on semi-solidified medium, the rate of swelling is further slowed and high levels of K in the medium help to reduce the effects of rapid K leakage upon imbibition.

The finding that no cell rupture was evident during hydration of white spruce somatic and zygotic embryos indicates that more subtle membrane changes are responsible for the levels of K leaked here. Therefore, these results would better support the gel-to-liquid crystalline phase theory of Crowe *et al.* (1989), but further work would be required to confirm this. The dynamics of imbibition in somatic embryos, zygotic embryos and seeds still requires further investigation. Results from this study and other studies will prove invaluable in the potential development of a dry synthetic seed, which can be imbibed and germinated in the same manner as natural seeds.

CHAPTER 7:
DISCUSSION OF KEY FINDINGS

Somatic embryo production provides numerous advantages for reforestation practices. Somatic embryogenesis can be used to produce virtually unlimited numbers of identical embryos continuously throughout the year (Attree and Fowke, 1993). By selecting explant sources based on desired characteristics, somatic embryos have the potential for producing genetically superior trees with better wood quality, increased vertical growth rates and better wood dimension increments (Attree and Fowke, 1993). Utilizing gene manipulation techniques, it may soon become possible to also use somatic embryos to produce trees that are resistant to disease, pests and environmental stresses like drought and frost (Attree and Fowke, 1993). Advancements in the ability to produce somatic embryos may result in faster and more efficient reforestation of logged areas, which potentially may help to correct some of the vast damage that human logging has had on the world's forests.

Development and refinement of the techniques used in somatic embryo production also has many implications towards understanding the complex processes involved in embryogenesis. Collection of conifer zygotic embryos at various stages of development, in volumes sufficient enough to do large scale testing, is very difficult because of the relatively long reproductive cycle of conifers and the difficulty in extracting developing seeds from resinous cones (Owens and Molder, 1979). Somatic embryogenesis, however, can be used to produce large numbers of embryos at any stage of development by simply stopping the

culture at the appropriate time. Researchers can then study the processes involved in somatic embryo production with relative ease. If researchers compare mature somatic embryos to mature zygotic embryos and find that these two embryo types are very similar in both structure and composition, then it can be hypothesized that somatic embryos must go through similar physiological and morphogenic processes as occurs in zygotic embryogenesis. In this way, research can be performed on the more accessible somatic embryos and the results extrapolated to zygotic embryos. Researchers can then perform studies on developmentally immature zygotic embryo samples, which are harder to collect, to confirm that these extrapolations are valid.

Morphological and anatomical studies in this thesis and by Reid (1996) found that in general, white spruce somatic and zygotic embryos were very similar. Somatic embryos of white spruce differed from zygotic embryos of white spruce in that somatic embryos were larger, had more prominent suspensor regions and had flared cotyledon arrangements. Both types of embryos contained three primary meristems: protoderm, ground meristem and procambium. Somatic embryos of white spruce had ground meristem tissue that contained large intercellular air spaces and the cells had divided in various planes of division prior to maturation; whereas, white spruce zygotic embryos had ground meristem tissue that was more compact and had rows of cells formed by cell division perpendicular to the hypocotyl-root axis. Despite these few differences, somatic and zygotic embryos of white spruce were morphologically and anatomically very similar.

Chemical analyses of P reserves in white spruce somatic embryos and various parts of white spruce seeds revealed different trends when the data was expressed as per g DW and

as per tissue. On a DW basis there was a small, but significant, difference between white spruce somatic embryos produced in two separate batches. White spruce female gametophyte tissue, which is a living storage tissue surrounding the zygotic embryo, had significantly higher P per g DW than white spruce zygotic embryos and both had higher P per g DW than white spruce somatic embryos. The total amount of P in a single white spruce somatic embryo from either batch was statistically similar to the total amount of P in a single white spruce zygotic embryo. The large female gametophyte of a single white spruce seed contained 7.4 times more P than the zygotic embryo. A single white spruce seed contained between 6.9 and 7.4 times more P than a single white spruce somatic embryo. When a white spruce seed imbibes and begins to germinate, the P reserves in the embryo and in the female gametophyte tissue are made available to the developing seedling. A somatic embryo lacks the additional P reserve supplied from the female gametophyte and consequently somatic embryos must be carefully germinated in the lab using nutrient-rich germination medium.

Measurements of PA-P in white spruce somatic embryos revealed that significant variations can occur between different batches of somatic embryos. White spruce somatic embryos from Batch 2 contained significantly more PA-P per g DW and as a % of the total P than somatic embryos from Batch 1. A single somatic embryo from either batch had statistically similar PA-P levels, but a Batch 2 somatic embryo did have 2.3 times more PA-P. A white spruce somatic embryo from Batch 2 had a very similar PA-P concentration to a single white spruce zygotic embryo. It appears that the improved purification procedures used to produce the Batch 2 somatic embryos, which selects based on overall qualities, was also useful in eliminating those embryos that are deficient in PA-P.

Since somatic embryos synthesize storage reserves during the maturation phase of development, attempts were made to alter the amount of P bound to phytic acid in white spruce somatic embryos by altering the concentrations of *myo*-inositol and sucrose in the maturation medium. The level of *myo*-inositol in the medium had no effect on the amount of PA-P in the somatic embryos and maturation of somatic embryos on medium lacking *myo*-inositol still resulted in somatic embryos containing equivalent PA-P levels. From these results it appears that *myo*-inositol in the medium was not required to produce additional phytic acid. These white spruce somatic embryos appear to have gone through the biosynthetic processes of synthesizing phytic acid from other substrates.

The differences in PA-P levels of Batch 1 white spruce somatic embryos and white spruce zygotic embryos could be related to differences in the size and frequency of globoids, as found using transmission electron microscopy and EDX analysis. Globoids ranged in size from 0.5 to 3 μm in diameter and were found in the ground meristem and procambium tissue of both types of embryos. Globoids were, however, typically between 0.5 and 2 μm in diameter in white spruce somatic embryos and between 2 and 3 μm in diameter in white spruce zygotic embryos. The difference in the average sizes of the globoids is significant because globoids are spherical. Therefore a globoid 3 μm in diameter has a volume 3.4 times larger than a globoid 2 μm in diameter. Therefore the difference in average globoid size is consistent with the observation that white spruce somatic embryos had lower PA-P levels. Globoids in female gametophyte tissue were found to be significantly more frequent and larger, ranging in size from 0.5 to 6 μm in diameter, than found in either type of embryo. In both embryo types, globoids were smaller in the procambium than in the ground meristem.

Globoids were less frequent in white spruce somatic embryos, which had lower PA-P levels, than in white spruce zygotic embryos. Globoids from both embryo types showed the presence of P, K and Mg in digital x-ray maps; but globoids from white spruce zygotic embryos also contained significant levels of Fe.

Digital x-ray maps also revealed the presence of Fe-rich particles in the ground meristem and procambium of both types of embryos. Iron-rich particles were also found in the protoderm, but were not present in sufficient quantity to produce adequate maps. Digital x-ray maps revealed the presence of Fe and occasionally the P and K present in Fe-rich particles from both types of embryos were identifiable in these maps. There was no noticeable difference in the frequency of these deposits in white spruce somatic and zygotic embryos, but no Fe-rich particles were found in maps of female gametophyte tissue even though Reid (1996) reported their presence using spectral EDX analysis.

Spectral EDX analysis of globoids and Fe-rich particles in white spruce somatic embryos confirmed the results of digital x-ray mapping. Globoids had high levels of P, moderate levels of K and Mg and little if any Ca, Fe and Zn. Iron-rich particles contained high levels of P and Fe, moderate K and Mg and little if any Ca and Zn. Globoids and Fe-rich particles from white spruce zygotic embryos and female gametophytes have been shown to have similar EDX analysis spectra (Reid, 1996). One exception found when spectra from white spruce somatic embryos were compared to spectra from white spruce zygotic embryos was the presence of moderate Fe levels in globoids from the procambium tissue in the cotyledons of zygotic embryos. Comparison of P/B values and ratios of P/B values consistently showed that the Fe:P ratio was approximately 10 times higher in procambium

globoids from white spruce zygotic embryos than from white spruce somatic embryos. Iron-rich particles from white spruce somatic embryos typically had P peaks that were higher than the Fe peaks, whereas, in white spruce zygotic embryos the Fe peaks were typically higher than the P peaks. The Fe:P ratio was found to be consistently higher in Fe-rich particles from white spruce zygotic embryos than from white spruce somatic embryos.

Using AAS, the total levels of K, Mg, Ca, Fe and Zn were measured for white spruce somatic embryos and various parts of white spruce seeds. Potassium was found to be the most abundant of these elements with Mg found in moderate levels and Ca, Fe and Zn present in much smaller concentrations. On a DW basis, white spruce somatic embryos contained significantly more Ca and significantly less K, Mg, Fe and Zn than zygotic embryos of white spruce. White spruce female gametophyte tissue had significantly higher Mg, Ca, Fe and Zn per g DW than white spruce zygotic embryos. A single white spruce somatic embryo had similar concentrations of K, Mg, Ca, Fe and Zn as a single white spruce zygotic embryo. The female gametophyte of a single seed contained 6.5 times more K , 8.6 times more Mg , 12.5 times more Ca, 4.5 times more Fe and 12 times more Zn than the zygotic embryo. Since white spruce somatic embryos lack the mineral nutrient supplies of the female gametophyte, they cannot currently be germinated unless a nutrient-rich medium is supplied to the embryos.

In a review by Lott *et al.* (1985), it was proposed that the size and frequency of globoids was related to the ratio of divalent cations (Mg^{2+} and Ca^{2+}) to monovalent cations (K^{+}), as measured per g DW. According to this hypothesis, seed tissues with a high (Mg+Ca):K ratio have larger and more frequent globoids; whereas, a low ratio is correlated to smaller and less frequent globoids. A lower ratio would result in more K-phytate, which

is more water-soluble and therefore would be present throughout the proteinaceous matrix rather than in discrete globoids (Prattley and Stanley, 1982; Lott *et al.*, 1985). The AAS results in this thesis found (Mg+Ca):K ratios of 0.38, 0.49 and 0.62 for white spruce somatic embryos, zygotic embryos and female gametophytes, respectively. White spruce somatic embryos also had lower PA-P levels, smaller globoids and less frequent globoids than in either zygotic embryos or female gametophytes. Female gametophyte tissue from white spruce seeds had the highest PA-P levels, the largest globoids and the highest frequency of globoids. These results support the theory proposed by Lott *et al.* (1985) and this is the first report of this ratio for conifer seeds and somatic embryos. The relationship of this ratio to globoid size and frequency therefore appears to be valid in both gymnosperm and angiosperm seed tissues.

The final study of this thesis involved measuring K leakage and surface changes during imbibition using AAS and an ESEM. Desiccated white spruce somatic embryos leaked significantly less K per g DW and as a % of the total K present than white spruce zygotic embryos. Pretreatment of white spruce somatic embryos in a high RH environment resulted in significant decreases in the amount of K leaked per g DW and as a % of the total K present at both the 80 min. and 120 min. time intervals. A single white spruce zygotic embryo and a single white spruce somatic embryo (desiccated or pretreated) leaked similar amounts of K, but pretreatment resulted in values at 80 and 120 min. closer to those measured for zygotic embryos than did untreated somatic embryos. A whole white spruce seed leaked 3.5 times more K than a single white spruce zygotic embryo, but on a DW basis a whole seed leaked 3.8 times less of its total K than did a zygotic embryo. Removal of the seed coat from a single white spruce seed resulted in 2.3 times more K leakage, thus illustrating the significance of

the seed coat in slowing down imbibition and solute leakage.

Desiccated white spruce somatic embryos have shoot apices that are flat and consist of surface cells that were shrunken and wrinkled when viewed in an ESEM. In a dry zygotic embryo, the apex also had shrunken surface cells, but the apex itself was more lobed and was protected within the cavity formed by the closely packed cotyledons. The surface of the cotyledons and hypocotyl of a desiccated white spruce somatic embryo had cells that are wrinkled and arranged in discrete rows. The same regions in white spruce zygotic embryos had surface cells that were more shrunken in appearance. This is likely due to the fact that white spruce somatic embryos have higher lipid contents than zygotic embryos, which would restrict the amount of shrinkage that can occur during desiccation (Attree *et al.*, 1994; 1995).

Imbibition of white spruce somatic and zygotic embryos in germination medium resulted in some swelling of surface cells, especially in the hypocotyl region. Even after 120 min. exposure to the medium the surface cells still showed signs of wrinkling. The high osmotic conditions of the germination medium must have resulted in slower hydration than occurred in water alone. It is possible that the osmotic conditions of this germination medium are so high that full hydration will never occur. Currently, white spruce somatic embryos are imbibed on semi-solidified medium, which would additionally reduce the rate of water uptake. Observations of surface changes during imbibition indicate that K leakage during imbibition was due to leakage through the plasma membranes rather than by surface cell rupture.

The results of this current thesis show that a white spruce somatic embryo and a white spruce zygotic embryo are similar in morphology, amounts of P, K, Mg, Ca, Fe, Zn, as well as K leakage and surface changes during imbibition. Although differences were found from

batch-to-batch in the level of PA-P in a white spruce somatic embryo, it was shown that similar levels of PA-P as found in zygotic embryos can be achieved with the newest protocol used to produce these somatic embryos. The frequency and size of globoid deposits did differ between white spruce somatic and zygotic embryos, but this was likely due to the overall differences in phytic acid produced. The fact that globoids and Fe-rich particles were so similar in composition and location in white spruce somatic embryos and zygotic embryos indicates that similar biosynthetic processes must have occurred in the seed and tissue culture.

The female gametophyte clearly plays a major nutritional role in a seed and this must be taken into account when attempting to produce a synthetic seed. It may now be possible to take a desiccated somatic embryo and surround it with a mixture containing the appropriate levels of the nutrients and then package this inside a dry synthetic seed coat. The synthetic female gametophyte could either be in the form of various salts, which would include salts that dissolve upon imbibition at different rates, or it may be more appropriate to produce a living artificial female gametophyte through tissue culture so as to more closely mimic a natural female gametophyte. The optimum goal of somatic embryogenesis is to produce large volumes of dry synthetic seeds that could be used to produce high quality seedlings in the shortest time possible. Studies like the ones described here will be necessary in order to complete the production of a viable synthetic spruce seed. Now that white spruce somatic embryos resemble white spruce zygotic embryos in so many respects, researchers should focus their attention towards thoroughly studying the roles of the female gametophyte and the seed coat so that the final step in artificial seed production can be accomplished.

REFERENCES

Allen, S.E., Grimshaw, H.M., Parkinson, J.A. and Quarmby, C. 1974. Chemical Analysis of Ecological Materials. John Wiley & Son, Inc., New York, NY.

Ammirato, P.V. 1983. Embryogenesis. In: Evans, D.A., Sharp, W.R., Ammirato, P.V. and Yamada, Y. (Ed.), Handbook of Plant Cell Culture, Vol. 1, p. 82-123. Macmillan Publishing Co., New York, NY.

AOAC Official Methods of Analysis. 1990. 15th ed, p. 56, 800-801. Association of Official Analytical Chemists, Arlington, VA.

Ashton, F.L. 1936. Influence of the temperature of ashing on the accuracy of the determination of phosphorus in grass. J. Soc. Chem. Ind. **55**: 106-108.

Ashton, W.M. and Williams, P.C. 1958. The phosphorus compounds of oats. I. the content of phytate phosphorus. J. Sci. Food Agric. **9**: 505-511.

Attree, S.M., Bekkaoui, F., Dunstan, D.I. and Fowke, L.C. 1987. Regeneration of somatic embryos from protoplasts isolated from an embryogenic suspension culture of white spruce (*Picea glauca*). Plant Cell Rep. **6**: 480-483.

Attree, S.M., Budimir, S. and Fowke, L.C. 1990. Somatic embryogenesis and plantlet regeneration from cultured shoots and cotyledons of seedlings from stored seeds of black and white spruce (*Picea mariana* and *Picea glauca*). Can. J. Bot. **68**: 30-34.

Attree, S.M., Dunstan, D.I. and Fowke, L.C. 1989a. Plantlet regeneration from embryogenic protoplasts of white spruce (*Picea glauca*). Bio/Tech. **7**: 1060-1062.

Attree, S.M., Dunstan, D.I. and Fowke, L.C. 1989b. Initiation of embryogenic callus and suspension cultures, and improved embryo regeneration from protoplasts of white spruce (*Picea glauca*). Can. J. Bot. **67**: 1790-1795.

Attree, S.M. and Fowke, L.C. 1993. Embryogeny of gymnosperms: advances in synthetic seed technology of conifers. Plant Cell Tiss. Org. Cult. **35**: 1-35.

Attree, S.M. and Fowke, L.C. 1995. Conifer somatic embryogenesis, embryo development, maturation drying and plant formation. In: Gamborg, O.L. and Phillips, G.C. (Ed.), Plant Cell, Tissue and Organ Culture, Fundamental Methods, p. 103-113. Springer Verlag, New York, NY.

Attree, S.M., Moore, D., Sawhney, V.K. and Fowke, L.C. 1991. Enhanced maturation and desiccation tolerance of white spruce (*Picea glauca* [Moench.] Voss) somatic embryos: effects of a non-plasmolysing water stress and abscisic acid. Ann. Bot. **68**: 519-525.

Attree, S.M., Pomeroy, M.K. and Fowke, L.C. 1992. Manipulation of conditions for the culture of somatic embryos of white spruce for improved triacylglycerol biosynthesis and desiccation tolerance. Planta **187**: 395-404.

Attree, S.M., Pomeroy, M.K. and Fowke, L.C. 1994. Production of vigorous, desiccation tolerant white spruce (*Picea glauca* [Moench.] Voss.) synthetic seeds in a bioreactor. Plant Cell Rep. **13**: 601-606.

Attree, S.M., Pomeroy, M.K. and Fowke, L.C. 1995. Development of white spruce (*Picea glauca* (Moench.) Voss) somatic embryos during culture with abscisic acid and osmoticum, and their tolerance to drying and frozen storage. J. Exp. Bot. **46**: 433-439.

Barbi, N.C. 1979. Quantitative methods in biological x-ray microanalysis. Scanning Electron Microsc. **II**: 659-672.

Barré, M.R. 1956. Influence de l'acide phytique sur la digestion pepsique de differentes protéines. Ann. Pharm. Fr. **14**: 182-193.

Bassiri, A. and Nahapetian, A. 1977. Differences in concentrations and interrelationships of phytate, phosphorus, magnesium, calcium, zinc, and iron in wheat varieties grown under dryland and irrigated conditions. J. Agric. Food Chem. **25**: 1118-1122.

Becwar, M.R., Noland, T.L. and Wann, S.R. 1987. A method for quantification of the level of somatic embryogenesis among Norway spruce callus lines. Plant Cell Rep. **6**: 35-38.

Becwar, M.R., Noland, T.L. and Wyckoff, J.L. 1989. Maturation, germination, and conversion of Norway spruce (*Picea abies* L.) somatic embryos to plants. In Vitro Cell. Dev. Biol. **25**: 575-580.

Beecroft, P. and Lott, J.N.A. 1996. Changes in the element composition of globoids from *Cucurbita maxima* and *Cucurbita andreana* cotyledons during early seedling growth. Can. J. Bot. **74**: 838-847.

Bekkaoui, F., Pilon, M., Lainé, E., Raju, D.S.S., Crosby, W.L. and Dunstan, D.I. 1988. Transient gene expression in electroporated *Picea glauca* protoplasts. Plant Cell Rep. 7: 481-484.

Berlyne, G.M., Ari, J.B., Nord, E. and Shainkin, R. 1973. Bedouin osteomalacia due to calcium deprivation caused by high phytic acid content of unleavened bread. Amer. J. Clinical Nutr. **26**: 910-911.

Bewley, D.J. and Black, M. 1985. Seeds: Physiology of Development and Germination. Plenum Press, New York, NY.

Boltz, D.F. and Mellon, M.G. 1948. Spectrophotometric determination of phosphorus as molybdiphosphoric acid. Analytical Chem. **20**: 749-751.

Bourgkard, F. and Favre, J.M. 1988. Somatic embryos from callus of *Sequoia sempervirens*. Plant Cell Rep. 7: 445-448.

Bozzola, J.J. and Russell, L.D. 1992. Electron Microscopy: Principles and Techniques for Biologists, p. 332-344. Jones and Bartlett Publishers, Inc., Boston, Mass.

Briggs, A.P. 1924. Some applications of the colorimetric phosphate method. J. Biol. Chem. **59**: 255-264.

Brown, E.C., Heit, M.L. and Ryan, D.E. 1961. Phytic acid: an analytical investigation. Can. J. Bot. **39**: 1290-1297.

Bruggink, H., Kraek, H.L., Dijkema, M.H.G.E. and Bejendam, J. 1991. Some factors influencing electrolyte leakage from maize (*Zea mays* L.) kernels. Seed Sci. Res. **1**: 15-20.

Buchholz, J.T. 1918. Suspensor and early embryos of *Pinus*. Bot. Gaz. **66**: 185-228.

Buchholz, J.T. 1926. Origin of cleavage polyembryony in conifers. Bot. Gaz. **81**: 55-71.

Buchholz, J.T. 1931. The pine embryo and the embryos of related genera. Ill. State Acad. Sci. **23**: 117-125.

Buchholz, J.T. 1939. The embryogeny of *Sequoia sempervirens* with a comparison of the sequoias. Amer. J. Bot. **26**: 248-257.

Caron, G.E., Wang, B.S.P. and Schooley, H.O. 1993. Variation in *Picea glauca* seed germination associated with the year of cone collection. Can. J. For. Res. **23**: 1306-1313.

Cavdek, V., Lott, J.N.A. and Kerr, P. 1987. Cell wall wrinkling and solute leakage in imbibing squash and carrot seeds. Scanning Microsc. **1**: 1413-1421.

Chalupa, V. 1985. Somatic embryogenesis and plantlet regeneration from cultured immature and mature embryos of *Picea abies* (L.) Karst. Comm. Inst. For. **14**: 57-63.

Chandler, J.A. 1977. X-ray microanalysis in the electron microscope. In: Glauert, A.M. (Ed.), Practical Methods in Electron Microscopy, p. 327-518. Elsevier/North-Holland Biomedical Press, Amsterdam, The Netherlands.

Chandler, J.A. 1979. Principles of x-ray microanalysis in biology. Scanning Electron Microsc. **II**: 595-606.

Chavez, V.M., Litz, R.E. and Norstog, K. 1992. Somatic embryogenesis from leaf callus of mature plants of the gymnosperm *Ceratozamia mexicana* var. Robustica (Miq.) Dyer (cycadales). In Vitro Cell. Dev. Biol. **28P**: 59-63.

Chilliers, J.L. and van Niekerk, P.J. 1986. LC determination of phytic acid in food by postcolumn colorimetric detection. J. Agric. Food Chem. **34**: 680-683.

Chowdhury, C.R. 1962. The embryogeny of conifers: a review. Phytomorphology **12**: 313-338.

Clarkson, D.T. and Hanson, J.B. 1980. The mineral nutrition of higher plants. Annu. Rev. Plant Physiol. **31**: 239-298.

Clegg, M.S., Keen, C.L., Lonnerdal, B. and Hurley, L.S. 1981. Influence of ashing techniques on the analysis of trace elements in biological samples. II. dry ashing. Biol. Trace Element Res. **3**: 237-244.

Cosgrove, D.J. 1966. The chemistry and bio-chemistry of inositol polyphosphates. Rev. Pure Appl. Chem. **16**: 209-224.

Crean, D.E.C. and Haisman, D.R. 1963. The interaction between phytic acid and divalent cations during the cooking of dried peas. J. Sci. Food Agric. **14**: 824-833.

Crowe, J.H., Hoekstra, F.A. and Crowe, L.M. 1989. Membrane phase transitions are responsible for imbibitional damage in dry organisms. Proc. Natl. Acad. Sci. USA **86**: 520-523.

Cyr, D.R., Lazaroff, W.R., Grimes, S.M.A., Quan, G., Bethune, T.D., Dunstan, D.I. and Roberts, D.R. 1994. Cryopreservation of interior spruce (*Picea glauca engelmanni* complex) embryogenic cultures. Plant Cell Rep. **13**: 574-577.

Cyr, D.R., Webster, F.B. and Roberts, D.R. 1991. Biochemical events during germination and early growth of somatic embryos and seeds of interior spruce (*Picea glauca engelmanii* complex). Seed Sci. Res. **1**: 91-97.

Danilatos, G.D. 1981a. The examination of fresh or living plant material in an environmental scanning electron microscope. J. Microsc. **121**: 235-238.

Danilatos, G.D. 1981b. Design and construction of an atmospheric or environmental SEM (Part 1). Scanning **4**: 9-20.

Danilatos, G.D. and Postle, R. 1982. The environmental scanning electron microscope and its applications. Scanning Electron Microsc. **I**: 1-16.

DeCarli, M.E., Baldan, B., Mariani, P. and Rascio, N. 1987. Subcellular and physiological changes in *Picea excelsa* seeds during germination. Cytobios **50**: 29-39.

Dogra, P.D. 1967. Seed sterility and disturbances in embryogeny in conifers with particular reference to seed testing and tree breeding in Pinaceae. Studia Forestalia Suecica, No. 45, Stockholm.

Downie, B. and Bewley, J.D. 1996. Dormancy in white spruce (*Picea glauca* [Moench] Voss.) seeds is imposed by tissues surrounding the embryo. Seed Sci. Res. **6**: 9-15.

Duke, S.H. and Kakefuda, G. 1981. Role of the testa in preventing cellular rupture during imbibition of legume seeds. Plant Physiol. **67**: 449-456.

Duke, S.H., Kakefuda, G. and Harvey, T.M. 1983. Differential leakage of intracellular substances from imbibing soybean seeds. Plant Physiol. **72**: 919-924.

Dunn, B.L., Obendorf, R.L. and Paolillo, D.J. Jr. 1980. Imbibitional surface damage in isolated hypocotyl-root axis of soybean. Plant Physiol. **65**: s764.

Durzan, D.J. and Gupta, P.K. 1987. Somatic embryogenesis and polyembryogenesis in Douglas-fir cell suspension cultures. Plant Sci. **52**: 229-235.

Ellis, R. and Morris, E.R. 1983. Improved ion-exchange phytate method. Cereal Chem. **60**: 121-124.

Evans, H.J. and Sorger, G.J. 1966. Role of mineral elements with emphasis on the univalent cations. Annu. Rev. Plant Physiol. **17**: 47-76.

Evans, H.J. and Wildes, R.A. 1971. Potassium and its role in enzyme activation. In: Potassium in Biochemistry and Physiology, p. 13-39. International Potash Institute, Berne, Switzerland.

Farjon, A. 1990. Pinaceae. Koeltz Scientific Books, Königstein, Germany.

Finer, J.J., Kriebel, H.B. and Becwar, M.R. 1989. Initiation of embryogenic callus and suspension cultures of Eastern white pine (*Pinus strobus* L.). Plant Cell Rep. **8**: 203-206.

Flinn, B.S., Roberts, D.R. and Taylor, I.E.P. 1991. Evaluation of somatic embryos of interior spruce. Characterization and developmental regulation of storage proteins. Physiol. Plant. **82**: 624-632.

Fourré, J.-L., André, P., Casimiro, F., Medjahdi, G. and Mestdagh, M. 1991. *In vitro* germination of encapsulated *Picea abies* (L.) Karst. somatic embryos: preliminary results. Med. Fac. Landbouww. Rijksuniv. Gent. **56**: 1449-1451.

Fowke, L.C., Attree, S.M. and Rennie, P.J. 1994. Scanning electron microscopy of hydrated and desiccated mature somatic embryos and zygotic embryos of white spruce (*Picea glauca* [Moench] Voss.). Plant Cell Rep. **13**: 612-618.

Friel, J.J. 1995. X-ray and Image Analysis in Electron Microscopy, p. 1-57. Princeton Gamma-Tech, Inc., Princeton, NJ.

Gibson, T.S., Speirs, J. and Brady, C.J. 1984. Salt tolerance in plants. II. *In vitro* translation of m-RNA's from salt-tolerant and salt-sensitive plants on wheat germ ribosomes response to ions and compatible organic solutes. Plant Cell Environ. **7**: 579-587.

Givelberg, A., Horowitz, M. and Poljakoff-Mayber, A. 1984. Solute leakage from *Solanum nigrum* L. seeds exposed to high temperatures during imbibition. J. Exp. Bot. **35**: 1754-1763.

Gjerde, D.T. and Fritz, J.S. 1987. Ion Chromatography, 2nd Ed. Heidelberg: Dr. Alfred Hüthig Verlag.

Glass, A.D.M. 1989. Plant Nutrition - an introduction to current concepts. Jones and Bartlett Publishers, Inc., Boston, MA.

Goldstein, J.I., Newbury, D.E., Echlin, P., Joy, D.C., Fiori, C. and Lifshin, E. 1981. Scanning Electron Microscopy and X-ray Microanalysis: A Text for Biologists, Material Scientists, and Geologists. Plenum Press, New York, NY.

Gorsuch, T.T. 1970. The destruction of organic matter. Pergamon Press, Oxford.

Greenwood, J.S. 1989. Phytin synthesis and deposition. In: Taylorson, R.B. (Ed.), Recent Advances in the Development and Germination of Seeds, p. 109-125. Plenum Press, NY.

Griffiths, D.W. and Thomas, T.A. 1981. Phytate and total phosphorus content of field beans (*Vicia faba* L.). J. Sci. Food Agric. **32**: 187-192.

Gupta, P.K., Dandekar, A.M. and Durzan, D.J. 1988. Somatic proembryo formation and transient expression of a luciferase gene in Douglas-fir and loblolly pine protoplasts. Plant Sci. **58**: 85-92.

Gupta, P.K. and Durzan, D.J. 1987. Somatic embryos from protoplasts of loblolly pine proembryonal cells. Bio/Tech. **5**: 710-712.

Gupta, P.K., Pullman, G., Timmis, R., Kreitinger, M., Carlson, W.L., Grob, J. and Welty, E. 1993. Forestry in the 21st century - the biotechnology of somatic embryogenesis. Bio/Tech. **11**: 454-459.

Hakman, I. and Fowke, L.C. 1987. Somatic embryogenesis in *Picea glauca* (white spruce) and *Picea mariana* (black spruce). Can. J. Bot. **65**: 656-659.

Hakman, I., Fowke, L.C., von Arnold, S. and Eriksson, T. 1985. The development of somatic embryos in tissue cultures initiated from immature embryos of *Picea abies* (Norway spruce). Plant Sci. **38**: 53-59.

Hakman, I., Stabel, P., Engström, P. and Eriksson, T. 1990. Storage protein accumulation during zygotic and somatic embryo development in *Picea abies* (Norway spruce). Physiol. Plant. **80**: 441-445.

Hakman, I. and von Arnold, S. 1988. Somatic embryogenesis and plant regeneration from suspension cultures of *Picea glauca* (white spruce). Physiol. Plant. **72**: 579-587.

Harry, I.S. and Thorpe, T.A. 1991. Somatic embryogenesis and plant regeneration from mature zygotic embryos of red spruce. Bot. Gaz. **152**: 446-452.

Hayat, M.A. 1978. Introduction to Biological Scanning Electron Microscopy. University Park Press, Baltimore, MD.

Hepler, P.K. and Wayne, R.O. 1985. Calcium and plant development. Annu. Rev. Plant Physiol. **36**: 397-439.

Hoekstra, F.A., Crowe, J.H. and Crowe, L.M. 1992. Germination and ion leakage are linked with phase transitions of membrane lipids during imbibition of *Typha latifolia* pollen. Physiol. Plant. **84**: 29-34.

Hoekstra, F.A. and Van der Wal, E.G. 1988. Initial moisture content and temperature of imbibition determine extent of imbibitional injury in pollen. J. Plant Physiol. **133**: 257-262.

Isaac, R.A. 1980. Atomic absorption methods for analysis of soil extracts and plant tissue digests. J. Assoc. Off. Anal. Chem. **63**: 788-796.

Isaac, R.A. and Johnson, W.C. 1975. Collaborative study of wet and dry ashing techniques for the elemental analysis of plant tissues by atomic absorption spectrophotometry. J. Assoc. Off. Anal. Chem. **58**: 436-440.

Jaffe, G. 1981. Phytic acid in soybeans. J. Amer. Oil Chemists' Soc. **58**: 493-495.

Johnson, L.F. and Tate, M.E. 1969. Structure of "phytic acids". Can. J. Chem. **47**: 63-73.

Joy, R.W., Yeung, E.C., Kong, L. and Thorpe, T. 1991. Development of white spruce somatic embryos: I. storage product deposition. In Vitro Cell. Dev. Biol. **27P**: 32-41.

Kartha, K.K., Fowke, L.C., Leung, N.L., Caswell, K.L. and Hakman, I. 1988. Induction of somatic embryos and plantlets from cryopreserved cell cultures of white spruce (*Picea glauca*). J. Plant Physiol. **132**: 529-539.

Kermode, A.R. 1990. Regulatory mechanisms involved in the transition from seed development to germination. CRC Crit. Rev. Plant Sci. **9**: 155-195.

Kermode, A.R. and Bewley, J.D. 1985. The role of maturation drying in the transition from seed development to germination. J. Exp. Bot. **36**: 1916-1927.

Kikunaga, S., Takahashi, M. and Huzisige, H. 1985. Accurate and simple measurement of phytic acid contents in cereal grains. Plant Cell Physiol. **26**: 1323-1330.

Klimaszewska, K., Ward, C. and Cheliak, W.M. 1992. Cryopreservation and plant regeneration from embryogenic cultures of larch (*Larix* x *eurolepis*) and black spruce (*Picea mariana*). J. Exp. Bot. **43**: 73-79.

Kong, L. and Yeung, E.C. 1992. Development of white spruce somatic embryos: II. continual shoot meristem development during germination. In Vitro Cell. Dev. Biol. **28P**: 125-131.

Korkisch, J. 1989. Handbook of Ion Exchange Resins: Their Application to Inorganic Analystical Chemistry, Vol. 1. CRC Press Inc., Boca Raton, Florida.

Krasowski, M.J. and Owens, J.N. 1993. Ultrastructural and histochemical postfertilization megagametophyte and zygotic embryo development of white spruce (*Picea glauca*) emphasizing the deposition of seed storage products. Can. J. Bot. **71**: 98-112.

Kristensen, M.M.H., Find, J.I., Floto, F., Møller, J.D., Nørgaard, J.V. and Krogstrup, P. 1994. The origin and development of somatic embryos following cryopreservation of an embryogenic suspension culture of *Picea sitchensis*. Protoplasma **182**: 65-70.

Krogstrup, P. 1986. Embryo like structures from cotyledons and ripe embryos of Norway spruce (*Picea abies*). Can. J. For. Res. **16**: 664-668.

Krogstrup, P. 1990. Effect of culture densities on cell proliferation and regeneration from embryogenic cell suspensions of *Picea sitchensis*. Plant Sci. **72**: 115-123.

Kunitake, H., Nakashima, T., Mori, K., Tanaka, M. and Mii, M. 1995. Plant regeneration from mesophyll protoplasts of lisianthus (*Eustoma grandiflorum*) by adding activated charcoal into protoplast culture medium. Plant Cell Tiss. Org. Cult. **43**: 59-65.

Lambert, M.J. 1976. Preparation of plant material for estimating a wide range of elements. Research Note No. 29, Forestry Commission of N.S.W., Wood Technology and Forest Research Division.

Larson, C.A. 1968. The effect soaking pea seeds with or without seedcoats has on seedling growth. Plant Physiol. **43**: 255-259.

LaRue, C.D. 1948. Regeneration in the megagametophyte of *Zamia floridana*. Bull. Torrey Bot. Club **75**: 597-603.

LaRue, C.D. 1954. Studies on the growth and regeneration in gametophytes and sporophytes of gymnosperms. Brookhaven Natl. Lab. Symp. **6**: 187-208.

Leal, I. and Misra, S. 1993. Developmental gene expression in conifer embryogenesis and germination. III. analysis of crystalloid protein mRNAs and desiccation protein mRNAs in the developing embryo and megagametophyte of white spruce (*Picea glauca* (Moench) Voss). Plant Sci. **88**: 25-37.

Leal, I., Misra, S., Attree, S.M. and Fowke, L.C. 1995. Effect of abscisic acid, osmoticum and desiccation on 11S storage protein gene expression in somatic embryos of white spruce. Plant Sci. **106**: 121-128.

Litvay, J.D., Johnson, M.A., Verma, D., Einspahr, D. and Weyrauch, K. 1981. Conifer suspension culture medium development using analytical data from developing seeds. Tech. Paper Series, Inst. Paper Chem. **115**: 1-17.

Loewus, F.A., Everard, J.D. and Young, K.A. 1990. Inositol metabolism: precursor role and breakdown. In: Morré, D.J., Boss, W.F. and Loewus, F.A. (Ed.), Inositol Metabolism in Plants, p. 21-45. Wiley-Liss, Inc., New York, NY.

Lolas, G.M. and Markakis, P. 1975. Phytic acid and other phosphorus compounds of beans (*Phaseolus vulgaris* L.). J. Agric. Food Chem. **23**: 13-15.

Loomis, E.L. and Smith, O.E. 1980. The effect of artificial aging on the concentration of Ca, Mg, Mn, K and Cl in imbibing cabbage seed. J. Amer. Soc. Hort. Sci. **105**: 647-650.

Lott, J.N.A. 1974. Cell walls in *Cucurbita maxima* cotyledons in relation to imbibition. Can. J. Bot. **52**: 1465-1468.

Lott, J.N.A. 1980. Protein bodies. In: Stumpf, P.K. and Conn, E.E. (Ed.), The Biochemistry of Plants, A Comprehensive Treatise, Vol. 1, p. 589-623. Academic Press, Inc., New York, NY.

Lott, J.N.A. 1981. Protein bodies in seeds. Nord. J. Bot. **1**: 421-432.

Lott, J.N.A. 1984. Accumulation of seed reserves of phosphorus and other minerals. In: Seed Physiology, Vol. 1, p. 139-166. Academic Press, Australia.

Lott, J.N.A. and Buttrose, M.S. 1978. Globoids in protein bodies of legume seed cotyledons. Aust. J. Plant Physiol. **5**: 89-111.

Lott, J.N.A., Cavdek, V. and Carson, J. 1991. Leakage of K, Mg, Cl, Ca and Mn from imbibing seeds, grains and isolated seed parts. Seed Sci. Res. **1**: 229-233.

Lott, J.N.A., Greenwood, J.S. and Batten, G.D. 1995a. Mechanisms and regulation of mineral nutrient storage during seed development. In: Kigel, J. and Galili, G. (Ed.), Seed Development and Germination, p. 215-235. Marcel Dekker, Inc., New York, NY.

Lott, J.N.A., Greenwood, J.S. and Vollmer, C.M. 1978a. An energy-dispersive x-ray analysis study of elemental loss from globoid crystals in protein bodies as a result of osmium tetroxide fixation. Can. J. Bot. **56**: 2408-2414.

Lott, J.N.A., Greenwood, J.S., Vollmer, C.M. and Buttrose, M.S. 1978b. Energy-dispersive x-ray analysis of phosphorus, potassium, magnesium, and calcium in globoid crystals in protein bodies from different regions of *Cucurbita maxima* embryos. Plant Physiol. **61**: 984-988.

Lott, J.N.A., Goodchild, D.J. and Craig, S. 1984. Studies of mineral reserves in pea (*Pisum sativum*) cotyledons using low-water-content procedures. Aust. J. Plant Physiol. **11**: 459-469.

Lott, J.N.A. and Kerr, P. 1986. Use of cryogenically prepared samples in the scanning electron microscopic study of dry-to-wet transitions. Scanning Electron Microsc. **III**: 979-986.

Lott, J.N.A. and Ockenden, I. 1986. The fine structure of phytate-rich particles in plants. In: Graf, E. (Ed.), Phytic Acid: Chemistry and Applications, p. 43-55. Pilatus Press, Minneapolis, MN.

Lott, J.N.A., Randall, P.J., Goodchild, D.J. and Craig, S. 1985. Occurrence of globoid crystals in cotyledonary protein bodies of *Pisum sativum* as influenced by experimentally induced changes in Mg, Ca and K contents of seeds. Aust. J. Plant Physiol. **12**: 341-353.

Lott, J.N.A. and Spitzer, E. 1980. X-ray analysis studies of elements stored in protein body globoid crystals of *Triticum* grains. Plant Physiol. **66**: 494-499.

Lott, J.N.A. and Vollmer, C.M. 1979. Composition of globoid crystals from embryo protein bodies in five species of *Cucurbita*. Plant Physiol. **63**: 307-311.

Lott, J.N.A., West, M.M., Clark, B. and Beecroft, P. 1995b. Changes in the composition of globoids in castor bean cotyledons and endosperm during early seedling growth with and without complete mineral nutrients. Seed Sci. Res. **5**: 121-125.

Lulsdorf, M.M., Tautorus, T.E., Kikcio, S.I. and Dunstan, D.I. 1992. Growth parameters of embryogenic suspension cultures of interior spruce (*Picea glauca-engelmanii* complex) and black spruce (*Picea mariana* Mill.). Plant Sci. **82**: 227-234.

Lüttge, U. and Clarkson, D.T. 1989. Mineral nutrition: potassium. In: Behnke, H.-D., Esser, K., Kubitzki, K., Runge, M. and Ziegler, H. (Ed.), Progress in Botany, Vol. 50, p. 51-69. Springer-Verlag, Berlin, Germany.

Luzzati, V. and Husson, F. 1962. The structure of the liquid-crystalline phases of lipid-water systems. J. Cell Biol. **12**: 207-219.

Maheshwari, P. and Singh, H. 1967. The female gametophyte of gymnosperms. Biol. Rev. **42**: 88-130.

Malik, V. and Timmer, V.R. 1995. Interaction of nutrient-loaded black spruce seedlings with neighbouring vegetation in greenhouse environments. Can. J. For. Res. **25**: 1017-1023.

McDonald, K.A. and Jackman, A.P. 1989. Bioreactor studies of growth and nutrient utilization in alfalfa suspension cultures. Plant Cell Rep. **8**: 455-458.

McDonald, M.B. Jr., Vertucci, C.N. and Roos, E.E. 1988. Seed coat regulation of soybean seed imbibition. Crop Sci. **28**: 987-992.

McKersie, B.D. and Stinson, R.H. 1980. Effect of dehydration on leakage and membrane structure in *Lotus corniculatus* L. seeds. Plant Physiol. **66**: 316-320.

Menden, E.E., Brockman, D., Choudhury, H. and Petering, H.G. 1977. Dry ashing of animal tissues for atomic absorption spectrometric determination of zinc, copper, cadmium, lead, iron, manganese, magnesium and calcium. Anal. Chem. **49**: 1644-1645.

Mengel, K. and Kirkby, E.A. 1982. Principles of plant nutrition. International Potash Institute, Bern, Switzerland.

Meredith, P., Donald, A.M. and Thiel, B. 1996. Electron-gas interactions in the environmental scanning electron microscopes gaseous detector. Scanning **18**: 467-473.

Misra, S. 1994. Conifer zygotic embryogenesis, somatic embryogenesis, and seed germination: biochemical and molecular advances. Seed Sci. Res. **4**: 357-384.

Misra, S., Attree, S.M., Leal, I. and Fowke, L.C. 1993. Effects of abscisic acid, osmoticum, and desiccation on synthesis of storage proteins during the development of white spruce somatic embryos. Ann. Bot. **71**: 11-22.

Misra, S. and Green, M.J. 1990. Developmental gene expression in conifer embryogenesis and germination. I. seed proteins and protein body composition of mature embryo and megagametophyte of white spruce (*Picea glauca* [Moench] Voss.). Plant Sci. **68**: 163-173.

Misra, S. and Green, M.J. 1991. Developmental gene expression in conifer embryogenesis and germination. II. crystalloid protein synthesis in the developing embryo and megagametophyte of white spruce (*Picea glauca* [Moench] Voss.). Plant Sci. **78**: 61-71.

Mo, L.H. and von Arnold, S. 1991. Origin and development of embryogenic cultures from seedlings of Norway spruce (*Picea abies*). J. Plant Physiol. **138**: 223-230.

Motomizu, S., Wakimoto, T. and Tôel, K. 1983. Spectrophotometric determination of phosphate in river waters with molybdate and malachite green. Analyst **108**: 361-367.

Munter, R.C., Grande, R.A. and Ahn, P.C. 1979. Analysis of animal tissue and food materials by inductively coupled plasma emission spectrometry in a university research service laboratory. Chem. Abs. **92**: 290.

Nagmani, R. and Bonga, J.M. 1985. Embryogenesis in subcultured callus of *Larix decidua*. Can. J. For. Res. **15**: 1088-1091.

Newbury, D.E., Joy, D.C., Echlin, P., Fiori, C.E. and Goldstein, J.I. 1986. Advanced Scanning Electron Microscopy and X-Ray Microanalysis. Plenum Press, New York, NY.

Nørgaard, J.V. and Krogstrup, P. 1991. Cytokinin induced somatic embryogenesis from immature embryos of *Abies nordmandiana* Lk. Plant Cell Rep. **9**: 509-513.

Norstog, K. 1982. Experimental embryology of gymnosperms. In: Johri, B.M. (Ed.), Experimental Embryology of Vascular Plants, p. 25-51. Springer-Verlag, New York, NY.

Norstog, K. and Rhamstine, E. 1967. Isolation and culture of haploid and diploid cycad tissues. Phytomorphology **17**: 374-381.

Ockenden, I., Falk, D.E. and Lott, J.N.A. 1997. Stability of phytate in barley grains and bean seeds stored under various conditions. J. Agric. Food Chem. **45**: 1673-1677.

Ockenden, I. and Lott, J.N.A. 1986. A possible enhancement of measured calcium in small samples of dry-ashed *Cucurbita* embryos as determined by atomic absorption analysis. Commun. in Soil Sci. Plant Anal. **17**: 601-626.

Ockenden, I. and Lott, J.N.A. 1991. Beam sensitivity of globoid crystals within seed protein bodies and commercially prepared phytates during x-ray microanalysis. Scanning Microsc. **5**: 767-778.

O'Brien, T.P. and McCully, M.E. 1981. The Study of Plant Structure Principles and Selected Methods. Termarcarphi Pty. Ltd., Melbourne, Australia.

Organ, M.G., Greenwood, J.S. and Bewley, J.D. 1988. Phytin is synthesized in the cotyledons of germinated castor-bean seeds in response to exogenously supplied phosphate. Planta **174**: 513-517.

Owens, J.N. and Blake, M.D. 1985. Forest tree seed production. Petawawa Natl. For. Inst. Inf. Rep. PI-X-53.

Owens, J.N. and Molder, M. 1979. Sexual reproduction in white spruce (*Picea glauca*). Can. J. Bot. **57**: 152-169.

Owens, J.N. and Molder, M. 1984a. The reproductive cycle of interior spruce. Inf. Serv. Branch, B.C. Ministry of Forests, Victoria, B.C.

Owens, J.N. and Molder, M. 1984b. The reproductive cycle of lodgepole pine. Inf. Serv. Branch, B.C. Ministry of Forests, Victoria, B.C.

Park, Y.S., Pond, S.E. and Bonga, J.M. 1993. Initiation of somatic embryogenesis in white spruce (*Picea glauca*): genetic control, culture treatment effects, and implications for tree breeding. Theor. Appl. Genet. **86**: 427-436.

Peters, K.-R. 1995. Digital differential hysteresis image processing displays what the microscope acquires but the eye can't see. In: Baily, G.W., Ellisman, M.H., Hennigar, R.A. and Zaluzec, N.J. (Ed.), Proc. Microscopy and Microanalysis, p. 642-643. Jones and Begell Publishing, New York, NY.

Peters, D.G., Hayes, J.M. and Hieftje, G.M. 1974. Atomic absorption spectroscopy. In: Chemical Separations and Measurements, p. 688-694. W.B. Saunders and Co., Philadelphia, PA.

Pittermann, J., West, M. and Lott, J.N.A. 1996. Characterization of globoids and iron-rich particles in cotyledons of *Pinus banksiana* seeds and seedlings. Can. J. For. Res. **26**: 1697-1702.

Plaami, S. and Kumpulainen, J. 1991. Determination of phytic acid in cereals using ICP-AES to determine phosphorus. J. Assoc. Off. Anal. Chem. **74**: 32-36.

Poovaiah, B.W. and Reddy, A.S.N. 1993. Calcium and signal transduction in plants. Crit. Rev. Plant Sci. **12**: 185-211.

Prattley, C.A. and Stanley, D.W. 1982. Protein-phytate interactions in soybeans. I. localization of phytate in protein bodies and globoids. J. Feed Biochem. **6**: 243-245.

Proe, M.F. and Millard, P. 1995. Effect of P supply upon seasonal growth and internal cycling of P in Sitka spruce (*Picea sitchensis* (Bong.) Carr.) seedlings. Plant and Soil **168-169**: 313-317.

Raboy, V. 1990. Biochemistry and genetics of phytic acid synthesis. In: Morré, D.J., Boss, W.F. and Loewus, F.A. (Ed.), Inositol Metabolism in Plants, Vol. 9, p. 55-76. Wiley-Liss, Inc., New York, NY.

Redenbaugh, K., Fujii, J.O. and Slade, D. 1991. Synthetic seed technology. In: Vasil, I.K. (Ed.), Scale-up and Automation in Plant Propagation. Cell Culture and Somatic Cell Genetics of Plants, Vol. 8, p. 35-74. Academic Press, San Diego, CA.

Reid, D.A. 1996. Investigation of globoid and Fe-rich particles in zygotic embryos and female gametophytes of white spruce (*Picea glauca*) seeds. Senior Thesis, McMaster University, Hamilton, Ontario, Canada.

Reid, D.A., Ducharme, H.C., West, M.M. and Lott, J.N.A. 1998. Iron-rich particles in embryos of seeds from the family Pinaceae. Accepted by Protoplasma.

Reinert, J. 1958. Morphogenese und ihre kontrolle and gewebekultures aus karotten. Naturwissen **45**: 344-345.

Reinert, J. 1959. Über die kontrolle der morphogenese und die induktion von adventivembryonen an gewebekulteren aus karotten. Planta **53**: 318-333.

Roberts, D.R., Flinn, B.S., Webb, D.T., Webster, F.B. and Sutton, B.C.S. 1990a. Abscisic acid and indole-3-butyric acid regulation of maturation and accumulation of storage proteins in somatic embryos of interior spruce. Plant Physiol. **78**: 355-360.

Roberts, D.R., Sutton, B.C.S. and Flinn, B.S. 1990b. Synchronous and high frequency germination of interior spruce somatic embryos following partial drying at high relative humidity. Can. J. Bot. **68**: 1086-1090.

Robinson, J.W. 1975. Atomic Absorption. Marcel Dekker, Inc., New York, NY.

Rocchiccioli, C. and Townshend, A. 1968. Some interferences in the atomic absorption spectrophotometry of calcium. Anal. Chim. Acta **41**: 93-98.

Rowland, G.G. and Gusta, L.V. 1977. Effects of soaking, seed moisture content, temperature and seed leakage on germination of faba beans (*Vicia faba*) and peas (*Pisum sativum*). Can. J. Plant Sci. **57**: 401-406.

Ruaud, J.-N., Berretche, J. and Pâques, M. 1992. First evidence of somatic embryogenesis from needles of 1-year-old *Picea abies* plants. Plant Cell Rep. **11**: 563-566.

Russ, J.C. 1972. Obtaining quantitative x-ray analytical results from thin sections in the electron microscope. In: Russ, J.C. and Panessa, B.J. (Ed.), Thin-section Microanalysis Proc. Symp. EDAX Laboratories, p. 115-133. Raleigh, NC.

Salisbury, F.B. and Ross, C.W. 1992. Plant Physiology, 4th Ed. Wadsworth Publishing Company, Belmont, CA.

Schoettle, A.W. and Leopold, A.C. 1984. Solute leakage from artificially aged soybean seeds after imbibition. Crop Sci. **24**: 835-838.

Schuller, A., Reuther, G. and Geier, T. 1989. Somatic embryogenesis from seed explants of *Abies alba*. Plant Cell Tiss. Org. Cult. **17**: 53-58.

Shkolnik, M.Y. 1984. Trace elements in plants. Elsevier Science, Amsterdam.

Simon, E.W. 1974. Phospholipids and plant membrane permeability. New Phytol. **73**: 377-420.

Simon, E.W. 1978. Membranes in dry and imbibing seeds. In: Crowe, J.H. and Clegg, J.S. (Ed.), Dry Biological Systems, p. 205-224. Academic Press, New York, NY.

Simon, E.W. and RajaHarun, R.M. 1972. Leakage during seed imbibition. J. Exp. Bot. **23**: 1076-1085.

Singh, H. 1978. Embryology of gymnosperms. In: Encyclopedia of Plant Anatomy, Vol. 10., p. 302. Gebrüder Borntraeger, Berlin, Germany.

Singh, H. and Owens, J.N. 1980. Sexual reproduction of Engelmann spruce (*Picea engelmanii*). Can. J. Bot. **59**: 793-810.

Skilnyk, H.R. and Lott, J.N.A. 1992. Mineral analyses of storage reserves of *Cucurbita maxima* and *Cucurbita andreana* pollen. Can. J. Bot. **70**: 491-495.

Skriver, K. and Mundy, J. 1990. Gene expression in response to abscisic acid and osmotic stress. The Plant Cell **2**: 503-512.

Spaeth, S.C. 1989. Seed physiology, production & technology: extrusion of protoplasm and protein bodies through pores in cell walls of pea, bean, and faba bean cotyledons during imbibition. Crop. Sci. **29**: 452-459.

Spitzer, E. and Lott, J.N.A. 1980. Thin-section, freeze-fracture, and energy dispersive x-ray analysis studies of the protein bodies of tomato seeds. Can. J. Bot. **58**: 699-711.

Steeves, T.A. 1983. The evolution and biological significance of seeds. Can. J. Bot. **61**: 3550-3560.

Steward, F.C., Mapes, M.O. and Mears, K. 1958. Growth and organized development of cultured cells. II. organization in cultures grown from freely suspended cells. Amer. J. Bot. **45**: 705-708.

Stewart, W.N. 1983. Paleobotany and the Evolution of Plants, p. 348-356. Cambridge University Press, Melbourne, Australia.

Stewart, A., Nield, H. and Lott, J.N.A. 1988. An investigation of the mineral content of barley grains and seedlings. Plant Physiol. **86**: 93-97.

Stuffins, C.B. 1967. The determination of phosphate and calcium in feeding stuffs. Analyst **92**: 107-111.

Štupar, J., Ajlec, R., Korošin, J. and Lobnik, F. 1987. A comparison of spectroscopic methods for determination of phosphorus in plant materials, soil extracts and fertilizers. Landwirtsch. Forschung **40**: 21-31.

Taiz, L. and Zeiger, E. 1991. Plant Physiology. The Benjamin/Cummings Publishing Company, Inc., Redwood City, CA.

Tautorus, T.E., Attree, S.M., Fowke, L.C. and Dunstan, D.I. 1990. Somatic embryogenesis from immature and mature zygotic embryos, and embryo regeneration from protoplasts in black spruce (*Picea mariana* Mill.). Plant Sci. **67**: 115-124.

Tautorus, T.E., Bekkaoui, F., Pilon, M., Datla, R.S.S., Crosby, W.L., Fowke, L.C. and Dunstan, D.I. 1989. Factors affecting transient gene expression in electroporated black spruce (*Picea mariana*) and jack pine (*Pinus banksiana*) protoplasts. Theor. Appl. Genet. **78**: 531-536.

Tautorus, T.E., Fowke, L.C. and Dunstan, D.I. 1991. Somatic embryogenesis in conifers. Can. J. Bot. **69**: 1873-1899.

Tautorus, T.E., Lulsdorf, M.M., Kikcio, S.I. and Dunstan, D.I. 1992. Bioreactor culture of *Picea mariana* Mill. (black spruce) and the species complex *Picea glauca-englemannii* (interior spruce) somatic embryos: growth parameters. Appl. Microbiol. Biotech. **38**: 46-51.

Taylor, T.G. 1965. The availability of the calcium and phosphorus of plant materials for animals. Proc. Nutr. Soc. **24**: 105-112.

Teasdale, R.D. and Buxton, P.A. 1986. Culture of *Pinus radiata* embryos with reference to artificial seed production. NZ J. For. Sci. **16**: 387-391.

Tetteroo, F.A.A., de Bruijn, A.Y., Henselmans, R.N.M., Wolkers, W.F., van Aelst, A.C. and Hoekstra, F.A. 1996. Characterization of membrane properties in desiccation-tolerant and -intolerant carrot somatic embryos. Plant Physiol. **111**: 403-412.

Thompson, R.G. and von Aderkas, P. 1992. Somatic embryogenesis and plant regeneration from immature embryos of western larch. Plant Cell Rep. **11**: 379-385.

Thomson, W.W. and Platt-Aloia, K. 1982. Ultrastructure and membrane permeability in cowpea seeds. Plant Cell and Environ. **5**: 367-373.

Thornton, J.M., Powell, A.A. and Matthews, S. 1990. Investigation of the relationship between seed leachate conductivity and the germination of *Brassica* seed. Ann. Appl. Biol. **117**: 129-135.

Timmer, V.R. and Miller, B.D. 1991. Effects of contrasting fertilization and moisture regimes on biomass, nutrients, and water relations of container grown red pine seedlings. New For. **5**: 335-348.

Tinker, B. and Läuchli, A. 1986. Advances in Plant Nutrition, Vol. 2. Praeger, New York, NY.

Toivonen, P.M.A. and Kartha, K.K. 1988. Regeneration of plantlets from in vitro cultured cotyledons of white spruce (*Picea glauca* (Moench) Voss). Plant Cell Rep. **7**: 318-321.

Tremblay, F.M. 1990. Somatic embryogenesis and plantlet regeneration from embryos isolated from stored seeds of *Picea glauca*. Can. J. Bot. **68**: 236-242.

Tremblay, L. and Tremblay, F.M. 1991. Carbohydrate requirements for the development of black spruce (*Picea mariana* (Mill.) B.S.P.) and red spruce (*P. rubens* Sarg.) somatic embryos. Plant Cell Tiss. Org. Cult. **27**: 95-103.

Tušl, J. 1972. Spectrophotometric determination of phosphorus in biological samples after dry ashing without fixatives. Analyst **97**: 111-113.

van den Driessche, R. 1985. Late-season fertilization, mineral nutrient reserves, and retranslocation in planted Douglas-fir (*Pseudotsuga menziesii* (Mirb.) Franco) seedlings. For. Sci. **31**: 485-496.

von Arnold, S. and Hakman, I. 1988. Regulation of somatic embryo development in *Picea abies* by abscisic acid (ABA). J. Plant Physiol. **132**: 164-169.

Wada, T. and Maeda, E. 1979. An improved method for the retention of globoids in aleurone grains in light microscopy and electron microscopy. Jpn. J. Crop Sci. **48**: 206-213.

Walsh, A. 1955. The application of atomic absorption spectra to chemical analysis. Spectrochim. Acta **7**: 108-117.

Walsh, A. 1982. Atomic absorption and atomic fluorescence methods of analysis: their merits and limitations. Phil. Trans. R. Soc. Lond. A **305**: 485-498.

Watt, I.M. 1985. The Principles and Practice of Electron Microscopy, p. 249-276. Cambridge University Press, Cambridge, UK.

Webb, M.A. and Arnott, H.J. 1982. Cell wall conformation in dry seeds in relation to the preservation of structural integrity during desiccation. Amer. J. Bot. **69**: 1657-1668.

West, M.M., Flannigan, D.T. and Lott, J.N.A. 1995. Elemental composition of globoids in the perisperm tissue of various seeds. Can. J. Bot. **73**: 954-957.

West, M.M. and Lott, J.N.A. 1993a. Studies of mature seeds of eleven *Pinus* species differing in seed weight. I. elemental concentrations in embryos and female gametophytes. Can. J. Bot. **71**: 570-576.

West, M.M. and Lott, J.N.A. 1993b. Studies of mature seeds of eleven *Pinus* species differing in seed weight. II. subcellular structure and localization of elements. Can. J. Bot. **71**: 577-585.

Westcott, R.J. 1994. Production of embryogenic callus from nonembryonic explants of Norway spruce *Picea abies* (L.) Karst. Plant Cell Rep. **14**: 47-49.

Wilson, S.M., Thorpe, T.A. and Moloney, M.M. 1989. PEG-mediated expression of GUS and CAT genes in protoplasts from embryogenic suspension cultures of *Picea glauca*. Plant Cell Rep. 7: 704-707.

Wyn Jones, R.G., Brady, C.J. and Spiers, J. 1979. Ionic osmotic relations in plant cells. In: Laidman, D.L. and Wyn Jones, R.G. (Ed.), Recent Advances in the Biochemistry of Cereals, p. 63-103. Academic Press, New York, NY.

Xu, N. and Bewley, J.D. 1992. Contrasting pattern of somatic and zygotic embryo development in alfalfa (*Medicago sativa* L.) as revealed by scanning electron microscopy. Plant Cell Rep. **11**: 279-284.

Yatsu, L.Y. 1983. Electron microscopy of dry peanut (*Arachis hypogaea* L.) seeds crushed for oil removal: fixation and embedding of anhydrously prepared tissues. Protoplasma **117**: 1-6.

Yofe, J. and Finkelstein, R. 1958. Elimination of anionic interference in flame photometric determination of calcium in the presence of phosphate and sulphate. Anal. Chim. Acta **19**: 166-173.

Young, J.A. and Young, C.G. 1992. Seeds of Woody Plants in North America, p. 243-247. Dioscorides Press, Portland, OR.

Zar, J.H. 1984. Biostatistical analysis. Prentice-Hall, Inc., Englewood Cliffs, NJ.

Zarei, J., Khyambashi, H., Emami, A., Farivar, H., Motamedi, G., Hedayat, H., Hekmatyar, F. and Barnett, R. 1972. High phytic acid content of wheat flour: a possible factor in the prevalence of bone deformities in Isfahan school children. Acta Biochim. Iranica **9**: 74-78.

APPENDIX A:

PEAK-TO-BACKGROUND RATIOS FOR INDIVIDUAL WHITE SPRUCE SOMATIC EMBRYOS

Note

* 5 spectra were used for each mean.
* For each table values in a single column that are followed by the same letter are not significantly different at $P > 0.05$.
* NS indicates values determined not to be significantly different from the background.

Table A1a: Mean (± SD) peak-to-background ratios of elements in globoids (> 0.33 µm) and Fe-rich particles (≤ 0.33 µm) for various tissues in resin embedded thick sections of white spruce somatic embryo #1.

Organ	Tissue	Particle	P	K	Mg	Ca	Fe	Zn
Cotyledons	Protoderm	Fe-rich Particle	3.69 ± 0.87 **e**	2.59 ± 0.57 **e**	0.80 ± 0.16 **d**	0.49 ± 0.08 **ab**	8.35 ± 1.86 **c**	0.06 ± 0.07 **b**
	Ground Meristem	Fe-rich Particle	6.23 ± 0.83 **bcde**	3.79 ± 0.87 **de**	1.33 ± 0.17 **d**	0.30 ± 0.11 **ab**	17.20 ± 2.41 **ab**	NS **b**
		Globoid	8.82 ± 1.08 **ab**	7.77 ± 0.52 **ab**	3.07 ± 0.65 **abc**	0.15 ± 0.09 **b**	0.21 ± 0.11 **d**	0.29 ± 0.15 **b**
	Procambium	Fe-rich Particle	5.23 ± 1.32 **de**	3.99 ± 1.42 **cde**	0.94 ± 0.08 **d**	0.30 ± 0.11 **ab**	14.34 ± 3.92 **abc**	NS **b**
		Globoid	7.98 ± 1.18 **abcd**	6.37 ± 1.68 **abc**	2.92 ± 0.56 **bc**	0.35 ± 0.22 **ab**	0.12 ± 0.09 **d**	0.84 ± 0.62 **a**
Hypocotyl	Protoderm	Fe-rich Particle	4.24 ± 1.08 **e**	2.21 ± 0.36 **e**	0.96 ± 0.22 **d**	0.44 ± 0.13 **ab**	9.51 ± 2.77 **c**	NS **b**
	Ground Meristem	Fe-rich Particle	3.85 ± 1.06 **e**	3.55 ± 0.90 **de**	0.75 ± 0.21 **d**	0.12 ± 0.08 **b**	11.50 ± 3.94 **bc**	NS **b**
		Globoid	10.16 ± 2.26 **a**	8.32 ± 1.83 **a**	3.91 ± 1.01 **ab**	0.18 ± 0.11 **ab**	0.36 ± 0.27 **d**	0.16 ± 0.16 **b**
	Procambium	Fe-rich Particle	4.00 ± 1.05 **e**	2.77 ± 0.54 **e**	0.55 ± 0.15 **d**	0.11 ± 0.04 **b**	9.09 ± 2.49 **c**	NS **b**
		Globoid	6.50 ± 1.06 **bcde**	5.60 ± 0.98 **bc**	2.83 ± 0.49 **c**	0.28 ± 0.17 **ab**	0.11 ± 0.05 **d**	0.07 ± 0.05 **b**
Radicle	Protoderm	Fe-rich Particle	5.59 ± 1.73 **de**	4.02 ± 1.43 **cde**	1.18 ± 0.31 **d**	0.35 ± 0.12 **ab**	18.79 ± 6.86 **a**	NS **b**
	Ground Meristem	Fe-rich Particle	3.69 ± 1.09 **e**	2.26 ± 0.82 **e**	0.65 ± 0.17 **d**	0.42 ± 0.09 **ab**	11.36 ± 4.38 **bc**	0.08 ± 0.07 **b**
		Globoid	8.71 ± 2.14 **abc**	6.58 ± 1.80 **ab**	4.00 ± 0.92 **a**	0.24 ± 0.12 **ab**	0.08 ± 0.09 **d**	0.41 ± 0.39 **ab**
	Procambium	Fe-rich Particle	4.20 ± 1.18 **e**	2.03 ± 0.64 **e**	0.74 ± 0.21 **d**	0.54 ± 0.44 **a**	12.31 ± 4.18 **abc**	0.08 ± 0.12 **b**
		Globoid	5.74 ± 1.12 **cde**	2.70 ± 0.94 **e**	2.69 ± 0.35 **c**	0.16 ± 0.09 **ab**	0.08 ± 0.02 **d**	0.09 ± 0.06 **b**

Table A1b: Ratios (± SD) of K to P, Mg to P, Ca to P, Fe to P, and Zn to P from peak-to-background ratios for thick sections of resin embedd white spruce somatic embryo #1.

Organ	Tissue	Particle	K:P	Mg:P	Ca:P	Fe:P	Zn:P
Cotyledons	Protoderm	Fe-rich Particle	0.71 ± 0.04 **abcd**	0.22 ± 0.06 **d**	0.13 ± 0.02 **a**	2.27 ± 0.18 **d**	0.01 ± 0.02 **b**
	Ground Meristem	Fe-rich Particle	0.61 ± 0.11 **bcde**	0.22 ± 0.04 **d**	0.05 ± 0.02 **cd**	2.77 ± 0.28 **bd**	NS **b**
		Globoid	0.89 ± 0.07 **a**	0.35 ± 0.09 **bc**	0.02 ± 0.01 **d**	0.02 ± 0.01 **a**	0.03 ± 0.02 **b**
	Procambium	Fe-rich Particle	0.75 ± 0.12 **abc**	0.19 ± 0.05 **d**	0.06 ± 0.02 **bcd**	2.72 ± 0.17 **cd**	NS **b**
		Globoid	0.79 ± 0.14 **ab**	0.37 ± 0.06 **ab**	0.04 ± 0.02 **d**	0.02 ± 0.01 **a**	0.11 ± 0.09
Hypocotyl	Protoderm	Fe-rich Particle	0.54 ± 0.12 **cde**	0.23 ± 0.03 **cd**	0.11 ± 0.03 **abc**	2.26 ± 0.38 **d**	NS **b**
	Ground Meristem	Fe-rich Particle	0.93 ± 0.09 **a**	0.20 ± 0.05 **d**	0.03 ± 0.02 **d**	2.96 ± 0.37 **bc**	NS **b**
		Globoid	0.82 ± 0.04 **ab**	0.38 ± 0.03 **ab**	0.02 ± 0.01 **d**	0.04 ± 0.03 **a**	0.02 ± 0.02 **b**
	Procambium	Fe-rich Particle	0.71 ± 0.12 **abcd**	0.14 ± 0.02 **d**	0.03 ± 0.01 **d**	2.30 ± 0.33 **d**	NS **b**
		Globoid	0.87 ± 0.15 **a**	0.44 ± 0.05 **ab**	0.04 ± 0.03 **d**	0.02 ± 0.01 **a**	0.01 ± 0.01 **b**
Radicle	Protoderm	Fe-rich Particle	0.72 ± 0.12 **abc**	0.22 ± 0.03 **d**	0.06 ± 0.01 **bcd**	3.35 ± 0.51 **b**	NS **b**
	Ground Meristem	Fe-rich Particle	0.61 ± 0.10 **bcde**	0.18 ± 0.04 **d**	0.12 ± 0.03 **ab**	3.03 ± 0.43 **bc**	0.02 ± 0.02 **b**
		Globoid	0.75 ± 0.07 **abc**	0.46 ± 0.06 **ab**	0.03 ± 0.02 **d**	0.01 ± 0.01 **a**	0.04 ± 0.03 **b**
	Procambium	Fe-rich Particle	0.49 ± 0.13 **de**	0.18 ± 0.03 **d**	0.11 ± 0.08 **ab**	2.90 ± 0.37 **bc**	0.02 ± 0.03 **b**
		Globoid	0.47 ± 0.12 **e**	0.48 ± 0.08 **a**	0.03 ± 0.01 **d**	0.01 ± 0.01 **a**	0.02 ± 0.02 **b**

Table A2a: Mean (± SD) peak-to-background ratios of elements in globoids (> 0.33 µm) and Fe-rich particles (≤ 0.33 µm) for various tissues in resin embedded thick sections of white spruce somatic embryo #2.

Organ	Tissue	Particle	P	K	Mg	Ca	Fe	Zn
Cotyledons	Protoderm	Fe-rich Particle	4.81 ± 0.84 **c**	2.10 ± 0.45 **e**	1.08 ± 0.31 **a**	0.50 ± 0.13 **a**	14.64 ± 2.79 **b**	NS **c**
	Ground Meristem	Fe-rich Particle	6.23 ± 2.30 **bc**	2.81 ± 1.80 **de**	1.45 ± 0.41 **a**	0.37 ± 0.28 **abc**	15.18 ± 4.53 **b**	NS **c**
		Globoid	11.01 ± 1.98 **a**	5.48 ± 0.95 **bc**	4.66 ± 0.70 **b**	0.19 ± 0.10 **bc**	0.36 ± 0.16 **a**	0.14 ± 0.10 **c**
	Procambium	Fe-rich Particle	3.87 ± 1.86 **c**	1.74 ± 0.52 **e**	1.02 ± 0.44 **a**	0.24 ± 0.03 **bc**	9.80 ± 4.59 **bc**	NS **c**
		Globoid	10.65 ± 0.95 **a**	5.03 ± 1.27 **bcd**	4.62 ± 0.65 **b**	0.31 ± 0.16 **bc**	0.02 ± 0.03 **a**	1.05 ± 1.02 **a**
Hypocotyl	Protoderm	Fe-rich Particle	4.66 ± 1.27 **c**	3.08 ± 0.77 **de**	0.96 ± 0.23 **a**	0.68 ± 0.11 **a**	15.15 ± 4.35 **b**	NS **c**
	Ground Meristem	Fe-rich Particle	4.79 ± 1.08 **c**	3.47 ± 0.73 **cde**	0.93 ± 0.25 **a**	0.38 ± 0.16 **abc**	12.99 ± 2.91 **bc**	NS **c**
		Globoid	9.26 ± 2.29 **ab**	6.76 ± 1.39 **ab**	4.55 ± 0.57 **bc**	0.11 ± 0.14 **b**	0.17 ± 0.13 **a**	0.31 ± 0.27 **abc**
	Procambium	Fe-rich Particle	4.96 ± 1.46 **c**	2.47 ± 0.51 **e**	1.24 ± 0.28 **a**	0.19 ± 0.05 **bc**	12.90 ± 4.30 **bc**	0.11 ± 0.16 **c**
		Globoid	10.04 ± 2.01 **a**	5.62 ± 1.28 **bc**	3.45 ± 1.00 **c**	0.18 ± 0.13 **bc**	NS **a**	0.56 ± 0.12 **abc**
Radicle	Protoderm	Fe-rich Particle	3.85 ± 1.29 **c**	2.50 ± 0.74 **e**	0.84 ± 0.16 **a**	0.48 ± 0.22 **ac**	10.79 ± 2.40 **bc**	NS **c**
	Ground Meristem	Fe-rich Particle	2.98 ± 0.56 **c**	2.16 ± 0.54 **e**	0.79 ± 0.12 **a**	0.12 ± 0.07 **b**	9.75 ± 1.07 **bc**	NS **c**
		Globoid	10.75 ± 2.08 **a**	8.03 ± 1.06 **a**	4.77 ± 0.91 **b**	0.25 ± 0.10 **bc**	0.17 ± 0.27 **a**	0.93 ± 0.72 **ab**
	Procambium	Fe-rich Particle	2.55 ± 0.79 **c**	1.97 ± 0.51 **e**	0.69 ± 0.09 **a**	0.12 ± 0.08 **b**	7.47 ± 1.60 **c**	0.16 ± 0.14 **bc**
		Globoid	9.84 ± 0.56 **a**	6.70 ± 1.36 **ab**	4.18 ± 0.52 **bc**	0.25 ± 0.08 **bc**	0.05 ± 0.11 **a**	0.18 ± 0.06 **bc**

Table A2b: Ratios (± SD) of K to P, Mg to P, Ca to P, Fe to P, and Zn to P from peak-to-background ratios for thick sections of resin embedd white spruce somatic embryo #2.

Organ	Tissue	Particle	K:P	Mg:P	Ca:P	Fe:P	Zn:P
Cotyledons	Protoderm	Fe-rich Particle	0.44 ± 0.03 **e**	0.22 ± 0.04 **d**	0.10 ± 0.02 **abc**	3.05 ± 0.29 **bc**	0.01 ± 0.02 **a**
	Ground Meristem	Fe-rich Particle	0.42 ± 0.14 **e**	0.24 ± 0.03 **cd**	0.06 ± 0.04 **cdef**	2.51 ± 0.50 **c**	NS **a**
		Globoid	0.50 ± 0.05 **cde**	0.43 ± 0.03 **ab**	0.02 ± 0.01 **ef**	0.03 ± 0.01 **a**	0.01 ± 0.01 **a**
	Procambium	Fe-rich Particle	0.49 ± 0.12 **de**	0.27 ± 0.04 **cd**	0.07 ± 0.03 **bcde**	2.53 ± 0.29 **c**	0.09 ± 0.08 **a**
		Globoid	0.47 ± 0.11 **de**	0.44 ± 0.08 **ab**	0.03 ± 0.02 **def**	NS **a**	0.01 ± 0.04 **a**
Hypocotyl	Protoderm	Fe-rich Particle	0.68 ± 0.15 **abcd**	0.21 ± 0.03 **d**	0.15 ± 0.03 **a**	3.25 ± 0.21 **bc**	NS **a**
	Ground Meristem	Fe-rich Particle	0.74 ± 0.12 **ab**	0.19 ± 0.02 **d**	0.08 ± 0.03 **bcd**	2.73 ± 0.26 **bc**	NS **a**
		Globoid	0.74 ± 0.12 **ab**	0.51 ± 0.08 **a**	0.01 ± 0.01 **f**	0.02 ± 0.02 **a**	0.04 ± 0.05 **a**
	Procambium	Fe-rich Particle	0.52 ± 0.10 **bcde**	0.26 ± 0.03 **cd**	0.04 ± 0.02 **def**	2.58 ± 0.27 **bc**	0.03 ± 0.04 **a**
		Globoid	0.57 ± 0.14 **abcde**	0.35 ± 0.08 **bc**	0.02 ± 0.02 **ef**	NS **a**	0.06 ± 0.01 **a**
Radicle	Protoderm	Fe-rich Particle	0.66 ± 0.06 **abcd**	0.23 ± 0.04 **cd**	0.12 ± 0.02 **ab**	2.97 ± 0.82 **bc**	NS **a**
	Ground Meristem	Fe-rich Particle	0.72 ± 0.05 **abc**	0.27 ± 0.04 **cd**	0.04 ± 0.02 **def**	3.32 ± 0.37 **b**	NS **a**
		Globoid	0.76 ± 0.10 **a**	0.45 ± 0.04 **ab**	0.02 ± 0.01 **ef**	0.02 ± 0.03 **a**	0.09 ± 0.08 **a**
	Procambium	Fe-rich Particle	0.79 ± 0.13 **a**	0.30 ± 0.11 **cd**	0.05 ± 0.02 **cdef**	3.03 ± 0.49 **bc**	0.06 ± 0.05 **a**
		Globoid	0.68 ± 0.15 **abcd**	0.43 ± 0.05 **ab**	0.03 ± 0.01 **def**	0.01 ± 0.01 **a**	0.02 ± 0.01 **a**

Table A3a: Mean (± SD) peak-to-background ratios of elements in globoids (> 0.33 μm) and Fe-rich particles (≤ 0.33 μm) for various tissues in resin embedded thick sections of white spruce somatic embryo #3.

Organ	Tissue	Particle	P	K	Mg	Ca	Fe	Zn
Cotyledons	Protoderm	Fe-rich Particle	3.43 ± 0.95 **d**	2.09 ± 0.55 **e**	0.58 ± 0.18 **d**	0.43 ± 0.07 **bcd**	12.32 ± 3.69 **c**	NS **a**
	Ground Meristem	Fe-rich Particle	4.00 ± 1.11 **d**	1.90 ± 0.44 **e**	0.85 ± 0.45 **d**	0.19 ± 0.06 **de**	9.45 ± 2.92 **c**	NS **a**
		Globoid	10.58 ± 2.19 **a**	4.74 ± 1.10 **bc**	4.41 ± 0.92 **a**	0.40 ± 0.14 **bcd**	0.04 ± 0.12 **a**	0.41 ± 0.42 **a**
	Procambium	Fe-rich Particle	4.39 ± 0.61 **cd**	2.75 ± 0.43 **cde**	0.95 ± 0.18 **d**	0.12 ± 0.07 **de**	13.76 ± 3.16 **c**	0.05 ± 0.05 **a**
		Globoid	10.01 ± 1.52 **a**	8.76 ± 1.01 **a**	4.47 ± 0.45 **a**	0.15 ± 0.06 **de**	0.04 ± 0.04 **a**	0.29 ± 0.11 **a**
Hypocotyl	Protoderm	Fe-rich Particle	4.71 ± 1.04 **cd**	2.99 ± 0.68 **bcde**	0.99 ± 0.20 **d**	0.59 ± 0.06 **abc**	14.92 ± 4.27 **c**	0.05 ± 0.09 **a**
	Ground Meristem	Fe-rich Particle	4.93 ± 1.91 **bcd**	4.56 ± 1.95 **bcd**	1.13 ± 0.25 **d**	0.05 ± 0.12 **e**	15.63 ± 7.40 **c**	NS **a**
		Globoid	12.46 ± 0.73 **a**	9.33 ± 1.19 **a**	5.08 ± 0.36 **a**	0.22 ± 0.08 **de**	0.14 ± 0.09 **a**	NS **a**
	Procambium	Fe-rich Particle	3.68 ± 0.84 **d**	2.77 ± 1.03 **cde**	0.79 ± 0.22 **d**	0.24 ± 0.21 **de**	12.53 ± 5.22 **c**	NS **a**
		Globoid	7.02 ± 2.39 **bc**	4.99 ± 1.03 **b**	2.60 ± 0.82 **b**	0.34 ± 0.06 **bcde**	0.22 ± 0.12 **a**	0.30 ± 0.74 **a**
Radicle	Protoderm	Fe-rich Particle	4.11 ± 0.44 **d**	2.72 ± 0.25 **cde**	0.96 ± 0.20 **d**	0.58 ± 0.11 **abc**	13.27 ± 3.32 **c**	NS **a**
	Ground Meristem	Fe-rich Particle	7.56 ± 0.31 **b**	4.86 ± 0.32 **b**	1.53 ± 0.08 **cd**	0.62 ± 0.05 **ab**	24.54 ± 3.10 **b**	NS **a**
		Globoid	10.27 ± 0.71 **a**	8.32 ± 1.24 **a**	4.20 ± 0.66 **a**	0.80 ± 0.41 **a**	0.17 ± 0.32 **a**	0.05 ± 0.04 **a**
	Procambium	Fe-rich Particle	3.93 ± 0.79 **d**	2.53 ± 0.55 **de**	0.83 ± 0.12 **d**	0.24 ± 0.07 **de**	12.03 ± 2.35 **c**	NS **a**
		Globoid	4.83 ± 0.64 **bcd**	3.80 ± 0.53 **bcde**	2.31 ± 0.27 **bc**	0.29 ± 0.06 **cde**	0.10 ± 0.07 **a**	0.05 ± 0.10 **a**

Table A3b: Ratios (± SD) of K to P, Mg to P, Ca to P, Fe to P, and Zn to P from peak-to-background ratios for thick sections of resin embedd white spruce somatic embryo #3.

Organ	Tissue	Particle	K:P	Mg:P	Ca:P	Fe:P	Zn:P
Cotyledons	Protoderm	Fe-rich Particle	0.61 ± 0.03 **bc**	0.18 ± 0.06 **a**	0.13 ± 0.04 **ab**	3.59 ± 0.45 **b**	0.02 ± 0.05 **a**
	Ground Meristem	Fe-rich Particle	0.49 ± 0.09 **c**	0.20 ± 0.07 **a**	0.05 ± 0.03 **cde**	2.36 ± 0.26 **c**	NS **a**
		Globoid	0.45 ± 0.03 **c**	0.42 ± 0.05 **b**	0.04 ± 0.01 **cde**	NS **a**	0.04 ± 0.04 **a**
	Procambium	Fe-rich Particle	0.63 ± 0.08 **bc**	0.22 ± 0.03 **a**	0.03 ± 0.02 **cde**	3.13 ± 0.62 **bc**	NS **a**
		Globoid	0.89 ± 0.13 **a**	0.45 ± 0.05 **b**	0.02 ± 0.01 **de**	NS **a**	0.03 ± 0.01 **a**
Hypocotyl	Protoderm	Fe-rich Particle	0.64 ± 0.06 **bc**	0.21 ± 0.02 **a**	0.13 ± 0.03 **ab**	3.17 ± 0.56 **bc**	NS **a**
	Ground Meristem	Fe-rich Particle	0.91 ± 0.12 **a**	0.24 ± 0.05 **a**	NS **e**	3.06 ± 0.49 **bc**	NS **a**
		Globoid	0.75 ± 0.12 **ab**	0.41 ± 0.01 **b**	0.02 ± 0.01 **de**	0.01 ± 0.01 **a**	NS **a**
	Procambium	Fe-rich Particle	0.73 ± 0.15 **ab**	0.21 ± 0.01 **a**	0.06 ± 0.05 **cd**	3.29 ± 0.74 **b**	0.06 ± 0.15 **a**
		Globoid	0.75 ± 0.15 **ab**	0.38 ± 0.05 **b**	0.05 ± 0.02 **cde**	0.03 ± 0.02 **a**	NS **a**
Radicle	Protoderm	Fe-rich Particle	0.66 ± 0.04 **bc**	0.23 ± 0.03 **a**	0.14 ± 0.02 **a**	3.22 ± 0.61 **bc**	NS **a**
	Ground Meristem	Fe-rich Particle	0.64 ± 0.05 **bc**	0.20 ± 0.02 **a**	0.08 ± 0.01 **bc**	3.26 ± 0.49 **bc**	NS **a**
		Globoid	0.81 ± 0.14 **ab**	0.41 ± 0.08 **b**	0.08 ± 0.04 **bc**	0.02 ± 0.03 **a**	NS **a**
	Procambium	Fe-rich Particle	0.64 ± 0.06 **bc**	0.21 ± 0.04 **a**	0.06 ± 0.01 **cd**	3.08 ± 0.44 **bc**	NS **a**
		Globoid	0.79 ± 0.09 **ab**	0.48 ± 0.06 **b**	0.06 ± 0.01 **cd**	0.02 ± 0.01 **a**	NS **a**

Table A4a: Mean (± SD) peak-to-background ratios of elements in globoids (> 0.33 μm) and Fe-rich particles (≤ 0.33 μm) for various tissues in resin embedded thick sections of white spruce somatic embryo #4.

Organ	Tissue	Particle	P	K	Mg	Ca	Fe	Zn
Cotyledons	Protoderm	Fe-rich Particle	5.16 ± 0.86 **de**	3.28 ± 0.61 **ef**	0.76 ± 0.17 **a**	0.76 ± 0.16 **ab**	12.94 ± 2.98 **cd**	NS **c**
	Ground Meristem	Fe-rich Particle	6.20 ± 0.93 **de**	3.37 ± 0.55 **ef**	1.51 ± 0.29 **a**	0.76 ± 0.14 **ab**	15.94 ± 3.11 **bcd**	NS **c**
		Globoid	9.37 ± 2.92 **abc**	6.84 ± 1.05 **bcd**	3.69 ± 0.94 **cd**	0.45 ± 0.27 **bcd**	0.35 ± 0.16 **a**	0.26 ± 0.15 **bc**
	Procambium	Fe-rich Particle	4.30 ± 0.86 **e**	2.30 ± 0.66 **f**	0.93 ± 0.25 **a**	0.74 ± 0.20 **ab**	11.15 ± 1.39 **d**	NS **c**
		Globoid	11.66 ± 0.86 **a**	5.36 ± 1.35 **cde**	4.98 ± 0.90 **b**	0.17 ± 0.09 **d**	0.17 ± 0.06 **a**	1.99 ± 1.32 **a**
Hypocotyl	Protoderm	Fe-rich Particle	5.89 ± 1.00 **de**	4.00 ± 0.85 **ef**	1.15 ± 0.12 **a**	0.78 ± 0.15 **a**	16.95 ± 1.69 **bc**	0.06 ± 0.11 **bc**
	Ground Meristem	Fe-rich Particle	6.03 ± 1.59 **de**	2.99 ± 0.84 **ef**	1.36 ± 0.23 **a**	0.59 ± 0.15 **abc**	16.99 ± 2.72 **bc**	NS **c**
		Globoid	11.06 ± 0.99 **ab**	7.19 ± 2.46 **a**	4.55 ± 0.30 **bc**	0.19 ± 0.13 **d**	0.35 ± 0.03 **a**	0.14 ± 0.17 **bc**
	Procambium	Fe-rich Particle	5.93 ± 1.46 **de**	3.57 ± 0.71 **ef**	1.41 ± 0.31 **a**	0.22 ± 0.07 **d**	17.76 ± 4.61 **bc**	NS **c**
		Globoid	10.93 ± 1.54 **ab**	8.81 ± 1.04 **b**	5.07 ± 0.63 **b**	0.33 ± 0.20 **cd**	0.01 ± 0.11 **a**	0.93 ± 0.66 **b**
Radicle	Protoderm	Fe-rich Particle	5.29 ± 0.84 **de**	3.53 ± 0.53 **ef**	0.89 ± 0.07 **a**	0.55 ± 0.11 **abc**	14.97 ± 2.96 **bcd**	NS **c**
	Ground Meristem	Fe-rich Particle	5.33 ± 1.30 **de**	2.97 ± 1.04 **ef**	1.21 ± 0.24 **a**	0.40 ± 0.19 **cd**	14.80 ± 4.63 **cd**	0.09 ± 0.10 **bc**
		Globoid	11.91 ± 1.43 **a**	7.32 ± 1.61 **bc**	4.99 ± 0.35 **b**	0.17 ± 0.03 **d**	0.10 ± 0.11 **a**	0.19 ± 0.13 **bc**
	Procambium	Fe-rich Particle	6.83 ± 1.38 **cde**	4.68 ± 1.10 **def**	1.52 ± 0.36 **a**	0.56 ± 0.15 **abc**	20.38 ± 2.55 **b**	NS **c**
		Globoid	8.04 ± 0.86 **bcd**	4.58 ± 0.59 **def**	3.35 ± 0.12 **d**	0.34 ± 0.66 **cd**	0.04 ± 0.06 **a**	0.05 ± 0.12 **bc**

Table A4b: Ratios (± SD) of K to P, Mg to P, Ca to P, Fe to P, and Zn to P from peak-to-background ratios for thick sections of resin embedd white spruce somatic embryo #4.

Organ	Tissue	Particle	K:P	Mg:P	Ca:P	Fe:P	Zn:P
Cotyledons	Protoderm	Fe-rich Particle	0.64 ± 0.09 **bcd**	0.15 ± 0.02 **b**	0.15 ± 0.03 **ab**	2.49 ± 0.19 **b**	NS **b**
	Ground Meristem	Fe-rich Particle	0.54 ± 0.04 **d**	0.18 ± 0.02 **b**	0.12 ± 0.01 **bcd**	2.57 ± 0.31 **b**	NS **b**
		Globoid	0.77 ± 0.16 **bc**	0.40 ± 0.06 **a**	0.06 ± 0.04 **fgh**	0.04 ± 0.02 **a**	0.03 ± 0.01 **b**
	Procambium	Fe-rich Particle	0.53 ± 0.05 **d**	0.21 ± 0.01 **b**	0.17 ± 0.02 **a**	2.63 ± 0.33 **b**	0.18 ± 0.13 **a**
		Globoid	0.46 ± 0.10 **d**	0.42 ± 0.05 **a**	0.01 ± 0.01 **i**	0.02 ± 0.01 **a**	NS **b**
Hypocotyl	Protoderm	Fe-rich Particle	0.68 ± 0.08 **bcd**	0.20 ± 0.02 **b**	0.13 ± 0.02 **bc**	2.92 ± 0.37 **b**	NS **b**
	Ground Meristem	Fe-rich Particle	0.50 ± 0.07 **d**	0.23 ± 0.05 **b**	0.10 ± 0.01 **cde**	2.90 ± 0.53 **b**	NS **b**
		Globoid	1.11 ± 0.26 **a**	0.41 ± 0.04 **a**	0.02 ± 0.01 **i**	0.03 ± 0.00 **a**	NS **b**
	Procambium	Fe-rich Particle	0.61 ± 0.05 **bcd**	0.24 ± 0.02 **b**	0.04 ± 0.01 **ghi**	2.99 ± 0.35 **b**	NS **b**
		Globoid	0.82 ± 0.18 **b**	0.47 ± 0.09 **a**	0.03 ± 0.01 **hi**	NS **a**	0.08 ± 0.05 **b**
Radicle	Protoderm	Fe-rich Particle	0.67 ± 0.09 **bcd**	0.17 ± 0.03 **b**	0.10 ± 0.01 **cde**	2.83 ± 0.36 **b**	NS **b**
	Ground Meristem	Fe-rich Particle	0.55 ± 0.07 **cd**	0.23 ± 0.03 **b**	0.07 ± 0.02 **defg**	2.75 ± 0.31 **b**	0.02 ± 0.03 **b**
		Globoid	0.61 ± 0.10 **bcd**	0.42 ± 0.06 **a**	0.01 ± 0.00 **i**	0.01 ± 0.01 **a**	0.02 ± 0.01 **b**
	Procambium	Fe-rich Particle	0.68 ± 0.05 **bcd**	0.23 ± 0.05 **b**	0.08 ± 0.01 **def**	3.05 ± 0.51 **b**	NS **b**
		Globoid	0.57 ± 0.07 **cd**	0.42 ± 0.04 **a**	0.04 ± 0.01 **ghi**	0.01 ± 0.01 **a**	NS **b**

Table A5a: Mean (± SD) peak-to-background ratios of elements in globoids (> 0.33 μm) and Fe-rich particles (≤ 0.33 μm) for various tissues in resin embedded thick sections of white spruce somatic embryo #5.

Organ	Tissue	Particle	P	K	Mg	Ca	Fe	Zn
Cotyledons	Protoderm	Fe-rich Particle	4.86 ± 1.06 **d**	3.03 ± 0.95 **e**	1.18 ± 0.21 **a**	0.49 ± 0.14 **abc**	15.67 ± 2.27 **bcde**	NS **a**
	Ground Meristem	Fe-rich Particle	4.91 ± 1.12 **d**	3.44 ± 0.91 **de**	1.09 ± 0.31 **a**	0.25 ± 0.08 **bcde**	15.05 ± 5.10 **cde**	NS **a**
		Globoid	11.74 ± 1.01 **ab**	5.51 ± 0.81 **bcd**	5.09 ± 0.69 **c**	0.65 ± 0.29 **a**	0.24 ± 0.17 **a**	0.14 ± 0.33 **ab**
	Procambium	Fe-rich Particle	6.21 ± 0.86 **cd**	2.75 ± 0.72 **e**	1.51 ± 0.18 **a**	0.45 ± 0.13 **abcd**	20.64 ± 2.73 **bc**	0.06 ± 0.06 **ab**
		Globoid	10.77 ± 1.74 **ab**	6.58 ± 1.76 **bc**	4.84 ± 0.54 **c**	0.22 ± 0.09 **bcde**	0.03 ± 0.07 **a**	0.11 ± 0.20 **ab**
Hypocotyl	Protoderm	Fe-rich Particle	4.69 ± 0.68 **d**	2.84 ± 0.21 **e**	0.96 ± 0.08 **a**	0.53 ± 0.11 **ab**	13.34 ± 1.39 **d**	NS **a**
	Ground Meristem	Fe-rich Particle	4.10 ± 0.82 **d**	3.21 ± 0.37 **de**	0.94 ± 0.28 **a**	0.39 ± 0.21 **abcde**	10.98 ± 1.38 **e**	NS **a**
		Globoid	12.59 ± 2.06 **a**	7.29 ± 1.53 **b**	4.97 ± 0.52 **c**	0.17 ± 0.05 **de**	0.11 ± 0.08 **a**	0.07 ± 0.05 **ab**
	Procambium	Fe-rich Particle	8.84 ± 2.53 **bc**	6.55 ± 1.16 **bc**	3.57 ± 0.85 **d**	0.23 ± 0.14 **bcde**	0.10 ± 0.11 **a**	0.39 ± 0.39 **b**
		Globoid	5.11 ± 0.66 **d**	3.62 ± 0.44 **de**	1.18 ± 0.10 **a**	0.24 ± 0.13 **bcde**	18.11 ± 4.37 **bcd**	NS **a**
Radicle	Protoderm	Fe-rich Particle	5.29 ± 0.83 **d**	4.23 ± 0.74 **de**	1.02 ± 0.15 **a**	0.37 ± 0.12 **abcde**	15.43 ± 3.47 **bcde**	NS **a**
	Ground Meristem	Fe-rich Particle	11.27 ± 1.29 **ab**	4.74 ± 0.93 **cde**	1.34 ± 0.18 **a**	0.09 ± 0.05 **e**	21.30 ± 2.95 **b**	NS **a**
		Globoid	6.49 ± 1.42 **cd**	11.21 ± 0.91 **a**	6.14 ± 0.72 **b**	0.59 ± 0.14 **a**	NS **a**	NS **a**
	Procambium	Fe-rich Particle	6.71 ± 1.57 **cd**	4.69 ± 0.96 **cde**	1.27 ± 0.25 **a**	0.26 ± 0.07 **bcde**	20.01 ± 5.57 **bc**	NS **a**
		Globoid	8.60 ± 1.97 **bc**	6.72 ± 1.61 **b**	3.44 ± 0.43 **d**	0.20 ± 0.10 **cde**	0.29 ± 0.36 **a**	NS **a**

Table A5b: Ratios (± SD) of K to P, Mg to P, Ca to P, Fe to P, and Zn to P from peak-to-background ratios for thick sections of resin embedd white spruce somatic embryo #5.

Organ	Tissue	Particle	K:P	Mg:P	Ca:P	Fe:P	Zn:P
Cotyledons	Protoderm	Fe-rich Particle	0.62 ± 0.10 **bc**	0.24 ± 0.02 **a**	0.10 ± 0.03 **ab**	3.27 ± 0.36 **bc**	NS **a**
	Ground Meristem	Fe-rich Particle	0.71 ± 0.12 **b**	0.22 ± 0.03 **a**	0.05 ± 0.02 **bcd**	3.01 ± 0.39 **bc**	NS **a**
		Globoid	0.47 ± 0.10 **c**	0.43 ± 0.03 **c**	0.06 ± 0.03 **abcd**	0.02 ± 0.01 **a**	NS **a**
	Procambium	Fe-rich Particle	0.44 ± 0.05 **c**	0.25 ± 0.04 **a**	0.07 ± 0.03 **abc**	3.33 ± 0.17 **bc**	NS **a**
		Globoid	0.60 ± 0.07 **bc**	0.45 ± 0.03 **c**	0.02 ± 0.01 **cd**	NS **a**	NS **a**
Hypocotyl	Protoderm	Fe-rich Particle	0.61 ± 0.07 **bc**	0.21 ± 0.03 **a**	0.11 ± 0.03 **a**	2.86 ± 0.16 **c**	NS **a**
	Ground Meristem	Fe-rich Particle	0.80 ± 0.17 **ab**	0.23 ± 0.04 **a**	0.10 ± 0.05 **ab**	2.71 ± 0.24 **c**	NS **a**
		Globoid	0.58 ± 0.08 **bc**	0.40 ± 0.04 **c**	0.01 ± 0.01 **d**	0.01 ± 0.01 **a**	NS **a**
	Procambium	Fe-rich Particle	0.78 ± 0.21 **ab**	0.41 ± 0.06 **c**	0.03 ± 0.02 **cd**	0.01 ± 0.01 **a**	0.05 ± 0.04 **a**
		Globoid	0.71 ± 0.09 **b**	0.23 ± 0.03 **a**	0.05 ± 0.03 **bcd**	3.52 ± 0.60 **b**	NS **a**
Radicle	Protoderm	Fe-rich Particle	0.80 ± 0.07 **ab**	0.19 ± 0.02 **a**	0.07 ± 0.03 **ab**	2.88 ± 0.27 **c**	NS **a**
	Ground Meristem	Fe-rich Particle	0.74 ± 0.13 **b**	0.21 ± 0.04 **a**	0.01 ± 0.01 **d**	3.34 ± 0.41 **bc**	NS **a**
		Globoid	1.00 ± 0.11 **a**	0.55 ± 0.03 **b**	0.05 ± 0.02 **bcd**	NS **a**	NS **a**
	Procambium	Fe-rich Particle	0.71 ± 0.06 **b**	0.19 ± 0.02 **a**	0.04 ± 0.01 **cd**	2.98 ± 0.34 **bc**	NS **a**
		Globoid	0.78 ± 0.04 **ab**	0.41 ± 0.06 **c**	0.02 ± 0.01 **cd**	0.03 ± 0.03 **a**	NS **a**

APPENDIX B:

PEAK-TO-BACKGROUND RATIOS FOR WHITE SPRUCE ZYGOTIC EMBRYOS AND FEMALE GAMETOPHYTES FROM REID (1996)

Note

* 25 spectra were used for each mean.
* For each table values in a single column that are followed by the same letter are not significantly different at $P>0.05$.
* NS indicates values determined not to be significantly different from the background.

Table B1a: Mean (± SD) peak-to-background ratios of elements in globoids (> 0.33 μm) and Fe-rich particles (≤ 0.33 μm) for various tissues from thick sections of five white spruce zygotic embryos (Taken from Reid, 1996).

Organ	Tissue	Particle	P	K	Mg	Ca	Fe	Zn
Cotyledons	Protoderm	Fe-rich Particle	4.86 ± 0.92 **c**	2.45 ± 0.96 **a**	1.07 ± 0.40 **a**	1.17 ± 0.69 **a**	16.98 ± 4.76 **bc**	NS **d**
	Ground Meristem	Fe-rich Particle	5.08 ± 1.34 **c**	2.72 ± 0.89 **a**	1.28 ± 0.33 **a**	0.80 ± 0.77 **ab**	18.62 ± 4.90 **b**	NS **d**
		Globoid	11.30 ± 2.32 **a**	7.59 ± 2.48 **cd**	4.15 ± 0.75 **cd**	0.19 ± 0.14 **cd**	0.45 ± 0.39 **a**	0.93 ± 0.88 **a**
	Procambium	Fe-rich Particle	4.73 ± 1.39 **c**	2.94 ± 0.98 **a**	1.03 ± 0.31 **a**	0.38 ± 0.25 **cd**	15.22 ± 2.99 **bcd**	NS **d**
		Globoid	6.93 ± 2.16 **b**	5.59 ± 1.23 **d**	3.23 ± 2.42 **b**	0.15 ± 0.26 **d**	7.37 ± 5.67 **e**	0.22 ± 0.25 **bcd**
Hypocotyl	Protoderm	Fe-rich Particle	3.81 ± 1.13 **c**	2.17 ± 1.03 **a**	4.74 ± 3.41 **c**	0.62 ± 0.42 **bc**	13.23 ± 4.26 **cd**	0.07 ± 0.18 **ab**
	Ground Meristem	Fe-rich Particle	3.53 ± 0.98 **c**	2.32 ± 0.67 **a**	2.25 ± 2.79 **a**	0.13 ± 0.17 **d**	14.46 ± 5.06 **bcd**	NS **d**
		Globoid	11.82 ± 2.01 **a**	9.68 ± 3.95 **b**	4.38 ± 0.91 **c**	0.11 ± 0.13 **d**	0.16 ± 0.23 **a**	0.27 ± 0.24 **bcd**
	Procambium	Fe-rich Particle	3.53 ± 1.14 **c**	2.70 ± 1.03 **a**	0.83 ± 0.25 **a**	0.10 ± 0.08 **d**	12.79 ± 3.57 **cd**	NS **d**
		Globoid	10.16 ± 2.45 **a**	7.28 ± 2.15 **cd**	3.60 ± 0.66 **d**	0.12 ± 0.11 **d**	0.25 ± 0.13 **a**	0.62 ± 0.92 **ab**
Radicle	Protoderm	Fe-rich Particle	4.01 ± 1.85 **c**	2.73 ± 1.92 **a**	1.32 ± 1.15 **a**	0.34 ± 0.32 **cd**	11.03 ± 4.08 **d**	0.10 ± 0.25 **cd**
	Ground Meristem	Fe-rich Particle	3.50 ± 0.94 **c**	2.14 ± 0.83 **a**	0.90 ± 0.29 **a**	0.24 ± 0.33 **cd**	13.28 ± 3.65 **cd**	NS **d**
		Globoid	11.98 ± 1.28 **a**	9.32 ± 3.44 **bc**	4.65 ± 0.71 **c**	0.19 ± 0.19 **cd**	0.09 ± 0.13 **a**	0.24 ± 0.14 **bcd**
	Procambium	Fe-rich Particle	3.56 ± 1.02 **c**	2.65 ± 0.89 **a**	0.85 ± 0.22 **a**	0.07 ± 0.07 **d**	13.83 ± 3.94 **cd**	NS **d**
		Globoid	10.51 ± 1.85 **a**	7.30 ± 1.53 **cd**	4.11 ± 0.77 **cd**	0.17 ± 0.16 **d**	0.19 ± 0.14 **a**	0.56 ± 0.39 **abc**

Table B1b: Ratios (± SD) of K to P, Mg to P, Ca to P, Fe to P, and Zn to P from peak-to-background ratios for thick sections of five resin embedded white spruce zygotic embryos (Taken from Reid, 1996).

Organ	Tissue	Particle	K:P	Mg:P	Ca:P	Fe:P	Zn:P
Cotyledons	Protoderm	Fe-rich Particle	0.50 ± 0.16 **c**	0.22 ± 0.06 **c**	0.26 ± 0.16 **a**	3.51 ± 0.79 **c**	NS **b**
	Ground Meristem	Fe-rich Particle	0.56 ± 0.17 **bc**	0.26 ± 0.06 **bc**	0.16 ± 0.15 **bc**	3.75 ± 0.85 **c**	NS **b**
		Globoid	0.69 ± 0.24 **abc**	0.37 ± 0.04 **ab**	0.02 ± 0.02 **e**	0.04 ± 0.04 **a**	0.09 ± 0.10 **a**
	Procambium	Fe-rich Particle	0.62 ± 0.10 **abc**	0.22 ± 0.06 **c**	0.08 ± 0.06 **de**	3.34 ± 0.71 **c**	NS **b**
		Globoid	0.85 ± 0.21 **a**	0.38 ± 0.15 **ab**	0.02 ± 0.04 **e**	1.07 ± 0.78 **b**	0.04 ± 0.04 **ab**
Hypocotyl	Protoderm	Fe-rich Particle	0.57 ± 0.18 **bc**	0.22 ± 0.07 **c**	0.17 ± 0.11 **bc**	3.53 ± 0.74 **c**	NS **b**
	Ground Meristem	Fe-rich Particle	0.66 ± 0.14 **abc**	0.28 ± 0.05 **abc**	0.04 ± 0.06 **de**	4.09 ± 0.75 **c**	NS **b**
		Globoid	0.81 ± 0.28 **ab**	0.38 ± 0.07 **ab**	0.01 ± 0.02 **e**	NS **a**	NS **b**
	Procambium	Fe-rich Particle	0.77 ± 0.18 **ab**	0.24 ± 0.06 **c**	0.03 ± 0.03 **de**	3.78 ± 0.92 **c**	NS **b**
		Globoid	0.71 ± 0.14 **abc**	0.37 ± 0.08 **ab**	0.01 ± 0.01 **e**	0.03 ± 0.02 **a**	0.07 ± 0.12 **a**
Radicle	Protoderm	Fe-rich Particle	0.64 ± 0.22 **abc**	0.30 ± 0.14 **abc**	0.10 ± 0.08 **bcd**	3.28 ± 1.49 **c**	NS **b**
	Ground Meristem	Fe-rich Particle	0.62 ± 0.20 **abc**	0.26 ± 0.06 **bc**	0.07 ± 0.10 **de**	3.85 ± 0.76 **c**	NS **b**
		Globoid	0.78 ± 0.30 **ab**	0.39 ± 0.04 **a**	0.02 ± 0.02 **e**	NS **a**	NS **b**
	Procambium	Fe-rich Particle	0.74 ± 0.11 **abc**	0.25 ± 0.06 **c**	0.02 ± 0.02 **e**	3.95 ± 0.73 **c**	NS **b**
		Globoid	0.70 ± 0.11 **abc**	0.39 ± 0.06 **a**	0.02 ± 0.02 **e**	0.02 ± 0.02 **a**	0.05 ± 0.04 **ab**

Table B2a: Mean (± SD) peak-to-background ratios of elements in globoids (> 0.33 µm) and Fe-rich particles (≤ 0.33 µm) from resin embedded thick sections for five white spruce female gametophytes (Taken from Reid, 1996).

Region	Particle	P	K	Mg	Ca	Fe	Zn
Cotyledon-Associated	Fe-rich Particle	3.31 ± 0.97 **a**	2.34 ± 0.75 **a**	0.87 ± 0.31 **a**	0.09 ± 0.11 **a**	9.82 ± 3.29 **a**	0.05 ± 0.12 **a**
	Globoid	11.36 ± 1.92 **b**	8.74 ± 2.42 **b**	3.90 ± 1.09 **b**	0.33 ± 0.22 **a**	0.52 ± 0.26 **b**	0.42 ± 0.28 **b**
Hypocotyl-Associated	Fe-rich Particle	3.34 ± 1.11 **a**	2.52 ± 0.87 **a**	0.93 ± 0.20 **a**	0.33 ± 0.80 **a**	10.91 ± 4.57 **a**	0.07 ± 0.14 **a**
	Globoid	11.99 ± 1.90 **b**	10.30 ± 1.37 **b**	4.49 ± 0.71 **b**	0.35 ± 0.15 **a**	0.30 ± 0.20 **b**	0.32 ± 0.14 **b**
Radicle-Associated	Fe-rich Particle	4.19 ± 1.69 **a**	2.72 ± 1.43 **a**	0.91 ± 0.33 **a**	0.64 ± 1.18 **a**	13.69 ± 5.88 **a**	0.10 ± 0.19 **a**
	Globoid	11.67 ± 2.24 **b**	9.93 ± 2.22 **b**	4.73 ± 1.11 **b**	0.32 ± 0.14 **a**	0.24 ± 0.22 **b**	0.31 ± 0.14 **b**

Table B2b: Ratios (± SD) of K to P, Mg to P, Ca to P, Fe to P, and Zn to P from peak-to-background ratios for various regions of resin embedded white spruce female gametophyte tissues from five seeds (Taken from Reid, 1996).

Region	Particle	K:P	Mg:P	Ca:P	Fe:P	Zn:P
Cotyledon-Associated	Fe-rich Particle	0.77 ± 0.34 **a**	0.26 ± 0.09 **ab**	0.03 ± 0.05 **a**	2.98 ± 0.61 **a**	0.02 ± 0.04 **a**
	Globoid	0.77 ± 0.19 **a**	0.34 ± 0.08 **ab**	0.03 ± 0.02 **a**	0.05 ± 0.03 **b**	0.04 ± 0.02 **a**
Hypocotyl-Associated	Fe-rich Particle	0.81 ± 0.31 **a**	0.30 ± 0.10 **ab**	0.07 ± 0.14 **a**	3.24 ± 0.56 **a**	0.02 ± 0.05 **a**
	Globoid	0.87 ± 0.13 **a**	0.38 ± 0.04 **ab**	0.03 ± 0.02 **a**	0.03 ± 0.02 **b**	0.03 ± 0.01 **a**
Radicle-Associated	Fe-rich Particle	0.76 ± 0.44 **a**	0.23 ± 0.07 **b**	0.11 ± 0.18 **a**	3.35 ± 0.82 **a**	0.03 ± 0.05 **a**
	Globoid	0.86 ± 0.13 **a**	0.40 ± 0.05 **a**	0.03 ± 0.02 **a**	0.02 ± 0.02 **b**	0.03 ± 0.01 **a**

APPENDIX C:

PEAK-TO-BACKGROUND RATIOS FOR ALL THE GLOBIODS COMBINED AND ALL THE FE-RICH PARTICLES COMBINED FOR BOTH WHITE SPRUCE SOMATIC AND ZYGOTIC EMBRYOS

Note

* 150 globoid spectra were used for each globoid mean.
* 225 Fe-rich particle spectra were used for each Fe-rich particle mean.
* Each mean was calculated using all the spectra for that embryo type (somatic or zygotic) and and for that type of particle (globoid or Fe-rich particle).

Table C1a: Mean (± SD) peak-to-background ratios of elements in all the globoids (> 0.33 μm) collected from white spruce somatic and zygotic embryos.

Embryo Type	P	K	Mg	Ca	Fe	Zn
Somatic	9.71 ± 2.42	6.79 ± 2.33	4.11 ± 1.10	0.29 ± 0.21	0.14 ± 0.17	0.35 ± 0.57
Zygotic	10.45 ± 2.64	7.79 ± 2.94	3.90 ± 1.05	0.16 ± 0.17	1.42 ± 3.52	0.47 ± 0.61

Table C1b: Mean (± SD) peak-to-background ratios of elements in all the Fe-rich particles (≤ 0.33 μm) collected from white spruce somatic and zygotic embryos.

Embryo Type	P	K	Mg	Ca	Fe	Zn
Somatic	4.88 ± 1.50	3.11 ± 1.12	1.03 ± 0.33	0.39 ± 0.24	14.27 ± 4.95	0.01 ± 0.10
Zygotic	4.07 ± 1.34	2.54 ± 1.09	1.01 ± 0.50	0.43 ± 0.54	14.38 ± 4.65	0.05 ± 0.16

Table C2a: Ratios (± SD) of K:P, Mg:P, Ca:P, Fe:P, and Zn:P for all the globoids (> 0.33 μm) collected from white spruce somatic and zygotic embryos.

Embryo Type	K:P	Mg:P	Ca:P	Fe:P	Zn:P
Somatic	0.71 ± 0.20	0.43 ± 0.07	0.03 ± 0.02	0.02 ± 0.02	0.04 ± 0.06
Zygotic	0.76 ± 0.23	0.38 ± 0.08	0.02 ± 0.02	0.20 ± 0.50	0.05 ± 0.07

Table C2b: Ratios (± SD) of K:P, Mg:P, Ca:P, Fe:P, and Zn:P for all the Fe-rich particles (≤ 0.33 μm) collected from white spruce somatic and zygotic embryos.

Embryo Type	K:P	Mg:P	Ca:P	Fe:P	Zn:P
Somatic	0.65 ± 0.14	0.22 ± 0.05	0.08 ± 0.05	2.93 ± 0.50	0.00 ± 0.03
Zygotic	0.63 ± 0.18	0.25 ± 0.08	0.10 ± 0.12	3.68 ± 0.91	0.01 ± 0.04

APPENDIX D:

COMPONENTS OF STANDARD LITVAY'S MEDIA (FROM LITVAY *ET AL.*, 1981)

Note

* Concentrations listed here were used at half strength in this project.

Compound	Levels (mg/L)
NH_4NO_3	1650.00
KNO_3	1900.00
$MgSO_4 \cdot 7H_2O$	1850.00
KH_2PO_4	340.00
$CaCl_2 \cdot 2H_2O$	22.00
KI	4.15
H_3BO_3	31.00
$MnSO_4 \cdot H_2O$	21.00
$ZnSO_4 \cdot 7H_2O$	43.00
$Na_2MoO_4 \cdot 2H_2O$	1.25
$CuSO_4 \cdot 5H_2O$	0.50
$CoCl_2 \cdot 6H_2O$	0.13
$FeSO_4 \cdot 7H_2O$	27.80
Na_2EDTA	37.30
Myoinositol	100.00
Nicotinic acid	0.50
Pyridoxine•HCl	0.10
Thiamine•HCl	0.10
Sucrose	30,000.00